Brief Primer on the Fundaments of Quantum Computing

Richard L Amoroso
amoroso@noeticadvancedstudies.us

PART 2 Cornucopia of Quantum Logic Gates

PART 3 Surmounting Uncertainty Supervening Decoherence

PART 4 Measurement With Certainty

PART 5 New Classes of Quantum Algorithms

This QC primer is based on excerpts from the breakthrough volume *Universal Quantum Computing* (ISBN: 978-981-3145-99-3) which touts having dissolved the remaining barriers to implementing Bulk Universal Quantum Computing (UQC), and as such most likely describes the most advanced QC development platform. Numerous books, hundreds of patents, thousands of papers and a Googolplex of considerations fill the pantheon of QC R&D. Of late QC mathemagicians claim QCs already exist; but by what chimeric definition. Does flipping a few qubits in a logic gate without an algorithm qualify as quantum computing? In physics, theory bears little weight without rigorous experimental confirmation, less if new, radical or a paradigm shift. This volume develops quantum computing based on '3rd regime' physics of Unified Field Mechanics (UFM). What distinguishes this work from a myriad of other avenues to UQC under study? Virtually all R&D paths struggle with technology and decoherence. If the currently highly favored room-sized cryogenically cooled quantum Hall anyon bilayer graphene QCs ever become successful, they would be reminiscent of the city block-sized Eniac computer of 1946. In 2017 quantum Hall techniques experimentally discovered additional dimension, said to be inaccessible and were called 'artificial'. This scenario will not last long; the floodgates will open momentarily. Then we will have actual QCs! The QC prototype proposed herein is room temperature and tabletop. It is dramatically different in that it is not confined to the limitations of quantum mechanics; since it is based on principles of UFM, the Uncertainty Principle and Decoherence no longer apply. Thus, this QC model could be implemented on any other quantum platform!

Preface – From the Volume

The breakthrough volume, from which the following excerpts come - (ISBN: 978-981-3145-99-3 print; ISBN: 978-981-3146-01-3 electronic) touts having conceptually dissolved the remaining barriers for immediate implementation of Bulk Universal Quantum Computing (UQC), and as such most likely describes the most advanced basis for developing Quantum Information Processing (QIP). Numerous books, many 100s of patents, 1,000s of papers and a Googolplex of considerations fill the pantheon of QC R&D. Of late QC mathemagicians claim QCs already exist; but by what chimeric definition. Does flipping a few qubits in a logic gate qualify as quantum computing?

In physics, theory bears little weight until it is supported by rigorous experimental confirmation, less if new, radical or an untested paradigm shift. This volume develops quantum computing based on '3rd regime' physics of Unified Field Mechanics (UFM). What distinguishes this work from myriad other avenues to UQC under study? Virtually all R&D paths struggle with refining technology and decoherence. If the highly favored room-sized cryogenically cooled QCs ever become successful, they would be reminiscent of the 1946 city block-sized Eniac computer that contained 17,468 vacuum tubes. Does the proposed by-pass of that step retard acceptance of the UFM model; maybe, maybe not as UFM modeling also puts an end to the need for large supercolliders like the CERN LHC.

The QC prototype proposed herein is room temperature, tabletop, surmounts uncertainty and supervenes decoherence during the general process of operation. It is dramatically different in that it is also not limited to the 'locality and unitarity' confines of the basis of quantum mechanics itself. Since it is based on principles of UFM, the Uncertainty Principle and Decoherence no longer apply. Thus, generally speaking, the UFM UQC model could putatively be implemented on any of the other viable quantum platforms. Albeit, here's the rub: a conundrum still exists; the complex algebra for correlating relativistic (r-qubits) with a new class of algorithms designed for a transform beyond the Galilean-Lorentz-Poincairé cast in HD UFM brane topology remains. A program is in place to finish the final mathematical derivation by spring 2017 and perform the 1st experiment by 2019 if our proposal is accepted and allocated a spot in the que applied to.

The last age of discovery occurred about 100 years ago. Incorporating the remaining requirements for UQC will usher in the next one. Scott Aaronson of MIT said, '*quantum computing requires a new discovery in physics, and if that discovery has been made is not been revealed to the physics community*.' Since the CIA has purchased a D-wave 'toy' QC, it seems reasonably clear no clandestine

discovery is in the hands of the US government. Gazing over the landscape of the QC research community, everyone seems to be about on the same page in battling decoherence as the final problem. With relative certainty then, the claim, '*Hypothesis non-Fingo'* as Newton is want to say, that the discovery is revealed in this volume is reservedly ballyhooed. The transition to UFM is not one discovery, but a 'bucket of discovery', perhaps that could be said of a similar bucket ladling out quantum mechanics a hundred years ago by the seventeen eventual Nobel laureates who attended the world of physics changing *Conseil Solvay* conferences in Brussels.

The framework for the imminent age of discovery we term unified field mechanics (UFM); a third regime of reality in the progression Classical Mechanics $\rightarrow$ Quantum Mechanics $\rightarrow$ UFM. Just as infinities (ultraviolet catastrophe) in the Raleigh-Jeans Law describing blackbody radiation led to Planck's 1900 formulation of the process of energy absorption and emission, becoming known as the quantum hypothesis - *any energy-radiating atomic system can theoretically be divided into a number of discrete 'energy elements',* ε with each element proportional to the frequency, v individually radiating energy, by: $\varepsilon = hv$.

There is an obvious parallel today in the renormalization of the troublesome infinities in quantum field theory. It is quite curious that in this case a reversal occurs and quantization is undone again by entry into the 3rd regime. Since quantum mechanics can no longer be considered the 'basement of reality' an initial discovery popping out of the UFM bucket is that QM uncertainty is a 'complex manifold of finite radius'. The new set of UFM transformations beyond the Galilean-Lorentz-Poincairé naturally cancel the infinities from fundamental principles, not in an *ad hoc* manner.

Physicists still 'believing' in a quantum universe where the Planck scale is the 'basement of reality', adamantly proclaim the impossibility of violating the quantum uncertainty principle. Here is the manner in which science fiction writer Isaac Asimov put it, "*You can't lick the uncertainty principle, man, any more than you can live on the sun, there are physical limits to what can be done*." [1]. Physical limits apply of course to the tools available to us. Currently, the smaller the scale we hope to observe the larger and larger supercollider the needs to be to create definitive particle spray cross-section. As you will hopefully be able to comprehend from my primitive ruminations, UFM provides a new type of low energy cross-section. The 4-space observation of microscopic matter demands at supercollider. From the point of view of a cosmology with a Planck-scale basement that is all there is; particles are singularities in spacetime. But the fundamental nature of matter is profoundly different once one is able to 'see' beyond the rigid barrier kept in place by the uncertainty manifold. In HD space, each particle is comprised additionally of a mirror-symmetric brane topology of conformal scale-invariant components. A Dirac-like spherical rotation occurs, cyclically separating each mirror symmetric half and reconnecting it again. If the 'measurement' is taken when the symmetry is reconnecting, the cross-section is revealed; the 3-sphere able to 'see' the insides of the circles in Abbot's book Flatland.

If this volume could evolve to a 3rd edition; I think I might finally be satisfied with it. Those who write 'books' suffer with the experience that a volume in many ways is never completely finished; and one polishes and rubs until a convenient or often inconvenient stopping place intervenes. I would not bother my dear readership with this misanthropic complaint if it were just a matter of time constraints, which of itself can be a serious derailment; but in performing the usual study and research to embellish, supplement and check for accuracy, something totally unexpected occurred. This has by no means been a more typical monograph preparation solidifying research done over a past five to ten or even twenty years; but *avant-garde* and thus perhaps sadly may be seen as a bit too radical for some mentalities. I remember when 1st reading Newton's *Principia*, it took an effort for me to find the basis for his historical introduction of Calculus. More pertinently however, what I mean is that the work has been a broad avenue of profound discovery, not a few, but many; that like the shift to quantum mechanics will take the next 100 years to develop.

For example, and this is not the kind of discovery I mean – something already out there that I didn't notice before: In preparing this manuscript I was delighted, surprised and nonplussed to find in what at first appeared to be an obscure nook and cranny in 2015, a discussion of relativistic quantum information processing and relativistic qubits. The originator of the concept, Vlasov, a Russian postdoc at the time, briefly introduced relativistic qubits at PhysComp96 [2]. On emailing him, I said, '*it looks*

like it took about 20 years, but finally the community is starting to catch up with your idea'. He promptly emailed me back with a link to a 2006 paper hinting at the concept [3]. As often is the case with a seminal thought, the presenter is timid, not sure himself and has less clarity than will appear soon afterwards, which almost immediately did, and now a new field of relativistic information processing (RIP) is in full swing. I'll only mention one more item at the moment – I never would have guessed in pondering solutions to the inherent problem of anyonic 'topologically protected' TQC, that I would discover the need for what I decided to term an 'Ontological-Phase Topological Field Theory (OPTFT).

> When the great innovation appears, it will almost certainly be in a muddled, incomplete and confusing form. To the discoverer himself it will be only half-understood; to everybody else it will be a mystery. For any speculation which does not at first glance look crazy, there is no hope. — Freeman Dyson [4].

If the author has an obvious shortcoming, while he is a practicing mathematical-theoretical physicist, he is equally or more so a philosopher of physics revealed in the more axiomatic approach peppered with *dessin enfant* (pun intended) utilized in this presentation.

OPTFT, essential UFM bulk UQC will end up taking us far into the future; with it, one leaves polynomial and quadratic algorithmic speedup in the dust as it will soon enough be possible to develop 'instantaneous algorithms' by utilizing the full EPR aspects of nonlocal holography and some sort of dual-amplituhedron as being developed by Nima Arkani-Hamed. Now let's get back to more immediate promulgations.

The salient premise of this volume is that UQC cannot be achieved without utilizing UFM. This is not a simple premise, but represents a major paradigm shift of the caliber of switching from classical mechanics to quantum mechanics. But to confound us, it is in addition more like a Galilean class paradigm shift complicated by additional epistemological issues involved; which even this 'fall guy' is too timid to address here without guile. The rest of the physics community is still lollygagging around finishing the standard model in 4D. I think dimensionality of the TOE is not addressed as a requirement in that escapade. Additional dimensionality (XD) is however, now testable by proposed experiments at CERN (or the low energy tabletop protocol outlined herein). It may be that the putative utility of UFM required for UQC here garners little attention until a version of M-theory becomes pragmatically realized.

Also note that, for a variety of reasons discussed, our version of M-theory differs dramatically on several key premises, because we feel Gravity is not quantized and that the regime of interaction is rather with the regime of UFM. This is also not a trivial dilemma, we have defined a duality between Newton's and Einstein's gravity; and it seems likely in that guise that in the semi-quantum limit some sort of quantized-like residue operates elevating the concept of wave-particle duality to a principle of cosmology applying to brane topology. This stems from our discovery that 'uncertainty' is a complex manifold of finite radius. Certainly, at the time of writing, the majority of QC developers still work within the confines of Bloch sphere Hilbert space concepts. Before even approaching the cornucopia of landmines proposed here; one must pass through the briar patch of leaving unitarity and locality behind, and also view differently the very recent forays into relativistic modes of QIP before coming to the threshold of what we think should be called a Ontological-Phase Topological Field Theory (OPTFT).

In Chap. 3 the author felt it necessary to take liberty and include material relating to the physical basis for the 'Mind of the Observer' as part of delineating the need for a new cosmological paradigm to fully develop UQC. For real progress to occur, even as the likes of von Neumann claimed, observer physics needs to be fully addressed sometime - Feynman said in his Nobel lecture:

> If [all physicists] follow the same current fashion in expressing and thinking about … field theory … hypotheses being generated ... is limited ... possibly the chance is high that the truth lies in the fashionable direction. But, on the off chance that it is in another direction - a direction obvious from an unfashionable view of field theory - who will find it? Only someone who sacrifices himself ... from a peculiar and unusual point of view, one may have to invent for himself - *Richard Feynman*,

Nobel Prize lecture.

There is still a lot of chatter about classical mechanics and classical field theory. The situation has been steadily evolving from quantum mechanics to quantum field theory. The concept of Quantum Computing (QC) began in 1981 when Nobelist Richard Feynman queried if '*quantum physics could be simulated on a computer*'. The discussion led to the insight that simulating quantum physics would require a new kind of computer called a '*quantum computer'*; thought to be the very first mention of the term. Later Feynman suggested: '*There is nothing in the laws of physics prohibiting quantum computers*' [5]. Feynman also proposed that quantum computation could be facilitated by incorporating the utility of a concept he termed a '*synchronization backbone'*. Until now this construct has remained mysterious and considered intractable by the QC development community. This impasse essentially occurred because the rational for attempting to implement a synchronization backbone approach is classed in terms of what is known as a 'bi-local' phenomenon [3,4] that didn't really add a proper 'backbone' to the quantum system in that style of attempt. In the extended model delineated here, based on elements of UFM [5-7], a viable synchronization backbone is discovered to be an inherent part of the topology of the higher dimensional (HD) M-Theoretic Calabi-Yau mirror symmetric backcloth; which turns out to be essentially like getting half the quantum computer for 'free'! In terms of UFM the perceived local state is only a shadow of the HD nonlocal quantum reality; thus, our perception of Feynman's synchronization backbone is not feasible bi-locally but requires a duality of locality and HD nonlocal aspects of UFM. This key aspect of bulk UQC modeling could not have been discovered without the paradigm shift to UFM [8-10] revealing the true synchronization backbone as part of the mirror symmetry backcloth.

The purpose of the first two chapters is generally to review the current state of affairs in QC development and give a semblance of self-containment for the volume. Chapter 1 - *From Concept to Conundrum* briefly delineates the origins of Quantum Computing in terms of Feynman's ruminations on the subject; followed by a short description of the dozen or more research approaches currently considered most promising. Chapter 2 - *Cornucopia of Quantum Logic Gates* surveys and compares salient aspects of many of the main types of quantum logic gates studied.

Chapter 3 *Multiverse Cosmology – A New Basis of Reality* provides the initial foray into the basis for UFM providing a glimpse of the radical extension from the historical and current concept of observed reality as a Euclidean 3-space and outlines the new multiverse cosmology needed to go beyond the 4D Minkowski-Riemann spacetime of the standard model into the HD 3rd regime of Calabi-Yau mirror symmetric M-Theory.

Chapter 4 - *A Revolution in the Conception of Matter* sets the stage for Chap. 5 extending understanding of the ages old conundrum of the nature of the fermionic singularity or point particle; and defining why the current Bloch sphere rendition of a qubit must now be considered grossly inadequate and a relativistic r-qubit with more degrees of freedom is required. Chapters 4 and 5 tell us about conformal scale-invariant mirror symmetric 'copies' of a quantum state found in the topology of the HD brane world. In Chap 5 - *From Qubits to Relativistic Qubits* (*R-Qubits*) the basis for the standard definition of a qubit is redefined and extended to relativistic form for RIP where the additional degrees of freedom create compatibility with a 12D OPTFT which as shown later in Chaps. 6,7 and 8 provides the foundation for surmounting uncertainty and completely eliminating the problem of decoherence in the operation of a quantum computer. Chapter 9 - *Topological Quantum Field Theory* gives a technical review of TQFT and its utility in our model of bulk quantum computing. Chapters 7 and 8 - *Surmounting Uncertainty Supervening Decoherence*, and - '*Measurement' With Certainty,* respectively begin to explain more fully the core thrust of the volume. This is where the principles for actualizing a universal bulk quantum computer are explained for final prototyping in Chap. 16 and operation in Chap. 14.

Chapter 6 - *Utility of Unified Field Mechanics* describing a 3rd regime of reality beyond Classical and Quantum Mechanics provides clarity in understanding the bridge between TQFT, the essential large scale additional dimensionality (LSXD) of our new understanding of reality and utility of relativistic qubits (r-qubits). When the reader gets to Chapter 13 - *New Classes of Quantum Algorithms,* it should become obvious that an r-qubit with additional degrees of freedom cast in an LSXD cosmology associated with UFM requires a radical extension of existing quantum logic gates.

In Chapters 14 - *Class II Mesoionic Xanthines as Potential Ten Qubit Substrate Registers*, and 16 - *Universal QC Prototype Modeling* the class II mesoionic xanthine molecule chosen for prototyping and its bonding substrate is described. The mesoionic xanthine forms a stable crystal at room temperature with a 100-year shelf life and has 10 evenly spaced quantum states suitable for uniform scalability.

Chapter 15 - *Empirical Regimen - Proof of Concept* is essential. There is currently a program in the process of performing an experimental protocol aimed at falsifying the paradigm of unified field mechanics required to operate the quantum computer design offered herein. Success of the experiment will essentially confirm near term implementation of universal scalable bulk quantum computing as the methodology required parallels computer operations, albeit applied to the quantum system in a different manner.

References

[1] Asimov, I. (1989) The dead past, in Hartwell, D.G. (ed.) The World Treasury of Science Fiction, Little Brown.
[2] Vlasov, A.Y. (1999) Quantum theory of computation and relativistic physics, PhysComp96 Workshop, Boston MA, 22-24 Nov 1996, arXiv: quant-ph/ 9701027v4.
[3] Terno, D.R. (2006) Introduction to relativistic quantum information, arXiv:quant-ph/0508049v2; Peres, A. & Terno, D.R. (2003) Quantum information and relativity theory, arXiv:quant-ph/0212023v2.
[4] Dyson, F. (1958) Innovation in physics, Scientific American, 199, Collected in, From Eros to Gaia,1993.
[5] Feynman, R.P. (1986) Quantum mechanical computers, Foundations of Physics 16: 507-531.
[6] Floerchingerar, S. (2010) Quantum field theory as a bilocal statistical field theory, arXiv:1004.2250v1 [hep-th].
[7] Acatrinei, C. (2002) Bilocal dynamics in quantum field theory, arXiv:hep-th/0210040v1.

PART 1
From Concept to Conundrum: A Precis of Quantum Computing Substrates

The concept of quantum computing (QC) is generally credited to ratiocination by Nobelist Richard Feynman during the 1980's, who saw 'nothing in the laws of physics that precluded their development'. During the ensuing decades accelerating progress has been made in the ongoing development of quantum logic gates, a variety albeit dearth of algorithms and most assuring a plethora of potentially viable substrates for QC implementation. Proponents generally consider the remaining hurdle preventing bulk universal QC centers on problems associated with decoherence. In this work, a brief review, for the purpose of bringing the interested reader up to speed and as a semblance of self-containment, a precis of the dominant platforms under development is given; each platform is unique in substrate technology, implementation format and scaling challenges. This also prepares the reader for moving from qubits to a new class of relativistic qubits (r-qubits) whereby additional degrees of freedom are deemed essential for crossing the 'semi-quantum limit' into the realm of Unified Field Mechanics (UFM) allowing routine violation of the Quantum Uncertainty Principle and thereby supervening decoherence.

"… Trying to find a computer simulation of physics, seems … an excellent program to follow … I'm not happy with all the analyses that go with just the classical theory, because nature isn't classical, … and if you want to make a simulation of nature, you'd better make it quantum mechanical …", R. Feynman [1].

1.1 Preamble – Bits, Qubits and Complex Space

A classical Turing bit (short for binary digit) is the smallest unit of digital data and is limited to the two discrete binary states, 0 and 1; but a quantum bit (qubit) can additionally enter an entangled superposition of states, in which the qubit is effectively in both states simultaneously. While a classical register made up of n binary bits can contain only one of 2^n possible numbers, the corresponding quantum register can contain all 2^n numbers simultaneously. Thus, in theory, a QC could operate on seemingly infinite values simultaneously in parallel, so that a 30-qubit QC would be comparable to

a digital computer capable of performing 10^{13} (trillion) floating-point operations per second (TFLOPS) which is comparable to currently fastest supercomputers.

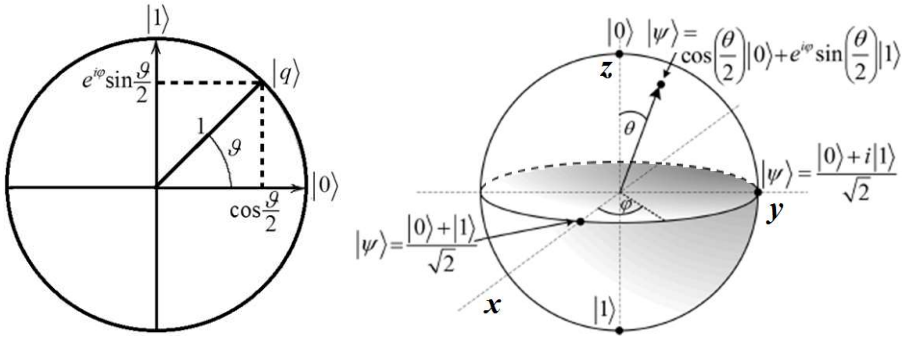

Fig. 1.1. Geometrical qubit representations. a) The qubit resides on the complex circle in the Hilbert space of all possible orientations of $|qi\rangle$. The complex unit circle is called the Hilbert space representation. In the logical basis, the two degrees of freedom of the qubit are expressed as two angles geometrically interpreted as Euler angles. b) The Bloch sphere in spin space showing the geometric representation of a qubit where $|\psi\rangle = \alpha|1\rangle + \beta|0\rangle$ for orthogonal eigenstates $|1\rangle$ and $|0\rangle$ of a single qubit on opposite poles, with superpositions located on the sphere's surface. Adapted from [2].

The qubit, a geometrical representation of the pure state space of a 2-level quantum mechanical system, is described in Dirac's 'bra-ket notation' by the state $\alpha|0\rangle+\beta|1\rangle$ where α and β are complex numbers satisfying the absolute value parameter $|\alpha|^2+|\beta|^2=1$; such that measurement would result in state $|0\rangle$ with probability $|\alpha|^2$ and $|1\rangle$ with probability $|\beta|^2$. Formally, a qubit is represented in the 2D complex vector space, $\mathbb{C}^2$ where the $\alpha|0\rangle+\beta|1\rangle$ can be represented in the standard orthonormal basis as $|0\rangle=\begin{bmatrix}1\\0\end{bmatrix}$ for the ground state or $|1\rangle=\begin{bmatrix}0\\1\end{bmatrix}$ for the excited state, or on the Bloch sphere as in Fig. 1.1b.

A qubit is shown in Fig. 1.1 in both its SU(2) Hilbert space representation (top), and the same qubit on the Bloch sphere in its O(3) representation (bottom). The SU(2) and O(3) representations are homomorphic, i.e. mapping preserves form between the two structures.

Vincenzo itemized what he felt were the major requirements for implementing practical bulk QC [3]:

- Physically scalable, allowing the number of qubits to be sufficiently increased for bulk implementation.
- Qubits must be able to be initialized to arbitrary values.
- Quantum gates that operate faster than the decoherence time.
- A universal gate set for running quantum algorithms.
- Qubits that can be easily read correctly.

None of Vincenzo's requirements are yet fulfilled; some are further along than others; system decoherence is among the most challenging aspects remaining. Recently, the fundamental basis of quantum information systems is undergoing an evolution in terms of the nature of reality with radical changes in the nature of the measurement problem. The recent introduction of parameters for relativistic information processing (RIP), including relativistic r-qubits, has brought into question the historical sacrosanct basis of 'locality and unitarity' in terms of Bell's inequalities, overcoming the no-cloning theorem [4,5]. The epistemic view of the Copenhagen Interpretation is challenged by ontic

considerations of objective realism and additionally as merged by W. Zurek's epi-ontic blend of quantum redundancy in quantum Darwinism [6].

1.2 Panoply of QC Architectures and Substrates – Limited Overview

The following list represents many prominent QC architectures and substrates currently under development. It seems useful to briefly review the challenges and merits of each system as distinguished by the computing model and physical substrates used to implement qubits.

- Quantum Turing Machine
- Quantum Circuit Quantum Computing Model
- Measurement Based Quantum Computing
- Adiabatic Quantum Computing
- Kane Nuclear Spin Quantum Computing
- QRAM Models of Quantum Computation
- Electrons-On-Helium Quantum Computers
- Fullerene-Based ESR Quantum Computer
- Superconductor-Based Quantum Computers
- Diamond-Based Quantum Computer
- Quantum Dot Quantum Computing
- Transistor-Based Quantum Computer
- Molecular Magnet Quantum Computer
- Bose–Einstein Condensate-Based Quantum Computer
- Rare-Earth-Metal-Ion-Doped Inorganic Crystal Quantum Computers
- Linear Optical Quantum Computer
- Optical Lattice Based Quantum Computing
- Cavity Quantum Electrodynamics (CQED) Quantum Computing
- Nuclear Magnetic Resonance (NMR) Quantum Computing
- Topological Quantum Computing
- Unified Field Mechanical Quantum Computing

1.2.1 *Quantum Turing Machine*

The quantum Turing machine (QTM) generalizes the classical Turing machine (CTM); the internal states of a CTM are replaced by pure or mixed states in a Hilbert space; The QTM is an idealistic platform not currently being developed. A QTM is a simple universal quantum computer used for modeling all the powerful parameters of quantum computing.

The QTM was proposed by Deutsch where he suggested that quantum gates could function similarly to traditional binary digital logic gates [7]. QTMs are not usually used for analyzing quantum computation; the quantum circuit model (QCM) is a more commonly used for such purposes.

1.2.2 *Quantum Circuit Computing Model*

The quantum circuit model (QCM) computes sequences of quantum gates which are reversible transformations on a quantum mechanical analog of a classical n-bit register. The QCM has only two observables, preparation of the initial state and observation of the final state in the same basis for the same variable at the end of the computation [8].

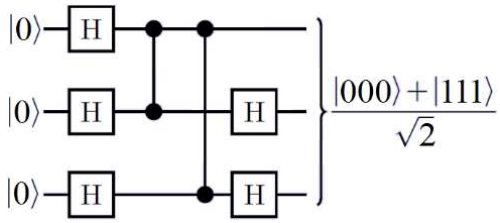

Fig. 1.2. Quantum circuit for 3 qubits using Hadamard gates.

1.2.3 *Measurement Based Quantum Computing*

The measurement based quantum computer (MBQC) model is also called the one-way model because the entangled resource state (usually a 'cluster state') is destroyed by the series of single qubit measurements on it. For a MBQC computation one starts with a given fixed entangled state of numerous qubits and performs a computation by applying a sequence of measurements to specific qubits in designated bases. The choice of basis for future measurements often depends on prior measurement outcomes. The final computation result is determined from the classical outcome data of all the measurements. In contrast to the more common gate array model in which computational steps are unitary operations, a large entangled state prior to some final measurements for the output is developed.

There are two principal schemes of MBQC:

1) Teleportation quantum computation (TQC) and the

2) Cluster state model or one-way quantum computer (1WQC)

Any one-way computation can be made into a quantum circuit by using quantum gates to prepare the resource state. For cluster and graph resource states, this requires only one 2-qubit gate per bond, which is very efficient [9-13].

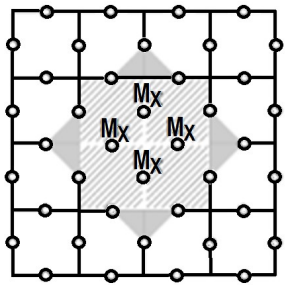

Fig. 1.3. Topological Cluster-State Quantum Computing (CSQC) on a 2D Cluster state surface code with 1° of freedom introduced via the measurement M_X of 4 qubits in the X basis and removal of 5 stabilizers. Note that new 3-term X stabilizers are not necessarily created with positive sign as in the shaded triangles. Redrawn from [14].

The face or region of such faces (shaded squares) is called a smooth defect. The degree of freedom can be phase flipped by any ring of Z-operators encircling the defect and bit flipped by any chain of X operators connecting the defect to a smooth boundary. The qubit inside the defect plays no further role in the computation unless the defect moves.

For the cluster-state model of quantum computation, in which coherent quantum information processing is accomplished via a sequence of single-qubit measurements applied to a fixed quantum state known as a cluster state; it has been proven that the cluster state cannot occur as the exact ground state of any naturally occurring physical system, proving that measurements on any quantum state which is linearly prepared in one dimension can be efficiently simulated on a classical computer, and thus are not candidates for use as a substrate for quantum computation [10,11].

1.2.4 *Adiabatic Quantum Computer*

Adiabatic quantum computation (AQC) is an alternative to the more common gate model which is based on the Turing approach to computing. It has been mathematically shown that the adiabatic model and the gate model are equivalent. The gate model approach creates quantum equivalents of digital logic gates and puts these gates together to build a quantum computer; it is a one-way quantum computer using quantum gates. It operates by setting up an initial entangled resource state pertaining to the problem, applies logic gates, then takes a measurement destroying the initial resource state. There is a high amount of error in this method requiring many trials or error correction sequences.

An AQC is based on Quantum annealing (finding the global minimum of a function over a given set of solutions by using quantum fluctuations), a process where computation is decomposed into a slow continuous transformation of an initial Hamiltonian into a final Hamiltonian, where the ground states of the system contain the solution [15].

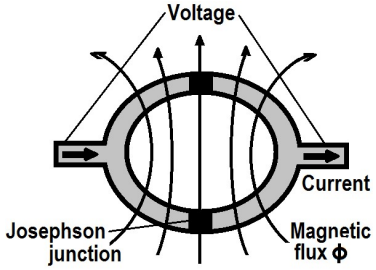

Fig. 1.4. An rf-SQUID with a Josephson junction from a D-Wave device. An array of coupled superconducting flux qubits acts as an artificial Ising spin system with programmable spin-spin couplings and transverse magnetic fields. Josephson junctions are integral elements in SQUID QC as flux qubits and other substrates where phase and charge act as conjugate variables.

A system of connected qubits in SQUID form is prepared with a magnetic field going a certain way. Then the initial state is slowly turned off while slowly turning on the final state. Basically, processing a mixed state of initial and final energy, and by the end there will be essentially no initial parts left in the state leaving only the final state. Alternatively, one can start with both states on, with the initial state much stronger than the final part of the state, and then slowly turn off the very large, initial state as shown in

$$H = \sum_i h_i Z_i + \sum_{i<j} J^{ij} Z_i Z_i + \sum_{i<j} K^{ij} X_i X_i, \qquad (1.1)$$

where *H* is the Hamiltonian, (matrix for total energy of the system). The three terms could be grouped into two terms because *Z* and *X* refer to the spin matrices; therefore, the initial state is governed by the last term, and the final state is governed by the first two terms. The spin matrices show the change from the *X*-basis state to the *Z*-basis state. When preparing the initial system of qubits, they are all put into the *X*-spin state and then 'annealed' to the *Z*-spin state. Imagine that *h* and *J* are tiny compared to *K* initially. When annealing, *K* is slowly turned off so that in the finished state, you're only left with the content of first two terms. This is how the annealing process works; when annealing, you need to be in the ground state. This is why you must move slowly, because if you move too quickly energy is imparted into the system, causing excitations and jumps to higher energy levels causing errors [15].

Researchers have performed the largest protein-folding problem solved to date using a quantum computer. The researchers solved instances of a lattice protein folding model, known as the Miyazawa-Jernigan model, on a D-Wave I quantum computer [16]. The D-Wave Systems QC has a quantum annealing processor, currently increased to 1,000 qubits.

The AQC unit cell array of coupled superconducting flux qubits is designed to solve instances of the classical optimization problem - given a set of local longitudinal fields, $\{h_i\}$ and an interaction

matrix, $\{j_{ij}\}$ find the assignment, $s^* = s_1^* s_2^* ... s_N^*$ that minimizes the objective function $E(\boldsymbol{s})$, where,

$$E(s) = \sum_{1 \le i \le N} h_i s_i + \sum_{1 \le i < j \le N} j_{ij} s_i s_j, \tag{1.2}$$

with $|h_i| \le 1, |j_{ij}| \le 1,$ and $s_i \in \{+1, -1\}$. Finding the optimal s* is equivalent to finding the ground state of the corresponding classical Ising Hamiltonian,

$$H_p = \sum_{1 \le i \le N}^{N} h_i \sigma_i^z + \sum_{1 \le i < j \le N}^{N} j_{ij} \sigma_i^z \sigma_j^z \tag{1.3}$$

where σ_i^z are Pauli matrices acting on the *i*th spin [16].

Experimentally, the time-dependent quantum Hamiltonian implemen-ted in the superconducting qubit array is given by

$$H(\tau) = A(\tau) H_b + B(\tau) H_b, \quad \tau = t / t_{\text{run}}, \tag{1.4}$$

with, $H_b = -\sum_i \sigma_i^x$ responsible for quantum tunneling among the localized classical states, which correspond to eigenstates of Hp (computational basis). Time-dependent functions, $A(\tau)$ and $B(\tau)$ are such that t_{run} denotes time elapsed between preparation of the initial state and the measurement [16].

1.2.5 *The Kane Nuclear Spin QC*

The Kane QC is based on an array of phosphorus donor atoms embedded in a silicon lattice is considered a hybrid between quantum dot and NMR QC platforms. The Kane QC utilizes the nuclear spins of the donors and the spins of the donor electrons in the computation. Phosphorus donors are placed in an array with a 20 nm spacing. An insulating oxide layer is grown on top of the silicon. As shown in Fig. 1.5 Metal A-gates are deposited on the oxide above each donor, and J-gates between adjacent donors [17].

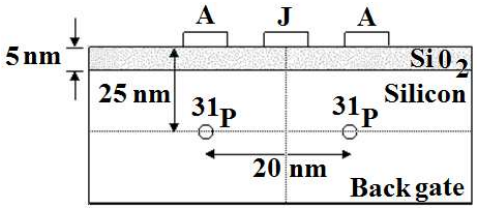

Fig. 1.5. Kane Nuclear Spin QC substrate with ^{31}P+ impurities embedded in ^{28}Si.

The phosphorus, ^{31}P donors and silicon, ^{28}Si substrate are isotopically pure, with nuclear spins of ½ and spin 0 respectively. The nuclear spin of the P donors used to encode qubits has two important advantages;

1) The state has an extremely long decoherence time, on the order of 1018 seconds at mK temperatures.

2) Qubits can be manipulated by applying an oscillating NMR field.

Theoretically, altering the voltage on the A gates, makes it possible to alter the Larmor frequency (precession of angular momentum about the axis of an applied external magnetic field) of

individual donors allowing them to be addressed individually, by bringing specific donors into resonance with the applied oscillating magnetic field [17,18].

Nuclear spins alone will not interact significantly with other nuclear spins 20 nm away. Nuclear spin is useful to perform single-qubit operations, but to make a quantum computer, 2-qubit operations are also required. This is the role of electron spin in this design. Under A-gate control, the spin is transferred from the nucleus to the donor electron. Then, a potential is applied to the J-gate, drawing adjacent donor electrons into a common region, greatly enhancing the interaction between the neighboring spins. By controlling the J-gate voltage, 2-qubit operations are possible [18].

Kane's proposal for readout is to apply an electric field to encourage spin-dependent tunneling of an electron to transform two neutral donors to a D+–D– state, where two electrons orbit the same donor. The charge excess is then detected using a single-electron transistor. This method has two major difficulties. Firstly, the D– state has strong coupling with the environment and hence a short decoherence time. Secondly, it's not clear that the D– state has a sufficiently long lifetime to allow for readout because the electron tunnels into the conduction band. Unlike many quantum computation schemes, the Kane quantum computer is in principle scalable to an arbitrary number of qubits. This is possible because qubits may be individually manipulated by hyperfine electrical means above each impurity [17,18].

1.2.6 *QRAM Models of Quantum Computation*

Quantum Random Access Machine (QRAM) Models of Quantum Computation have a quantum processor controlled by classical instructions. The processor follows the QRAM model, a quantum memory and a quantum ALU (qALU) Arithmetic and Logical Unit using a reversible control unit [19] containing a group of quantum gates, which are controlled by classical signals. The processor's instructions are written using a quantum assembly (QASM) language. As test cases, several well-known quantum circuits are described using the QASM language and executed by the model. The QRAM model hopes to be integrated with classical components forming a hybrid quantum computer [20].

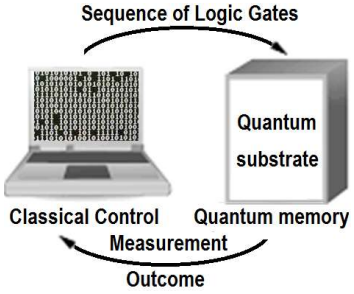

Fig. 1.6. Hybrid QRAM Quantum Computer with classical input.

1.2.7 *Electrons-On-Helium Quantum Computers*

Electrons-On-Helium Quantum Computers (EOH) are attractive because the scalable electron traps have very long relaxation times, and the highest mobility known in a condensed-matter system [21]. The system of electrons on the surface of superfluid ^{4}H is made by submerging a system of individually addressed micro-electrodes beneath the helium surface. The large $\sim$1 μm interelectron simplifies fabrication of an electrode array. The electrode potential, the high barrier that prevents electrons from penetrating into the helium, and the helium image potential together create a single-electron quantum dot above each electrode. The parameters of the dot can be controlled by the electrode potential [22,23].

The Hamiltonian describing $|2\rangle \rightarrow |1\rangle$ transitions induced by excit-ations in helium has the form

$$H_i^{(d)} = \sum_n |2\rangle_n \; {}_n\langle 1| \sum_q \hat{V}_q e^{iqr_n} \tag{1.5}$$

where, $|1\rangle_n$ and $|2\rangle_n$ are the states of the nth electron normal to the surface, and $\hat{V}_q$ is the operator depending on the coordinates of helium vibrations, such as phonons or ripplons. The wavelengths of the vibrations involved in electron scattering are much smaller than the interelectron distance so that each electron has its own thermal bath of helium excitations [22].

As shown in Fig. 1.7, the EOH QC is operated by a constant voltage, V applied to the rings creating a static electric field with voltage valleys that trap electron bubbles along the z-axis. The oscillating voltage, $\tilde{V}$ is applied to opposing rods trapping electrons in the x-y plane.

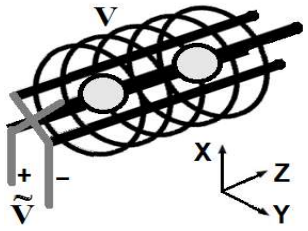

Fig. 1.7. Architecture for electrons on liquid helium QC. The qubit is the electron spin. At each end of the qubit array is a single-electron transistor (SET) detector.

The spin of electrons floating on the surface of liquid ^{4}H makes excellent qubits because these electrons can be electrostatically held and manipulated like electrons in semiconductor heterostructures, and being in a vacuum the spins on ^{4}H are less likely to decohere. The spin-orbit interaction is reduced so that moving the qubits with voltages applied to gates has little effect on coherence times which can be expected to exceed 100 s which is enough time for more than 105 operations at 10 mK [23].

The $|0\rangle$ and $|1\rangle$ qubits are assigned the ground and 1st excited Rydberg states of the electrons above the liquid ^{4}H. An electron can be excited from $|0\rangle$ to $|1\rangle$ with a microwave pulse at frequency, fR with individual qubits tuned by voltages on the underlying electrodes using the linear Stark effect. Quantum gates are operated by tuning neighboring qubits through mutual resonance generating entangled quantum states in XOR, $\sqrt{\ }$ swap or other quantum gates [22,23].

1.2.8 *Fullerene-Based ESR Quantum Computer*

Endohedral buckyball or Fullerene-based ESR quantum computer qubits are based on the electronic spin of atoms or molecules encased in fullerenes. Atoms can be embedded in a permanent nanoscale molecular scaffolding to form an array. Electron paramagnetic resonance (EPR) or electron spin resonance (ESR) spectroscopy is a technique for manipulating materials with unpaired electrons. The basic concepts of EPR/ESR spectroscopy is similar to nuclear magnetic resonance (NMR), but electron spins are excited instead of the spins of atomic nuclei as in NMR spectroscopy.

All electrons have a magnetic moment and spin quantum number, $s = 1/2$, with magnetic components $m_s = +(1/2)$ and $m_s = -(1/2)$. In the presence of an external magnetic field with strength, B_0 the electron's magnetic moment aligns itself either parallel, $m_s = -(1/2)$ or antiparallel $m_s = +(1/2)$ to the field with each alignment having a specific energy due to the Zeeman effect, $E = m_s g_e \mu_B B_0$, where g_e is the electron g-factor, g_e = 2.0023 for the free electron and μ_B is the Bohr magneton [24]. Therefore, the separation between the lower and the upper state is $\Delta E = g_e \mu_B B_0$ for

free unpaired electrons implying that the splitting of the energy levels is directly proportional to the magnetic field strength, as shown in Fig. 1.8.

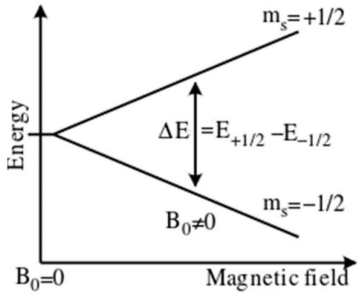

Fig. 1.8. Splitting of the electrons magnetic moment in the presence of an external magnetic field with strength, B_0.

An unpaired electron can move between the two energy levels by either absorbing or emitting a photon of energy, $h\nu$ such that the resonance condition, $h\nu = \Delta E$ is obeyed. This leads to the fundamental equation of EPR spectroscopy: $h\nu = g_e \mu_B B_0$.

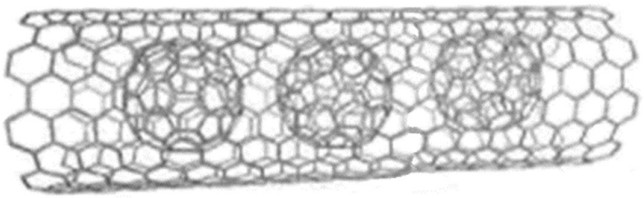

Fig. 1.9. 'Peapod' – Carbon nanotube filled with nitrogen doped buckyball fullerenes.

A nitrogen atom is bonded to the center of the fullerene cage with its electron wavefunction extending the cage boundary with a 2% overlap. 'Peapod' nanotubes contain fullerenes packed in a pseudo-helical phase. These nanotube 'Peapods' could help in the implementation of quantum computing. A pea pod is made up of a tiny carbon nanotube filled with buckyball fullerenes [25].

1.2.9 *Superconductor-Based Quantum Computers*

There are two main types of Superconductor-Based Quantum Computers under study:

a) SQUID-based Superconductor quantum computers with the qubit implemented by the state of small superconducting circuits such as Josephson junctions.
b) Superconductor-based quantum computers with qubits implemented by the internal state of near Absolute Zero, mK trapped ions.

1.2.9.1 SQUID-BASED SUPERCONDUCTOR QC

The SQUID quantum annealing QC is summarized briefly in Sect. 1.2.4, Adiabatic Quantum Computers, as the two models are very similar. Quantum annealing (QA) is a classical randomized algorithm. Meaning, there is no part of QA that necessarily depends on quantum hardware. In classical annealing (CA), temperature is the source of random perturb-ations that allow the algorithm to explore a problem's solution space. In QA, the temperature is replaced by a term analogous to the quantum tunneling field strength, where quantum tunneling would be carried out directly in hardware.

D-Wave processors are designed to harness a fundamental principle operating in both quantum and classical regimes - the propensity for all physical systems to minimize their free energy. Free energy minimization in a classical system is referred to as annealing. Free energy minimization in a quantum system is referred to as quantum annealing. D-Wave has demonstrated that quantum annealing can hasten the energy minimization process. D-Wave processors compute by piggybacking on quantum annealing which can be operated as a UQC. In this regime of operation, the computational model is referred to as adiabatic quantum computation (AQC), which can be thought of as the long-time limit of quantum annealing [26].

1.2.9.2 TRAPPED ION-BASED SUPERCONDUCTOR QC

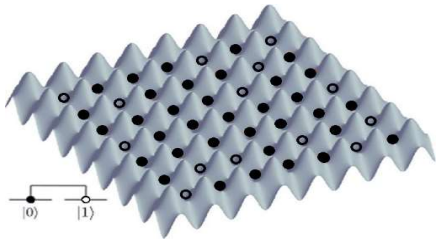

Fig. 1.10. Cold atoms confined in an optical lattice formed by multidimensional optical standing-wave potentials, with solid balls depicted as $|0\rangle$ and clear spheres as $|1\rangle$.

The most successful demonstrations of quantum computing have involved atoms trapped in magnetic fields One method for building a trapped-ion computer connects ions through common motions of a string of ions electrically levitated between two arrays of electrodes. Because the positively charged particles repel one another, any oscillatory motions imparted to one ion by a laser will oscillate the whole string of ions. Lasers can also flip an ions' magnetic orientations encoding the data carried by the string [27].

Scaling these systems is difficult because longer strings containing more than ~20 ions seem impossible to control because the collective modes of common motion would interfere with one another. Now grid-like-traps (Fig. 1.10) allow ions to be moved from a string in the system's memory to another data processing string. Quantum entanglement of the ions allows data to be transferred from one trap zone to another [26-29].

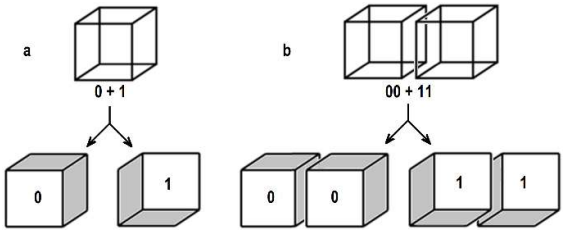

Fig. 1.11. The "ambiguous cube" (a) is like an ion in a superposition state—a measurement of the ion will lock it into one of two definite states (0 or 1). When two ions are in an entangled superposition (b), a measurement will force both ions into the same state (either 0 or 1) even though there is no physical connection between them. Redrawn from [30].

It should be easy to scale trapped ions to large numbers of qubits by merely connecting several types of quantum logic gates made from trapped ions; and if the qubits are encoded with multiple ions, the system should be fault tolerant. In this manner, Wineland suggests "*a useful trapped-ion quantum computer would most likely entail the storage and manipulation of at least thousands of ions, trapped in complex arrays of electrodes on microscopic chips*". Wineland's team created a 4-qubit quantum computer by entangling four ionized beryllium atoms in an em-trap. After linearly confining the ions,

they were laser cooled to a few mK and their spin states synchronized. Finally, a laser was used to entangle the particles, creating a superposition of both spin-up and spin-down states simultaneously for all four ions. Wineland goes on to say:

'Firstly, a UQC requires reliable memory where decoherence will not occur before the data is processed and measured. Trapped ions have been shown to have coherence times over 10 minutes long'.

'Secondly, the ability to manipulate individual qubits is essential. Oscillating magnetic fields applied for a specified duration, can be used to flip a trapped ion qubits magnetic orientation. Currently, the small distances between trapped ions (millionths of a meter), make it difficult to localize the oscillating magnetic fields to an individual ion' [30].

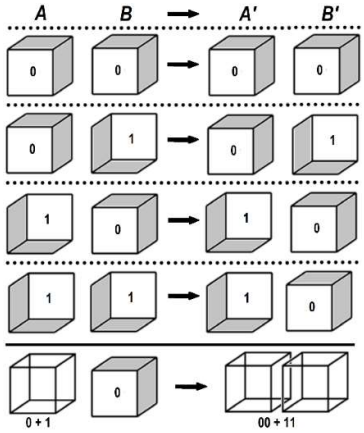

Fig. 1.12. Trapped ion truth table from ambiguous cubes. A trapped-ion computer would rely on logic gates such as the CNOT, which consists of two ions, *A* and *B.* The truth table shows that if *A* (control bit) has a value of 0, the gate leaves *B* unchanged. But if *A* is 1, the gate flips *B,* changing its value from 0 to 1, and vice versa. And if *A* is in a superposition state of 0 and 1, the gate puts the two ions in an entangled superposition state identical to the one in Fig. 1.11. Redrawn from [30].

Trapped atom qubits can also be measured with nearly 100% efficiency through the use of state dependent fluorescence detection. Trapped atomic ions are particularly attractive quantum computer architectures, because the individual charged atoms can be confined in free space to nanometer precision, and nearby ions interact strongly through their mutual Coulomb repulsion. A collection of atomic ions can be confined with appropriate em-fields from nearby electrodes, forming a 3D harmonic confinement potential, as depicted in Fig. 1.10. When the ions are laser cooled to a center of the trap, the balance between the confinement and the Coulomb repulsion forms a stationary atomic crystal. The most typical geometry is a 1D linear atomic crystal, where one dimension is made significantly weaker than the other two. In such a linear trap, the collective motion of the ion chain can be described accurately by quantized normal modes of harmonic oscillation, and these modes can couple the individual ions to form entangled states and a variety of quantum gates [29-31].

1.2.10. *Diamond Based Quantum Computers*

Diamond-based quantum computers are being realized by qubits with an electronic or the nuclear spin of nitrogen-vacancy centers in synthetic diamond crystals. Among solid-state systems, the nitrogen-vacancy (NV) in diamond is found to have an excellent optically addressable memory with satisfactory electron spin coherence times. Recent efforts have demonstrated quantum entanglement and teleportation between two NV-memories, but as true for scaling virtually any proposed QC substrate to larger networks, NV diamond qubits will require more efficient spin-photon interfaces such as optical resonators. Situating nitrogen atoms next to gaps in a diamond's crystal lattice produces 'nitrogen vacancies', which enable optical control of the magnetic orientation (spin) of individual electrons and atomic nuclei.

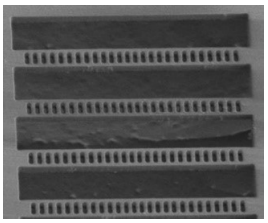

Fig. 1.13. Nitrogen-vacancy (NV) diamond qubit substrate. The NV consists of a substitutional nitrogen atom adjacent to a vacancy in the diamond lattice. The diamond photonic cavities are integrated on a Si substrate with metallic strip lines for coherent spin control. They are optically addressed using a confocal setup with 532 nm CW excitation and photoluminescence collected > 630 nm ladder-like structure etched into diamond. The gaps between the ladder's 'rungs' act like a mirror, temporarily trapping light particles emitted at the ladder's center. Adapted from [32].

Among all crystals, diamond is particularly good for capturing an atom, because the diamond nuclei are essentially free of magnetic dipoles, which can cause noise on the electron spin. Diamond NV spin superpositions have been found to last almost a second. But in order to communicate with each other, NV qubits need to be able to transfer information via photons, requiring the vacancy to be positioned inside an optical resonator. As shown in Fig. 1.13 a Diamond NV device consists of a ladder-like diamond structure with a NV at its center suspended horizontally above a silicon substrate.

Shining light perpendicularly onto the ladder kicks an NV electron into a higher energy state. When it drops back to ground, it releases the excess energy as a photon. The gaps in the diamond structure - spaces between rungs in the ladder, act as a photonic crystal, confining the photon so that it bounces back and forth across the vacancy thousands of times. When the photon finally emerges, it has a high likelihood of traveling along the axis of the ladder, so that it can be guided into an optical fiber [32].

1.2.11. *Quantum Dot Quantum Computer*

A quantum dot (QD) is a type of nanoscale atomic/molecular structure or nanocrystal made of silicon and semiconductor materials of which there are at least 200 kinds. Generally, a QD is any nanocrystalline material which tightly confines its excitons in all three spatial directions. A QD can be designed as a single qubit. There are numerous methods for utilizing quantum dots in quantum information processing; and QD technology is among the more promising candidates being studied for use in solid-state quantum computation.

In semiconductors, thermal energy is sufficient to cause a small number of electrons to escape from the valence bonds between the atoms (valence band); allowing them to orbit in the higher energy conduction band instead where they are relatively free. Gaps in the valence band are called holes. The hole within an exciton is called the Bohr radius of the exciton; and Excitons are coupled electron-hole pairs via a Coulomb force.

A significant factor for using QDs for quantum information processing is that QDs can have a radius close to or smaller than the Bohr radius value, which in a typical semiconductor is a few nanometers. This is the scenario where a particle reveals its specific quantum mechanical properties:

> "In bulk semiconductors, the exciton can move freely in all directions. When the length of a semiconductor is reduced to the same order as the exciton radius, i.e., to a few nanometers, quantum confinement effect occurs and the exciton properties are modified. Depending on the dimension of the confinement, three kinds of confined structures are defined: quantum well (sometimes termed QW), quantum wire (QWR) and quantum dot (QD). In a QW, the material size is reduced only in one direction and the exciton can move freely in other two directions. In a QWR, the material size is reduced in two directions and the exciton can move freely in one direction only. In a QD, the material size is reduced in all directions and the exciton cannot move freely in any direction" [33].

By applying small voltages to the leads, the flow of electrons through the quantum dot can be controlled and thereby precise measurements of the spin and other properties therein can be made. With several entangled quantum dots, or qubits, plus a way of performing operations, quantum calculations and the quantum computers that would perform them might be possible.

The two main types of QD quantum computing being studied are:

- Spin-based Quantum dot computer, such as the Loss-Di Vincenzo quantum computer where the qubit occurs as the spin states of trapped electrons [34-36].

- Spatial-based Quantum dot computer, where the qubit occurs from the position of electrons in double quantum dot. QC researchers have been focusing on QDs formed in GaAs heterostructures, nanowire-based QDs, and self-assembled QDs [37].

In Fig. 1.14 a gallium arsenide semiconductor is coated with plastic and the nanoscale lines are cut into the plastic with a beam of electrons. Then the lines were filled with metal and the plastic dissolved, leaving lines ~ 50 nanometers wide (5-10 atoms). The quantum dots (center of the image) are pools of ~ 20-40 electrons. Each dot is ~180 nanometers in diameter. The modulated Swap operation is achieved by applying a pulsed gate voltage between the dots, making the exchange constant in the Hamiltonian time-dependent:

$$H_S(t) = J(t)\vec{S}_L \cdot \vec{S}_R. \tag{1.6}$$

which is valid only if the level spacing in the quantum-dot is much greater than kT, the pulse time scale, τ_S is greater than $\hbar/\Delta E,$ so there is no time for transitions to higher orbital levels to happen and also the decoherence time Γ^{-1} is longer than τ_S [37].

According to Jeong and his team, the QD are defined by ten independently tunable QD gates on a GaAs/AlGaAs heterostructure containing a 2D electron gas (2 ^{o}K) located 80 nm below the surface. The low temperature sheet electron density and mobility are n = 3.8 × 1011cm^{-2} with μ = 9 × 105 cm$^{2/Vs}$, respectively. The lithographic dot size is 180 nm in diameter and each dot contains about 40 electrons. To reduce unnecessary degrees of freedom in controlling the double dot, gates sitting on the opposite side are connected together, giving a total of five pairs of controllable gates. Gate pair V1 and V5 are used to set tunneling barriers, while the V3 sets the inter-dot tunnel coupling. V2 and V4 control the number of electrons and energy levels in each dot separately [37].

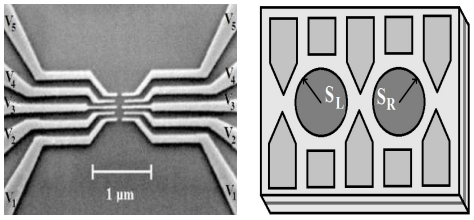

Fig. 1.14. a) Depicting a double quantum dot. Each S_L or S_R electron spin defines one 2-level system (qubit) in the 'Loss-Di Vincenzo Model'. The narrow gate between the two dots modulates the spin coupling, allowing swap operations. b) Physical realization of the quantum dots utilizing electron beam lithography. Figs. Redrawn from [37].

1.2.12. *Transistor-Based Quantum Computer*

A Transistor-based quantum computer is a string quantum computer with an entrainment of positive holes using an electrostatic trap. A microwave field is used to gain control over an electron bound to a single phosphorous atom implanted next to a specially-designed silicon transistor, a device made in a manner similar to making common silicon computer chips.

From team member Morello: "*This is the quantum equivalent of typing a number on your keyboard. This has never been done before in silicon, a material that offers the advantage of being well understood scientifically and more easily adopted by industry. Our technology is fundamentally the same as is already being used in countless everyday electronic devices, and that's a trillion-dollar industry*."

Veldhorst's team presents a 2-qubit logic gate, which uses a single spin in isotopically enriched silicon and is realized by performing single- and 2-qubit operations in a QD system using the exchange interaction, as envisaged in the Loss-Di Vincenzo proposal discussed briefly in 1.2.11, the Quantum Dot Quantum Computer [34,35]. He realizes CNOT gates by controlled-phase operations combined with single-qubit operations. Direct gate-voltage control provides single-qubit addressability, together with a switchable exchange interaction that is used in the 2-qubit controlled-phase gate. By independently reading out both qubits, the transistor-based QC can measure anti-correlations in the 2-spin probabilities of the CNOT gate [38].

1.2.13. *Molecular Magnet Quantum Computer*

A Molecular Magnet Quantum Computer (MMQC) is an additional form of the Loss-Di Vincenzo proposal [34-35]. The potential of molecular magnets as the building blocks of a UQC is the attractive simplification in the control procedure for the quantum gates provided by many-spin systems coming from the high symmetry shown to lead to a relatively simple way to address spin degrees of freedom in molecular magnets. The advantage of an anisotropic effective spin interaction in QC memory applications is demonstrated by using Grover's quantum search algorithm in a generic easy-axis molecular magnet. Electric control of spin-spin coupling has been shown to enable 2-qubit quantum gates in polyoxometalates [39,40].

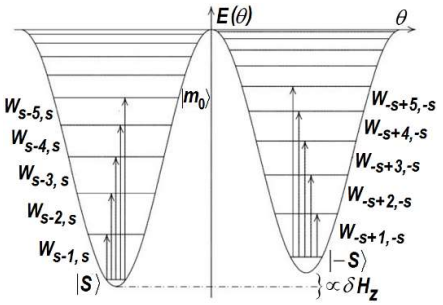

Fig. 1.15. High symmetry properties of single-molecule magnets for QC. Shows the double well potential of the spin due to magnetic anisotropies in ^{12}Mn with the initial state, $|\psi_0\rangle = |s\rangle$. Arrows depict transitions between spin eigenstates driven by the external magnetic field *H*. Figure adapted from [40].

It is of interest to briefly summarize the Leuenberger & Loss [40] proposal for what they call 'a feasible implementation of Grover's factoring algorithm' utilizing ^{8}Fe and ^{12}Mn as molecular magnets. The initial state, $|\psi_0\rangle = |s\rangle$ is prepared by applying a strong field in the *z* direction. Then field brought near zero (to bias δH_z) so that all $|m\rangle -$states become localized.

Once a state is marked and amplified (decoded) readout is performed by standard pulsed ESR spectroscopy. Then the magnet is irradiated with a single pulse of duration, *T* with frequencies, $\omega_{m-1,m}$, with $m = s-2,...,m_0,$ inducing transitions of 1st order amplitudes, $S^{(1)}_{m-1,m}$. To illustrate, Leuenberger & Loss assume state, $|7\rangle$ is populated, from which stimulated emission can be observed in the transition from $|7\rangle$ to $|8\rangle$ at frequency, $\omega = \varpi_{6,7}$ uniquely identifying the marked level. They go on to say generally that, if states, $|m_1\rangle, |m_2\rangle, ..., |m_k\rangle,$ where $1 \le k \le n,$ are marked, the following absorption/emission intensity is measured:

$$I^{m_0}_{s-2} = \sum_{i=1}^{k} \left(\left| S^{(1)}_{m_i-1,m_i} \right|^2 + \left| S^{(1)}_{m_i+1,m_i} \right|^2 \right). \qquad (1.7)$$

The spectrum identifies all marked states clearly. In this manner implementing the entire Grover algorithm (input, decoding, read-out) is achieved by three pulses of duration, T with $\tau_d > T > \omega_0^{-1} > \omega_m^{-1}, \omega_{m,m\pm1}^{-1}$, giving a clock speed of ~10 GHz for Mn_{12} such that the complete process takes only 10^{-10} s [40].

1.2.14. *Bose–Einstein Condensate-Based Quantum Computer*

In 1924 Einstein pointed out that unlimited bosons could condense into a single ground state [41,42]. Recently QC based on Bose–Einstein condensation (BEC), the state of matter composed of a dilute gas of bosons cooled close to absolute zero, has been proposed.

Recent progress in solid-state quantum computing using super-conducting qubits on Cooper pairs of charged electrons met limitations due to decoherence effects caused by the strong Coulomb interaction of the superconducting qubit with the environment. To solve the problem, Andrianov and Moiseev have proposed a solution by trying another BEC setup utilizing uncharged long-lived magnons, where the magnon BEC qubit can be realized due to a magnon blockade isolating pairs of the magnon condensate energy levels in mesoscopic and nanoscopic ferromagnetic dielectric samples [43].

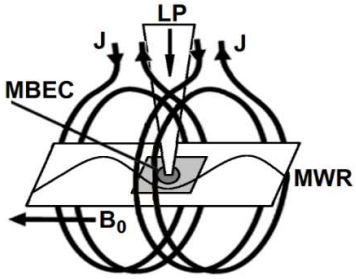

Fig. 1.16. Layout of the single qubit gate, Magnon Bose-Einstein Condensate (MBEC), laser pumping (LP), microwave resonator (MWR), current in the magnetic coil, J and the magnetic field, B_0. The MBEC is excited by laser pulse. Qubit rotation is achieved by the interaction with a standing microwave field in a high-quality resonator. Redrawn from [43].

Andrianov and Moiseev want to demonstrate single-qubit gates by operating quantum transitions between these states in the external microwave field. They are also studying implementation of the 2-qubit gate by using the interaction between the MBEC qubits due to exchange of virtual photons in a microwave cavity. They hope to achieve conditions for long-lived MBEC qubits, a scalable architecture, and utility of the promising advantages of the multi-qubit QC the MBEC qubit offers [43].

Hecht presents a different scheme for BEC quantum computation utilizing atomic many-body states. The system she has in mind consists of a 2-species interacting BEC, which, under the right conditions, behaves like a robust 2-level system protected by an energy gap from higher excited levels. The two states can be used to encode a qubit. Hecht claims to show how to create a universal set of quantum gates by inducing energy shifts on the atomic levels, by changing the Raman coupling between atomic states and allowing tunneling between pairs of the BEC condensates. The scheme is limited by particle losses as a key source of decoherence, but Hecht suggests that for small numbers of particles and weak Feshbach resonance, maximally entangled states between two qubits can be produced [43,44].

1.2.15. *Rare-Earth-Metal-Ion-Doped Inorganic Crystal QC*

Rare-earth-metal-ion-doped inorganic crystal based quantum computers are being developed to use the internal electronic state of dopants put in optical fibers. The aim of initial experiments towards constructing simple quantum gates in such solid-state materials using these specially tailored crystals, is to select a subset of randomly distributed ions in the ion-doped material, ones which have the interaction necessary to control each other and can therefore be used for quantum logic operations.

Experimental results demonstrate that part of an inhomogeneously broadened absorption line can be selected as a qubit and that a subset of ions in the material can control the resonance frequency of other ions. This is the key to opening the way for the construction of quantum gates in rare-earth-ion doped crystals.

Rare-earth-ion doped crystals have several attractive features for implementing quantum gates. Because of the existence of a partially filled inner shell (4f) that is shielded from the environment by outer electrons, they have optical transitions with very narrow line-widths. For Eu doped into Y_2SiO_5 for example, some transitions have homogeneous line-widths of less than 1 kHz. The narrow line-width makes it possible to coherently manipulate the ions with long sequences of laser pulses. Most rare-earths have a hyperfine splitting of the ground state, due to nuclear quadrupole interactions. Any nucleus with more than one unpaired nuclear particle (protons or neutrons) will have a charge distribution which results in an electric quadrupole moment. NMR of the anisotropy of the magnetic hyperfine and nuclear quadrupole interactions in rare-earth orthochromites in the vicinity of the order-order type magnetic phase transition, with GdCrO, as the rare-earth example, show that the nuclear quadrupole interactions, along with the magnetic anisotropies of the hyperfine interactions, contribute to the splitting of the NMR lines of ^{53}Cr in the transition region [45].

The relaxation between different hyperfine levels is very slow and lifetimes are as long as hours or days. Measurements of the dephasing time between the hyperfine levels are lacking for many materials, but it is at least of the order of milliseconds for some combinations of dopants and hosts. When doped into inorganic host crystals, the differently located ions experience shifts of their optical absorption frequencies because of imperfections in the crystal host lattice. Because of the differences between different positions in the lattice, the shifts will be different for different ions, creating an inhomogeneous broadening of the optical transition. The broadening can be several GHz, making it possible to address more than 106 different spectrally distinct channels. [46]

Another rare-earth-ion doped crystal QC research team headed by Walther is studying a high-fidelity readout scheme for a 'single instance' approach to quantum computing in rare-earth-ion-doped crystals. The scheme is based on using a different species of qubit and readout ions; Walther shows that by allowing the closest qubit ion to act as a readout buffer, readout error can be reduced by more than an order of magnitude. The scheme is shown to be robust against certain experimental variations, such as varying detection efficiencies. Walther's team has found a way to use the scheme to predict the expected quantum fidelity of a CNOT gate in a variety of solid state systems that he predicts are scalable.

By monitoring the cavity-enhanced fluorescence from one rare-earth ion using another long-lived rare-earth ion species as a buffer stage that can be repeatedly cycled, several buffer stages can be concatenated to yield a very long effective detection times reaching $\varepsilon = 10^{-3}$ for a wide variety of collection efficiencies and background levels. The team then used this result, together with known error sources, to obtain expected fidelities for a CNOT gate of 99 % and for larger GHz states remaining above 92 % for up to 10 qubits. One of the present limitations of his assumptions is that the expected increase in performance for qubit rotations when switching from Pr to Eu has not been fully experimentally verified as of yet [47,48].

1.2.16. *Linear Optical Quantum Computer (LOQC)*

Linear optical quantum computer (LOQC) development attempts to realize qubits by processing different modes of light as quantum states (photonic qubits) through linear elements like mirrors, beam splitters and phase shifters, which is a form of the quantum circuit model as in 1.2.2 [8]. Optical quantum technologies are highly sought for quantum information processing (QIP) because they link QC with quantum communications in the same framework.

Up to N x N unitary matrix $U(N)$ operations can be realized using just mirrors, beam splitters and phase shifters which preserve the quantum state of light; but the intrinsic challenge as well-known, is that photons only interact minimally. Initially this problem was partly solved by adding nonlinearity via the Kerr effect to LOQC; this allowed operations such as the single-photon CNOT gate. This was

followed by discovery of the KLM protocol by Knill, Laflamme and Milburn that uses linear optical elements to promote nonlinear operations [49].

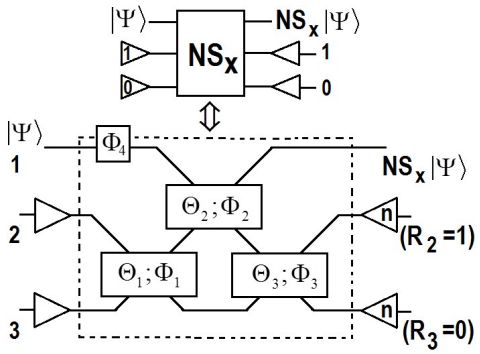

Fig. 1.17. Linear optics implementation of Nondeterministic Sign-Flip gate (NS-gate). The elements framed in the box (dashed border) is the linear optics implementation with three beam splitters and one phase shifter. Modes 2 and 3 are ancilla modes. Adapted from [49].

Photon states for a 2-qubit representation could be written as $|01\rangle_{\alpha\beta} \equiv |0\rangle_{\alpha}|1\rangle_{\beta}$ for two orthogonal photon polarization modes prepared by optical parametric down-conversion which emits EPR correlated photons. Linear optics in LOQC is supported by a complete set of *SU*(2) operators. If a unitary matrix is correlated with an optical beam splitter, $\mathrm{B}_{\theta,\phi}$, the 2 x 2 matrix is

$$U\left(\mathrm{B}_{\theta,\phi}\right)=\begin{bmatrix}\cos\theta & -e^{-i\phi}\sin\theta\\ e^{-i\phi}\sin\theta & \cos\theta\end{bmatrix}; \tag{1.8}$$

the reflection and transmission amplitudes determine θ and ϕ [49-51].

A nonlinear sign-flip gate implements the transform:

$$\mathrm{NS}:\alpha_0|0\rangle+\alpha_1|1\rangle+\alpha_2|2\rangle\rightarrow\alpha_0|0\rangle+\alpha_1|1\rangle-\alpha_2|2\rangle, \tag{1.9}$$

which is the basis, along with ancilla, for implementing the CNOT-gate [52]. The nonlinear sign gate can be implemented non-deterministically by three beam splitters, two photo-detectors, and one ancilla photon. The implementation of conditional sign flip gate is then made by the combination of the nonlinear sign gate and the physics of Hong-Ou-Mandel (HOM) interferometer. For an arbitrary two qubits [53]

$$\begin{aligned}|Q_1\rangle&=\alpha_0|0\rangle_L+\alpha_1|1\rangle_L=\alpha_0|0\rangle_1|1\rangle_2+\alpha_1|1\rangle_1|0\rangle_2,\\ |Q_2\rangle&=\alpha_0'|0\rangle_L+\alpha_1'|1\rangle_L=\alpha_0'|0\rangle_3|0\rangle_4+\alpha_1'|1\rangle_3|0\rangle_4\end{aligned}. \tag{1.10}$$

The NS-gate in Fig. 1.17 gives a nonlinear phase shift on one mode conditioned on two ancilla modes. The output is accepted only if there is one photon in mode 2 and zero photons in mode 3 detected, where the ancilla modes 2 and 3 are prepared as the $|10\rangle_{2,3}$ state [49, 53-55].

1.2.17. *Optical Lattice Based Quantum Computing (OLQC)*

In an Optical Lattice Based Quantum Computer (OLQC) qubits are implemented by internal states of neutral atoms such as, ^{6}Li and ^{133}Cs trapped in an optical lattice as shown in Fig. 1.18.

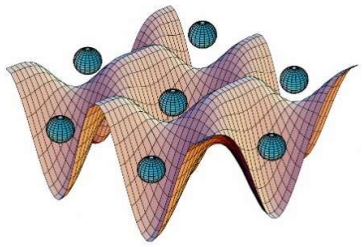

Fig. 1.18. Optical lattice of qubits trapped potential minima by the Stark shift.

Optical lattices are often formed by counterpropagating laser beams, interfering to form spatially periodic polarization patterns. The resulting periodic potential traps neutral atoms by the Stark shift (shifting and splitting of spectral lines of atoms and molecules due to presence of an external electric field). The neutral atoms are cooled and congregate in locations of potential minima where the trapped atoms resemble a crystal lattice [56-58].

One novel scheme uses Li-Cs molecular states to entangle ultracold ^{6}Li and ^{133}Cs atoms held in independent optical lattices. The ^{6}Li atoms act as the qubits, and the ^{133}Cs atoms serve as messenger qubits aiding in q-gate operations to mediate entanglement between distant qubit atoms. The separated species can be overlapped by translating the lattices. When the ^{133}Cs messenger and ^{6}Li qubit atoms are overlapped, targeted single spin operations and entangling operations would be performed by coupling the atomic states to a molecular state with rf-pulses. By controlling frequency and duration of the rf-pulses, entanglement can either be created or swapped between a qubit messenger pair [59].

1.2.18. *Cavity Quantum Electrodynamics Quantum Computing*

In Cavity Quantum Electrodynamics Quantum Computing (CQEDQC) a qubit is based on the internal state of trapped atoms coupled to high-finesse cavities. Following Burell, an essential component of CQEDQC is the Fabry-Perot partially silvered mirror cavity, which partially reflects and transmits incident light E_a and E_b, which has the effect of producing output fields $E_{a'}$ and $E_{b'}$, which are related by the unitary transformation:

$$\begin{bmatrix} E_{a'} \\ E_{b'} \end{bmatrix} = \begin{bmatrix} \sqrt{R} & \sqrt{1-R} \\ \sqrt{1-R} & -\sqrt{R} \end{bmatrix} \begin{bmatrix} E_a \\ E_b \end{bmatrix} \tag{1.11}$$

where R is the reflectivity of the mirror. A Fabry-Perot (FP) cavity is made from two plane parallel mirrors of reactivities R_1 and R_2, incident upon which is light from outside the cavity E_{int}. Inside the cavity, light bounces back and forth between the two mirrors acquiring a phase shift $e^{i\phi}$ on each trip. The internal cavity field is

$$E_{\text{cav}} = \sum_k E_k = \frac{\sqrt{1-R}E_{\text{in}}}{1+e^{i\phi}\sqrt{R_1 R_2}} \tag{1.12}$$

One of the most important things about the Fabry Perot cavity for purposes of CQEDQC is the power in the internal cavity field mode as a function of the power and frequency of the input field,

$$\frac{P_{\text{cav}}}{P_{\text{in}}} = \left|\frac{E_{\text{cav}}}{E_{\text{in}}}\right|^2 = \frac{1-R_1}{\left|1+e^{i\phi}\sqrt{R_1 R_2}\right|^2} \tag{1.13}$$

Frequency selectivity arises because of constructive and destructive interference between the cavity mode and the reflected light front. Another indispensable feature is that on resonance, the cavity field achieves a maximum which is approximately $(1 - R)^{-1}$ times the incident field [60].

An optical CQEDQC could be almost entirely comprised of optical interferometers. The quantum information would be encoded in both the photon number states and the photon phase. The Interferometers would perform the switching function between the two representations. Stability is a major issue, because the relatively short scale of the de Broglie wavelengths of the qubits would make stable interferometers a challenge to construct [60].

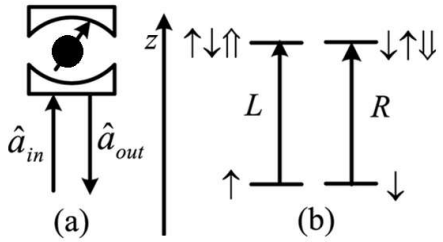

Fig. 1.19. Schematic CQED dipole spin-dependent transitions with circularly polarized photons for utility in CQEDQC modeling. a) A charged quantum dot inside a 1-side micropillar-microcavity interacting with circularly polarized photons, where $\hat{a}_{\text{in}}$ and $\hat{a}_{\text{out}}$ are the input and output field operators of the waveguide, respectively. (b) Optical selection rules by the Pauli exclusion principle. *L* and *R* denote left and right circular polarization respectively, ↑ and ↓ represent spins of excess electrons and ↑↓⇑ and ↓↑⇓ negatively charged excitons. Figure redrawn from [61].

1.2.19. *Nuclear Magnetic Resonance (NMR) Quantum Computing*

Nuclear Magnetic Resonance Quantum Computing (NMRQC) is among the 1st and most mature technologies for implementing quantum computation. It utilizes the motion of spins of nuclei in a variety of molecules such as the hydrogen and the carbon nuclei of chloroform, manipulated by rf-pulses. The spin-lattice (T_1) and spin-spin (T_2) relaxation processes in NMR are key factors in the ability to implement NMRQC quantum algorithms. NMRQC has taken two forms:

- Liquid-state NMRQC on molecules in solution with the qubit provided by nuclear spins within the dissolved molecule [62].
- Solid-state NMR Kane quantum computers with qubits realized by the nuclear spin state of phosphorus donors in silicon [17].

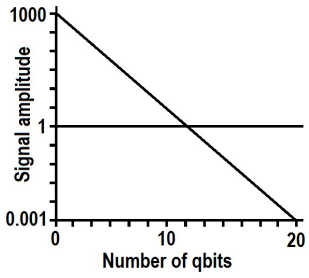

Fig. 1.20. Signal amplitude loss in NMRCC due to preparation of pure states as a function of the size of the quantum register, causing NMR QC to be difficult beyond a few qubits.

1.2.19.1 LIQUID-STATE NMRQC

NMR differs from other implementations of QC in that it uses an ensemble of systems, in this case molecules. The ensemble is initialized to be the thermal equilibrium state as given by the density matrix:

$$\rho = \frac{e^{-\beta H}}{\mathrm{Tr}\left(e^{-\beta H}\right)}, \tag{1.14}$$

where H is the Hamiltonian matrix for a single molecule with $\beta = 1/kT$, k Boltzman's constant and T the temperature. Ensemble operations are performed through rf-pulses applied orthogonally to a strong, static field, created by a large NMR magnet [62].

It is very difficult to prepare NMRQC systems in pure spin states because of the tiny energy gap between nuclear spin states. This seriously challenges the scalability of NMRQC because the procedure for preparing the required pseudo-pure states averages all the populations but one. As long as the spin system can be described by the high temperature approximation, the population of an individual spin state is inversely proportional to the number of states. But this scenario decreases as 2^{-N} with an increase in the number of spins, N. The detectable signal size therefore limits the possible number of spins to be used in NMR quantum information processors. The reduction of sensitivity associated with the preparation of pseudo-pure states can be avoided by using algorithms that do not require pure states to work with [63].

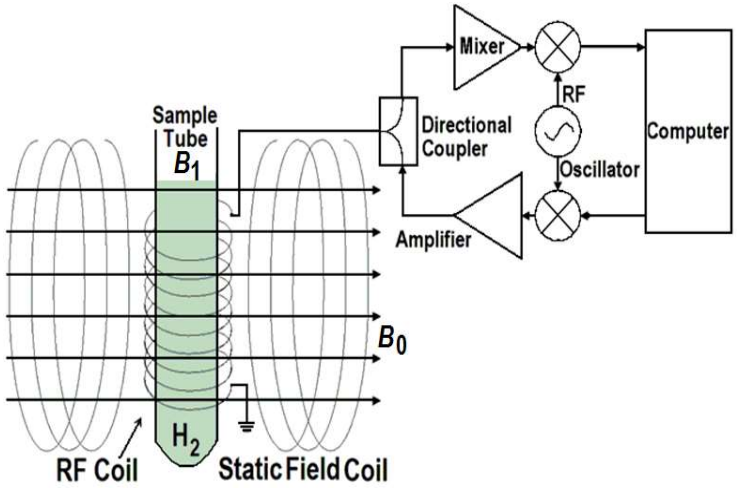

Fig. 1.21. Experimental set up for Liquid-state NMRQC on molecules in solution with the qubit provided by nuclear spins within the dissolved molecule. For a time, NMRQC was very appealing leading model for QC research, but as shown in Fig. 1.20 severe tactical problems have removed it from the limelight until these problems are solved.

It has also been shown that liquid state ensemble NMRQC do not possess quantum entanglement as required for quantum information processing; thus it appears that NMRQC are only classical simulations of a QC. Quantum ensembles represent possible states of a mechanical system of particles that are maintained thermodynamically with a reservoir. The system is open in the sense that it can exchange energy and particles with a reservoir, so that various possible states of the system can differ in both their total energy and total number of particles. The system's volume, shape, and other external coordinates are kept the same in all possible states of the system [64].

1.2.19.2 SOLID-STATE NMRQC

For solid-state NMRQC see Sect. 1.2.5, the brief review of Kane Nuclear Spin QC where:

1) The state has an extremely long decoherence time, on the order of 10^{18} seconds at mK temperatures.

2) Qubits can be manipulated by applying an oscillating NMR field [17].

1.2.20. *Topological Quantum Computing (TQC)*

Topological Quantum Computing (TQC) is based on the braiding of anyons in a 2D lattice at cryogenic temperatures near absolute zero. TQC is among the most promising considerations for Bulk UQC; and the scenario that Microsoft has placed it's bet on [65]. Anyons are 2D quasiparticles that are neither Bosons or Fermions operating with the Fractional quantum Hall effect. Common substrates are doped GaAs, Pb or Si, InSb and InAs semiconducting nanowires some of which support Majorana Zero Modes (MZM). Non-Abelian anyons are the key requirement for the anyonic model of TQC, but their existence has not yet been experimentally confirmed. But recent experimental work following theoretical predictions, has shown signatures consistent with the existence of Majorana modes localized at the ends of semiconductor nanowires in the presence of a superconducting proximity effect [66].

The topological braiding of these anyonic non-Abelian fractional quantum Hall effect quasiparticle Majorana fermions provides a high degree of error protection from decoherence by interaction with the environment (the braid state has remained experimentally inaccessible). The actual TQC is done by the edge states of a fractional quantum Hall effect. When anyons are braided the quantum information which is stored in the state of the system is impervious to small errors in the trajectories. Braiding acts as a matrix on a degenerate space of states. The relevant quasiparticle in the Moore-Read state is a 'Majorana fermion' which is its own antiparticle, 'half' of a normal fermion. The effect of the exchange on the ground state need not square to 1. 'Anyon' statistics: the effect of an exchange is neither +1 (bosons) or -1 (fermions), but a phase [67].

Freedman, Kitaev, Larsen, & Wang (FKLW) found that a conventional QC device, with an error-free operation of its logic circuits, gives a solution with an absolute level of accuracy, whereas a FKLW device with flawless operation will give the solution with only finite accuracy; but any level of precision for a readout can be obtained by adding more anyon braid twists (logic circuits) to the TQC, in a simple linear relationship. In other words, a reasonable increase in elements (braid twists) can achieve a high degree of accuracy in the answer [68]. Note that this solution can be considered the same as applying the Quantum Zeno Effect (QZE) to Interaction Free Measurement (IFM), discussed in detail in Ch. 7.

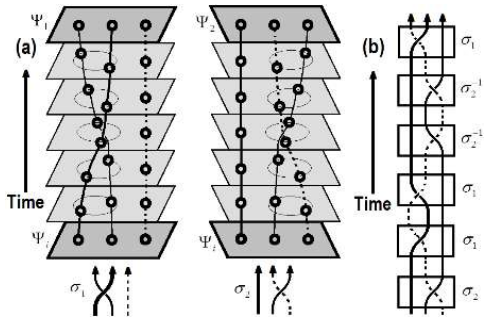

Fig. 1.22. Topological quantum computing schema of quasiparticle exchange. (a) Basic operations, σ_1 and σ_2 on a system of three quasiparticles. Top: Temporal evolution of the system from the initial state ψ_i to the final state $\psi_{1(2)} = \sigma_{1(2)}\psi_i$. Bottom: diagrammatic representations of the quasiparticle exchange operations. (b) Example of logic gate operations for the basic operations σ_1 and σ_2 shown in (a) and their inverses σ_1^{-1} and σ_2^{-1}. Redrawn from [67].

Even though quantum braids are inherently more stable than trapped quantum particles, there is still a need to control for error inducing thermal fluctuations, which produce random stray pairs of anyons which interfere with adjoining braids. Controlling these errors is simply a matter of separating the anyons to a distance where the rate of interfering strays drops to near zero [67].

TQC provides a possible new architecture for QC with a low error rate by exploiting anyon braiding in the topology of quasiparticles. Anyons have different statistics than Bosons (Bose-Einstein spin 1 statistics) and Fermions (Fermi-Dirac spin 1/2 statistics). Semiconductor devices are expected to host

these exotic quasiparticle states, predicting that TQC will have properties sufficient for error-free quantum computation. A more detailed analysis of TQC is given in Chaps. 9 and 10. TQC is considered a 'toy model' for the introduction of the Unified Field Mechanical (UFM) Ontological-Phase Topological Field Theoretic QC presented as the main purpose of this volume. See Chap. 12.

1.2.21. *Unified Field Mechanical Quantum Computing*

Unified Field Mechanical Quantum Computing (UFMQC) is probably the newest QC model; although under theoretical development for over a decade, understanding its formulation only began to gel while writing this volume. Its Group Theory is not fully known yet; and its basis has been given the provisional name: Ontological-Phase Topological Field Theory or in terms of quantum information processing: Ontological-Phase Topological Quantum Computing (OPTQC), which we will do our best to make a case for in Chaps. 12, 13 and 15.

What this currently highly speculative model has to offer is pointed out acutely in the subtitle of this volume 'Surmounting Uncertainty – Supervening Decoherence'. Those UFM scenarios, if correct totally remove conditions plaguing virtually all the other QC models outlined in this chapter. Its most redeeming factor is that it is experimentally testable; and preparations are underway to do such [69,70].

1.3 Concept

Computation whether classical or quantum is Boolean, utilizing a symbolic system of algebraic notation for binary variables that are used to represent logical propositions or logical operators having two possible values denoted as 'true' and 'false', 1 and 0 or $|\uparrow\rangle$ or $|\downarrow\rangle$ [71]. Information is physical and cannot exist without a physical representation. The question is how to move from current more symbolic representations to methods of representing algorithms in a manner connoting physical reality to the extent now required by UFM? The supposition is that a purely mathematical space such as the multidimensional Hilbert space currently in use can no longer be considered adequate for implementing universal quantum information processing (QIP). It is a fairly recent idea to worry about the fact that information is physical in this respect [72-74], and that while mere binary representations have been adequate for Turing machines for the last 70 years, and even all the QIP done to date at the semi-classical limit; the scenario is not sufficient for QC at a UQC level, especially as we pass beyond the historical basis of Unitarity and Locality to the requirements for relativistic QIP effects and further to incorporate the necessary phenomena imposed by UFM and the associated OPTFT.

Moore's Law has approached unity as we speak; and as everyone knows computing at the quantum level is plagued by a lack of control of quantum degrees of freedom by interaction with the environment and vacuum fluctuations. The wavefunction, $|\psi\rangle = \alpha|0\rangle + \beta|1\rangle$ complicates the concept of reality for Euclidean observers. In order to determine the state of a physical object we have to interact with it; don't we?

Two quantum systems as represented by the wavefunction above are entangled by a standard unitary operation, $U_{ent}|\psi\rangle|0\rangle = \alpha|0\rangle|0\rangle + \beta|1\rangle|1\rangle$, $|\psi\rangle$ can be unknown and $|0\rangle$ a known state, that can be extended to an *N*-qubit product state which can be operated on simultaneously by *U*:

$$U_{\text{ent}} \underbrace{|0\rangle|0\rangle|0\rangle|0\rangle...|0\rangle|0\rangle}_{N \text{ times}} \sim |00000...00\rangle + |00000...01\rangle + |00000...10\rangle + \\ +... + |1111...00\rangle + |1111...01\rangle + |1111...10\rangle + |1111...11\rangle \left(2^N \text{ terms}\right). \tag{1.15}$$

We have been at this point for a long time for all QC systems under study; all plagued by decoherence with severity increasing with the number of qubits. Error correcting techniques have been proposed for arbitrary size qubit registers [75-77].

Any quantum system such as electron spin whose state space can be described by a 2D complex vector space can be used to implement a qubit. By current thinking, 'The QC must operate in a Hilbert space whose dimensions may be grown exponentially as an infinite-dimensional analog of Euclidean space such that an abstract vector space possessing the structure of an inner product allows length and angle to be measured'. This scenario has been good in principle until now, and probably retains utility in some QC mathematical and algorithm preparation processes; but since the Bloch 2-sphere representation is not physical, it can no longer be considered a sufficient description for practical implementations of UQC.

1.4. Conundrum - *Hypotheses non Fingo*

Newton claimed he did not make use of fictions, "*Whereas the main business of natural Philosophy is to argue from Phaenomena without feigning Hypotheses*" [78]. I have no idea what the most myopic hypothesis in the in the history of science is; I do know that theory drives experiment and experiment drives theory and that finally the much-criticized string/M-Theory has finally become testable after several decades of criticism. I say this because a very radical model of UQC is presented in this volume. It has been tinkered with for 20 years and finally is sufficiently testable to promote. One corner of the QC community has finally caught up with the premise of relativistic qubits in the last couple years. The TQC anyon quasiparticle Hall effect model seems to be a 2D toy model of our model. As far as the penultimate requirement of UFM; we seem first to use the term.

Few physicists consider Large-Scale Additional Dimensionality (LSXD), but sufficiently so, that experiments at CERN are being developed to search for them. Our UFM protocol to find them is table top and low energy, which if successful will put an end to the need for supercolliders. We are formulating an Ontological-Phase Topological Field Theory (OPTFT) to address the putative parameters. Our view of a UFM fortunately makes easy correspondence to HD extensions of the Wheeler-Feynman-Absorber Cramer-Transactional De Broglie-Bohm-Vigier causal interpretations of quantum theory as well as dual 3-tori Calabi-Yau brane mirror symmetry (thus OPTFT). Even though I'm riding a wild stallion, it is a very radical paradigm shift that blows even the author's mind. The most difficult part for colleagues to embrace/comprehend is the 'continuous-state' evolution of the HD brane topology; along with the fact that 'the Earth is not the center of the Universe', flagrantly meaning that we, as physical observers, must give up observation from the perspective of Euclidean 3-space as the primary vantage. It's always like this in a paradigm shift; get over it, leap-frog over and beyond me and enter the 'brave new world'. The late Karl H. Pribram, noted Stanford neuroscientist (holographic brain model), once asked me on a beach approaching sunset, in Long Beach, CA USA "*Aren't we all in this together*?", while we were pondering the reflection of the sun on the water, arguing about how many images there were…

1.4.1 *The Church-Turing Hypothesis*

The Church-Turing Hypothesis states, every function naturally regarded as computable can be computed by the universal Turing machine, interpreted quasi-mathematically as the conjecture that all possible formalizations of the mathematical notion of algorithm or computation are equivalent to each other. But Deutsch says, "*we shall see that it can also be regarded as asserting a new physical principle, which I shall call the Church-Turing principle to distinguish it from other implications and connotations of the conjecture. My statement of the Church-Turing principle is manifestly physical … computable as the functions which may in principle be computed by a real physical system*" [79].

Deutsch then states, "*I can now state the physical version of the Church- Turing principle: 'Every finitely realizable physical system can be perfectly simulated by a universal model computing machine operating by finite means'. This formulation is both better defined and more physical than Turing's*

own way of expressing it, because it refers exclusively to objective concepts such as 'measurement', 'preparation' and 'physical system', which are already present in measurement theory." [79]. And further:

> Every existing general model of computation is effectively classical. That is, a full specification of its state at any instant is equivalent to the specification of a set of numbers, all of which are in principle measurable. Yet according to quantum theory there exist no physical systems with this property. The fact that classical physics and the classical universal Turing machine do not obey the Church-Turing principle in the strong physical form is one motivation for seeking a truly quantum model. The more urgent motivation is, of course, that classical physics is false. Benioff (1982) has constructed a model for computation within quantum kinematics and dynamics, but it is still effectively classical in the above sense. It is constructed so that at the end of each elementary computational step, no characteristically quantum property of the model - interference, non-separability, or indeterminism - can be detected. Its computations can be perfectly simulated by a Turing machine [79].

The Church-Turing thesis generally defines an 'algorithm' as a description of a calculation that needs to be realized physically; thus, the device executing the calculation has to be considered a physical system also. In this regard a calculation is defined as the execution of a physical process, where the result is provided by the observation of the process. Underlying the Church-Turing hypothesis there is an implicit physical assertion, which as Deutsch states:

> "is presented explicitly as a physical principle*: 'every finitely realizable physical system can be perfectly simulated by a universal model computing machine operating by finite means*'. Classical physics and the universal Turing machine, because the former is continuous and the latter discrete, do not obey the principle, at least in the strong form above. A class of model computing machines that is the quantum generalization of the class of Turing machines is described, and it is shown that quantum theory and the 'universal quantum computer' are compatible with the principle. Computing machines resembling the universal quantum computer could, in principle, be built and would have many remarkable properties not reproducible by any Turing machine. [79].

This includes 'quantum parallelism', whereby certain probabilistic tasks can be performed faster by a UQC than by any classical restriction of it. "*The intuitive explanation of these properties places an intolerable strain on all interpretations of quantum theory other than Everett's*" [79].

1.4.2. *The Church-Turing-Deutsch Thesis*

The idea of the Turing machine dates back to the year 1936. At this time, the physical world seemed to be dominated by mechanical forces; correspondingly, the definition of a Turing machine is based on the ideas of classical mechanics. And though the physical realization of a Turing machine, the digital computer, actually uses quantum mechanics, its construction principles aims at the suppression of any effect associated with the quantum world. With ever-tighter package density, however, this is not achievable anymore in a perfect way. The effects of quantum theory may begin to have an influence on the outcome of the calculation.

Consequently, it seems to be questionable whether the Turing machine provides a 'natural' model of computation. Searching for alternatives and taking the quantum nature of the world into consideration, Feynman had the idea of quantum computation in 1982. As a model executing such a quantum computation, he proposed the quantum Turing machine as quantum theoretical analogon to the Turing machine. Similar ideas were developed independently by Manin [80]. Accordingly, David Deutsch famously generalized the Church-Turing thesis to the Church-Turing-Deutsch thesis in 1985, which states that every computation, which can be realized physically, can be executed using a quantum Turing machine [81, 82].

1.4.3. *Perspicacious Perspicacity – Who Has it? Where can I get Some?*

I remember when I was about 12 years old and my father would take the old fashioned steam locomotives from West Medford, MA to Boston to work. That railroad company had kept a few steam locomotives about a decade longer than any others in the country. The last age of discovery occurred at

the beginning of the 20th century; this next one will pale all others in the history of human consciousness. A big part of me wishes I wasn't with the utmost alacrity, becoming a codger and could transfer my mind to an android for a couple hundred years; Yea, I mean 'where's my flying car', less than a decade ago it took four guys to barely be able to move a 50-inch TV out the door, now they can be carried with one arm, and paper thin, roll up into a tube, wallpaper TVs are coming out the door. The toys UCQ will provide are not unimaginable; I want some. Let's
get with the program…

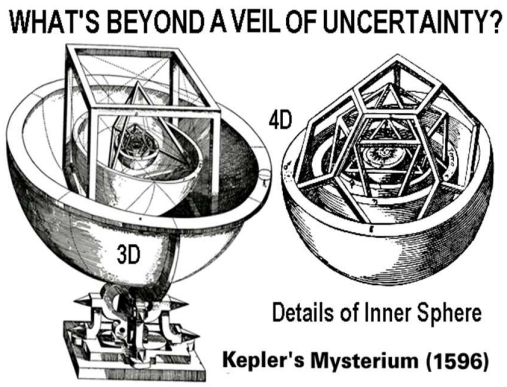

Fig. 1.23. Kepler's *Mysterium Cosmographicum* Platonic solid solar system model [83].

We offer Kepler's *Mysterium Cosmographicum* Platonic solid as a metaphor suggesting the additional hidden semi-quantum dimensionality for UFM required to represent QC operations in a physically real manner. It is important to realize, that just as the Earth was found not to be the center of the universe, as difficult as it may seem at the moment; Euclidean 3-space can no longer be considered the sole basis of observation.

For that important reason we repeat Feynman's message quoted at the beginning of this chapter:

> "… Trying to find a computer simulation of physics, seems … an excellent program to follow … I'm not happy with all the analyses that go with just the classical theory, because nature isn't classical, … and if you want to make a simulation of nature, you'd better make it quantum mechanical …", R. Feynman [1].

Thirty-four years have passed. I take liberty to impress upon you the necessity for updating Feynman:

> *I'm not happy with all the analyses that go with just classical and quantum theory, because nature isn't classical or quantum, … if you want to make a simulation of nature, you'd better make it unified field mechanical,* R.L. Amoroso.

References

[1] Feynman, R.P. (1982) Simulating physics with computers, Intl J Theoretical Physics 21, pp. 467-488.
[2] Vandersypen, L.M.K. & Chuang, I.L. (2004) NMR techniques for quantum control and computation, Rev Mod Phys, 76, 1037-1069.
[3] Di Vincenzo, D.P. (2000) The physical implementation of quantum computation, arXiv:quant-ph/0002077.
[4] Bell, J.S. (1966) On the problem of hidden variables in quantum mechanics, Reviews of Modern Physics, 38(3), 447.
[5] Lindblad, G. (1999) A general no-cloning theorem, Letters in Mathematical Physics, 47(2), 189-196.
[6] Zurek, W.H. (2009) Quantum Darwinism, arXiv:0903.5082v1 [quant-ph].
[7] Deutsch, D. (1985) Quantum theory, the Church-Turing principle and the universal quantum computer, Proceedings Royal Society, A 400 (1818): 97-117.
[8] Benioff, P. (1980) The computer as a physical system: A microscopic quantum mechanical Hamiltonian model of computers as represented by Turing machines, Journal of Statistical Physics, 22(5):563-591.
[9] Jozsa, R. (2005) An introduction to measurement based quantum computation, arXiv:quant-ph/0508124v2.
[10] Raussendorf, R., Browne, D.E. & Briegel, H. J. (2003) Measurement based quantum computation on cluster states, Phys Rev A 68 (2):022312; arXiv:quantph/0301052.
[11] Raussendorf, R., Harrington, J. & Goyal, K. (2007) Topological fault tolerance, New Journal of Physics 9:

199; arXiv:quant-ph/0703143.
[12] Walther, P., Resch, K.J. Rudolph, T., Schenck, E. Weinfurter, H. Vedral, V.M. Aspelmeyer, M. & Zeilinger, A. (2005) Nature 434 (7030): 169-76; arXiv:quant-ph/0503126.
[13] Fowler, A.G., Stephens, A.M. & Groszkowski, P. (2009) High-threshold universal quantum computation on the surface code, Phys Rev A, 80: 052312.
[14] Nielsen, M.A. (2005) Cluster-state quantum computation, arXiv:quant-ph/0504097v2.
[15] Johnson, M.W. et al. (2011) Quantum annealing with manufactured spins, Nature, 473,194-198.
[16] Perdomo-Ortiz, A., Dickson, N., Drew-Brook, M., Rose, G. & Aspuru-Guzik, A. (2012) Finding low-energy conformations of lattice protein models by quantum annealing, Scientific Reports 2, 571.
[17] Kane, B.E. (1998) A silicon-based nuclear spin quantum computer, Nature, 393, p. 133.
[18] O'Gorman, J., Nickerson, N.H., Ross, P., Morton, J.L. & Benjamin, S.C. (2015) A silicon-based surface code quantum computer, arXiv:1406.5149v3 [quant-ph].
[19] Dixit, A. & Kapse, V (2012) Arithmetic & logic unit (ALU) design using reversible control unit, Intl J Eng and Innovative Tech (IJEIT) Vol 1, No. 6.
[20] Elhoushi, M., El-Kharashi, M.W. & Elrefaei, H. (2011) Modeling a quantum processor using the QRAM model, in Communications, Computers and Signal Processing (PacRim), 2011 IEEE Pacific Rim Conf., pp. 409-415.
[21] Shirahama, K., Ito, H.S., Suto, S.I. & Kono, K. (1995) J. Low Temp. Phys. 101, 439.
[22] Platzman, P.M. & Dykman, M.I. (1999) Quantum computing with electrons floating on liquid helium, Science, Vol. 284, No. 5422, pp. 1967-1969.
[23] Platzman, P.M., Dykman, M.I. & Seddighrad, P. (2003) Dynamics in quantum dots on helium surface, arXiv:cond-mat/0308572v1.
[24] Odom, B., Hanneke, D., D'Urso, B. & Gabrielse, G. (2006) New measurement of the electron magnetic moment using a one-electron quantum cyclotron, Physical Review Letters 97 (3): 030801.
[25] Harneit, W. (2002) Fullerene-based electron-spin quantum computer, Phys. Rev. A 65, 032322.
[26] Rose, G. & Macready, W.G. (2007) An Introduction to quantum annealing, DWAVE/ Technical Document 0712.
[27] Clarke, J. & Wilhelm, F. (2008) Superconducting quantum bits, Nature 453 (7198): 1031-1042.
[28] Kaminsky, W.M. (2004) Scalable superconducting architecture for adiabatic quantum computation, arXiv:quant-ph/0403090.
[29] Bouchiat, V., Vion, D., Joyez, P., Esteve, D. & Devoret, M.H. (1988) Quantum coherence with a single Cooper pair, Physica Scripta, T76: 165.
[30] Monroe, C.R. & Wineland, D.J. (2008) Quantum computing with ions, Scientific American, pp. 64-71.
[31] Monroe, C.R. (2002) Quantum information processing with atoms and photons, Nature, V. 416, No. 6877, pp. 238-246.
[32] Li, L. et al. (2015) Coherent spin control of a nanocavity-enhanced qubit in diamond, Nature Communications, 6, 6173.
[33] Xu, S.J. Physics of nanomaterials, www.physics.hku.hk/~phys2235/lectures/ lecture9.pdf.
[34] Loss, D. & DiVincenzo, D.P. (1998) Quantum computation with quantum dots, Phys. Rev. A 57, p120; arXiv.org.
[35] DiVincenzo, D.P. (1997) in Mesoscopic Electron Transport, Vol. 345, NATO Advanced Study Institute, Series E: Applied Sciences, L. Sohn, L. Kouwenhoven, & G. Schoen (eds.) Dordrecht: Kluwer; arXiv.org.
[36] Kloeffel, C. & Loss, D. (2012) Prospects for spin-based quantum computing, arXiv:1204.5917v1 [cond-mat.mes-hall].
[37] Jeong, H., Chang, A. M., Melloch, M. R. (2001) The Kondo effect in an artificial quantum dot molecule, Science 293, 2221-2223.
[38] Veldhorst, M. et al. (2015) A two-qubit logic gate in silicon, Nature, 526, 410-414.
[39] Stepanenko, D., Trif, M. & Loss, D. (2008) Quantum computing with molecular magnets, *Inorganica Chimica Acta*, Vol. 361, Is. 14-15, pp. 3740-3745.
[40] Leuenberger, M.N. & Loss, D. (2001) Quantum computing in molecular magnets, arXiv.org/ftp/cond-mat/papers/0011/0011415.pdf.
[41] Andrianov, S.N. & Moiseev, S.A. (2014) Magnon qubit and quantum computing on magnon Bose-Einstein condensates, Phys. Rev. A 90, 042303.
[41] Bose, S.N. (1924) *Plancks gesetz und lichtquantenhypothese, Zeitschrift für Physik* 26: 178–181.
[42] Einstein, A. (1925) *Quantentheorie des einatomigen idealen Gases, Sitzungsberichte der Preussischen Akademie der Wissenschaften,* 1: 3.
[43] Hecht, T. (2004) Quantum computation with Bose-Einstein condensates, www2.mpq.mpg.de/Theorygroup/CIRAC/wiki/images/7/79/Hecht_Diplomarbeit.pdf.
[44] Timmermans, E., Tommasini, P., Hussein, M. & Kerman, A. (1999) Feshbach resonances in atomic Bose-Einstein condensates, Physics Reports-Review Section of Physics Letters, 315(1-3):199–230.
[45] Karnachev, A.S., Klechin, Y.I., Kovtun, N.M., Moskvin, A.S., Solov'ev, E.E. & Tkachenko, A.A. (1983) Spin-flip and nuclear quadrupole interactions in the rare-earth orthochromites $GdCr0_3$, Sov. Phys. JETP 58 (2), *Zh. Eksp. Teor. Fiz.* 85, 670-677.
[46] Nilsson, M., Levin, L., Ohlsson, N., Christiansson, T. & Kröll, S. (2001) Initial experiments concerning quantum information processing in rare-earth-ion doped crystals, arxiv.org/ftp/quant-ph/papers/0201/0201141.pdf.
[47] Chang, H., Xie, J., Zhao, B., Liu, B., Xu, S., Ren, N., Xie, X., Huang, L. & Huang, W. (2015) Rare earth ion-doped up conversion and surface modification, Nanocrystals: Synthesis, Nanomaterials, 5, 1-25.

[48] Walther, A., Rippe, L., Yan, Y. Karlsson, J., Serrano, D., Nilsson, A.N., Bengtsson, S. & Kroll, S. (2015) High fidelity readout scheme for rare-earth solid-state quantum computing, arXiv:1503[quant-ph].
[49] Knill, E., Laflamme, R., Milburn, G.J. (2001) A scheme for efficient quantum computation with linear optics, Nature (Nature Publishing Group) 409 (6816): 46-52.
[50] Kok, P., Munro, W.J., Nemoto, K., Ralph, T.C., Dowling, J.P. & Milburn, G.J. (2007) Linear optical quantum computing with photonic qubits, Rev. Mod. Phys, 79: 135-174; arXiv:quant-ph/0512071.
[51] Adami, C. & Cerf, N.J. (1999) Quantum computation with linear optics, in Quantum Computing and Quantum Communications, Lecture Notes in Computer Science, Springer, 1509: 391-401.
[52] Malinovskaya, S.A. & Novikova, I. (2015) From Atomic to Mesoscale: The Role of Quantum Coherence in Systems of Various Complexities, Singapore: World Scientific.
[53] Ralph, T.C., White, A.G., Munro, W.J. & Milburn, G.J. (2001) Simple scheme for efficient linear optics quantum gates, Phys. Rev. A 65, 012314.
[54] Hong, C.K., Ou, Z.Y. & Mandel, L. (1987) Measurement of subpicosecond time intervals between two photons by interference, Phys. Rev. Lett. 59, 2044.
[55] Knill, E. (2002) Quantum gates using linear optics and postselection. Physical Review A 66 (5): 052306; arXiv:quant-ph/0110144.
[56] Hutchinson, G.D. & Milburn, G. J. (2004) Nonlinear quantum optical computing via measurement, Journal of Modern Optics 51 (8): 1211-1222; arXiv:quant-ph/0409198.
[57] Lloyd, S. (1992) Any nonlinear gate, with linear gates, suffices for computation, Physics Letters A 167 (3): 255-260.
[58] Bloch, I. (2005) Ultracold quantum gases in optical lattices, Nature Physics 1 (1): 23-30.
[59] Soderberg, K-A B., Gemelke, N. & Chin, C. (2008) Ultracold molecules: Vehicles to scalable quantum information processing, arXiv:0812.1606v1 [quant-ph].
[60] Burell, B. (2012) An introduction to quantum computing. arXiv:1210.6512v1 [quant-ph].
[61] Luo, M-X, Deng, Y., Li, H-R & Ma, S-Y (2015) Photonic ququart logic assisted by the cavity-QED system, Scientific Reports 5, No.: 13255.
[62] Vandersypen, L.M.K., Yannoni, C.S. & Chuang, I.L. (2002) Liquid state NMR quantum computing, in D.M. Grant & R.K. Harris (eds.) Encyclopedia of Nuclear Magnetic Resonance, Vol. 9, pp 687-697, Chichester: John Wiley & Sons.
[63] Peng, X., Zhu, X., Fang, X., Feng, M., Gao, K., Yang, X. & Liu, M. (2000) Preparation of pseudo-pure states by line-selective pulses in Nuclear Magnetic Resonance, ar Xiv:quant-ph/0012038v2.
[64] Menicucci, N.C. & Caves, C.M. (2002) Local realistic model for the dynamics of bulk-ensemble NMR information processing, Phys Rev Let 88 (16); arXiv:quant-ph/0111152.
[65] Freedman, M.H., Kitaev, A., Larsen, M.J. & Wang, Z. (2002) Topological quantum computation, Bulletin (new series) Am Mathematical Society vol. 40, no. 1, pp. 31-38.
[66] Sarma, S.D., Freedman, M. & Nayak, C. (2015) Majorana zero modes and topological quantum computation, NPJ Quantum Information 1, 15001.
[67] Muraki, K. (2012) Unraveling an exotic electronic state for error-free quantum computation, NTT Technical Review, Vol. 10 No. 10.
[68] Sarma, S.D., Freedman, M. & Nayak, C. (2005) Topologically protected qubits from a possible non-abelian fractional quantum Hall state, Physical Review Letters 94 (16): 166802; arXiv:cond-mat/0412343.
[69] Amoroso, R.L. (2013) Evidencing 'tight bound states' in the hydrogen atom: Empirical manipulation of large-scale XD in violation of QED, in R.L. Amoroso (ed.) The Physics of Reality: Space, Time, Matter, Cosmos, Singapore: World Sci.
[70] Amoroso, R.L. (2010) Simple resonance hierarchy for surmounting quantum uncertainty, AIP Conf. Proc. 1316, 185 or http://vixra.org/pdf/1305.0098v1.pdf.
[71] Nielsen, M.A. (2002) Rules for a complex quantum world, Scientific American, Vol. 287, No. 5, pp. 66-75.
[72] Shannon, C.E. (1958) Channels with side information at the transmitter, IBM journal of Research and Development, *2*(4), 289-293.
[73] Landauer, R. (1991) Information is physical, Phys. Today 44 (5) 22.
[74] Landauer, R. (1996) The physical nature of information, Phys Let. A 217, 188-193.
[75] Lidar, D. & Todd Brun T. (eds.) (2013) Quantum Error Correction, Cambridge: Cambridge University Press.
[76] Shor, P.W. (1996) Fault-tolerant quantum computation, 37th Symposium on Foundations of Computing, IEEE Computer Society Press, pp. 56-65.
[77] Preskill, J. (1998) Fault-tolerant quantum computation, in Introduction to Quantum Computation, H-K Lo, S. Popescu, T. P. Spiller (eds.) Singapore: World Scientific.
[78] Newton, I. (1689) Scholium to the Definitions in *Philosophiae Naturalis Principia Mathematica*, Bk. 1; Andrew Motte (trans.) (1729), rev. F. Cajori (1934) Berkeley: University of California Press, pp. 6-12.
[79] Deutsch, D. (1985) Quantum theory, the Church-Turing principle and the universal quantum computer, Proceedings of the Royal Society of London, A 400, pp. 97-117.
[80] Manin, Y.I. (1980) *Vychislimoe i* nevychislimoe [Computable and Noncomputable] *(in Russian)* Sov.Radio. pp. 13-15.
[81] Quantum Turing machine, Encyclopedia of Mathematics, www.encyclopediaofmath.org/index.php/Quantum_Turing_machine.
[82] Aaronson, S. (2008) The limits of quantum computers, Scientific American, Vol. 298, No. 3, pp. 62-69.
[83] Kepler, J. (1596) *Mysterium Cosmographicum*, Platonic solid model of the Solar system.

PART 2
Cornucopia of Quantum Logic Gates

A logic gate is the elementary building block of a computing circuit or algorithm practically applying the concept of binary Boolean bits to circuits using combinational logic. Logic gates are of recent origin. From the time that Leibniz refined binary numbers and showed that mathematics and logic could be combined in 1705, it took well over a hundred years before Babbage devised geared mechanical logic gates in 1837 for use in his proposed Analytical Engine. Another sixty years passed before the first electronic relays appeared in the late 1890s. Then it wasn't until the 1940s that the first working computer was built. Now, with the arrival of quantum logic gates the evolution continues; and universal quantum computers (UQC) wait in the wings while finishing the absorption of required remaining discovery in physics.

2.1 Fundamental Properties of Gate Operations

Linear algebra concerns vector spaces and linear mappings between such spaces. The 3D Euclidean space $\mathbb{R}^3$ is a vector space, where lines and planes passing through the origin are vector subspaces in $\mathbb{R}^3$. The most important space in basic linear algebra is $\mathbb{R}^n$, a Euclidean space in *n* dimensions where a typical element is an *n*-element vector of real numbers. The space of infinite-dimensional vectors defines the Hilbert space, $\ell^2(\mathbb{N})$. Such a Hilbert space, *H* is a vector space endowed with an inner or dot product, $\|x\|$ and associated norm and metric, $\|x-y\|$ such that every Cauchy sequence (converges to a limit) in $\mathbb{R}^n$ making $\mathbb{R}^n$ a Hilbert space. Complex Hilbert spaces are used to represent the pure states of a quantum mechanical system utilizing unit vectors, called state vectors.

What is the difference between classical and quantum information? As shown in the matrices below, the classical bit is described by two nonnegative real numbers for probabilities P(0) = 1/3 and P(1) = 2/3. In contrast the quantum bit has two complex amplitudes giving the same probabilities by taking the square of the absolute value.

$$\text{Classical bit: } \begin{bmatrix} 1/3 \\ 2/3 \end{bmatrix} \quad \text{Qubit } \begin{bmatrix} -1/\sqrt{3} \\ 1+i/\sqrt{3} \end{bmatrix} \qquad (2.1)$$

A quantum system described like this with nonzero amplitudes is said to be in a superposition of the 0 and 1 configurations.

The basis of all computing is the logic gate [1]. A quantum logic gate is most often represented by a matrix. For example, a gate acting on *n* qubits takes the form of a $2^n \times 2^n$ unitary matrix. The number of qubits input and the number of qubits output from any gate must be equal. The operation of the gate is determined by multiplying the gate's unitary matrix by the vector representation of the quantum state. For example, the vector representation of a solitary qubit and of two qubits is represented respectively as:

$$v_0|0\rangle + v_1|1\rangle \to \begin{bmatrix} v_0 \\ v_1 \end{bmatrix}, \quad v_{00}|00\rangle + v_{01}|01\rangle + v_{10}|10\rangle + v_{11}|11\rangle \to \begin{bmatrix} v_{00} \\ v_{01} \\ v_{10} \\ v_{11} \end{bmatrix}. \qquad (2.2)$$

For the 2-qubit state $|ab\rangle$, *a* represents the value of the 1st qubit and *b* represents the 2nd qubit.

A single qubit wave function takes the form $|\Psi\rangle = \psi_0|0\rangle + \psi_1|1\rangle$ such that $|\psi_0|^2 + |\psi_1|^2 = 1$; with this as the case observation gives a result of either a 0 or a 1 with a probability for 0 as $|\psi_0|^2$ and the probability for observing a 1 is $|\psi_1|^2$.

2.2 Unitary Operators as Quantum Gates

The state of a quantum computer is described by a state vector, Ψ which is a complex linear superposition of all binary states of the qubits $x_n \in \{0,1\}$:

$$\Psi(t) = \sum_{x_n \in \{0,1\}^n} \alpha_x |x_1,...,x_n\rangle, \quad \sum_x |\alpha_x|^2 = 1. \qquad (2.3)$$

The state's evolution in time, *t* is described by a unitary operator, *U* on the same vector space, meaning any linear transformation is bijective and length-preserving. This unitary evolution on a normalized state vector is known to be the correct physical description of an isolated system evolving in time according to the laws of quantum mechanics [2-5]. Quantum physics is reversible because the reverse-time evolution specified by the unitary operator, $U^{-1} = U^{\dagger}$ always exists; as a consequence, reversible computation could be executed within a quantum-mechanical system.

Quantum physics postulates that quantum evolution is unitary (reversible); i.e., if we have an arbitrary quantum system, *U* taking an input state, $|\phi\rangle$ that outputs a different state, $U|\phi\rangle$, then we describe *U* as a unitary linear transformation, defined as follows. If *U* is any linear transformation, the adjoint (functions related by transposition) of *U*, denoted $U^{\dagger}$, is defined in the relation $(U\vec{v},\vec{w}) = (\vec{v},U^{\dagger}\vec{w})$. In a basis, $U^{\dagger}$ is the conjugate transposition of *U*; for example,

$$U = \begin{pmatrix} a & b \\ c & d \end{pmatrix} \Rightarrow U^{\dagger} = \begin{pmatrix} \overline{a} & \overline{c} \\ \overline{b} & \overline{d} \end{pmatrix}. \qquad (2.4)$$

By definition *U* is unitary if $U^{\dagger} = U^{-1}$. Thus, rotations and reflections are unitary. Also, the composition of two unitary transformations is also unitary, and for a unitary transformation *U*, the rows and columns also form an orthonormal basis [6].

Evolution of the state, $|\psi\rangle$ of a quantum system in time, *t* is a unitary transform, $|\psi\rangle \rightarrow \hat{U}|\psi\rangle$. Temporal evolution of a quantum system is linear because it does not depend on the state, $|\psi\rangle$. For example, any linear combination in *t* of state, $|\psi\rangle$ and $|\phi\rangle$ has the same operator

$$(\alpha|\psi\rangle + \beta|\phi\rangle) \rightarrow \hat{U}(\alpha|\psi\rangle + \beta|\phi\rangle) = \alpha\hat{U}|\psi\rangle + \beta\hat{U}|\phi\rangle. \qquad (2.5)$$

Unitary operators conform to the Schrödinger equation

$$\frac{d|\psi\rangle}{dt} = -i\frac{\hat{H}(t)|\psi\rangle}{\hbar} \qquad (2.6)$$

with $\hat{H}(t) = \hat{H}^{\dagger}(t)$ the system's Hamiltonian.

The general Hamiltonian for a spin-1/2 system is $\hat{H} = b\hat{X} + c\hat{Y} + d\hat{Z} = E_0 \vec{n} \cdot \hat{\vec{\sigma}}$ with $E_0 = \sqrt{b^2 + c^2 + d^2}, \vec{n} = \left(n_x, n_y, n_z\right) = \left(b / E_0, c / E_0, d / E_0\right)$, $n_x^2 + n_y^2 + n_z^2 = 1$ and $\hat{\vec{\sigma}} = \left(\hat{X}, \hat{Y}, \hat{Z}\right)$. Thus the unitary is

$$\exp\left(-\frac{i\hat{H}t}{\hbar}\right) = \cos\left(\frac{E_0 t}{\hbar}\right)\hat{I} - i\sin\left(\frac{E_0 t}{\hbar}\right)\vec{n} \cdot \hat{\vec{\sigma}}. \qquad (2.7)$$

This is a rotation about the $\vec{n}$ axis in the Bloch sphere representation with a rotation rate of $E_0 / \hbar$. For spin-1/2 this is the most general unitary transform [6].

Assuming we can turn the Hamiltonian off and on, the state can be rotated by a specific angle; again for spin-1/2 a unitary transform takes the form, $\hat{U}(\theta) = \cos(\theta/2)\hat{I} - i\sin(\theta/2)\vec{n} \cdot \hat{\vec{\sigma}}$. It is important to realize that any product of unitary operators is also unitary [7]

$$\hat{U}^\dagger \hat{U} = \hat{V}^\dagger \hat{V} = \hat{I} \Rightarrow \left(\hat{U}\hat{V}\right)^\dagger \left(\hat{U}\hat{V}\right) = \hat{V}^\dagger \hat{U}^\dagger \hat{U}\hat{V} = \hat{I} \qquad (2.8)$$

The Copenhagen Interpretation's restriction of time evolution to unitary operators suggests that certain kinds of evolution are deemed impossible. Two such operations are the quantum no-cloning and non-erasure theorems [8-15]. In ensuing chapters, we intend to show that this is a condition of the 4D standard model Copenhagen Interpretation up to the 'semi-quantum limit' and is no longer the case for UFM topology.

2.3 Some Fundamental Quantum Gates

Unitary transformations, or quantum gates can be built from sets of unitaries, $\hat{U}$. The simplest spin-1/2 quantum system, the qubit, has two quantum states with the basis $|0\rangle \equiv |\uparrow Z\rangle$, $|1\rangle \equiv |\downarrow Z\rangle$. Some examples of simple single and 2-qubit unitary transforms, or 'quantum gates' follow:

- **The Hadamard Gate:**

The Hadamard transform, known as the Hadamard gate in quantum computing is an example of a generalized class of Fourier transforms. It is able to perform orthogonal, symmetric, involute and linear operations. The Hadamard gate acts on a single qubit. It maps the basis state $|0\rangle$ to $|0\rangle + |1\rangle/\sqrt{2}$ and $|1\rangle$ to $|0\rangle - |1\rangle/\sqrt{2}$ representing a rotation of π about the axis $(\hat{x} + \hat{z})/\sqrt{2}$. This is equivalent to the combination of the two rotations, $\pi/2$ about the y-axis followed by π about the x-axis. The Hadamard gate is represented by the Hadamard matrix which is a square matrix with mutually orthogonal rows with entries of ± 1.

$$H = \frac{1}{\sqrt{2}}\begin{bmatrix} 1 & 1 \\ 1 & -1 \end{bmatrix}. \qquad (2.9)$$

Since $HH^* = I$ and I is an identity matrix, H is a unitary matrix. The Hadamard gate operates as a reflection around π/8, or as a π/4 rotation followed by a reflection. Notice that $H^\dagger = H$ and $H^2 = 1$ because H is real and symmetric.

$$H = \frac{1}{\sqrt{2}}\begin{pmatrix} 1 & 1 \\ 1 & -1 \end{pmatrix} = -\boxed{H}- = \begin{bmatrix} \frac{1}{\sqrt{2}} & \frac{1}{\sqrt{2}} \\ \frac{1}{\sqrt{2}} & -\frac{1}{\sqrt{2}} \end{bmatrix} \tag{2.10}$$

The circuit representation of Hadamard gate is

$$-\boxed{H}-.$$

- **The Phase Shift Gate:**

Phase Shift gates are a family of single qubit gates that leave basis state $|0\rangle$ unchanged and map $|1\rangle$ to $e^{i\theta}|1\rangle$. The Phase Shift Gate 2 × 2 matrix and symbol are:

$$R_\theta = \begin{bmatrix} 1 & 0 \\ 0 & e^{i\theta} \end{bmatrix} \quad \text{with symbol} \quad -\boxed{R_\theta}-$$

The phase shift gate is a generalization of an infinity of gates. The Pauli-Z gate, Phase shift gate, and $\pi/8$ gates are all special cases of the phase shift gate for specific values of θ (the phase shift).

- **The Swap Gate:**

The Swap Gate swaps two qubits in terms of the basis $|00\rangle, |01\rangle, |10\rangle, |11\rangle$ and is represented by the matrix:

$$\text{SWAP} = \begin{bmatrix} 1 & 0 & 0 & 0 \\ 0 & 0 & 1 & 0 \\ 0 & 1 & 0 & 0 \\ 0 & 0 & 0 & 1 \end{bmatrix}$$

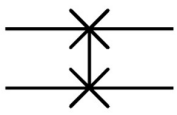

- **The Pauli *X* (NOT) Gate:**

The Pauli-X gate acts on a single qubit. It is the quantum equivalent of a classical NOT gate (with respect to the standard basis $|1\rangle$, $|0\rangle$, which privileges the Z-direction). It equates to a rotation of the Bloch Sphere around the X-axis by π radians; and maps $|0\rangle$ to $|1\rangle$ and $|1\rangle$ to $|0\rangle$. Due to this operation, it is sometimes called the bit-flip gate. It is represented by the Pauli matrix:

$$\begin{bmatrix} 0 & 1 \\ 1 & 0 \end{bmatrix} = -\boxed{X}-$$

- **The Pauli *Y* Gate:**

The Pauli-Y gate acts on a single qubit. It equates to a rotation around the Y-axis of the Bloch Sphere by π radians. It maps $|0\rangle$ to $i|1\rangle$ and $|1\rangle$ to $-i|0\rangle$. It is represented by the Pauli Y matrix:

$$\begin{bmatrix} 0 & -i \\ i & 0 \end{bmatrix} = -\boxed{Y}-$$

- **The Pauli *Z* Gate:**

The Pauli-Z gate acts on a single qubit. It produces a rotation around the *Z*-axis of the Bloch Sphere by π radians. Thus, it is a special case of a phase shift gate with $\theta = \pi$. It leaves the basis state, $|0\rangle$ unchanged and maps $|1\rangle$ to $-|1\rangle$. Due to this nature, it is sometimes called the phase-flip gate. It is represented by the Pauli *Z* matrix:

$$\begin{bmatrix} 1 & 0 \\ 0 & -1 \end{bmatrix} = -\boxed{Z}-$$

- **The CNOT (Controlled NOT) Gate:**

Controlled gates act on 2 or more qubits, with one or more qubits acting as a control for a specific operation. For example, a CNOT Gate acts on 2 qubits, and performs the NOT operation on the second qubit. The first bit of a CNOT gate is the 'control bit'; the second is the 'target bit'. The control bit never changes, while the target bit flips if and only if the control bit is 1. Here is the matrix representation of CNOT, and its operation upon a general 2-qubit state column vector:

$$\text{CNOT} = \begin{bmatrix} 1 & 0 & 0 & 0 \\ 0 & 1 & 0 & 0 \\ 0 & 0 & 0 & 1 \\ 0 & 0 & 1 & 0 \end{bmatrix}$$

$$\text{CNOT}\,\Psi = \begin{bmatrix} 1 & 0 & 0 & 0 \\ 0 & 1 & 0 & 0 \\ 0 & 0 & 0 & 1 \\ 0 & 0 & 1 & 0 \end{bmatrix} \begin{bmatrix} \alpha \\ \beta \\ \gamma \\ \delta \end{bmatrix} = \begin{bmatrix} \alpha \\ \beta \\ \delta \\ \gamma \end{bmatrix}$$

The CNOT gate is usually depicted as follows, with the control bit on top

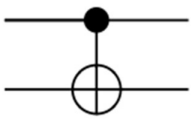

and the target bit on the bottom.

When unitary gates are combined they form a quantum circuit; the example below uses three CNOT gates to swap the 1st and 2nd qubits.

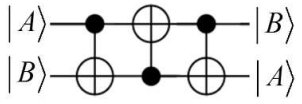

$$\begin{aligned} \hat{U}\text{CNOT}|00\rangle &= |00\rangle, \quad \hat{U}\text{CNOT}|01\rangle = |01\rangle, \\ \hat{U}\text{CNOT}|10\rangle &= |11\rangle, \quad \hat{U}\text{CNOT}|11\rangle = |10\rangle. \end{aligned} \tag{2.11}$$

This has two inputs and two outputs. The first input is passed through unchanged to the corresponding output. When this first input is **0**, the second input is also passed through unchanged to its corresponding output. But when the first input is **1**, the second input gets inverted as through an **X** gate.

- **The Toffoli Gate:**

Introduction of an additional control line to the CNOT gate results in the CCNOT gate (controlled-controlled NOT) which is also called the Toffoli gate. The Toffoli Gate is a 3-bit controlled gate also called the CCNOT gate which is universal for classical computing. The quantum Toffoli gate is the same gate defined instead for 3 qubits; but this gate is not universal for quantum Computing.

The Toffoli gate is depicted as follows:

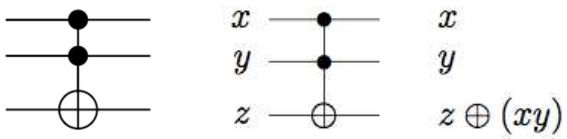

If the first two bits are in the state $|1\rangle$, a Pauli-X is applied on the 3rd bit, otherwise it does nothing. Its permutation matrix is:

$$\text{CCNOT} = \begin{pmatrix} 1 & 0 & 0 & 0 & 0 & 0 & 0 & 0 \\ 0 & 1 & 0 & 0 & 0 & 0 & 0 & 0 \\ 0 & 0 & 1 & 0 & 0 & 0 & 0 & 0 \\ 0 & 0 & 0 & 1 & 0 & 0 & 0 & 0 \\ 0 & 0 & 0 & 0 & 1 & 0 & 0 & 0 \\ 0 & 0 & 0 & 0 & 0 & 1 & 0 & 0 \\ 0 & 0 & 0 & 0 & 0 & 0 & 0 & 1 \\ 0 & 0 & 0 & 0 & 0 & 0 & 1 & 0 \end{pmatrix}$$

Essentially, the Toffoli gate reverses the bottom qubit if the top two qubits are 1, otherwise it leaves the qubit the same. This lets us simulate the classical AND gate if we initialize the bottom qubit in state $|0\rangle$, then we know it is in state $|1\rangle$ if and only if both top qubits are in state $|1\rangle$, thus the bottom qubit is essentially the output of an AND operation.

Any reversible gate can be implemented on a quantum computer, thus the Toffoli gate is a quantum operator. However, the Toffoli gate cannot be used by itself for UQC, it has to be implemented along with some inherently quantum gate(s) in order to be universal for quantum computation. Any single-qubit gate with real coefficients that can create a nontrivial quantum state suffices [6]. Recently a quantum mechanical Toffoli gate has been realized [16,17].

- **The Fredkin Gate:**

The Fredkin Gate, also called the CSWAP gate, is logic gate combining the logic of the SWAP and CNOT gates, is a universal reversible 3-bit gate that by performing a controlled-swap operation, swaps the last two bits if the first bit is 1. The Fredkin gate is universal for classical computation. As with the Toffoli gate it has the useful property that the number of 0s and 1s are conserved throughout operation, which in the billiard ball model means that the same number of balls are output as input.

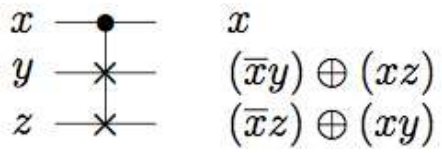

$$\begin{bmatrix} 1 & 0 & 0 & 0 & 0 & 0 & 0 & 0 \\ 0 & 1 & 0 & 0 & 0 & 0 & 0 & 0 \\ 0 & 0 & 1 & 0 & 0 & 0 & 0 & 0 \\ 0 & 0 & 0 & 1 & 0 & 0 & 0 & 0 \\ 0 & 0 & 0 & 0 & 1 & 0 & 0 & 0 \\ 0 & 0 & 0 & 0 & 0 & 0 & 1 & 0 \\ 0 & 0 & 0 & 0 & 0 & 1 & 0 & 0 \\ 0 & 0 & 0 & 0 & 0 & 0 & 0 & 1 \end{bmatrix}$$

- **The Controlled *U* Gate:**

The Controlled-*U* Gate is a gate that operates on two qubits in such a way that the 1st qubit serves as a control. It maps the basis states as:

$$\begin{aligned} &|00\rangle \mapsto |00\rangle \\ &|01\rangle \mapsto |01\rangle \\ &|10\rangle \mapsto |1\rangle U|0\rangle = |1\rangle \left(x_{00}|0\rangle + x_{10}|1\rangle\right) \\ &|11\rangle \mapsto |1\rangle U|1\rangle = |1\rangle \left(x_{01}|0\rangle + x_{11}|1\rangle\right) \end{aligned}$$

$$\mathrm{C}(U) = \begin{bmatrix} 1 & 0 & 0 & 0 \\ 0 & 1 & 0 & 0 \\ 0 & 0 & x_{00} & x_{01} \\ 0 & 0 & x_{10} & x_{11} \end{bmatrix},$$

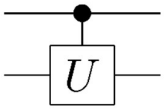

- **The Rotation Gate:**

This gate rotates the plane by θ:

$$U_R = \begin{bmatrix} \cos\theta & -\sin\theta \\ \sin\theta & \cos\theta \end{bmatrix} \tag{2.12}$$

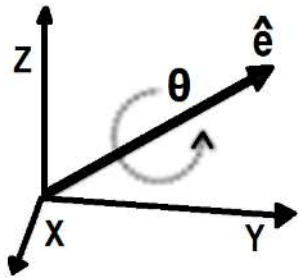

Fig. 2.1 The rotation gate showing axis of rotation.

2.4 Properties of the Hadamard Gate

The Hadamard Gate is an important special transform that maps qubit basis states $|0\rangle$ and $|1\rangle$ to two superposition states with a 50/50 weight of the computational basis states $|0\rangle$ and $|1\rangle$:

$$H|0\rangle = \frac{1}{\sqrt{2}}|0\rangle + \frac{1}{\sqrt{2}}|1\rangle; \quad H|1\rangle = \frac{1}{\sqrt{2}}|0\rangle - \frac{1}{\sqrt{2}}|1\rangle \tag{2.13}$$

This is the reason the Hadamard Gate is often used in the first steps of quantum algorithms to test all possible parallel input values.

$$-\boxed{H}- = \begin{bmatrix} \frac{1}{\sqrt{2}} & \frac{1}{\sqrt{2}} \\ \frac{1}{\sqrt{2}} & -\frac{1}{\sqrt{2}} \end{bmatrix}; \quad H|0\rangle = \frac{|0\rangle + |1\rangle}{\sqrt{2}}; \quad H|1\rangle = \frac{|0\rangle - |1\rangle}{\sqrt{2}}$$

The Hadamard operator is also hermitian and unitary, being its own inverse, $U\left(H,t\left|\psi(0)\right\rangle\right)$, where $U(H,t)$ is a unitary operator called the propagator. The propagator gives the probability amplitude for a particle to travel from one point to another in a given time, t, or to travel with a certain energy and momentum.

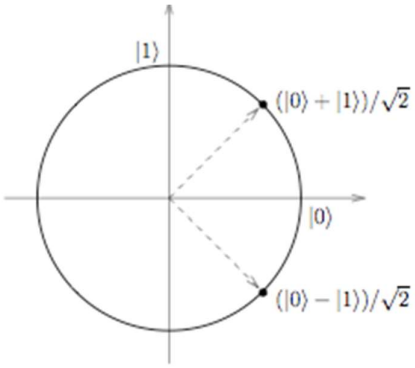

Fig. 2.2. Hadamard gate shown as R_y, R_z state rotations on the Bloch plane.

$$R_y(\pi/2)R_z(\pi) = -iH, \; R_y(\pi/2) = \frac{1}{\sqrt{2}}\begin{bmatrix} 1 & -1 \\ 1 & 1 \end{bmatrix}, \; R_z(\pi) = \begin{bmatrix} -i & 0 \\ 0 & i \end{bmatrix} = -iZ \tag{2.14}$$

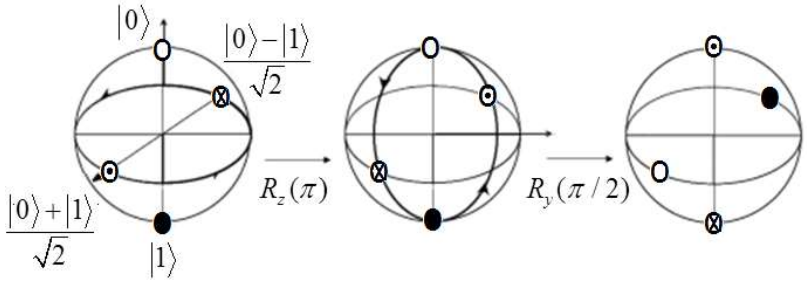

Fig. 2.3. Hadamard Bloch sphere rotation.

2.5 Rotation Gate Quantum Multiplexer

Finally, we give a brief review of recent work by Abdollahi and colleagues on their proposed multiple-control Toffoli gates for a quantum multiplexer [18]. The approach explores the synthesis of reversible functions by gates other than generalized Toffoli and Fredkin gates. They show that applying the proposed approach improves circuit size for multiple-control Toffoli gates from exponential in [19] to polynomial and circuit size for quantum multiplexers [19,20].

The θ – rotation gate $\left(0 \le \theta \le 2\pi\right)$ around the *x,y,z* axes acting on a single qubit is defined as

$$R_x(\theta) = \begin{bmatrix} \cos\frac{\theta}{2} & -i\sin\frac{\theta}{2} \\ -i\sin\frac{\theta}{2} & \cos\frac{\theta}{2} \end{bmatrix}, \quad R_y(\theta) = \begin{bmatrix} \cos\frac{\theta}{2} & -\sin\frac{\theta}{2} \\ \sin\frac{\theta}{2} & \cos\frac{\theta}{2} \end{bmatrix},$$
$$R_z(\theta) = \begin{bmatrix} e^{\frac{-i\theta}{2}} & 0 \\ 0 & e^{\frac{i\theta}{2}} \end{bmatrix}. \tag{2.14}$$

In review, the single qubit NOT gate, $X = \begin{bmatrix} 0 & 1 \\ 1 & 0 \end{bmatrix}$, the (controlled NOT), $\text{CNOT} = \begin{bmatrix} 1 & 0 & 0 & 0 \\ 0 & 1 & 0 & 0 \\ 0 & 0 & 0 & 1 \\ 0 & 0 & 1 & 0 \end{bmatrix}$, acting on two qubits (control and target) and the Hadamard gate, $H = \frac{1}{\sqrt{2}}\begin{bmatrix} 1 & 1 \\ 1 & -1 \end{bmatrix}$ are represented. A unitary matrix, *U* implemented by several gates acting on several qubits can be calculated by the tensor products of their matrices; and two or more q-gates can be cascaded to form a quantum circuit. For a set of *k* gates, $g_1, g_2, \ldots, g_k$ cascaded in a q-circuit, *C* sequentially, the matrix of *C* can be calculated as $M_k M_{k-1} \ldots M_1$ where $_{Mi}$ is the matrix of the i^{th} gate $\left(1 \le i \le k\right)$. For a quantum circuit with unitary matrix, *U* and input vector, ψ_1 the output vector is, $\psi_2 = U\psi_1$ [18].

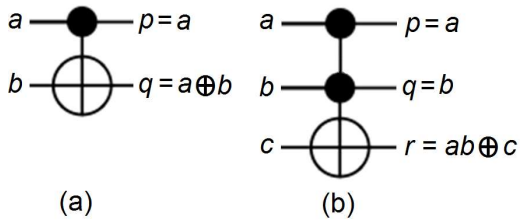

Fig. 2.4. a) CNOT gate, b) Toffoli gate.

Given any unitary, *U* over *m* qubits $\left|x_1 x_2 \ldots x_m\right\rangle$, a Controlled-*U* gate with *k* control qubits $\left|y_1 y_2 \ldots y_k\right\rangle$ can be defined as an (*m* + *k*)-qubit gate that applies *U* on $\left|x_1 x_2 \ldots x_m\right\rangle$ if $\left|y_1 y_2 \ldots y_k\right\rangle = \left|11 \ldots 1\right\rangle$. For example, CNOT is the controlled-NOT with a single control, the Toffoli

gate is a NOT gate with two controls, and $CR_x(\theta)$ is an $R_x(\theta)$ gate with a single control. Likewise, a multi-control Toffoli gate C^{k}NOT is a NOT gate with k controls as shown below [17,18].

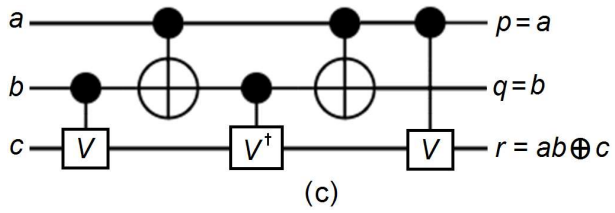

Fig. 2.5. c) Decomposition of a Toffoli gate into 2-qubit gates where $V = (1 - i)(I + iX)/2$. Redrawn from [16].

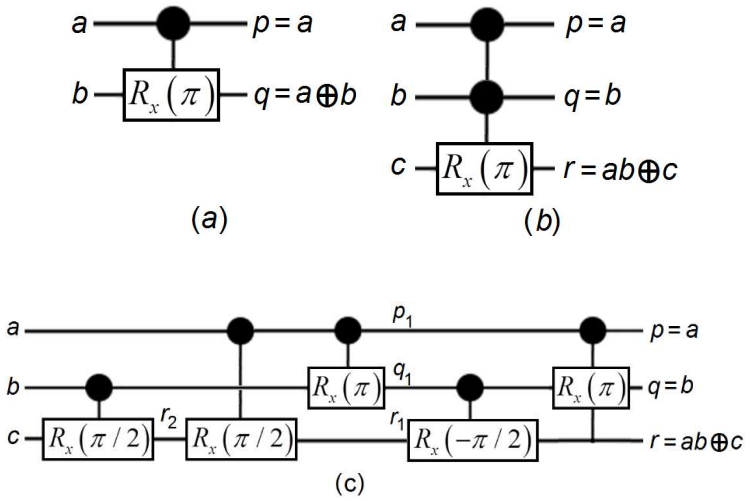

Fig. 2.6. New definitions for CNOT (a) and Toffoli (b) gates using controlled rotation gates. Decomposition of a Toffoli gate into five 2-qubit controlled-rotation gates (c). Redrawn from [16].

Under these parameters Boolean functions can be automatically synthesized by using rotations and controlled-$R_x(\pi)$ rotation gates around the x axis [18], which changes the basis states to $\hat{0} = \begin{bmatrix} 1 & 0 \end{bmatrix}^T$ and $\hat{1} = R_x(\pi)\hat{0} = \begin{bmatrix} 0 & -i \end{bmatrix}^T$. The superscript, T stands for the conjugate transpose matrix of a vector provided the bases are orthonormal. By this basis definition of $\hat{0}$ and $\hat{1}$, the basis states remain orthogonal and inversion (NOT gate) from one basis state to the other is easily obtained by a $R_x(\pi)$ rotation gate. This means that the CNOT gate can be described using the $CR_x(\pi)$ operator shown in the figure. Additionally, the Toffoli gate can be described by the $C^2R_x(\pi)$ operator also illustrated in the figure. Finally, recall that a 3-qubit Toffoli gate needs five 2-qubit gates if $|0\rangle$ and $|1\rangle$ are used as the basis states [19].

References

[1] Peirce, C.S. & Eisele, C. (eds.) (1976) The New Elements of Mathematics, Atlantic Highlands: Humanities Press.
[2] Dirac, P.A.M. (1958) The Principles of Quantum Mechanics, Oxford: Oxford Univ. Press.
[3] Feynman, R.P. (1985) Quantum mechanical computers, Optics News, 11, p. 11; reprinted in Foundations of Physics 16(6) 507-531.

[4] Nielsen, M. & Chuang, I. (2000) Quantum Computation and Quantum Information, Cambridge: Cambridge Univ. Press.
[5] Barenco, A. et al. (1995) Elementary gates for quantum computation, *Phys. Rev. 52 (5): 3457-3467*; arXiv:quant-ph/9503016v1.
[6] http://www-inst.eecs.berkeley.edu/~cs191/sp05/lectures/lecture4.pdf
[7] http://www-bcf.usc.edu/~tbrun/Course/lecture05.pdf.
[8] Abramsky, S. (2008) No-Cloning in categorical quantum mechanics, in I. Mackie & S. Gay (eds) Semantic Techniques for Quantum Computation, Cambridge: Cambridge University Press.
[9] Bužek V. & Hillery, M. (1996) Quantum copying: Beyond the no-cloning theorem, Phys. Rev. A 54, 1844.
[10] Buzek, V. & Hillery, M. (2001) Quantum cloning, Physics World 14 (11), pp. 25-29.
[11] Wootters, W. K. & Zurek, W. H. (1982). A single quantum cannot be cloned, Nature 299 (5886): 802-803.
[12] Dieks, D. (1982) Communication by EPR devices, Phys. Let. A 92 (6): 271-272.
[13] Herbert, N. (1982) FLASH-A superluminal communicator based upon a new kind of quantum measurement, Found. Physics 12 (12): 1171-1179.
[14] Peres, A. (2003) How the no-cloning theorem got its name, Fortschritte der Physik 51 (45): 458-461; arXiv:quant-ph/0205076.
[15] Vlasov, A.Y. (2002) Comment on 'How the no-cloning theorem got its name', arXiv:quant-ph/0205195.
[16] Monz, T., Kim, K., Hänsel, W., Riebe, M., Villar, A. S., Schindler, P., Chwalla, M., Hennrich, M. & Blatt, R. (2009) Realization of the quantum Toffoli gate with trapped ions, Am Phys Soc, 102 (4): 040501; arXiv:0804.0082.
[17] Toffoli, T. (1980) Reversible computing, in J. W. de Bakker & J. van Leeuwen (eds,) Automata, Languages and Programming, Seventh Colloquium, Noordwijkerhout, Netherlands: Springer Verlag, pp. 632-644.
[18] Abdollahi, A., Saeedi, M. & Pedram, M. (2013) Reversible logic synthesis by quantum rotation gates, arXiv:1302.5382v2 [cs.ET].
[19] Barenco, A., Bennett, C.H., Cleve, R., DiVincenzo, D.P., Margolus, N. & Shor P. (1995) Elementary gates for quantum computation, Physical Review A, 52:3457-3467.
[20] Cuccaro, S.A., Draper, T.G., Kutin, S.A. & Moulton, D.P. (2004) A new quantum ripple-carry addition circuit, arXiv:0410184.

PART 3
Surmounting Uncertainty Supervening Decoherence

Eliminating ensemble decoherence time and uncertainty in the operation and measurement process of Quantum Information Processing (QIP) systems are remaining problems considered to be of paramount importance in the task of implementing viable bulk scalable Universal Quantum Computing (UQC). Most teams currently attempt to supervene decoherence by utilizing multimillion dollar room sized cryogenic apparatus. If our model is correct, it will allow tabletop room temperature UQC. We theoretically illustrate (in a manner empirically testable) that these conditions essentially become irrelevant in terms of the radical new Unified Field Mechanical (UFM) approach to QIP introduced here. It should be noted that the recent relativistic restrictions the QC research community has imposed on QIP point the way to our model. The additional degrees of freedom obtained by leaving the 3D realm of Euclidean space associated with Newtonian Classical Mechanics and entering the 4D domain of Minkowski 4-space had a profound effect on physics during the last century. Now as we enter a 12D M-Theoretic (String Theory) dual Calabi-Yau mirror symmetric 3-torus 3rd regime associated with UFM, more surprises like the ability to surmount the quantum uncertainty principle are proffered. In this chapter we review a UFM protocol for allowing uncertainty and decoherence to be routinely surmounted and supervened respectively, 100% of the time with probability, $P \equiv 1$. We begin with a discussion of Interaction-Free Measurement (IFM), an interesting 4D precursor providing another indicium of the 12D brane topology model introduced here. IFM is a novel quantum mechanical procedure for detecting the state of an object without an interaction occurring with the measuring device. What we propose is a radical extension of the various experimental protocols spawned by the recent Elitzur-Vaidman IFM thought experiment.

3.1 Phenomenology Versus Ontology

The highly speculative, at time of writing, UFM alternative to IFM protocols, is a single pass ontological method for surmounting uncertainty, without (phenomenological) quantal field interaction or collapse of the wave function. Surmounting the Quantum Uncertainty Principle with probability, $P \equiv 1$ is

achieved through utility of the additional degrees of freedom inherent in a new cyclic interpretation of the Calabi-Yau mirror symmetric SUSY regime of string/brane theory. Just as the UV catastrophe provided a clue for the immanent transition from Classical to Quantum Mechanics, duality in the Turing Paradox (quantum Zeno Effect where an unstable particle observed continuously will never decay), suggests another imminent new horizon in our understanding of reality.

IFM as mentioned provides an intermediate indicator of this developing scenario. The quantum Zeno paradox experimentally implemented in IFM protocols hints at the duality between the regular phenomenological quantum theory and a completed unified or ontological model beyond the usual 4D Gauge formalism of the standard Copenhagen interpretation. Utilizing extended theoretical elements associated with a new formulation for the topological transformation of a 'cosmological least unit' (LCU), a putative empirical protocol for producing IFM with probability, $P \equiv 1$ is introduced in a manner representing a direct causal violation or absolute surmounting of the putatively inviolate quantum Uncertainty Principle imposed by 4D Copenhagen restrictions.

In the 1970's the concept of quantum non-demolition (QND) [1] arose as a process for performing very sensitive measurements without disturbing an extremely weak signal which led to the Weber approach for gravitational interferometry. But there was a trade-off between the accuracy of a QND measurement and its inevitable back-action on the conjugate observable to that being measured. Recently myriad new terms have been introduced for programs exploring manipulation of the quantum uncertainty principle [2,3] for non-collapse of the wave function: Negative Result Measurement (NRM) [4], Quantum Non-Demolition (QND) [3,5,6], Interaction Free Measurement (IFM) [7-15], Quantum Zeno Effect (QZE) [16-19], Bang-Bang Decoupling (BBD) [20], Quantum Error Correction (QEC) [21], Quantum Interrogation Measurement (QIM) [22,23], Counter Factual Computing (CFC) [24,25], Absorption-Free Measurement (AFM) [26,27], Quantum Seeing in the Dark (QSD) [28], Quantum Erasure Experiment (QEE) [29,30], Interaction Free Imaging (IFI) [31] and the Bomb Testing Experiment (BTE) [7].

By definition an interaction (phenomenological) is any action, generally a force, mediated by an exchange particle for a field such as the photon in electromagnetic field interactions. This physical concept of a fundamental interaction regards phenomenological properties of matter (Fermions) mediated by the exchange of an energy/momentum field (Bosons) as described by the Galilean, or Lorentz-Poincairé groups of transformations. "*There has been some controversy and misunderstanding of the IFM system concerning what is meant by 'interaction' in the context of 'interaction-free' measurements. In particular, we stress that there must be a coupling (interaction) term in any Hamiltonian description*." [32].

This is the distinction we are talking about. The Hamiltonian, H is generally used to express a systems energy in terms of momentum and position coordinates based on forces. While it might bring abject clarity to differentiate the differences between our model and the usual framework of Hamiltonian Mechanics; to do so is beyond the scope of this volume and will be addressed in detail elsewhere. Here we wish to introduce a new ontological type of homeomorphic transformation without the phenomenology of an exchange particle mediated by an ontological interactionless or 'energyless' topological switching process based on the concept of 'topological charge' in M-Theoretic brane configurations [33].

As indelibly ingrained in the current mindset; it is *impossible by definition* to violate the uncertainty principle, $\Delta x \Delta p_x \geq \hbar/2$ or $\Delta E \Delta t_x \geq \hbar/2$ within the framework of Copenhagen phenomenology arising from operation of a 'Heisenberg Microscope'. This is a *fundamental empirical fact* demonstrated by the Stern-Gerlach experiment where space quantization is produced arbitrarily along the z axis by continuous application of a non-uniform magnetic field to an atomic spin structure [34], or as demonstrated by Young's double-slit experiment [35] for example. Recent work stemming from the Elitzur-Vaidman bomb-test thought experiment [7] has begun to change the interpretation of this 'immutable law'! The Elitzur-Vaidman bomb-test experiment was first demonstrated experimentally in 1994 [36] using a Mach-Zehnder interferometer (Fig. 3.1); and soon led to two main procedures for improving probability outcomes:

1) Multiple recycled Measurements and
2) Multiple array of Interferometers.

The Mach-Zehnder interferometer [37] works by using pairs of correlated photons produced by spontaneous parametric down-conversion from a molecular crystal such as $LiIO_3$. Initially in the first experiments for a 50-50 beam splitter with a 1-time measurement cycle, the IFM probability was 25% according to the formula in Eq. (3.1) [36]; but for repeated measurements and/or various forms of multiple interferometers it was found IFM probability could be arbitrarily increased toward unity as in Fig. 3.2.

$$\eta = \frac{P(Det2)}{P(Det2) + P(Bomb)} \tag{3.1}$$

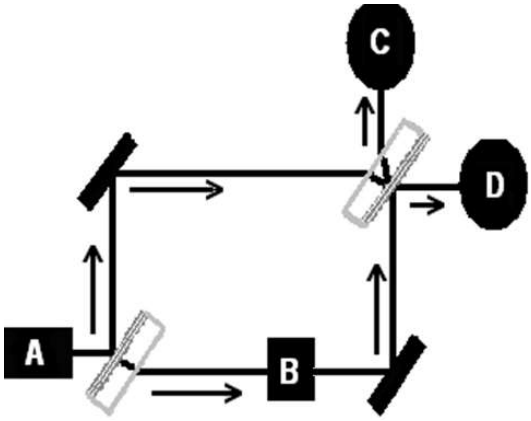

Fig. 3.1 General form of a Mach-Zehnder interferometer used to determine the phaseshift caused by placing a sample in the path of one of two collimated laser beams. **A** is the beam source, B the sample and C & D the detectors. Note the two types of mirrors utilized.

The probability for the IFM model was suggested to occur in powers of $\pi/2N$ by $P_{IFM} = [1 - 1/2(\pi/2N)^2 + ...]^{2N}$ where N is the number of beam splitters in the Max-Zehnder interferometer. In his seminal paper (A thought experiment) Elitzur suggested a maximum IFM of 50%. Thereafter Kwiat's team developed a method to improve the model to 80% with $P_{QSD} = 1 - (\pi^2/4N) + O(1/N^2)$ where in this case N is the number of photon cycles through the apparatus [36]. In regards to the Elitzur and Vaidmann consideration that their model could be explained by the 'Many-Worlds' interpretation Cramer proposed, "*they suggest that the information indicating the presence of the opaque object can be considered to come from an interaction that occurs in a separate Everett-Wheeler universe and to be transferred to our universe through the absence of interference*" [38].

In terms of creative processes in the history of scientific progress, it is profoundly interesting to note that Cramer's suggestion, 'the idea of a Many-Worlds interpretation to explain how IFM works', is an LD shadow the new HD UFM model! In the UFM model of LSXD Calabi-Yau mirror symmetry the supposition is that the 4D Cavity-QED 'particle in a box' state has conformal scale-invariant Supersymmetric (SUSY) 'mirror copies' inherent in the HD Calabi-Yau brane topology [39,40]. Thus if the experimental protocol proposed here is successful it will demonstrate that the IFM model is not suggestive of a reality with 'many parallel worlds' but provides instead indicia of Calabi-Yau mirror symmetric topological 'copies' extending 'our' reality beyond the veil of stochastic spacetime [40] to a 3rd UFM regime with LSXD; and that these extra degrees of freedom, when properly accessed, allow the uncertainty principle to be surmounted in one pass with probability, $P \equiv 1$.

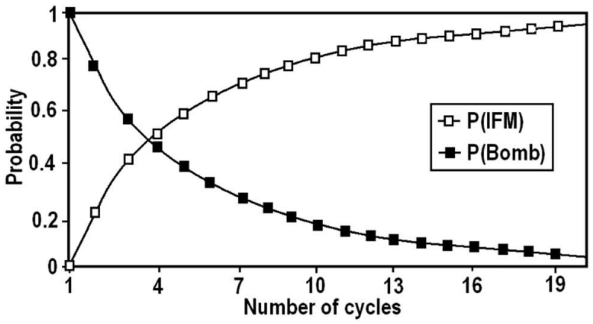

Fig. 3.2 IFM probability as shown to be arbitrarily increased toward unity by repeated measurements. Figure adapted from [36].

In this chapter a putative protocol is delineated, not for another sophisticated improvement of the varied stepwise degrees of violating the uncertainty relation by the several IFM protocols; but for completely surmounting the uncertainty relation directly, in a straight forward manner, for any and every singular resonant action, with probability, $P \equiv 1$. As stated in an unexpected way our model has similarities to IFM/QSD, but instead uses extended quantum theory and newly developing UFM theory [40] to fully complete the task of uncertainty violation. The HD regime of the unified protocol is like a complete IFM fun house 'hall of mirrors' where the whole battery of interferometers and multiple cycling routines is inherent in the HD mirror symmetric brane regime, such that only one 'ontological measurement' is required to obtain probability, $P \equiv 1$. We emphasize that the methodology of this new empirical protocol is completely ontological (rather than usual phenomenological field couplings mediated by energy exchange quanta) with action in the HD SUSY regime in causal violation of the 4D Copenhagen phenomenology, not in an Everett 'many-worlds' sense [41], but in a manner that extends to completion the de Broglie-Bohm-Vigier causal interpretation of quantum theory [42] with a so-called 'super-quantum potential', the ontological 'force of coherence' of UFM (not a 5^{th} force). The ontological basis is realized utilizing the additional degrees of freedom of a 12D version of M-Theory [43] along with the key supposition of conformal scale-invariance pertaining to the state of quantum informational SUSY brane mirror symmetric copies extended to Large-Scale Additional Dimensions (LSXD) [39].

While considerations of the vacuum bulk are of paramount concern for string theory, much of its putative essential parameters used here are ignored in the avid exploration of other parameters. The $P \equiv 1$ model also relies heavily on the existence of a Dirac covariant polarized vacuum [44-46]. Of primary concern at this point of our development is the Dirac vacuum inclusion of extended electromagnetic theory [47-49] which is a key element in manipulating the structural-phenomenology of LSXD SUSY brane topology with a spin-exchange resonant hierarchy.

The experimental design relies heavily on the utility of a new fundamental action principle inherent in the LSXD cyclical brane topology putatively driving the evolution of self-organization in spacetime as a complex system of cellular automata-like Least Cosmological Units (LCU) tessellating space [39]. Stated more directly, space, spacetime (no longer considered fundamental but emergent) and the HD mirror symmetric Calabi-Yau brane structure is an evolutionary form of self-organized complex system.

The new action principle is suggested not to be a 5^{th} force of nature per se, but a combination of the four known forces as united in the unified field (not quantized). Initially this can appear confusing because the three known forces are phenomenological in action, i.e. mediated by the Hamiltonian for phenomenological energetic field exchange quanta, whereas the topological field is mediated by an 'ontological charge' of the unified field. Which is therefore is energyless by definition, albeit it acts as a 'force of coherence' in conjunction with the driving of LSXD brane conformation dynamics. Continuous evolution of the ontology is a form of 'becoming' or merging of one informational aspect with another without the exchange of energy, as in the until now usual sense of a physical field [39]. This key UFM aspect is difficult to comprehend at first, because it is also a challenge for us to explain.

Topologically, the HD Calabi-Yau mirror symmetric copies, $\pm\mathbb{C}^4$ in Fig. 3.2 are in constant motion [39,40]. Later we will see this inherent synchronization backbone (as called for by Feynman) is essential to providing a resonance hierarchy 'beat frequency' for surmounting uncertainty, and of paramount importance to QIP for bulk UQC.

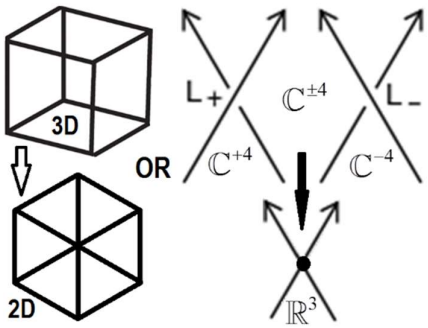

Fig. 3.3. Euclidean 3-space, $\mathbb{R}^3$ as a 'fixed' shadow of LSXD Calabi-Yau, L, R mirror symmetric topological brane (crossover) components in continuous-state cyclic evolution, with 4 complex HD dimensions suppressed for simplicity.

The field concept is a supporting paradigm of the entire edifice of modern physics; until now specifically for phenomenological field dynamics only. Be reminded that physically, physicists have no idea what a field is, we are only able to associate it with a metric and parametrize various phenomena. Our view of what constitutes an ontological field is radically different. We do not feel equipped to definitively define the distinction rigorously in this volume (as the whole nascent edifice of UFM has yet to even reach infancy); but realize we cannot get away with saying nothing either, (Chap. 12). We want to let experiment drive theory at this moment in development [39,40]. Suffice it to say the ontological properties of the dynamics inherent in the HD unified field theoretic topological brane world do not transfer energy, and the 'exchange' of information also does not occur in time; further hinting at bringing into question the historically fundamental basis of 'locality and unitarity'. The best metaphor we know for energyless ontological charge is the switching of central vertices of the ambiguous Necker cube when stared at (Fig. 3.4a).

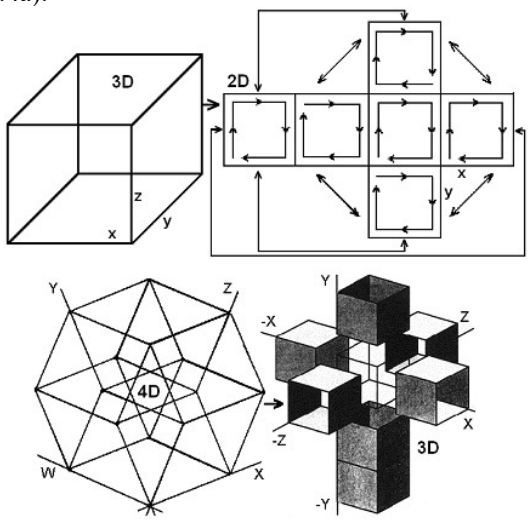

Fig. 3.4. Dimensional reduction. The suggestion is that the central translucent cube in the lower right represents a 4D CQED 'particle in a box' quantum state that through conformal scale-invariance remains physically real when the metaphor is carried to 12D where the nilpotent space-antispace state components become like the 'mirror image of a mirror image' and in that sense is causally free of the localized, E_3 quantum state, thereby open to ontological 'energyless' information transfer in violation of Copenhagen uncertainty.

Regarding Fig. 3.4, there is no 'event' relative to the perceived switching of the vertices of the metric of the cube in 3D (rather suggested to occur in 4D extensions like the spherical rotation of the Dirac electron requiring 720^{o} to complete). For a cellular automata-like close-packed 12D dual space tessellation of an array of such hyperspherical objects, (the 3D nilpotent resultant designated as quantum particle/states in a box) we propose that quantum entanglement occurs in a conformal scale-invariant LSXD brane topology with inherent cyclic mirror symmetric copies of the usually considered stationary 3D Cavity-QED quantum 'particle in a box'. This provides sufficient degrees of freedom for allowing quantum uncertainty to be surmounted, thus avoiding problems associated with decoherence times in QC. In this scenario quantum mechanical uncertainty is a manifold of finite radius separating two regimes of infinite size dimensionality - the 3(4)D Euclidean/Minkowski and a complexified mirror symmetric 8D LSXD M-Theoretic brane world [40].

The de Broglie-Bohm-Vigier Causal [42] and Cramer Transactional Interpretations [38,50] have generally been ignored by the physics community for various reasons; most saliently considered to add nothing new or are incomplete interpretations. The Quantum Potential-Pilot Wave model is extended to a form of 'Super Quantum Potential' synonymous with a putative action of the Unified Field; the future-past parameters of Cramer's model [50] enhance the hierarchy of Calabi-Yau mirror symmetry annihilation-creation parameters. The two theories together form key pillars for an ontological basis of the predicted 'Force of Coherence' of the Unified Field which is a mandatory requirement in the new model for developing UQC.

If the metaphor in Fig. 3.4 if carried to the 5D 'cross' in the lower right corner would be comprised of 4D hypercubes instead of the 3-cubes shown in the dimensional reduction. Table 3.2 below shows the geometric content of spacetime carried to 12D. Our scale-invariant theory predicts that the 12D copy of the quantum state is causally free of the 3D shadow of this quantum state or 'particle in a box' (3D generator is a misnomer as used in terms of the usual sense of a Euclidean observer - The 3D quantum state or particle in a box is the resultant in terms of the 12D model of nilpotent potentia [39]). The task of this chapter is to elucidate the methodology for surmounting uncertainty in this LSXD context. The experimental apparatus, a multi-level rf-pulsed interferometer, is designed to focus/ mediate/manipulate this unitary field. It is going to be a severe challenge for a while longer to encapsulate the observer physically. The 3-space we observe is virtual; the physically real space is the hidden HD space [39,40]. Fortunately, we can perform our proposed experiment without getting any acceptance of this temporary 'heresy'; be advised von Neumann said something similar, only now we are nearly able to do something about it.

As we hope to show the protocol relies on the symmetry conditions of new self-organized cosmological parameters amenable to a resonant hierarchy of coherently controlled topological interactions able to undergo what Toffoli calls 'topological switching' as the energyless basis for the Micromagnetics [33] of information exchange. Finally, to complete the concatenation of concepts we utilize theoretical modeling in conjunction with the parameters associated with a covariant polarized Dirac vacuum [44-46] (another heresy) as described from the context of extended electromagnetic theory [47-49] (more heresy). In other Chaps. we show how this model relates to an M-Theoretic dual form of Calabi-Yau mirror symmetry; the conceptual mantra of which is: Continuous-state, spin-exchange, dimensional reduction, compactification process. Not a unique 4D compactification to the standard model as sought by string theorists, but a continuous cyclic dimensional reduction 12D $\rightleftarrows$ ~0D symmetry exchange through pertinent aspects all five M-Theories [39,40].

3.2 The Turing Paradox and Quantum Zeno Effect

By using the quantum Zeno effect, also known as the Turing paradox, the efficiency of an IFM can be made arbitrarily close to unity.

> "*It is easy to show using standard theory that if a system starts in an eigenstate of some observable, and measurements are made of that observable N times a second, then, even if the state is not a stationary one, the probability that the system will be in the same state after, say, one second, tends to one as N tends to infinity*

... continual observations will prevent motion ...” – A. Turing [51].

The Turing Paradox also called the Quantum Zeno Effect is a scenario where a particle observed continuously will never decohere; in a sense the evolution of the system is frozen by frequent measurement in its initial state. More technically the Quantum Zeno Effect can suppress unitary time evolution not only by constant measurement, but applying a series of sufficiently strong fast pulses with appropriate symmetry can also decouple a system from its decohering environment or other stochastic fields [52-60].

Cramer has suggested that IFM can be interpreted by utilizing the Everett ‘Many Worlds Hypothesis’ to explain the subtleties of the quantum Zeno paradox [3,38]. While Cramer’s hypothesis is certainly logical we believe nature in higher dimensions (HD) is more surprising [39,40]. The Standard Model of Quantum Mechanics predicts that physical reality is influenced by events that can potentially happen (Heisenberg potentia) but factually do not occur. Peise [58] suggests that IFM exploits this counterintuitive influence to detect the presence of an object without requiring any interaction with it. “*Here we propose and realize an IFM concept based on an unstable many-particle system. In our experiments, we employ an ultracold gas in an unstable spin configuration, which can undergo a rapid decay. The object (realized by a laser beam) prevents this decay because of the indirect quantum Zeno effect and thus, its presence can be detected without interacting with a single atom. Contrary to existing proposals, our IFM does not require single-particle sources and is only weakly affected by losses and decoherence. We demonstrate confidence levels of 90%, well beyond previous optical experiments*.” [58].

Our UFM model is radically different [39,40]. There is in a sense no interaction [32,39], but not in the sense Paise suggests. His claim is based on the usual ‘quantal or phenomenological’ form of interaction. But as we shall see in later chapters, there is another UFM type of ‘energyless’ ontological interaction or exchange of information based on ‘topological charge’ in HD brane topology [39,40] described by a new 3rd regime theory we call ‘Ontological-Phase Topological Field Theory’(OPTFT). This model arises in answer to recent forays into relativistic information processing [61-64] calling for an end to the historically fundamental utility of ‘locality and unitarity’ as the basis for describing the nature of reality [65-67]. The measurement problem is not yet solved.

The recent introduction of relativistic parameters, including relativistic r-qubits, into quantum information processing has compounded the dilemma bringing up new questions in terms of Bell’s inequalities, the no-cloning and quantum erasure theorems. Correspondence to the epistemic view of the Copenhagen Interpretation versus the ontic consideration of objective realism and as merged by W. Zurek’s epi-ontic blend of quantum redundancy in quantum Darwinism will be discussed [68,69]. Finally, after making further correspondence to current thinking in terms of the dual amplituhedron we delve into the ontological topology of UFM requiring a new set of topological transformations beyond the Galilean, Lorentz-Poincairé. We hope to have taken a bold step at least philosophically correct into the new UFM arena.

3.3 From the Perspective of Multiverse Cosmology

Comprehending the $P \equiv 1$ model from the perspective of cosmology is only necessary for more fully understanding the context from which developing the experimental protocol arises; otherwise the reader may skip to the next section, especially since no one seems to understands it very well yet anyway. When physicists last embraced a 3D Newtonian world view about a hundred years ago, the universe was believed to be a predictable mechanical clockwork. Since the advent of Quantum Theory (QT) reality has been considered to be stochastic and statistical or uncertain with a Planck scale basement. Following this line of reasoning when a Theory of Everything (TOE) is realistically discovered based on formalizing a unified field, should some form of fundamental monism be embraced? Although the fermionic point-particle is considered the basic unit of physics, this concept is embedded in the global context of cosmology. We postulate that additional cosmology is required to understand the basis for

bulk Universal Quantum Computing (UQC) because cosmology ultimately speaks to the nature of reality and the ultimate basis for the Fermionic singularity or point particle; and we are finding out that using a nonphysical mathematical calculation space is not sufficient for UQC implementation. The three regimes stated above (classical, quantum and unified field TOE) are currently thought to have a Planck-scale 'basement of reality'. It remains impossible to surmount uncertainty in this context; it is perceived as an inadequate view requiring a reality with an open LSXD 'continuous-state' process instead of an impenetrable basement barrier [39]. Not seeing XD because they are curled up at the Planck scale is not the only interpretation. If the continuous-state process includes a form of 'subtractive interferometry', like discrete frames of film passing through a movie projector appearing continuous on the screen, additional dimensionality can be large scale. Experiments under development at CERN are trying to make this discovery, our proposal however, is tabletop and low energy [39,40].

Regarding 'Continuous-State': Imagine Einstein's elevator metaphor with an observer inside in freefall. Next imagine an amusement park pin raster (pins as points in spacetime) with the little ball bouncing stochastically off the nails towards a slot at the bottom of the device. Now consider the observer inside the elevator to be the falling ball. But instead of the ball being drawn gravitationally toward a final slot at the bottom (pulled toward center of the Earth by G), imagine that the pin raster continuously rotates (hyperspherically) so that the ball perpetually remains at the center as if it were in continuous freefall. Also that the ball is not a OD vertex, but comprised of HD cyclic brane topology [39]; with a point in reality a dynamic transformation comprised of a Wheeler-Feynman-Cramer-like complementarity [50,70] of the three regimes in a background independent environment [71-74] as outlined in another chapter.

Einstein stated that 'all of physics' is based on measurements of *duration* and *extension*. This has occurred historically within the parameters of a 3D Euclidean, and in recent times, a 4D Minkowski-Riemann energy dependent spacetime metric, $\hat{M}_4$ under Gauge parameters utilizing various forms of the $E_3 / \hat{M}_4$ Galilean-Lorentz-Poincairé transformations describing classical, quantum and relativistic conditions. These criteria are perceived herein as insufficient for UQC operations, and indeed our protocol for surmounting the uncertainty principle requires inclusion of another cosmological regime - Unified Field Mechanics (UFM) [39,40] described by a new set of 12D transformations we propose calling the 'Noetic UFM Transformation' because of its relevance to aspects of a Holographic Anthropic Multiverse correlated with the observer and meaning of the Greek term noetic as 'hidden'. In this regard in spite of Bell's theorem, following Einstein's dice playing conundrum, we restate his complaint that quantum theory is incomplete and therefore inadequate in current form for supervening some quantum processes.

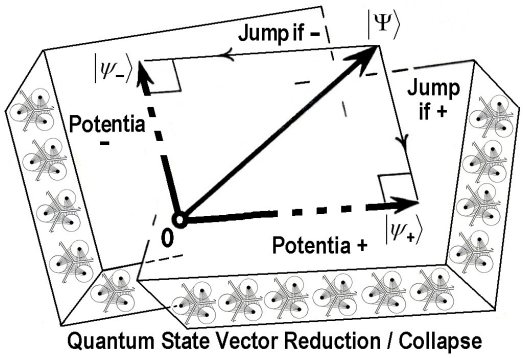

Fig. 3.5 A way to conceptualize a transaction as a collapse, $|\Psi\rangle$ to the 2D Euclidian plane from, in this case, an HD potentia of two possible orthogonal states, $|\psi_+\rangle, |\psi_-\rangle$ mediated by the underlying nilpotent annihilation-creation process inherent in the Least Cosmological Units (LCU) tessellating space behind the finite radius veil of uncertainty. The LCUs are the gatekeepers of spontaneous symmetry breaking. The LCU array can be compared to Fig. 3.7 where a Euclidean cube emerges from spacetime 'lattice gas'. (Illustrated here as a 3rd dimension with 9 others suppressed).

Cramer's transactional model of QT [50] has been ignored by the physics community for a variety of reasons we will not address now. Its marginalization means that it's utility as a key foundation of extended UFM cosmology is not well received. Cramer based his interpretation on the Wheeler-Feynman Absorber Theory [70]. Thus a *Cramer transaction* entails Wheeler-Feynman-like future-past, standing-wave symmetry conditions to describe a present instant which when extended to the HD SUSY regime readily lends itself as a foundation for Calabi-Yau mirror symmetry conditions inherent in a unique background independent 12D brane iteration of M-Theory [43] (derived elsewhere). Note: Some have criticized Cramer's standing-wave concept as simplistic. This might of course be valid for a line element as a 1D string; but we feel the model when sufficiently developed for 9D hyperspherical brane topology as required by our model; it is sufficient as it becomes synonymous with a 6D Calabi-Yau Kahler manifold. In differential geometry, a Kahler manifold has three mutually compatible structures; a complex structure, a Riemannian structure, and a smooth symplectic differential 2-form.

Furthermore, we suggest that the UFM 12D noetic transform adds additional de Broglie-Bohm piloting-super-quantum potential [39,40] parameters, suggesting a duality to the regime of quantum mechanics – that of the observed 4D phenomenological interaction associated with the uncertainty principle; and another ontological HD nilpotent 'piloted' regime associated with the coherent force of the unified field. There seems to be a 'semi-quantum limit' associated with a manifold of uncertainty (MOU) of finite radius as the lower bound with an inherent gating mechanism (uncertainty) blocking entry to the LSXD beyond. Experiment will settle this issue [39,40].

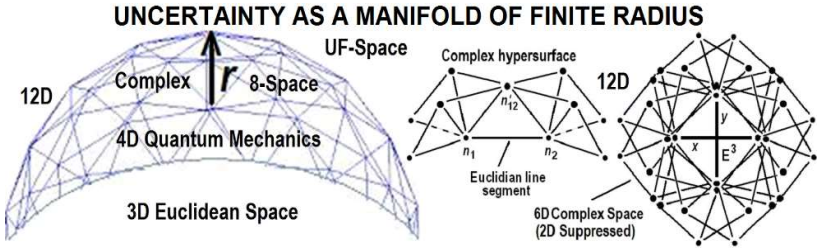

Fig. 3.6. Manifold of uncertainty of finite radius in the semi-quantum limit as a transition barrier between infinite dimensional Euclidean space and LSXD infinite dimensional UFM space. Because of Calabi-Yau dual 3-tori mirror symmetry we suspect it is a 5D manifold with the 6th dimension degenerate ending the domain wall. Experiment will test this limit.

As discussed in Chap. 3, reality completed by UFM, is a multi-tiered duality of a virtually static Euclidean subspace manifold with a dynamic HD de Broglie-Bohm piloted Cramer-like continuous-state standing-wave cyclical evolution. Because the external world we observe is this limited virtual submanifold of a more complete nilpotent (sums to zero) [39] contiguous superspace, some elements are removed from observation by subtractive interferometry [39]. This interpretation suggests that the reason additional XD brane dimensionality is not observed is not because it is curled up microscopically at the Planck scale, but because subtractive interferometric annihilation-creation vectors of the nilpotent standing-wave process of the localized line element 'erase' the HD generators of the present moment keeping those parameters hidden from the observer's view by a Heisenberg microscope because of the observational limit to our sensory apparatus provided by the veil of uncertainty.

In the standard Copenhagen Interpretation of QT an event emerges only as a result of measurement and objective reality is considered limited to probability. Cramer considers 'all off diagonal elements of the line element physically real' during the process of the offer-wave-confirmation-wave process preceding a local transaction (event) [50]. We may call the final event a resultant of the conditions of Heisenberg Potentia. Here we wish to consider (a more complete) reality that has remained illusory to the Minkowski observer hidden to the temporal observer behind the veil of the uncertainty principle.

Issues regarding the nature of the fundamental cosmological background continue to be debated with disparate views jockeying for philosophical supremacy; a scenario remaining tenable because experimental avenues for testing physics beyond the standard model have remained elusive. In our favor deeper and deeper cracks are occurring in QED violation [75]. QED is a relativistic quantum field theory

of electrodynamics; the most stringently tested and most accurate theory in physics specifically for measurements of the fine structure constant, α, where $\alpha^{-1} = 137.035999074(44)$, from CODATA 2010. QED violation suggests we are on the brink of falsifying quantum mechanics in 4D [39,40,75]. Absolute truth occurs in science when a theory becomes falsified. In this respect with the advent of Quantum Mechanics the Newtonian Classical world view became an 'absolute truth' in the finite domain it describes. UFM is presenting a similar scenario for the falsification of Quantum Mechanics.

Here a putative empirical protocol is devised for manipulating a HD form of the so-called covariant Dirac polarized vacuum (DPV) [47-49] providing a methodology for both surmounting uncertainty and low energy protocols for testing the dimensionality of string theory. The DPV has a sixty-year history in the physics literature [44-49] which has for the most part been ignored by the main stream physics community for a number of philosophical conflicts most notably the DPV, and its associated Extended Electromagnetic Theory which includes photon mass, is erroneously perceived to conflict with the highly successful Gauge Theory. As well-known Gauge theory is an approximation, suggesting additional physics. The problem of surmounting uncertainty is simplistically solved by the utility of additional degrees of freedom introduced by a UFM multiverse cosmology and the associated extended theoretical elements. We will develop salient features as we proceed.

3.4 Micromagnetics and LSXD Topological Charge Brane Conformation

An extensive body of literature exists for phenomena related to the zero-point field; but relative to unified theory this work is considered metaphorically descriptive only of the 'fog over the ocean' rather than the structural-phenomenology of the ocean itself. Instead a deep HD structure with a real covariant DPV at its foundation is utilized [44-46]. The Casimir, Zeeman, Aharanov-Bohm and Sagnac effects are considered evidence for a Dirac vacuum. New assumptions are made concerning the DPV relating to the topology of spacetime and the structure of matter cast in a 12D form of Relativistic Quantum Field Theory (RQFT) in the context of the Holographic Anthropic Multiverse (HAM) cosmological paradigm [39]. In this cosmology the observed Euclidian-Minkowski spacetime present, $E_3 - \hat{M}_4$ is a virtual standing wave of highly ordered Wheeler-Feynman-Cramer retarded-advanced future-past parameters respectively [50,70]. See Figs. 3.22 & 3.23 for a graphic illustration of this paradigm. An essential ingredient of HAM cosmology is that a new action principle synonymous with the force of coherence of the unified field arises naturally and is postulated to drive self-organization and evolution through all levels of scale [39,40].

In this context an experimental design [39,40] is introduced to isolate and utilize the new UFM action to test empirically its putative ability to effect conformational structure of the topology of spacetime to surmount the usual phenomenologically based uncertainty in an ontological matter with probability, $P \equiv 1$. Properties of the Least Cosmological Unit (LCU) is an essential key factor in the experimental design.

Unified Theory postulates that spacetime topology is 'continuously transformed' by the self-organizing properties of the long-range coherence of the unified field [39,40]. In addition to manipulating conformational change in HD brane topology, from the experimental results we attempt to calculate the energy Hamiltonian required to manipulate Casimir-like boundary conformation in terms of the unified field equation, $F_N = \aleph / \rho$ (simple unexpanded form - derived in Chap 3). This resonant coupling produced by the teleological action of the unified field driving its hierarchical self-organization has local, nonlocal and supralocal [1](complex LSXD) parameters. The Schrödinger equation, extended by the addition of the de Broglie-Bohm quantum potential-pilot wave mechanism

[1] Nonlocal, complex regime of instantaneous action at a distance; by 'supralocal' we mean LSXD aspects with additional UFM complex topological properties. It may be that nonlocal should incorporate what we call here supralocal UFM parameters; but a distinction needs to be made and we are not there yet with clarity in that decision.

has been used to describe an electron moving on a manifold; but this is not a sufficient extension to describe HD unified aspects of the continuous-state (Chap. 3) symmetry breaking of spacetime topology which requires further extension to include action of the unified field in additional dimensions.

The basic time dependent Schrödinger equation takes the form

$$i\hbar\frac{\partial}{\partial t}\Psi(r,t)=\left[-\frac{\hbar^2}{2m}\nabla^2+V(r,t)\right]\Psi(r,t) \tag{3.2}$$

where i is the square root of -1, $\hbar$ the reduced Planck constant, t time, r position, $\Psi(r,t)$ the wave function, ∇^2 the Laplacian operator and $V(x)$ is the potential energy as a function of position. The simplest de Broglie-Bohm pilot wave addition is

$$i\hbar\frac{\partial}{\partial t}\Psi(r,t)=\left[-\frac{\hbar^2}{2m}\nabla^2+V(r,t)-Q\right]\Psi(r,t) \tag{3.3}$$

with the quantum force potential $Q=-\dfrac{\hbar^2}{2m}\dfrac{\nabla^2\sqrt{\rho}}{\sqrt{\rho}}$.

I have not found any attempt in the literature to extend the de Broglie-Bohm pilot wave-quantum potential to String/M-Theory in the literature, which is one of several key criteria for developing our UFM model. But there is a small body of literature correlating de Broglie-Bohm with the Dirac equation [76].

The nilpotent Dirac equation is an intermediate step for our UFM needs. Following Rowlands [77], who firmly believes in the utility of quaternionic algebra in simplifying particle physics [78-84].

Rowlands claims particle physics is more easily understood if the Dirac equation is expressed algebraically, replacing the gamma matrices by equivalent operators from vector and quaternion algebra [78-84]. Unit quaternion operators (1, ***i, j, k***) are defined according to the usual rules:

$$\begin{gathered} i^2=j^2=k^2=ijk=-1 \\ ij=-ji=k;\ jk=-kj=i;\ ki=-ik=j, \end{gathered} \tag{3.4}$$

with multivariate 4-vector operators (i, **i, j, k**), which are isomorphic to complex quaternions or Pauli matrices:

$$\begin{gathered} \mathrm{i}^2=\mathrm{j}^2=\mathrm{k}^2=1 \\ \mathrm{ij}=-\mathrm{ji}=i\mathrm{k};\quad \mathrm{jk}=-\mathrm{kj}=i\mathrm{i};\quad \mathrm{ki}=-\mathrm{ik}=i\mathrm{j}. \end{gathered} \tag{3.5}$$

Combination these two sets of units produces a 32-part algebra (group of order 64, with both + and – signs), which can be directly related to that of the five γ matrices, with mappings of the form:

$$\gamma^0=\text{-}i\boldsymbol{i};\ \gamma^1=\mathrm{i}\boldsymbol{k};\ \gamma^2=\mathbf{j}\boldsymbol{k};\ \gamma^3=\mathbf{k}\boldsymbol{k};\ \gamma^5=i\boldsymbol{j}. \tag{3.6}$$

or, alternatively,

$$\gamma^0=\text{-}i\boldsymbol{k};\ \gamma^1=\mathrm{i}\boldsymbol{i};\ \gamma^2=\mathbf{j}\boldsymbol{i};\ \gamma^3=\mathbf{k}\boldsymbol{i};\ \gamma^5=i\boldsymbol{j}. \tag{3.7}$$

Application directly to the conventional form of the Dirac equation,

$$\left(\gamma^0\frac{\partial}{\partial t}+\gamma^1\frac{\partial}{\partial x}+\gamma^2\frac{\partial}{\partial y}+\gamma^3\frac{\partial}{\partial z}+im\right)\psi=0, \quad (3.8)$$

we obtain:

$$\left(-i\boldsymbol{i}\frac{\partial}{\partial t}+\boldsymbol{k}\mathbf{i}\frac{\partial}{\partial y}+\boldsymbol{k}\mathbf{j}\frac{\partial}{\partial x}+\boldsymbol{k}\mathbf{k}\frac{\partial}{\partial z}+im\right)\psi=0\,. \quad (3.9).$$

Multiplying the equation from the left by ***j*** alters the algebraic representation to (3.9) and the Dirac equation becomes:

$$\left(i\boldsymbol{k}\frac{\partial}{\partial t}+\boldsymbol{i}\mathbf{i}\frac{\partial}{\partial y}+\boldsymbol{i}\mathbf{j}\frac{\partial}{\partial x}+\boldsymbol{i}\mathbf{k}\frac{\partial}{\partial z}+ij m\right)\psi=0. \quad (3.10)$$

The Dirac equation allows four solutions, corresponding to the four fermion – antifermion combinations, with spin up and spin down, which can be arranged in a column vector, or as a Dirac 4-spinor. Here, we identify the solutions as produced by the combinations of $\pm E,\pm\ \mathbf{p}$ (or $\boldsymbol{\sigma}\cdot\mathbf{p}$). . Rowlands writes these terms in the form:

$$\begin{aligned}
\psi_1&=\left(\boldsymbol{k}E+i\boldsymbol{i}\mathbf{p}+ij m\right)e^{-i(Et-\mathbf{p}\cdot\mathbf{r})}\\
\psi_2&=\left(\boldsymbol{k}E-i\boldsymbol{i}\mathbf{p}+ij m\right)e^{-i(Et+\mathbf{p}\cdot\mathbf{r})}\\
\psi_3&=\left(\boldsymbol{-k}E+i\boldsymbol{i}\mathbf{p}+ij m\right)e^{i(Et-\mathbf{p}\cdot\mathbf{r})}\\
\psi_4&=\left(\boldsymbol{-k}E-i\boldsymbol{i}\mathbf{p}+ij m\right)e^{i(Et+\mathbf{p}\cdot\mathbf{r})}
\end{aligned} \quad (3.11)$$

and apply a single differential operator, but it is more useful to remove the variation in the signs of E and $\mathbf{p}$ from the exponential term, by making the differential operator a 4-term row vector, which, in the equation, forms a scalar product with the Dirac 4- spinor. Incorporating all four terms into a single expression, we obtain

$$\left(\pm i\boldsymbol{k}\frac{\partial}{\partial t}\pm\boldsymbol{i}\,\boldsymbol{\nabla}+ij m\right)\left(\pm\boldsymbol{k}E\pm i\boldsymbol{i}\mathbf{p}+ij m\right)e^{-i(Et-\mathbf{p}\cdot\mathbf{r})}=0 \quad (3.12)$$

as the new version of the Dirac equation for a free particle [81]. Reducing this to the eigenvalue form, and multiplying out, produces the classical relativistic momentum-energy conservation equation:

$$\left(\pm\boldsymbol{k}E\pm i\boldsymbol{i}\mathbf{p}+ij m\right)\left(\pm\boldsymbol{k}E\pm i\boldsymbol{i}\mathbf{p}+ij m\right)=E^2-p^2-m^2=0. \quad (3.13)$$

It is significant that there are exactly four solutions to the Dirac equation. Both quaternion and complex operators require equal representation for + and – signs, suggesting eight possible sign combinations for $\pm\boldsymbol{k}E\pm i\boldsymbol{i}\mathbf{p}+ij m$; but only four of these will be independent, since the overall sign for the state vector is an arbitrary scalar factor. Thus, the sign of one ***kE, ii*** **p** or ***ij*** *m* must behave as if fixed. With only E and $\mathbf{p}$ terms represented in the exponent, it is evident that the fixed term is m. Four solutions also result from the fact that quaternionic structure of the state vector can be related to the

conventional 4 x 4 matrix formulation with quaternionic matrices. The conventional formulation is itself uniquely determined by the 4D spacetime signature of the equation, a 2nD spacetime requiring a 2^n x 2^n matrix representation of the Clifford algebra [82].

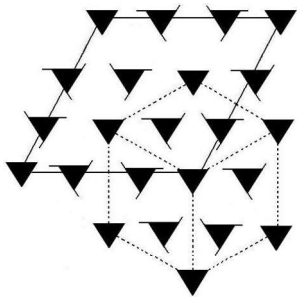

Fig. 3.7 HD emergence of structure from a LD lattice gas tessellation. If the central vertex of the projective cube represents a Euclidian point, the 12 satellite points represent HD control parameters. The triangles with obverse tails represent left-right raising and lowering nilpotent symmetry.

In the case of quaternionic matrices, it is significant that the hidden quaternion operators ***i, j, k*** applied, along with 1, to the rows and columns, and also to the rows of the Dirac 4-spinor, are identical in meaning to the same operators applied to the terms in the nilpotent state vector, as one can be derived from the other. There are good reasons for believing that the nilpotent form of the Dirac equation is the most fundamental. It is automatically second quantized, fulfilling all the requirements of a quantum field theory; it removes the infrared divergence in the fermion propagator, and the divergent loop calculation for the self-energy of the non-interacting fermion; and it introduces supersymmetry as a mathematical operation without the need for additional particles [84].

> Physically, the fermion can be considered to see in the vacuum its 'image' or virtual antistate, producing a kind of virtual bosonic combination, and leading to an infinite alternating series of virtual fermions and bosons. Each real fermion state creates a virtual antifermion mirror image of itself in the vacuum, while each real antifermion state creates a virtual fermion mirror image of itself. The combined real and virtual particle creates a virtual boson state. Real fermions and real antifermions, of course, provide real mirror images of each other [84].

This is far as we will take the model in terms of development in this Chapter; what is needed for the next step is an additional space-antispace doubling, requiring a Complex Quaternion Clifford Algebra to describe. Compounded by development of the new UFM transformation cast in what we propose as an Ontological-Phase Topological Field Theory (OPTFT) going beyond the historic requirement for a fundamental basis of 'locality and unitarity' possibly utilizing an amplituhedron [65-67].

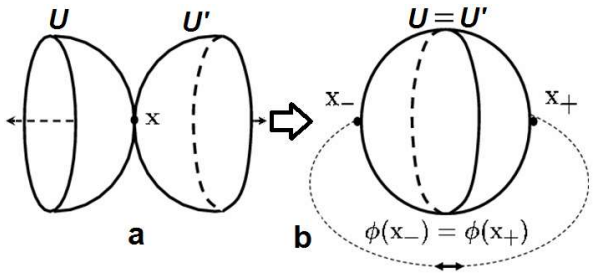

Fig. 3.8. Shadow point, *x* becomes unknotted (or knotted) in the continuous-state cyclic process that when various topological moves are performed dimensional raising and lowering may occur as part of cyclically opening and closing the algebraic description.

The Unified Field [40] produces periodic symmetry variations with long-range coherence that can

lead to a topological phase effect like a coherently controlled Ising model lattice gas rotation of the Riemann sphere spacetime backcloth [85] (catastrophe theory Sect. 7.5). This can be described by a form of double-cusp catastrophe dynamics (Fig. 3.11).

The coupled modes of this process rely on a special form of the harmonic oscillator called the Dubois incursive oscillator [86-90]. There is an inherent force of coherence [39,40,91]. For example, for an Earth observer's temporal perception in Euclidean 3-space, railroad tracks recede into a point at the horizon. For an atemporal HD observer, the tracks remain parallel. This is the cyclic action of the coherence force forming an exciplex-like spacetime cellular automata logic gate driving equilibrium of the topologically charged Casimir boundaries to parallel or degenerate modes thus giving rise to the possibility of effecting conformational state interactions 'opened' and 'closed' by resonant incursion [92]. These efforts will be clarified in Chaps. 9 & 11 on topological field theory.

Fig. 3.7 An attempt to illustrate an Ising model lattice gas mechanism for boosting and compactifying dimensionality as inherently driven by a de Broglie-Bohm super-quantum potential or ontological force of coherence of the unified field. We are still developing a format to clarify our explanation. Given that it is postulated that points in Euclidean space are knotted or braided 'shadows' of an HD topological brane structure that is continuously cycling stepwise through a L – R symmetry breaking compactification process; a structure of this sort applies. Relative to Figs. 3.3,3.8, there is no known sequence of Reidemeister moves that will untie a trefoil but moves based on Chern-Simons skein relations can [93].

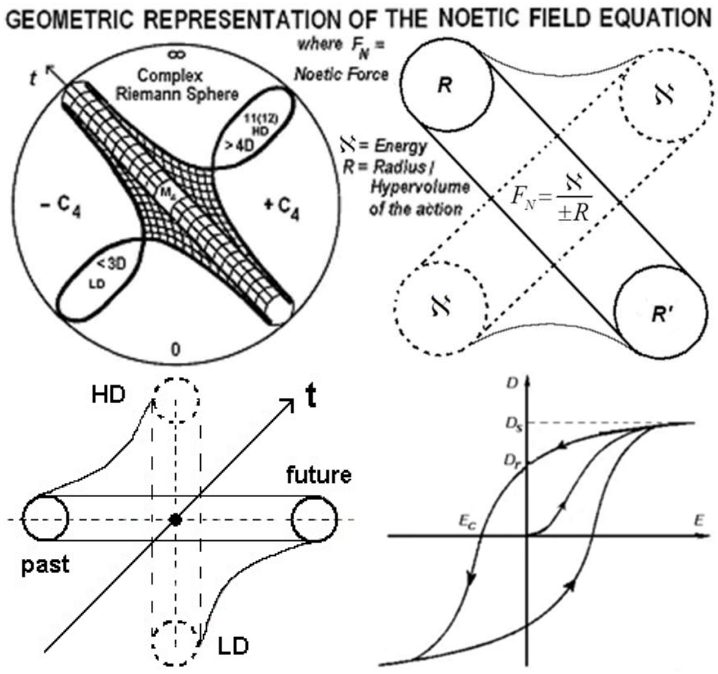

Fig. 3.9. Several topological and geometric idealizations of the putative unified field equation, $F_{(N)} = \aleph / \rho$ describing an action of the unified field, a catastrophic 'coherence effect', on both biological and spacetime manifolds. Fig. 3.9d is a spacetime/brane hysteresis loop signifying the inherent energy of topological charge driving the 'topological switching' of catastrophe.

This is a boundary condition problem; here probably of the Born-von Karman type where the boundary conditions restrict the wave function to periodicity on a Bravais lattice of hexagonal symmetry, stated simply as $\psi(r + N_i a_i) = \psi_r$, where *i* runs over the dimensions of the Bravais lattice, a_i are the lattice vectors and N_i are integers [85,91]. In this model presence of the periodic spherical rotation effects of the cyclical coherence-decoherence modes allow the cyclic action of the unified field.

This Unified Processing is governed by the fundamental equation of unitarity, $F_{(N)} = \aleph / \rho$ (Fig. 3.9). Cyclotron resonance, logarithmic spiral, Kaluza-Klein or genus-1 helicoid 'parking garage symmetry hierarchies (Chaps. 3,4) may be involved in maintaining piloting effects by the unified field or induce an electromotive 'radiation pressure' or topological switching coherence force that effects the topology of spacetime leading to conformational change in the static-dynamic [94-96] leapfrogging' cycle of the topologically charged Casimir-like boundary conditions of HD Calabi-Yau mirror symmetric topological brane states.

We can't be sure yet which of the hierarchical formalisms might be the physical one until some empirical work is performed. Intellectually we lean toward the concept of the action of a cyclotron resonance hierarchy acting on the genus-1 helicoid parking garage structure (Chaps. 3,4) modulated by a form of Bessel function embedded in the complex quaternionic Clifford algebra under study because this format also seems to meld well with catastrophe theory and the future-past symmetry breaking parameters we postulate in to be inherent in the structural-phenomenology of UFM continuous-state spacetime topology. We are utilizing a complex quaternionic Clifford algebra to develop this formalism in order to predict the resonance hierarchy bandwidth.

The structural-phenomenology of atoms and molecules is full of domain walls amenable to description by combinations of Gauss' and Stokes' theorems ordered in terms of Bessel Functions where boundary conditions create resonant cavities built up by alternating static and dynamic Casimir-like conditions [94-96]. As frequency increases central peaks occur with opposite or zero polarity at the domain edges. These properties are relevant to Ising Model [85] spin flips of the domains of the Riemann-Block Spheres effecting homeostatic planes of equilibrium (Fig. 3.11b). The UFM force of coherence can maintain equilibrium or produce catastrophes causing conformational change in the Casimir-like HD spacetime structures [92,97].

The UF 'Coherence Effect' is not a 5th phenomenological force (mediated by quantal field exchange); but an ontological charge or 'Force of Coherence' of energyless Calabi-Yau mirror symmetric (6D dual 3-tori) brane dynamics mediated by what is called topological switching [33] as described by a new set of transformations beyond the Galilean-Lorentz-Poincairé we chose to call the Noetic Transformation in terms of the meaning of the Greek term noetic as 'hidden' because it is deemed to operate in the regime of the as yet unobserved (LSXD) higher dimensions of spacetime [39,40] See Chap. 8 for complete delineation of the complex quaternionic Clifford algebra used for developing the preliminary formalism.

3.5 Catastrophe Theory and the M-Theoretic Formalism

Regarding *dynamical systems* that generally operate in a framework of stability and equilibrium – Technically these systems have a restrictive class called gradient systems which contain singularities or points of *extrema*. Some causal action can institute a bifurcation of an extrema that can initiate a qualitative change in the physical state of the system.

Catastrophe theory[2] describes the breakdown of stability of any equilibrium system causing the system to jump to another state as the control parameters change. The changes in the singularities associated with the bifurcation of extrema are called elementary catastrophes [98-100] and can be described by real mathematical functions

$$f : R^N \to R. \qquad (3.15)$$

[2] The groundwork for Catastrophe Theory began with Poincaré's efforts in 1880 on the qualitative properties of solutions to differential equations; formalized in the 1950's by R. Thom's work mapping singularities in structural stability, he called catastrophes.

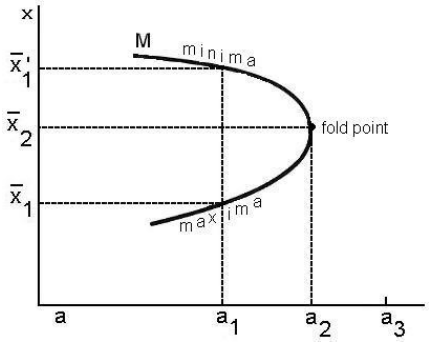

Fig. 3.10. Fundamental minima-maxima fold point basis of catastrophe theory.

The equation describing an elementary catastrophe utilizes variables representing *Control* and *State* parameters of the system and is a smooth real function of r and n where R represents the resultant singularity or catastrophe

$$f : R^r \times R^n \to R\,. \tag{3.16}$$

r (Control Factors)	Number of Catastrophes	Name		Dimensions
r = 1	1	A_2	Fold Catastrophe	2D
r = 2	1	$A_{\pm 3}$	Cusp Catastrophe	3D
r = 3	3	A_4	Swallowtail	4D
r = 4	2	$A_{\pm 5}$	Butterfly	5D
r = 5	4	A_6	Wigwam	6D
r = 3	-	D_{-4}	Eliptic Umbilic	5D
r = 3	-	D_{+4}	Hyperbolic Umbilic	5D
r = 4	-	D_5	Parabolic Umbilic	6D
r = 5	-	D_{-6}	2nd Elliptic Umbilic	7D
r = 5	-	D_{+6}	2nd Hyperbolic Umbil	7D
r = 5	-	$E_{\pm 6}$	Symbolic Umbilic	7D
r = 6	∞	X_9	Double Cusp	9-11D

Table 3.1 The general forms of catastrophes showing how dimensions increase as the number of control factors increase. The names bear some resemblance to the geometric pattern of the catastrophe. The double-cusp catastrophe is perceived as an aid to understanding the resonance hierarchy for surmounting uncertainty.

The r variables are the control parameters of the state variables, n. The function f is therefore an r-parameter family of functions of n variables.

If we let

$$f\left(a_i,...a_r;\;\; x_j,..x_n \right) \tag{3.17}$$

be a smooth real-valued function of $r + n$ real variables we get equation (3.17). The number of elementary catastrophes depends only on r and is finite for $r \geq 5$ totalling eleven (Table 3.1) and infinite for $r \geq 6$.

UNIFIED ACTION ON THE EQUILIBRIUM PLANE OF A DOUBLE-CUSP CATASTROPHE

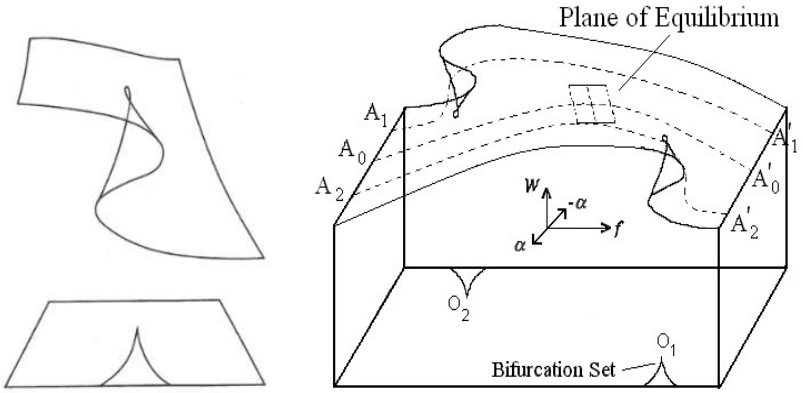

Fig. 3.11. The double-cusp catastrophe (DCC) illustration shows cusps at each end of the plane of equilibrium. The DCC occurs in ≥ 9 dimensions and thought to be the catastrophe form most compatible with UFM symmetry where the plane of equilibrium would be a topological manifold tiled of *least cosmological units* (LCU). This equilibrium manifold operates in conjunction with the inherent Feynman 'synchronization backbone' when undergoing a directed quantum computation best described as interactive computation.

This model can be utilized to call for a new field of vacuum engineering based on the structural-phenomenology of the unified field and whether resultant action of the 'force of coherence' of the unified field is positive or negative. Spacetime cellular automata exhibit complex self-organization. The unified field is the factor driving this self-organization [39,40]; therefore, we postulate hyperincursion and anticipatory properties are inherent in the fundamental hierarchical basis of this self-organization which could be formally described by Double-Cusp Catastrophe Theory.

Unit Circle and Associated Flag Manifold of Temporal Evolution for Noetic Catastrophe Cycle

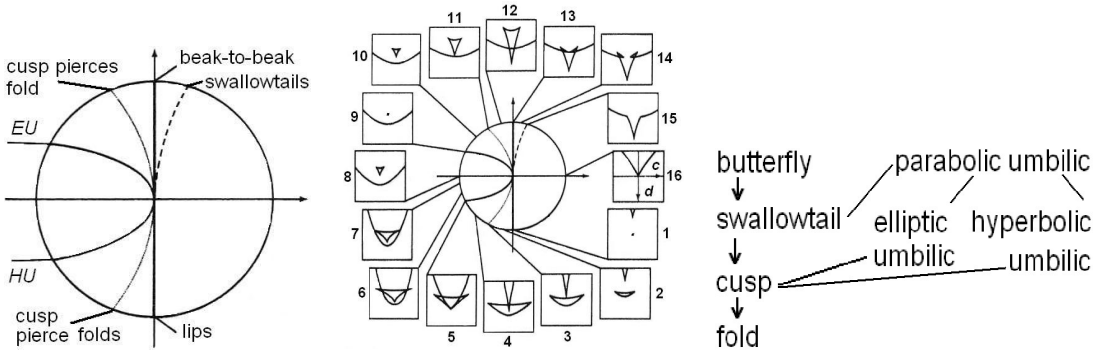

Fig. 3.12 a) represents a plane of the unit circle with corresponding cross sections in b: for example, shows a cusp. A single point in 1 grows to the 'lips' in 2. In 3 to 4 the original cusp 16 penetrates the mouth becoming a hyperbolic umbilic point at 5, turning into an elliptic umbilic at 6, shrinking to a point in 9. Growing again in 10 to pierce the fold line in 11 and through it in 12. A 'beak-to-beak singularity in 13 breaks in 14, collapsing to a swallowtail 15. The seven fundamental catastrophes contain 'subcatastrophes according to the diagram in c. Figures adapted from [98-100].

Fig. 3.11b (bottom) graphically illustrates the fundamental scale-invariant unified field equation

$F_{(N)} = \aleph / \rho$ of the 'force of coherence' of unified field action. Any internal or external stress or change in $\aleph$ is a nonlinear dynamic process producing stability or instability in the boundary conditions of ρ ; an instability in $\aleph \rightarrow$ stress $\rightarrow$ displacement $\rightarrow$ catastrophe $\rightarrow$ jump…whereas stable flux is homeostatic. Further regarding Fig. 3.11b the plane of equilibrium entails a form of hysteresis loop of the Hamiltonian generalized in Fig. 3.9d as future-past parameters of HD spacetime. The area of the hysteresis loop represents the energy, $\aleph$ of the unified force, F_N effecting the stability of the catastrophe as applied to manipulating the process for surmounting uncertainty.

TABLE 3.2 GEOMETRIC CONTENT OF 12D SPACETIME

N-Space	Points	Lines	Squares	Cubes	Tesseracts	5T	6T	7T	8T	9T	10T	11T	12T
0	1												
1	2	1											
2	4	4	1										
3	8	12	6	1									
4	16	32	24	8	1								
5	32	80	80	40	10	1							
6	64	192	240	160	60	12	1						
7	128	448	672	560	280	84	14	1					
8	256	1,024	1,792	1,792	1,120	448	112	16	1				
9	512	2,304	4,608	5,376	4,032	2,016	672	144	18	1			
10	1,024	5,120	11,520	15,360	13,440	8,064	3,360	960	180	20	1		
11	2,048	11,264	28,160	42,240	42,240	29,568	14,784	5,280	1,320	220	22	1	
12	4,096	24,576	67,584	112,640	126,720	101,376	59,136	25,344	7,920	1,760	264	24	1

The structural-phenomenology of Double-Cusp Catastrophe (DCC) Theory in $\geq 9D$ appears homeomorphic to the Riemannian manifold of both 10(11)D M-Theory and the 12D topological geometry of the mantra for the continuous-state spin-exchange dimensional reduction compactif-ication process inherent in the action of the corresponding scale-invariant cosmological least-unit of UFM superspace as cast in UFM cosmology [39,40]. In this general framework the DCC equilibrium surface is analyzed in terms of a hierarchy of Ising-like lattice gas jumps in state providing a framework for considering the least-unit tiling [101] of the Planck backcloth as a complex HD catastrophe manifold mediated by the force of coherence of the unified field which because of the polarized properties of the Dirac vacuum lends itself to empirical mediation under certain restrictions.

The putative significance of Table 3.2 for the application of DCC theory to the UFM formalism is that the structure of possible boundary conditions and the number of control points is revealed. For example, in this simplistic view, a 3D point in real spacetime might have 16 control photon-gravitons (noeons - UF exchange unit) covering it. Carrying the analogy up to the 12D brane topology of the Multiverse, the same 3D point might be controlled or guided by a total of 8,176 noeon units. The number arrived at by summing the points of D4 to D12. No point in the universe is isolated; so this metaphor does not include the possible power factor by associated points in both the HD and LD UFM backcloth. Within the inherent continuous-state dimensional reduction compactification process, the LD domain (dimensions less than 3) might be coupled to orders of magnitude of more photon-gravitons. This detail of Unified Theory has not been completely worked out yet. $F_{(N)} = \aleph_{(N)} / \rho$

One can say that the cosmological least-unit [101] tiling the fabric of the continuous-state virtual Planck-scale backcloth is a complex HD catastrophe manifold with Dirac spherical rotation symmetry mediated by the unitary action of the unified field. Any internal or external stress or change in energy, $\aleph$ is a nonlinear dynamical process producing stability or instability in the boundary conditions of ρ ; a causal instability in $\aleph \rightarrow$ stress $\rightarrow$ displacement $\rightarrow$ catastrophe $\rightarrow$ Ising jump…whereas stable flux is homeostatic. The hysteresis loop of the unified field (Fig. 3.9d) is conformally scale invariant; the same processes occur in UFM cosmology and domains of the chemistry of living systems. The area

represents the energy of the string tension, T_0. This energy, $\aleph_{(N)}$ is measured in a unit similar to the *Einstein* in photometry, the fundamental physical quantity defined as a 'mole'-Avogadro's number (6.02×10^{23}) of bosons, defined here as noeons, the exchange unit of the unitary field.

Equation (3.18) describes the equilibrium surface of the DCC [98-100] as modeled in (Fig. 3.11); where $B \pm Q$ is the state variable and μ_d and υ_d are the control parameters.

$$(B+Q)^3 + (B+Q)\mu_d + \upsilon_d = 0 \qquad (3.18)$$

The position of the two cusps is found at $\mu_d = 0$ and $\upsilon_d = 0$. At any moment temporal permutations of the unified field catastrophe cycle evolve in time from future to past and higher to lower dimensions in the same manner as the spacetime present of the cosmological least-unit of UFM cosmology for the spatial domains: $R^{12} \supseteq ... \; R^4 \supseteq R^3 \supseteq R^2 \supseteq R^1 \supseteq R^0$; followed by a Riemann sphere Ising rotation where the cycle repeats.

3.6 Protocol for Empirically Testing Unified Theoretic Cosmology

Extrapolating Einstein's energy dependent or deformed spacetime metric, $\hat{M}_4$ [102-104] to a supersymmetric 12D standing-wave future-past advanced-retarded topology for a holographic multiverse we have designed a spacetime resonance hierarchy protocol for a covariant Dirac polarized vacuum which has properties akin to an 'ocean of light' or Wheeler Geon 'beyond the veil of spacetime [40]. If this is true emergent aspects of spacetime act like a 'surface wave' (Fig. 3.13) on the upper regime of the complex self-organized Dirac Sea and is therefore amenable to descriptive methods of nonlinear dispersive wave phenomena generally of the basic form

$$L(\mu) = \varepsilon N(\mu) \qquad (3.19)$$

where *L* and *N* are Linear and Nonlinear operators respectively in the linear limit where $\varepsilon = 0$ with elementary dispersive wave solutions $\mu_i = A_i \cos\theta_i,\ \theta_i = k_i x - \omega(k_i)t$ for one dimension plus time where nonlinearity creates resonant interactions between the μ_i solutions and the Amplitude A_i depends on *t*, creating potentially substantial effects where initial absent modes can become cumulative interactions producing shock wave effects.

Motion of a one-dimensional *classical* harmonic oscillator is given by $q = A\sin(\omega t + \varphi)$ and $p = m\omega A\cos(\omega t + \varphi)$ where A is the amplitude and φ is the phase constant for fixed energy $E = m\omega^2 A^2/2$. For state $|n\rangle$, with $n = 0,1,2...\infty$ and Hamiltonian $E_n = (n+1/2)\hbar\omega$ the *quantum* harmonic oscillator becomes

$$\langle n|q^2|n\rangle = \hbar/2m\omega\langle n|(a^\dagger a + aa^\dagger)|n\rangle = E_n/m\omega^2 \qquad (3.20)$$

and

$$\langle n|p^2|n\rangle = 1/2(m\hbar\omega)\langle n|a^\dagger a + aa^\dagger = mE_n \qquad (3.21)$$

where a & $a^\dagger$ are the annihilation and creation operators,

$q = \sqrt{\hbar/2m\omega}(a^\dagger + a)$ and $p = i\sqrt{m\hbar\omega/2}(a^\dagger a)$.

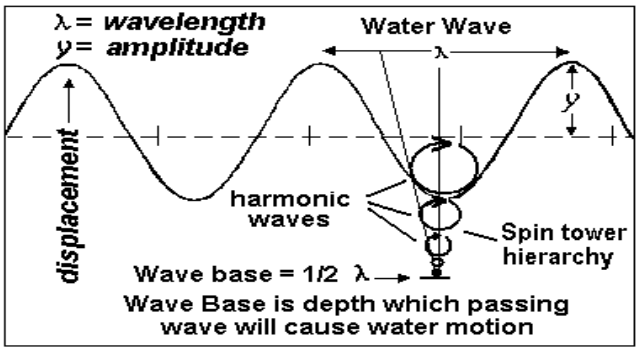

Fig. 3.13. The spacetime topological hierarchy may have properties like water waves where the wave (HD branes) moves but the water surface (local) remains stationary.

For the 3D harmonic oscillator each equation is the same with energies

$$E_x = (n_x + 1/2)\hbar\omega_x, E_y = (n_y + 1/2)\hbar\omega_y \qquad (3.22a)$$

and

$$E_z = (n_z + 1/2)\hbar\omega_z \text{ [77,78].} \qquad (3.22b)$$

In Dubois' notation the classical 1D harmonic oscillator for Newton's second law in coordinates *t* and *x(t)* for a mass, *m* in a potential $U(x) = 1/2(kx^2)$ takes the differential form

$$\frac{d^2x}{dt^2} + \omega^2 x = 0 \qquad where \qquad \omega = \sqrt{k/m} \qquad (3.23)$$

which can be separated into the coupled equations

$$\frac{dx(t)}{dt} - v(t) = 0 \qquad and \qquad \frac{dv(t)}{dt} + \omega^2 x = 0. \qquad (3.24)$$

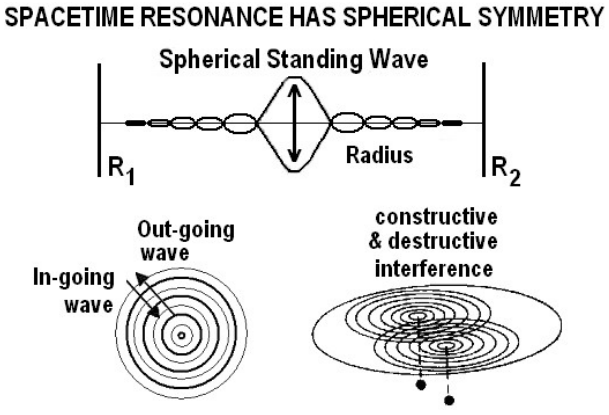

Fig. 3.14. The Dirac covariant polarized vacuum has hyperspherical symmetry. a) Metaphor for standing-wave present showing future-past elements, R_1, R_2, 11D of 12D suppressed for simplicity. b) Top view of a) a 2D spherical standing-wave. c) Manipulating the relative phase of oscillations creates nodes of destructive and constructive interference as a substrate for incursion.

From incursive discretization, Dubois creates two solutions $x(t+\Delta t)$ $v(t+\Delta t)$ providing a structural bifurcation of the system which together produce Hyperincursion. The effect of increasing the time interval discretizes the trajectory as in Fig. 3.15 below. This represents a background independent discretization of spacetime [86-90].

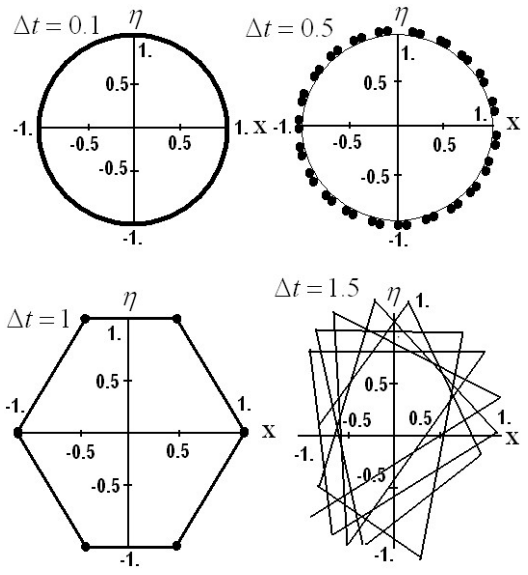

Fig. 3.15. Numerical simulation of the phase space trajectory of the Dubois *superposed incursive oscillator* based on coordinates and velocities $x_n = 1/2[x_n(1) + x_n(2)]$ $v_n = 1/2[v_n(1) + v_n(2)]$ is shown in the figure for values of $\Delta\tau = \omega t$ equal to 0.1, 0.5, 1.0 and 1.5. Initial conditions are $\chi_0 = 1, \eta_0 = 0 \,\&\, \tau_0 = 0$ with total simulation time $\tau = \omega t = 8\pi$. Figure adapted from [86-90].

3.7 Introduction to a $\mathbf{P \equiv 1}$ Experimental Design

In a homogeneous magnetic field, the forces exerted on opposite ends of the dipole cancel each other out and the trajectory of the particle is unaffected. if the particles are classical 'spinning' particles then the distribution of their spin angular momentum vectors is taken to be truly random and each particle would be deflected up or down by a different amount producing an even distribution on the screen of a detector. Instead quantum mechanically, the particles passing through the device are deflected either up or down by a specific amount. This means that spin angular momentum is quantized (also called space quantization), i.e. it can only take on discrete values. There is not a continuous distribution of possible angular momenta. This is the usual fundamental basis of the standard quantum theory and where we must introduce a new experimental protocol to surmount it. This is the crux of our new methodology: If application of a homogeneous magnetic field along a Z-axis produces quantum uncertainty upon measurement, then simplistically "*do something else*".

In NMR spectroscopy often it is easier to make a first order calculation for a resonant state and then vary the frequency until resonance is achieved. Among the variety of possible approaches that might work best for a specific quantum system, if we choose NMR for the UFM Interferometer it is relatively straight forward to determine the spin-spin resonant couplings between the modulated electrons and the nucleons. But achieving a critical resonant coupling with the wave properties of matter with a putative beat frequency inherent in the HD spacetime backcloth is another matter. Firstly, for UFM cosmology $\hbar$ is not a rigid barrier as in Standard Model Big Bang-Copenhagen cosmology; $\hbar$ is a virtual limit of retarded-advanced elements of the continuous-state standing-wave present as it cyclically recedes into

the past where the least unit [101] cavities tiling the spacetime backcloth can have cyclical radii ≤ the Larmor radius of the hydrogen atom. This new Planck length ($\hbar + T_s$), where T_S is string tension, oscillates through a limit cycle from the Larmor radius of the hydrogen atom to standard $\hbar$, as asymptote never reached. As discussed in Chaps. 3,4, we utilize the original hadronic form of string tension which is variable, not the current M-Theoretic form which is fixed.

This cycle is like a wave-particle duality – Larmor radius at the future-retarded moment and $\hbar$ at the past-advanced moment that opens and closes periodically into the HD regime. The dynamics are different for future-retarded elements which have been theorized to have the possibility of infinite radius for D > 4 [105]. This scenario is a postulate of string theory. Considering the domain walls of the least-unit structure, the $\pm\Delta\hbar$-Larmor cyclical regime is considered internal-nonlocal and the Larmor-infinity regime rotation considered external-supralocal.

For simplicity we introduce our review of NMR concepts for the hydrogen atom, a single proton with magnetic moment, μ, angular momentum, J related by the vector $\mu = \gamma J$ where γ is the gyromagnetic ratio and $J = \hbar I$ where I is the nuclear spin. The magnetic energy $U = -\mu \cdot B$ of the nucleus in an external magnetic field in the z direction is $U = -\mu_z B_0 = -\gamma \hbar I_z B_0$ where the usual values of I_z, m_I are quantized according to $m_I = I, I-1, I-2, I-3, \ldots -1$ [106,107].

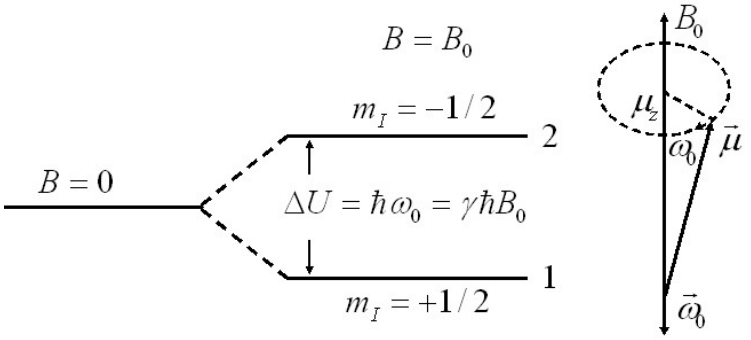

Fig. 3.16. a) The two magnetic energy states for the spin, I = ½ single proton of a hydrogen atom in a magnetic field. b) Time variation of the magnetic moment of the proton in magnetic field B_0 with precession frequency, $\omega_0 = \gamma B_0$, the fundamental resonant frequency from a).

For most nuclear species the z-component of the magnetization, M grows exponentially until reaching equilibrium according to the formula $M_z(t) = M_0(1 - e\exp - t/T_1)$ where T_1 is the spin-lattice relaxation time. Of interest for the noetic interferometer is the fact that (Fig. 3.16) as μ precesses cyclically from $m_I = -1/2$ to $m_I = +1/2$ the nucleons experience a torque, with τ changing J by $\tau = dJ/dt$ or $\mu \times B = dJ/dt$. Under thermal equilibrium the x-y components are zero; but M_z can be rotated into the x-y plane creating additional transverse M_x and M_y components $dM/dt = \gamma M \times B$ for the entire system by applying a rotating circularly polarized oscillating magnetic field $2B_1 \cos\omega t\hat{i}$ of frequency ω in addition to the constant magnetic field, $B_0\hat{k}$. Now the total time dependent field decomposes into the two counterpropagating fields

$$B_1(\cos\omega t\hat{i} + \sin\omega t\hat{j}) + B_1(\cos\omega t\hat{i} - \sin\omega t\hat{j}). \qquad (3.25)$$

This more complicated form for use with multiple applied fields is necessary, as described below for use with the Sagnac Effect, quadrupole, and dipole dynamics [108,109] required to operate the

noetic interferometer.

Nuclear Quadrupole Resonance (NQR) is a form of NMR in which quantized energy level transitions are induced by an oscillating rf-magnetic field in the electric quadrupole moment of nuclear spin systems rather than the magnetic dipole moment. The nuclear quadrupole moment, Q is based on the nuclear charge distributions $\rho(r)$ departure from spherical symmetry defined as the average value of $1/2(3z^2 - r^2)\rho(r)$ over the nuclear volume. Q has the dimension of area where the nuclear angular momentum, for which $m_I = I$ where I is the nuclear spin quantum number and m_I is the quantum number for the z component of the spin, $m_I = -1, +1, ..., I-1, I$. Nuclei with $I = 0$ have no magnetic moment and are therefore magnetically inert. Similarly, in order for $Q = 0$ the nucleus must be spherical with spin, $I \geq 0$. For spin I = 1/2 nuclei have dipole moments, μ but no Q. Q is positive for prolate nuclei and negative for oblate nuclei [110,111].

For an isolated nucleus in a constant magnetic field, H_0 with nuclear spin number $I > 0$ the nucleus possesses a magnetic moment. From QT the length of the nuclear angular momentum vector is $[I(+1)]^{1/2}\hbar$ where measurable components are given by $m\hbar$ with m the magnetic quantum number taking any $(2I + 1)$ value from the series $I, I-1, I-2, ..., -(I-1), -I$. For the I = 3/2 case there are four values along the direction of the applied magnetic field, H_0.

Of the three types of spin-spin coupling, this experiment relies the hyperfine interaction for electron-nucleus coupling, specifically the interaction of the nuclear electric quadrupole moment induced by an applied oscillating rf-electric field acting on the nuclear magnetic dipole moment, μ. When electron and nuclear spins are strongly aligned along their z-components the Hamiltonian is $-m \cdot B$, and if B is in the z direction

$$H = -\gamma_N I \cdot B = -\gamma_N B I_x \tag{3.26}$$

with $m = \gamma_N I$, γ_N the magnetogyric ratio $\gamma_N = e\hbar / 2m_p$ and m_p the mass of the proton [112].

Radio frequency excitation of the nuclear magnetic moment, μ to resonance occurs for a nucleus collectively which rotates μ to some angle with respect to the applied field, B_0. This produces a torque $\mu_i \times B_0$ causing the angular momentum, μ itself to precess around B_0 at the Larmor frequency $\omega_L = \gamma_N B_0$ [112-114]. This coherent precession of μ can also induce a 'voltage' in surrounding media, an energy component of the Hamiltonian to be utilized (Figs. 3.17,3.18) to create interference in the structure of spacetime.

Metaphorically this is like dropping stones in a pool of water: One stone creates concentric ripples; two stones create domains of constructive and destructive interference. Such an event is not considered possible in the standard models of particle physics, quantum theory and cosmology. However, UF science uses extended versions of these theories wherein a new teleological action principle is utilized to develop what might be called a 'transistor of the vacuum'. Just as standard transistors and copper wires provide the basis for almost all modern electronic devices; This Laser Oscillated Vacuum Energy Resonator using the information content of spacetime geodesics (null lines) will become the basis of many forms of new UF technologies.

Simplistically in this context, utilizing an array of modulated tunable lasers, atomic electrons are rf-pulsed with a resonant frequency that couples them to the magnetic moment of the nucleons such that a cumulative interaction is created to dramatically enhance the Haisch-Rueda inertial back-reaction [115-118] in conjunction with the Dubois incursive oscillator [86-90]. The laser beams are counter-propagating producing a Sagnac Effect Interferometry to maximize the small-scale local violation of Special Relativity. This is the 1st stage of a multi-tier experimental platform designed (according to the

tenets of UFT) to periodically 'open a hole' in the fabric of spacetime in order to isolate and utilize the force $\hat{F}_U$ of the UFM Field.

The interferometer utilized as the basis for the vacuum engineering research platform is a multi-tiered device. The top tier is comprised of counter-propagating Sagnac effect ring lasers that can be built into an IC array of 1,000+ ring lasers. If each microlaser in the array is designed to be counterpropagating, an interference phenomenon called the Sagnac Effect occurs that violates special relativity in the small scale [119]. This array of rf-modulated Sagnac-Effect ring lasers provides the top tier of the multi-tier Laser Oscillated Vacuum Energy Resonator. Inside the ring of each laser is a cavity where quantum effects called Cavity-Quantum Electrodynamics (C-QED) may occur. A specific molecule is placed inside each cavity. If the ring laser array is modulated with resonant frequency modes chosen to achieve spin-spin coupling with the molecules electrons and neutrons, by a process of Coherent Control [120] of Cumulative Interaction an inertial incursive back-reaction is produced whereby the electrons also resonate with the spacetime backcloth in order to 'open an oscillating hole' in it. This requires a TFT compatible with the 12D version of M-theory [43] relying on the key 'continuous-state' symmetry conditions of UFM cosmology in which it is cast (Chap. 3).

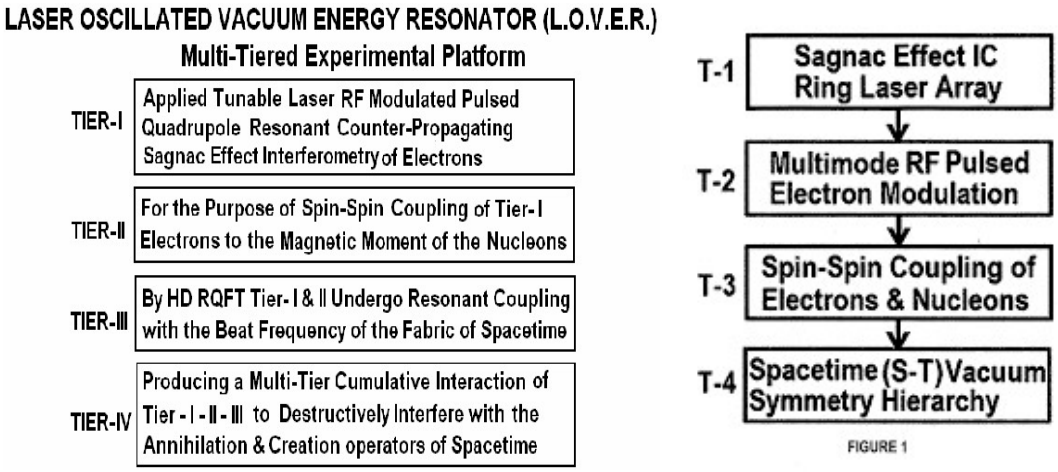

Fig. 3.17. Design elements for the HD Cavity-QED trap of the UFM Noetic Interferometer postulated to constructively-destructively interfere with the topology of the 12D spacetime manifold to manipulate the unified field. Substantial putative effects are possible if cumulative interactions of the interference nodes of the cyclotron resonance hierarchy produce reactive incursive shock waves. **Fig. 3.18.** Simplified description of the rf-pulsed resonance hierarchy for HD access.

The first step in the interference hierarchy (Fig. 3.17) is to establish an inertial back-reaction between the modulated electrons and their coupled resonance modes with the nucleons. The complete nature of inertia remains a mystery [121]. It may later be shown that the continuous-state energy in conjunction with the UF force of coherence will solve this mystery of Mach's Principle.

It is critical to realize that the Standard Model contains no fundamental 'beat frequency' of a spacetime annihilation-creation cycle. Physicists have come to the realization recently that spacetime is not fundamental, but little has been said yet of the nature of its emergence. In our cosmological model, a key breakthrough is that this beat frequency arises as an inherent property of the continuous-state cycling.

But if one follows the Sakarov [122] and Puthoff [123] conjecture, regarding the force of gravity and inertia, the initial resistance to motion, are actions of the vacuum zero-point field. Therefore, the parameter m in Newton's second law $f = ma$ is a function of the zero-point field [115-118,125-126]. Newton's third law states that 'every force has an equal and opposite reaction'. Haisch & Rueda [115-118] claim vacuum resistance arises from this reaction force, $f = -f$. We have also derived an electromagnetic interpretation of gravity and electromagnetism [127] that suggests this inertial back-

reaction is like an electromotive force[3] of the de Broglie matter-wave field in the spin exchange annihilation creation process inherent in a hysteresis of the relativistic spacetime fabric (Fig. 3.9b,d). In fact, we go further to suggest that the energy responsible for Newton's third law is a result of the continuous-state flux of the ubiquitous UFM noetic field. For the Laser Oscillated Vacuum Energy Resonator we assume the Haisch-Rueda postulate is sufficiently correct to be adapted for use in our rf-pulsed Sagnac Effect resonance hierarchy.

$$f = \frac{d\rho}{dt} - \lim_{\Delta t \to 0} \frac{\Delta\rho}{\Delta t} \quad \equiv \quad \frac{d\rho_*}{dt_*} - \lim_{\Delta t_* \to 0} \frac{\Delta\rho_*}{\Delta t_*} = f_* \tag{3.27}$$

where $\Delta\rho$ is the impulse given by the accelerating agent and thus $\Delta\rho_*^{zp} = -\Delta\rho_*$ [115-118].

The cyclotron resonance hierarchy must also utilize the proper spacetime beat frequency according to the mantra of the continuous-state dimensional reduction spin-exchange compactification process inherent in the symmetry of UF spacetime naturally 'tuned' to make the speed of light $c \equiv c$ and not infinite. With this apparatus in place noetic theory suggests that destructive-constructive C-QED interference of the spacetime fabric occurs such that the UFM noeon wave, $\aleph$ of the unified field, U_F is harmonically (like a light house beacon or holophote) released periodically into the cavity of the detector array. Parameters of the Dubois incursive oscillator are also required for aligning the interferometer hierarchy with the beat frequency of spacetime.

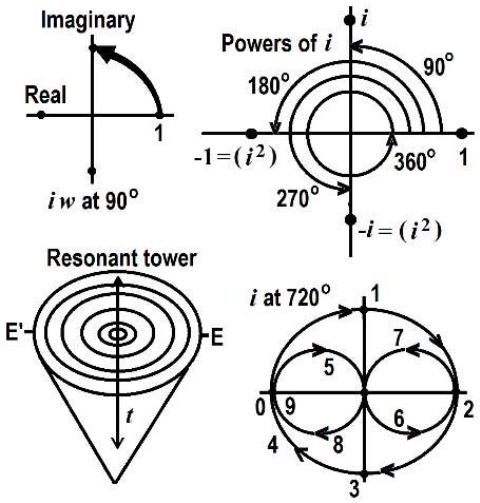

Fig. 3.19 Powers of *i* in the complex plane. For 90° to 360° the concept can be readily illustrated in 2D; but for 720° and above 4D is required which cannot easily be depicted in 3D so the representation in d) is used, which might also be represented by a Klein bottle which was not used because the torus in d) more easily shows the rotation topology, which for spin 1/2 is the Dirac rotation of the electron. c) is a simplistic representation of a powers of *i* resonance hierarchy.

If the water wave conception for the 'Dirac sea' is correct, the continuous state compactification process contains a tower of spin states from spin 0 to spin 4. Spin 4 represents the unified field making cyclic correspondence with spin 0 where Ising lattice Riemann sphere spin flips create dimensional jumps. Spin 0, 1/2, 1, & 2 remain in standard form. Spin 3 is suggested to relate to the orthogonal properties of atomic energy levels and space quantization. Therefore, the spin tower hierarchy precesses through 0, 720º, 360º, 180º, 90º & 0 (∞) as powers of *i* as illustrated in Fig. 3.19.

[3] Electromotive force, *E*: The internal resistance *r* generated when a load is put upon an electric current *I* between a potential difference, *V,* i.e. $r = (E - V)/I$.

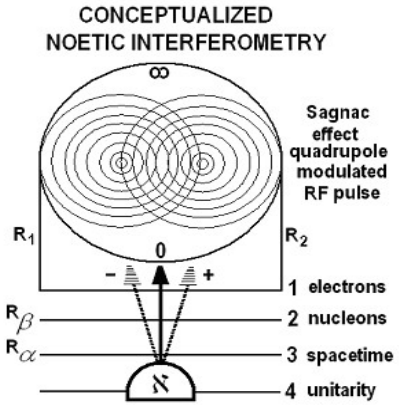

Fig. 3.20. Conceptualized Ising model Riemann sphere cavity-QED multi-level Sagnac effect interferometer designed to cyclically 'penetrate' space-time to emit the 'noeon wave, ℵ'. Experimental access to vacuum structure or for surmounting the uncertainty principle can be done by two similar methods. One is to utilize an atomic resonance hierarchy and the other a spacetime resonance hierarchy. The spheroid is a 2D representation of a HD Ising model Riemann sphere able to spin-flip from zero to infinity in conjunction with the putative 'beat frequency' of spacetime.

As illustrated in Figs. 3.17, 3.18 the coherent control of the multi-level tier of cumulative interactions relies on full utilization of the continuous-state cycling inherent in parameters of Multiverse cosmology. What putatively will allow noetic interferometry to operate is the harmonic coupling to periodic modes of Dirac spherical rotation in the symmetry of the HD brane geometry. The universe is no more classical than quantum as currently believed; reality rather is a continuous state cycling of nodes of classical to quantum to unified, $C \to Q \to U$. We elevate the concept of wave-particle duality to a principle of cosmology especially in terms of the HD continuous-state cycle; this is what allows the UFM 'mantra' to operate. The salient point is that cosmology, the HD topology of spacetime itself, has a conformal rotation like the wave-particle duality Dirac postulated for electron spin. Recall that the electron requires a 4D topology and 720° for one complete rotation instead of the usual 360° to complete a rotation in 3D. The hierarchy of noetic cosmology is cast in 12D such that a pertinent form of ontological-phase topological field theory has significantly more degrees of freedom, whereby the modes of resonant coupling may act on the structural-phenomenology of the Dirac 'sea' itself rather than just the superficial zero-point field surface approaches to vacuum engineering common until now.

Hierarchical Harmonic Oscillator Parameters	
classical	$X = A\cos(\omega t)$
quantum	$\frac{\hbar^2}{2m}\frac{d^2\psi}{dx^2} + \left(E - \frac{kx^2}{2}\right)\psi = 0$
annihilation creation	$x(t) = x_0\left[a\exp(-i\omega t) + a^\dagger \exp(i\omega t)\right]$
future-past retarded-advanced	$F_1 = F_0 e^{-ikx}e^{-2\pi i\beta t}$, $F_2 = F_0 e^{ikx}e^{-2\pi i\beta t}$, $F_3 = F_0 e^{-ikx}e^{2\pi i\beta t}$, $F_4 = F_0 e^{ikx}e^{2\pi i\beta t}$
incursive	$\frac{dx(t+\Delta t)}{dt} - v(t) = 0, \frac{dv(t+\Delta t)}{dt} + \omega^2 = 0$

Fig. 3.21. Basic conceptual mathematical components of the applied harmonic oscillator: classical, quantum, relativistic, transactional and incursive are all required in order to achieve coherent control of the cumulative resonance coupling hierarchy in order to produce harmonic nodes of destructive and constructive interference in the spacetime backcloth by incursion.

The parameters of the noetic oscillator (Figs. 3.17, 3.18) seem best be implemented by an OPTFT using a form of de Broglie fusion. According to de Broglie a spin 1 photon can be considered a fusion of a pair of spin 1/2 corpuscles linked by an electrostatic force. Initially de Broglie thought this might be an electron-positron pair and later a neutrino and antineutrino. "*A more complete theory of quanta of light must introduce polarization in such a way that to each atom of light should be linked an internal state of right and left polarization represented by an axial vector with the same direction as the propagation velocity*" [128]. These prospects suggest a deeper relationship in the structure of spacetime of the Cramer Transaction type [50] (Fig. 3.22).

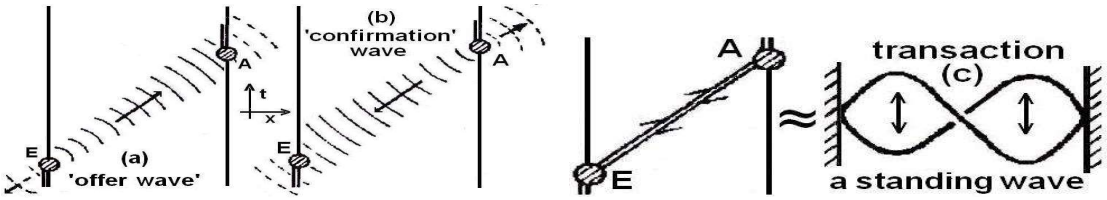

Fig. 3.22. Transactional model. a) Offer-wave, b) confirmation-wave combined into the resultant transaction c) which takes the form of an HD future-past advanced-retarded standing or stationary wave. Figs. Adapted from Cramer [50].

The epistemological implications of a 12D OPTFT must be delineated. The empirical domain of the standard model relates to the 4D phenomenology of elementary particles. It is the intricate notion of what constitutes a particle that concerns us here – the objects emerging from the quantized fields defined on Minkowski spacetime. This domain for evaluating physical events is insufficient for our purposes. The problem is not only the additional degrees of freedom and the associated XD, or the fact that 'particles' can be annihilated and created but that in UFM cosmology they are continuously annihilated and recreated within the holograph as part of the annihilation and recreation of the fabric of spacetime itself. This property is inherent in the 12D Multiverse because temporality is a subspace of the atemporal 3rd regime of the UF. This is compatible with the concept of a particle as a quantized field. What we are suggesting parallels the wave-particle duality in the propagation of an electromagnetic wave. We postulate this as a property of all matter and spacetime albeit as continuous-state standing waves.

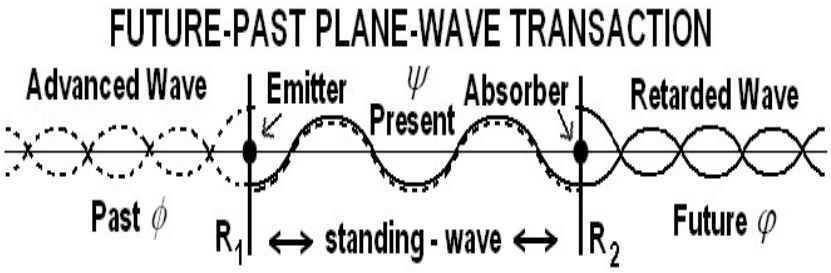

Fig. 3.23 Structure of a Cramer transaction (present state or event) where the present is a standing-wave of future-past elements. The separation of these parameters in terms of de Broglie's fusion model is suggested to allow manipulation of the harmonic tier of the UF interferometer with respect to T-Duality or Calabi-Yau mirror symmetry.

For a basic description, following de Broglie's fusion concept, assume two sets of coordinates x_1, y_1, z_1 and x_2, y_2, z_2 which become

$$X = \frac{x_1 + x_2}{2}, \quad Y = \frac{y_1 + y_2}{2}, \quad Z = \frac{z_1 + z_2}{2}. \qquad (3.28)$$

Then for identical particles of mass *m* without distinguishing coordinates, the Schrödinger equation (for the center of mass) is

$$-i\hbar\frac{\partial\psi}{\partial t}=\frac{1}{2M}\Delta\psi,\quad M=2m \tag{3.29}$$

In terms of Fig. 3.23, Eq. 3.29 corresponds to the present and Eq. 3.30a corresponds to the advanced wave and (3.30b) to the retarded wave [98].

$$-i\hbar\frac{\partial\phi}{\partial t}=\frac{1}{2M}\Delta\phi,\qquad -i\hbar\frac{\partial\varphi}{\partial t}=\frac{1}{2M}\Delta\varphi. \tag{3.30}$$

Extending Rauscher's concept for a complex 8-space differential line element $dS^2=\eta_{\mu\nu}dZ^{\mu}dZ^{*\nu}$, where the indices run 1 to 4, $\eta_{\mu\nu}$ is the complex 8-space metric, Z^{μ} the complex 8-space variable where $Z^{\mu}=X^{\mu}_{\mathrm{Re}}+iX^{\mu}_{\mathrm{Im}}$ and $Z^{*\nu}$ is the complex conjugate [129,130]. This can be extended to 12D continuous-state UFM spacetime; we write just the dimensions for simplicity and space constraints:

$$x_{\mathrm{Re}},y_{\mathrm{Re}},z_{\mathrm{Re}},t_{\mathrm{Re}},\pm x_{\mathrm{Im}},\pm y_{\mathrm{Im}},\pm z_{\mathrm{Im}},\pm t_{\mathrm{Im}} \tag{3.31}$$

where ± signifies Wheeler-Feynman/Cramer type future-past/retarded-advanced dimensions. This dimensionality provides an elementary framework for applying the hierarchical harmonic oscillator parameters suggested in Figs. 3.17 and 3.21.

The concept conceptualized is that although commutativity was sacrificed by Hamilton in creating a closed quaternion algebra utilizing a 12D complex quaternion Clifford algebra approach to describe the Fermionic singularity; the additional degrees of freedom allow anticommutativity and commutativity to cycle periodically through the constraints of the algebra. This scenario when applied to the continuous-state cycle can be utilized to periodically via the suggested resonance hierarchy protocol to surmount the quantum uncertainty principle.

3.8 Conclusions

If the noeon interferometer resonance hierarchy is able to surmount the uncertainty principle as outlined and can isolate and manipulate the LSXD brane world, in addition to quantum computing it will lead to a new research platform for developing a whole new class of vacuum based technologies; whereas one could say virtually all electronic devices up to now are based on transistors and copper wires. The Laser Oscillated Vacuum Energy Resonator could lead to a transistor of vacuum cellular automata, where rather than copper wires, the geodesics or null lines of space would be utilized to transfer information topologically with no quantal exchange particle mediating the 'interaction' in this scenario distinguishing phenomenology from unified field ontology.

This brief introduction is a primitive overview introducing the anticipated new field of vacuum engineering as Cramer stated in the 1st sentence of this chapter should revolutionize many fields of science [131].

> When the great innovation appears, it will most certainly be in a muddled, incomplete form. To the discoverer himself it will be only half-understood; to everyone else it will be a mystery. For any speculation which does not at first glance look crazy, there is no hope [132].

Finally, we stress that vacuum energy is not 'produced' by the noeon interferometer. The interferometer manipulates the boundary conditions 'insulating' or 'hiding' the unitary geodesics of HD spacetime by constructive and destructive interference allowing vacuum energy to be 'emitted' as a form of cursory superradiance [133] of the dynamics of the hysteresis loop of inherent least-unit

synchronization backbone energy (topological charge) in continuous-state parallel transport.

We have found already that a fair number of colleagues want to summarily dismiss this model because of its utilization of LSXD. This is the sort of myopic view that has consistently plagued the history of science whenever 'big-leap' innovation occurs. We hope readers here will not fall into this quagmire! The model is empirically testable hopefully making up for some of the lack of precision in our axiomatic approach or thin rigor in portions of our attempts at formalism. In addition to the protocol presented here we have described elsewhere an additional experiment to utilize the noeon $\aleph$-wave to study the putative manipulation of prion protein conformation responsible for degenerative neuropathies [92,97].

References

[1] Thorne, K.S., Drever, R.W.P., Caves, C.M., Zimmermann, M. & Sandberg, V.D. (1978) Quantum nondemolition measurements of harmonic oscillators, Phys. Rev. Lett. 40; 667-671.
[2] Teuscher, C. (ed.) (2004) Alan Turing: Life and Legacy of a Great Thinker, quoted by A. Hodges, p. 54, New York: Springer.
[3] Cramer, J.G. (2000) The Alternate View: "Interaction-Free" Quantum Measurement and Imaging, Vol. CXX No. 6, pp. 78-81, Analog Science Fiction & Fact, Dell Magazines.
[4] Gurvitz, S.A. (2003) Negative result measurements in mesoscopic systems, Physics Letters A, 311:4-5;292-296.
[5] Braginsky, V.B., Vorontsov, Y.I. & Thorne, K.S. (1980) Quantum nondemolition measurements, Science, 209:4456, 547-557.
[6] Ralph, T.C., Bartlett, S.D., O'Brien, J.L., Pryde, G.J & Wiseman, H.M. (2004) Quantum non-demolition measurements on qubits, arXiv:quant-ph/0412149v1.
[7] Elitzur, A.C. & Vaidman, L. (1993) Quantum mechanical interaction-free measurements. Found. Phys. 23; 987-997.
[8] Kwiat, P., Weinfurter, H., Herzog, T., Zeilinger, A. & Kasevich, M. (1995) Interaction-free quantum measurements. Phys. Rev. Lett. 74, 4763-4766.
[9] du Marchie Van Voorthuysen, E.H. (1996) Realization of an interaction-free measurement of the presence of an object in a light beam, Am. J. Phys. 64:12; 1504-1507; or arXiv:quant-ph/9803060 v2 26.
[10] Simon, S.H. & Platzman, P.M. (1999) Fundamental limit on "interaction free" measurements, arXiv:quant-ph/9905050v1.
[11] Vaidman, L. (1996) Interaction-free measurements, arXiv:quant-ph/9610033v1.
[12] Paraoanu, G.S. (2006) Interaction-free measurements with superconducting qubits, Physical Rev. Letters, 97.
[13] Vaidman, L. (2001) The meaning of the interaction-free measurements, arXiv:quant-ph/0103081v1.
[14] Vaidman, L. (2001) The paradoxes of the interaction-free measurements, arXiv:quant-ph/0102049v1.
[15] Vaidman, L. (2000) Are interaction-free measurements interaction free?, arXiv:quant-ph/0006077v1.
[16] Helmer, F., Mariantoni, M., Solano, E. & Marquardt, F. (2008) Quantum, Zeno effect in the quantum non-demolition detection of itinerant photons, arXiv:0712.1908v2.
[17] Facchi, P. Lidar, D.A. & Pascazio, S. (2004) Unification of dynamical decoupling and the quantum Zeno effect, Phys Rev A 69, 032314; or arxiv:quant-ph/0303132.
[18] Sudarshan, E.C.G. & Misra, B. (1977) The Zeno's paradox in quantum theory, J Mathematical Physics 18:4; 756-763.
[19] Facchi, P. & Pascazio, S. (2002) Quantum Zeno subspaces, arXiv:quant-ph/0201115v2.
[20] Wocjan. P. (2004) Efficient decoupling schemes with bounded controls based on "Eulerian" orthogonal arrays, arXiv:quant-ph/0410107v1.
[21] Knill, E., Laflamme, R., Ashikhmin, A., Barnum, H., Viola, L. & Zurek, W.H. (1999) Introduction to quantum error correction, arXiv:quant-ph/0207170v1.
[22] Kwiat, P.G. White, A.G., Mitchell, J.R., Nairz, O., Weihs, G. Weinfurter, H. & Zeilinger, A. (1999) High-efficiency quantum interrogation measurements via the quantum Zeno effect, Phys. Rev. Lett. 83, 4725-4728; or arXiv:quant-ph/9909083v1.
[23] Carroll, S.M. (2006) Quantum Interrogation, reprinted in The Open Laboratory: The Best Writing on Science Blogs, B. Zivkovic (ed.) (Lulu: Morrisville, NC), p. 123.
[24] Jozsa, R. (1996) Counterfactual quantum computation, University of Plymouth preprint, unpublished.
[25] Mitchison, G. & Jozsa, R. (2000) Counterfactual computation, Proc. Roy. Soc. (Lond) A; or arXiv:quant-ph/9907007v2.
[26] Mitchison, G. & Massar, S. (2000) Absorption-free discrimination between semi-transparent objects, arXiv:quant-ph/0003140v2.
[27] Nakanishi, T., Yamane, K. & Kitano, M. (2002) Absorption-free optical control of spin systems: The quantum Zeno effect in optical pumping, arXiv:quant-ph/0103034v2.
[28] Kwiat, P.G., Weinfurter, H. & Zeilinger, A. (1996) Quantum seeing in the dark, Scientific American, Nov.
[29] Elitzur, A.C. & Dolev, S. (2000) Nonlocal effects of partial measurements & quantum erasure, arXiv:quant-ph/0012091v12000.
[30] Hiley, B.J. & Callaghan, R.E. (2006) What is erased in the quantum erasure? Foundations of Physics, 36:12.
[31] White, A.G., Mitchell, J.R. Nairz, O. & Kwiat, P.G. (1998) Interaction-free imaging, Physical Review A 58; 605.

[32] White, A.G., Mitchell, J.R., Nairz, O. & Kwiat, P.G. (1998)
"Interaction-free" imaging, arXiv:quant-ph/9803060v2.
[33] Kotigua, R.P. & Toffoli, T. (1998) Potential for computing in micromagnetics via topological conservation laws, Physica D, 120:1-2, pp. 139-161.
[34] Gerlach, W & Stern, O. (1922) *Das magnetische moment des silberatoms, Zeitschrift für Physik* 9, 353-355.
[35] Young, T. (1804) Experiments and calculations relative to physical optics, Philosophical Trans. of the Royal Society of London 94, 1-16.
[36] Kwiat, P.G., Weinfurter, H., Herzog, T., Zeilinger, A. & Kasevich, M. (1995) Experimental realization of 'interaction-free' measurements,
in D.M. Greenberger & A. Zelinger (eds.) Fundamental Problems in Quantum Theory, A Conference held in Honor of Professor John A. Wheeler, Annals of the New York Academy of Science, Vol. 755, p. 383, New York: New York Academy of Science.
[37] Jaekel, M.T. & S. Reynaud, S. (1990) Quantum limits in interferometric measurements, Europhys. Lett. 13, 301.
[38] Cramer, J.G. (2006) A transactional analysis of interaction-free measurements, Foundations of Physics Letters 19: 1; 63-73; or arXiv:quant-ph/0508102v23, 2008.
[39] Amoroso, R.L., Kauffman, L.H. & Rowlands, P. (eds.) (2013) The Physics of Reality: Space, Time, Matter, Cosmos, Singapore: World Scientific.
[40] Amoroso, R.L., Kauffman, L.H. & Rowlands, P. (eds.) (2015) Unified Field Mechanics; Natural Science Beyond the Veil of Spacetime, Singapore: World Scientific.
[41] Everett, H. (1957) Relative state formulation of quantum mechanics, Reviews of Modern Physics, Vol 29, pp 454-462.
[42] Bohm, D. & Vigier, J-P (1954) Model of the causal interpretation of quantum theory in terms of a fluid with irregular fluctuations, Phys. Rev. 96:1; 208-217.
[43] Kaku, M. (1999) Introduction to Superstrings and M-Theory, New York: Springer.
[44] Dirac, P.A.M. (1952) Is there an ether? Nature, 169: 172.
[45] Pettroni, N.C. & Vigier, J-P (1983) Dirac's aether in relativistic quantum mechanics, Foundations Phys, 13:2, 253-285.
[46] Vigier, J-P (1980) De Broglie waves on Dirac aether: A testable experimental assumption, *Lettere al Nuovo Cimento*, 29; 467-475.
[47] Lehnert, B. (2002) New developments in electromagnetic field theory, in R.L. Amoroso, G. Hunter, M. Kafatos & J-P Vigier (eds.) Gravitation & Cosmology: From the Hubble Radius to the Planck Scale, Dordrecht: Kluwer Academic.
[48] Lehnert, B. (1998) Electromagnetic theory with space-charges in vacuo, in G. Hunter, S. Jeffers & J-P Vigier (eds.) Causality and Locality in Modern Physics, Dordrecht: Kluwer Academic.
[49] Proca, A, (1936) *Compt. Rend*., 202, 1420.
[50] Cramer, J.G. (1986) The transactional interpretation of quantum mechanics, Rev. Mod. Phys 58, 647-687.
[51] Hofstadter, D. (2013) Alan Turing: Life and legacy of a great thinker, in C. Teuscher (ed.) p. 54, Springer Science & Business Media.
[52] Sudarshan, E.C.G. & Misra, B. (1977) The Zeno's paradox in quantum theory, Journal of Mathematical Physics 18 (4): 756–763.
[53] Nakanishi, T., Yamane, K., Kitano, M. (2001) Absorption-free optical control of spin systems: The quantum Zeno effect in optical pumping, Physical Review A 65 (1): 013404; arXiv:quant-ph/0103034.
[54] Facchi, P., Lidar, D.A. & Pascazio, S. (2004) Unification of dynamical decoupling and the quantum Zeno effect, Physical Review A 69 (3).
[55] Degasperis, A., Fonda, L. & Ghirardi, G.C. (1974) Does the lifetime of an unstable system depend on the measuring apparatus? *Il Nuovo Cimento* A 21 (3): 471-484.
[56] von Neumann, J. (1932*) Mathematische Grundlagen der Quantenmechanik,* Springer; von Neumann, J. (1955) Mathematical Foundations of Quantum Mechanics, Princeton University Press. p. 366.
[57] Menskey, M.B. (2000) Quantum Measurements And Decoherence, Springer.
[58] Peise, J., Lücke, B., Pezzé, L., Deuretzbacher, F., Ertmer, W., Arlt, J., Smerzi, A., Santos, L. & Klempt, C. (2015) Interaction-free measurements by quantum Zeno stabilization of ultracold atoms, Nature Communications, 6,14.
[59] Renninger, M. (1953) *Zum Wellen-Korpuskel-Dualismus. Zeitschrift fiir Physik* 136, 251–261.
[60] Misra, B. & Sudarshan, E.C.G. (1977) The Zeno's paradox in quantum theory, J. Math. Phys 18, 756-763.
[61] Vlasov, A.Y. (1999) Quantum theory of computation and relativistic physics, PhysComp96 Workshop, Boston MA, 22-24 Nov 1996, arXiv: quant-ph/ 9701027v4.
[62] Peres, A. & Terno, D.R. (2004) Quantum information and relativity theory, Rev. Mod. Phys. 76, 93; arXiv:quant-ph/0212023v2; Introduction to relativistic quantum information (2006) arXiv:quant-ph/0508049v2.
[63] Jafarizadeh, M.A. & Mahdian, M. (2011) Quantifying entanglement of two relativistic particles using optimal entanglement witness, Quantum Information Processing, 10:4, pp. 501-518.
[64] Felicetti, S., Sabın, C., Fuentes, I., Lamata, L., Romero, G. & Solano, E. (2015) Relativistic motion with superconducting qubits, arXiv:1503.06653v2 [quant-ph].
[65] Arkani-Hamed, N., & Trnka, J. (2013) The amplituhedron, arXiv:1312.2007.
[66] Bai, Y., He, S., & Lam, T. (2015) The amplituhedron and the one-loop Grassmannian measure, arXiv:1510.03553.
[67] Arkani-Hameda, N., Hodgesb, A. & Trnkac, J. (2014) Positive amplitudes in the amplituhedron, arXiv:1412.8478v1 [hep-th].
[68] Wootters, W.K. & Zurek, W.H. (1982) A single quantum cannot be cloned, Nature, 299 (5886) 802-803.
[69] Jaynes, E.T. (1990) in W.H. Zurek (ed.) Complexity, Entropy, and the Physics of Information, Reading: Addison-Wesley.

[70] Wheeler, J.A., & Feynman, R. (1945) Rev. Mod. Physics, 17, 157;
[71] Witten, E. (1993) Quantum background independence in string theory, arXiv:hep-th/9306122v1
[72] Sen, A. & Zwiebach, B. (1994) Local background independence of classical closed string field theory, Nucl. Phys. B414, 649.
[73] Sen, A. & Zwiebach, B. (1994) Quantum background independence of closed string field theory, Nucl. Phys. B423, 580.
[74] Chu, S-Y (1993) Physical Rev. Letters, 71, 2847.
[75] Chantler, C.T. et al. (2012) Testing three-body quantum electrodynamics with trapped Ti^{20} ions: evidence for a *Z*-dependent divergence between experiment and calculation, PRL 109, 153001.
[76] Ranganathan, D. (1988) The Dirac equation in the de Broglie-Bohm theory, Physics Letters A, Volume 128, Issues 3-4, pp. 105-108.
[77] Rowlands, P. (2003) The nilpotent Dirac equation and its applications in particle physics; http://arxiv.org/ftp/quant-ph/papers/0301/0301071.pdf.
[78] Rowlands, P. (1994) An algebra combining vectors and quaternions, Speculat. Sci. Tech., 17, 279-282.
[79] Rowlands, P. (1996) Some interpretations of the Dirac algebra, Speculat. Sci. Tech., 19, 242-246.
[80] Rowlands, P. (1998) The physical consequences of a new version of the Dirac equation, in G. Hunter, S. Jeffers, and J-P. Vigier (eds.), Causality and Locality in Modern Physics and Astronomy: Open Questions and Possible Solutions. Fundamental Theories of Physics, vol. 97, Kluwer Academic Publishers, Dordrecht, 397- 402.
[81] Rowlands, P. & Cullerne, J.P. (2001) The connection between the Han-Nambu quark theory, the Dirac equation and fundamental symmetries, Nuc Phys A 684, 713-5.
[82] Rowlands, P. & Cullerne, J.P. (2002) The Dirac algebra and its physical interpretation, arXiv:quant-ph/00010094.
[83] Rowlands, P. & Cullerne, J.P. (2002) Applications of the nilpotent Dirac state vector, arXiv:quant-ph/0103036.
[84] Rowlands, P. & Cullerne, J.P. (2004) The Dirac algebra and grand unification, arXiv:quant-ph/0106111.
[85] Mackay, A.L. & Pawley, G.S. (1963) Bravais Lattices in Four-dimensional Space, Acta. cryst. 16: 11–19.
[86] Antippa, A.F. & Dubois, D.M. (2004) Anticipation, orbital stability and energy conservation in discrete harmonic oscillators, in D.M. Dubois (ed.) Computing Anticipatory Systems, AIP Conf. Proceedings Vol. 718, pp.3-44, Melville: American Inst. of Physics.
[87] Dubois, D.M. (2001) Theory of incursive synchronization and application to the anticipation of delayed linear and nonlinear systems, in D.M. Dubois (ed.) Computing Anticipatory Systems: CASYS 2001, 5th Intl Conf., Am Inst of Physics: AIP Conf. Proceedings 627, pp. 182-195.
[88] Antippa, A.F. & Dubois, D.M. (2008) The synchronous hyperincursive discrete harmonic oscillator, in D. Dubois (ed.) AIP proceedings of CASYS07.
[89] Dubois, D.M. (2008) The quantum potential and pulsating wave packet in the harmonic oscillator, in D. Dubois (ed.) AIP proceedings of CASYS07.
[90] Dubois, D.M. (2016) Hyperincursive algorithms of classical harmonic oscillator applied to quantum harmonic oscillator separable into incursive oscillators, in R.L. Amoroso, L.H. Kauffman & P. Rowlands (eds.) Unified Field Mechanics: Natural Science Beyond the veil of Spacetime, Singapore: World Scientific.
[91] Icke, V. (1995) The Force of Symmetry, Cambridge: Cambridge Univ. Press.
[92] Amoroso, R.L. & Chu, M-Y.J. (2008) Empirical mediation of the primary mechanism initiating protein conformation in prion propagation, in D. Dubois (ed.) Partial Proceedings of CASYS07, IJCAS, Vol. 22, Univ. Liege Belgium.
[93] Gambini, R. & Pullin, J. (1996) Variational derivation of exact skein relations from Chern-Simons theories, arXiv:hep-th/9602165v1.
[94] Schwinger, J. (1992) Casimir energy for dielectrics, Proc. Nat.Acad. Sci. 89, 4091-3.
[95] Schwinger, J. (1993) Casimir light: The source, Proc. Nat. Acad. Sci 90, 2105-6.
[96] Schwinger, J. (1994) Casimir energy for dielectrics: spherical geometry, Proc. Nat. Acad. Math. Psych. 41:64-67, San Francisco: W.H. Freeman.
[97] Amoroso, R.L. (2005) Application of double-cusp catastrophe theory to the physical evolution of qualia: Implications for paradigm shift in medicine & psychology, in G.E. Lasker & D.M. Dubois (eds.) Anticipative & Predictive Models in Systems Science, Vol. 1, pp. 19-26, Windsor: The International Institute for Advanced Studies in Systems Research & Cybernetics.
[98] Gilmore, R. (1981) Catastrophe Theory for Scientists & Engineers, New York: Dover.
[99] Poston T. & Stewart, I (1978) Catastrophe Theory & Its Applications, New York: Dover; Gilmore, R. (1981) Catastrophe Theory for Scientists & Engineers, Dover.
[100] Qin, S. et al. (2001) Int. J of Solids & Structures, 38, pp. 8093-8109.
[101] Stevens, H.H. (1989) Size of a least unit, in M. Kafatos (ed.) Bell's Theorem, Quantum Theory and Conceptions of the Universe, Dordrecht: Kluwer Academic.
[102] Cardone, F. & Mignani, R. (2004) Energy and Geometry - An Introduction to Deformed Special Relativity, Singapore: World Scientific.
[103] Cardone, F., Marrani, A. & Mignani, R. (2003) The electron mass from deformed special relativity, Electromagnetic Phenomena Vol.3, N.1; 9, special number dedicated to Dirac's centenary; (2008) hep-th/0505134.
[104] Cardone, F., Marrani, A. & Mignani, R. (2008) A new pseudo-Kaluza-Klein scheme for geometrical description of interactions, arXiv:hep-th/0505149v1.
[105] Randall, L. (2005) Warped Passages, Unraveling the Mysteries of the Universe's Hidden Dimensions, New York: Harper-Collins.
[106] Slichter, C.P. (1990) Principles of Magnetic Resonance, 3rd edition, Springer Series in Solid-State Sciences 1, New York:

Springer.
[107] Schumacher, R.T. (1970) Introduction to Magnetic Resonance, Menlo Park: Benjamin-Cummings.
[108] Farrar, T.C. & Becker, E.D. (1971) Pulsed and Fourier Transform NMR, New York: Academic Press.
[109] Abragam, A. (1961) Principles of Nuclear Magnetism, Oxford: Clarendon Press.
[110] Dehmelt, H.G. (1954) Nuclear quadrupole resonance, Am. J. Physics, 22:110.
[111] Semin, G.K, Babushkina, T.A. & Yakobson, G.G. (1975) Nuclear Quadrupole Resonance in Chemistry, NY: Wiley.
[112] Atkinson, P.W. (1994) Molecular Quantum Mechanics, 2nd edition, Oxford: Oxford University Press.
[113] Hausser, O. (1974) Coulomb reorientation, in J. Cerny (ed.) Nuclear Spectroscopy and Reactions, Part C, New York: Academic Press.
[114] Humieres, D., Beasley, M.R., Huberman, B.A. & Libchaber, A. (1982) Chaotic states and routes to chaos in the forced pendulum, Physical Rev A, 26:6, 3483-34.
[115] Rueda, A. & Haisch, B. (1998) Contributions to inertial mass by reaction of the vacuum to accelerated motion, Found. of Phys, 28:7, 1057-1108.
[116] Rueda, A. & Haisch, B. (1998) Physics Lett. A, 240, 115.
[117] Rueda, A., Haisch, B.& Puthoff, H.E. (1994) Phys.Rev. A, 49, 678.
[118] Rueda, A. & Haisch, B. (2002) The inertia reaction force and its vacuum origin, in R.L. Amoroso, G. Hunter, M. Kafatos & J-P Vigier (eds.), Gravitation & Cosmology: From the Hubble Radius to the Planck Scale, pp. 447-458, Dordrecht: Kluwer Academic.
[119] Vigier, J-P (1997) New non-zero photon mass interpretation of the Sagnac effect as direct experimental justification of the Langevin paradox, Physics Let. A, 234:2, 75-85.
[120] Garcia-Ripoli, J.J., Zoller, P. & Cirac, J.I. (2005) Coherent control of trapped ions using off-resonant lasers, Phys. Rev. A 71, 062309; 1-13.
[121] Vigier-J-P (1995) Derivation of inertial forces from the Einstein-de Broglie-Bohm causal stochastic interpretation of quantum mechanics, Found. Phys. 25:10, 1461-1494.
[122] Sakharov, A.D. (1968) Sov. Phys. Dokl. 12, 1040.
[123] Puthoff, H.E. (2002) Polarizable vacuum approach to General Relativity, in R.L. Amoroso, G. Hunter, M. Kafatos & J-P Vigier (eds.), Gravitation & Cosmology: From the Hubble Radius to the Planck Scale, pp. 431-446, Dordrecht: Kluwer Academic.
[124] Burns, J.E. (1998) Entropy and vacuum radiation, Found. Phys. 28 (7), 1191-1207.
[125] Burns, J.E. (2002), Vacuum radiation, entropy and the arrow of time, in R.L. Amoroso, G. Hunter, S. Jeffers & M. Kafatos, (eds.) Gravitation & Cosmology: From the Hubble Radius to the Planck Scale, Dordrecht: Kluwer Academic.
[126] Zeh, H.D. (1989) The Physical Basis of the Direction of Time, New York: Springer-Verlag.
[127] Vigier, J-P & Amoroso, R.L. (2002) Can one unify gravity and electromagnetic fields? in R.L. Amoroso, G. Hunter, S. Jeffers & M. Kafatos, (eds.), Gravitation & Cosmology: From the Hubble Radius to the Planck Scale, Dordrecht: Kluwer Academic.
[128] Borne, T., Lochak, G. & Stumpf, H. (2001) Nonperturbative Quantum Field Theory and the Structure of Matter, The theory of light and wave mechanics, pp. 4-38, Volume 114, Fundamental Theories of Physics Dordrecht: Kluwer.
[129] Rauscher, E.A. (1983) Electromagnetic Phenomena in Complex Geometries and Nonlinear Phenomena, Non-Hertzian Waves and Magnetic Monopoles, Millbrae: Tesla Books; (2009) 2nd edition, Oakland: The Noetic Press, and references therein.
[130] Rauscher, E. (2002) Non-Abelian gauge groups for real & complex Maxwell's equations, in R.L. Amoroso, G. Hunter, S. Jeffers & M. Kafatos, (eds.), Gravitation & Cosmology: From the Hubble Radius to the Planck Scale, Dordrecht: Kluwer.
[131] Messiah, A. (1999) Quantum Mechanics, pp. 438-444, New York: Dover.
[132] Dyson, F.J. (1958) Innovation in Physics, Scientific American, 199, No. 3.
[133] Eberly, J.H. (1972) Superradiance revisited, AJP, 40; 1374-1383.

PART 4
Measurement with Certainty

Because of what Unified Field Mechanics (UFM) appears to tell us about the fundamental basis of matter (albeit a preliminary foray); it is postulated that a bulk UQC cannot be built without utilizing UFM parameters with an inherent ability to supervene the quantum uncertainty principle. Although no attempt has been made yet to make correspondence with M-Theoretic supersymmetry, since it remains sufficiently unfinished; the topological order envisioned for UFM additions to the structure of matter can probably readily be made to do so. Concepts required to supervene uncertainty, such as a Dirac polarized vacuum, the de Broglie-Bohm causal interpretation and Cramer's transactional interpretation are already well-known to physics, but generally ignored. Concepts like Large-Scale Additional Dimensions (LSXD), brane topology and the vision that spacetime is not fundamental, but emergent, are already known and under ongoing development. The three main additions we apply are the discovery of a

manifold of uncertainty (MOU) with finite radius, to which the unified field provides an ontological force of coherence (not 5th force) and that the underlying bulk hidden behind the 'veil of uncertainty' is a tessellation of 'Least Cosmological Units' (LCU) annihilated and recreated with a cyclic beat frequency. May it become obvious, that this inherent LCU beat frequency is the key factor in supervening uncertainty for measurement with certainty.

> The general principle of superposition of quantum mechanics applies to the states ... of any one dynamical system. It requires us to assume that between these states there exist peculiar relationships such that whenever the system is definitely in one state we can consider it as being partly in each of two or more other states … indeed in an infinite number of ways. Conversely any two or more states may be superposed to give a new state ... The non-classical nature of the superposition process is brought out clearly if we consider the superposition of two states, *A* and *B*, such that there exists an observation which, when made on the system in state *A*, is certain to lead to one particular result, *a* say, and when made on the system in state *B* is certain to lead to some different result, *b*. What will be the result of the observation when made on the system in the superposed state? The answer is that the result will be sometimes *a* and sometimes *b*, according to a probability law depending on the relative weights of *A* and *B* in the superposition process. It will never be different from both *a* and *b*. The intermediate character of the state formed by superposition thus expresses itself through the probability of a particular result for an observation being intermediate between the corresponding probabilities for the original states, not through the result itself being intermediate between the corresponding results for the original states – Dirac [1].

4.1 Introduction – Summary of Purpose

Generally, the 4-space of observation is restricted to a manifold inside a HD space, called the 'bulk' (hyperspace) by M-Theorists. If additional dimensions are compactified, then the observed universe would contain any possible extra dimensions; and no reference to a bulk is required. However, if a bulk with Large-Scale Additional Dimensionality (LSXD) does exist, a rich interacting brane-world influencing 4-space is postulated.

Kaluza-Klein XD compactification in string theory differs from the particle theory version in that a closed string can be wound several times around a rolled up dimension. A string with this property, has what is called winding mode oscillations that add additional symmetry not found in particle physics. A theory with a rolled up dimension of size R was found to be equivalent to a theory with a rolled up dimension of size L_s^2/R with winding modes and momentum modes exchanged in XD. (L_s is the string length scale.)

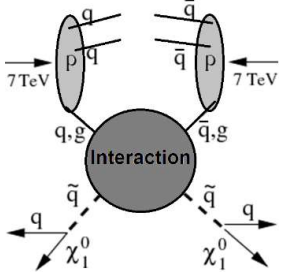

Fig. 4.1. An LHC p-p collision producing supersymmetric particles. Protons, p from the beams, are made of quarks, q and gluons, g. Their collisions produce supersymmetric particle pairs, $\tilde{q}$. The supersymmetric particles subsequently decay into ordinary particles and dark matter particles, χ_1^0. Redrawn from [2].

This symmetry allows correspondence between theories with small XD to theories with LSXD, which is known as T-Duality. In superstring theory, Kaluza-Klein compactification must be applied to a 6D space. The well-known method of doing so is to use a heterotic dual Calabi-Yau 3-torus which determines the geometric topology of the symmetries and spectrum of the particle theory [3]. In our theory the manifold of uncertainty has a 6D topology [4,5] compatible with this type of supersymmetry. Braneworld models generally radically differ from superstring Kaluza-Klein compactification models because they require few steps between the Planck scale and electroweak scale. This huge difference between the Planck and the electroweak scale is called the gauge hierarchy problem [6-8].

Sufficient theoretical insight related to a new anthropic multiverse UFM cosmology [4,9-44] has occurred during the 17 intervening years since the prior work [45] to design rigorous empirical protocols for isolating and manipulating fundamental parameters related to long-range coherence in semi-quantum systems. A key premise is that the so-called Planck scale stochastic regime is not fundamental and need no longer be a barrier to the study coherent phenomena in quantum systems generally or biological systems. Since Heisenberg's 1927 discovery, the quantum uncertainty principle (4D) has been by empirical definition a barrier to accessing certain kinds of complementary biophysical information. As will be shown, the simple solution is - Do something else! That is, use a different fundamental basis for quantum and biophysical 'measurement' criteria by utilizing additional degrees of freedom inherent in a noetic UFM cosmology. Nine experimental protocols are outlined for testing postulates of the model; which if successful will lead to bulk UQC, a standardized biophysical research platform and a new class of biosensors.

Noetic UFM cosmology makes correspondence to 11D M-Theoretic dual Calabi-Yau mirror symmetry, $M_{10} \to M_4 \times K_6$ [46-48] albeit with the addition of a twelfth dimension to incorporate Unified Field, U_F dynamics, $M_{12} \to M_4 \times K_8 \to \hat{M}_4 \times \hat{\mathbb{C}}_4^+ \times \hat{\mathbb{C}}_4^-$ [4,30]. String Theory has struggled to discover one unique vacuum compactification from the googolplex, 10^{googol} or infinite potentia provided by XD, with Standard Model Minkowski space, M_4 as the sought resultant [46-48]. Noetic UFM cosmology is different - All dimensionalities from 12D to 0D are cycled through continuously defined as a 'Continuous-state spin exchange dimensional reduction compactification process' that led to discovery of a unique string vacuum [4,44]. Note: The 'continuous-state' LCU is radically different than a Big Bang singularity [4,21,40,41].

Summary of salient theoretical postulates:

- The Unified Field, U_F provides an evolutionary 'force of coherence' guiding evolution in quantum systems.
- The HD U_F regime is accessible by surmounting the uncertainty principle (limitation imposed by space-quantization parameters of the Copenhagen Interpretation) by manipulating new cosmological parameters described by additional degrees of freedom related to a Large-Scale Additional Dimensionality (LSXD) version of M-Theory [41].
- Utilizing U_F parameters provides a new action principle with an inherent force of coherence acting like a 'super-quantum potential' or pilot wave [4,49-51] guiding the 'continuous-state' spin-exchange dimensional reduction compactification process of spacetime and evolution of complexity in quantum and the Self-Organized Living Systems (SOLS) it pervades [9].
- The putative unique 12D M-Theoretic regime of U_F action correlates parameters of Calabi-Yau mirror symmetry [49-51] with heretofore generally ignored properties of de Broglie-Bohm Causal and Cramer Transactional interpretations of quantum theory [49-52] and their higher dimensional (HD) extensions utilized in the new paradigm of noetic UFM cosmology [4,44].
- This unique string vacuum forms a conformal scale-invariant covariant polarized Dirac-Einstein energy dependent spacetime metric, $\hat{M}_4 \times \pm\mathbb{C}_4$ [4,53-55] which by nature of its inherent continuous-state dimensional reduction process [4] acts as a Feynman 'synchronization backbone' [56] facilitating/simplify-ing empirical accessibility.
- This empirical mediation of the LSXD polarized Dirac-Einstein metric, $\hat{M}_4 \times \pm\mathbb{C}_4$ (12D) [4,10,44,53-55] can be performed by a specialized incursive form of rf-modulated Sagnac Effect resonant interference hierarchy able to surmount the uncertainty principle [4,11].

Since 1993 the so-called Elitzur-Vaidman Interaction-Free Measurement (IFM) paradigm [57-65], a procedure for detecting the quantum state of an object without a phenomenological interaction occurring with the measuring device that ordinarily collapses the quantum wave function, Ψ provides

an indicia of our model suggesting it may be possible in general, as proposed here, to completely override the quantum uncertainty principle with probability, $p \equiv 1$ through utility of additional degrees of freedom inherent in the supersymmetric regime of string/brane theory. Note: in Newtonian mechanics the universe was 3D, Einstein introduced a 4D cosmology; now the next step seems to require 12D as the minimal dimensionality for producing causal separation from $\hat{M}_4$.

The disadvantages of the IFM model is that in order to improve probability towards certainty more and more Mach-Zehnder interferometers and more and more cycles through the apparatus are required [58-61]; while our apparatus acts with a single cycle because it represents a true and complete overriding of the quantum uncertainty principle by utilization U_F dynamics [4,11]. We emphasize our position that it is impossible to violate the uncertainty principle in 4D (by empirical fact) which the IFM method is limited to. This duality in the Quantum Zeno Paradox as experimentally implemented in IFM protocols suggests a duality between the regular phenomenological quantum theory [66-70] and a completed unified or ontological model beyond the formalism of the standard Copenhagen Interpretation as proposed here [4,5,44,45,71]. Utilizing extended theoretical elements, a putative empirical protocol for producing IFM with probability $p \equiv 1$ is introduced in a direct causal violation or absolute surmount of the methodology of the current 4D Copenhagen quantum Uncertainty Principle.

4.2. The Principle of Superposition

Classical waves can interact with constructive or destructive interference or a combination of both. When two waves interfere, the resulting displacement of the medium at any location is the algebraic sum of the displacements of the individual waves at that same location. Quantum mechanically waves can exist in all possible states simultaneously; this known as a superposition of states. A state vector corresponding to a pure quantum state takes the form, $|\Psi\rangle$. For example, if electron spin is measured in a Stern-Gerlach apparatus, there are two possible results. By convention electron spin is described by a 2D Hilbert space represented as a pure state complex vector, (α, β) with a length one by $|\alpha|^2 + |\beta|^2 = 1$ where $|\alpha|$ and $|\beta|$ are the absolute values of α and β. The superposition principle states that the net response at a given place and time caused by two or more stimuli is the sum of the responses which would have been caused by each stimulus individually. For example, a physically observable manifestation of superposition is interference peaks from an electron wave in a double-slit experiment or a qubit state as a linear superposition of the quantum basis states $|0\rangle$ and $|1\rangle$ in Dirac notation which convert to classical logic 0 or 1 by a measurement.

Accounting for interference effects in waves requires superposition such that an ensemble of quantum systems is described by wave functions with states, $\Psi_1, \Psi_2 \ldots \Psi_n$. Thereby any linear combination

$$\Psi = c_1\Psi_1 + c_2\Psi_2 \ldots c_n\Psi_n \tag{4.1}$$

with $c_1, c_2 \ldots c_n$ being constants describes possible quantum states of the ensemble. The complex wave functions, $\Psi_1, \Psi_2 \ldots \Psi_n$ are written as

$$\Psi_1 = |\Psi_1| e^{i\alpha_1}, \quad \Psi_2 = |\Psi_2| e^{i\alpha_2} \ldots \Psi_n = |\Psi_n| e^{i\alpha_n} \tag{4.2}$$

From (4.1) (simplified) the squared modulus of Ψ is

$$|\Psi|^2 = |c_1\Psi_1|^2 + |c_2\Psi_2|^2 + 2\,\mathrm{Re}\left\{c_1 c_2^* |\Psi_1||\Psi_2| \exp\left[i(\alpha_1 - \alpha_2)\right]\right\} \tag{4.3}$$

Achieved by

$$\begin{aligned}
&|\Psi|^2 = \Psi^*\Psi = \left(c_1^*\Psi_1^* + c_2^*\Psi_2^*\right)\left(c_1\Psi_1 + c_2\Psi_2\right) = \\
&c_1^*\Psi_1^* c_1\Psi_1 + c_2^*\Psi_2^* c_2\Psi_2 + c_1^*\Psi_1^* c_2\Psi_2 + c_1\Psi_1 c_2^*\Psi_2^* = \\
&\left|c_1\Psi_1\right|^2 + \left|c_2\Psi_2\right|^2 + c_1\Psi_1 c_2^*\Psi_2^* + \left(c_1\Psi_1 c_2^*\Psi_2^*\right)^* = \\
&\left|c_1\Psi_1\right|^2 + \left|c_2\Psi_2\right|^2 + 2\,\mathrm{Re}\left(c_1\Psi_1 c_2^*\Psi_2^*\right)
\end{aligned} \tag{4.4}$$

and then substituting (4.1) one gets (4.2), such that in general

$$|\Psi|^2 \neq \left|c_1\Psi_1\right|^2 + \left|c_2\Psi_2\right|^2 \tag{4.5}$$

because of the Uncertainty Principle.

Note that $|\Psi|^2$ is unaffected if the wavefunction, Ψ is multiplied by a global phase factor, $\exp(i\alpha)$. However, if α is a real constant, it depends on the relative phase $(\alpha_1 - \alpha_2)$ of Ψ_1 and Ψ_2 which because of the third term on the right in (4.3) is an interference term [4,72].

4.3 Oscillatory Rabi NMR Resonance Cycles

A Rabi cycle is the cyclic behavior of a two-state quantum system in the presence of an oscillatory driving field. We are interested here in NMR-like Rabi cycles because our protocol for surmounting the uncertainty principle relies in part on a Rabi cycle resonance hierarchy. A two-state or two-level quantum system, such as the spin-1/2 electron $(\pm\hbar/2)$ or atomic orbital transitions, has two possible states and can become 'excited' if energy is absorbed. For hydrogen in an electromagnetic field with the frequency tuned to the excitation energy, the electron would be in either the ground state or an excited state. If we initialize the hydrogen atom to one of these states, time evolution will cause each level to oscillate with a characteristic angular Rabi frequency represented by the basis vectors, $|1\rangle = \begin{pmatrix}1\\0\end{pmatrix}, |2\rangle = \begin{pmatrix}0\\1\end{pmatrix}$ [73].

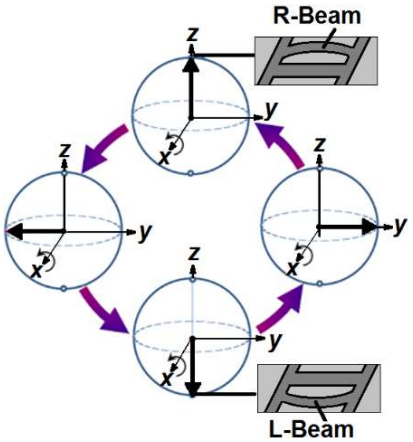

Fig. 4.2. Schematic evolution of coupled mechanical oscillators on the Bloch sphere when undergoing a Rabi cycle.

The NMR effect is produced by applying a strong static field, B_0, called the holding field, to a nucleus. When an additional weak transverse field, B_1 oscillating at an rf-frequency, ω_r rotating in the *xy*-plane around B_0 is applied to the holding field, $B_0\hat{z}$, one has the time-dependent field:

$$\mathrm{B} = \begin{pmatrix} B_1 \cos \omega_r t \\ B_1 \sin \omega_r t \\ B_0 \end{pmatrix} \text{ [73].} \qquad (4.6)$$

This is the right-handed rotating field; utilized in our protocol of counterpropagating Sagnac Effect rf-fields [4,5,44,71].

Whatever motions produce spectral lines, the application of a uniform magnetic field should produce changes because of Larmor precession. A general oscillation can be resolved into three harmonic components at right angles. If the magnetic field is in the +*z*-direction, then the oscillation in the z-direction will be unaffected by the magnetic field, while the *x* and *y* motions will precess with the Larmor angular velocity (*e*/2*mc*)B in a right-handed manner about the +*z*-axis. An *x*-vibration $x = a\cos\omega t$ can be expressed as the sum of two circular motions $(a/2)e^{i\omega t}$ and $(a/2)e^{-i\omega t}$ rotating in opposite directions, and similarly for a *y*-oscillation. Clockwise motion will speed up by Larmor precession to $\omega + \omega_L$, and anticlockwise motion will slow down by the same amount [73-75].

4.4. The Problem of Decoherence

It could be that the universe has a very rich structure, with many different branes, on which there exist very different physics, living in an as yet unknown geometry. - L. Randall [7].

Except perhaps for quantum Hall quasiparticle protected anyons, in principle, quantum systems are open and not isolated from environmental noise or coupling. Decoherence, the destroyer of quantum superstition is essentially the only remaining barrier to bulk UCQ. It is curious that although anyonic TQC apparently has solved this dilemma by the braiding of topological phase; as yet there is no known method of accessing the protected qubits [76,77]. We suspect our proposed Ontological-phase Topological Field Theory (OPTFT) will provide a method of doing so; but if such is the case, cryogenic temperatures would not be needed for UQC and an anyonic TQC might only be built as an interesting proof of concept.

One key to developing UQC is to have quantum states with lifetimes longer than it takes to perform a computing operation. Current records for maintaining coherence are curiously interesting. For isolated atoms in ultra-high vacuum chambers (no collisions with environment); the record for coherence is over 10 minutes. Solid-state silicon qubit systems cooled to absolute zero have long coherence times; but the new record is 39 minutes for room temperature silicon qubits [78].

In general, the problem of decoherence is strictly connected to the emergence of classicality in a world governed by the laws of quantum mechanics; and until now, any quantum information protocol must end up with a measurement converting quantum states into classical outcomes where decoherence plays a key role in this quantum measurement process [79-86]. The last statement is not true exactly in the manner stated. As we intend to show, the causally-free HD ontological-phase copy of the system may be read instead of the system itself, leaving the system itself untouched and free to continue its evolution. What this does to QC algorithms, or speedup remains to be determined [4,87,88] (Chap. 12).

The Heisenberg *uncertainty principle,* $\delta_x \delta_\rho \geq \hbar/2$ says that there is an inherent uncertainty in the relation between position and momentum in the *x* direction. Matter was thought to consist of localized particles, but matter exhibits wave-like properties, which means that matter, like waves, isn't localized in space. The uncertainty principle is a direct consequence of the wave-like nature of matter, because you

can't completely discretize a wave. As developed to a preliminary degree in Chap. 4, we move beyond these concepts of matter to one radically extended in HD UFM topology.

We concur with Randall that these dimensions can be of infinite size, which follows from the existence of branes with infinite spatial extent, a property of branes that occurs because they carry energy. If there is an energetic 4D flat brane in a 5D spacetime, the 5D space does not consist of flat, uniform, LSXD. To accommodate a flat brane requires that in addition to the tension of the brane itself, there is a bulk vacuum energy, closely aligned to the brane tension. The solution to Einstein's equations is then described locally as an anti-de Sitter (AdS) space, a space with a negative vacuum energy, although it is fundamentally 5D [7,89].

In this geometry, the length of a yardstick depends on position. Spacetime is 'warped' and HD do not have to be finite in size, because unlike the case of flat XD, the gravitational force spreads very little in the direction perpendicular to the brane. To derive this form for the gravitational force, one solves Einstein's equations of general relativity in the presence of the brane. General relativity tells us that not only do gravitational forces affect matter, but matter determines the surrounding gravitational potential. In this case, the presence of a massive brane leads to a gravitational force highly concentrated near the brane. So although XD can be very large (even infinite), the gravitational force is highly concentrated near the brane [6-8].

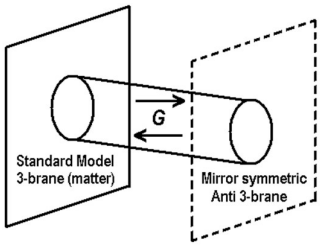

Fig. 4.3. Infinite size local 3-space and LSXD Braneworld and relate to gravity.

Randall says there is physics that ties XD to observable low energy scales. Such theories, in which the XD are tied to relatively low energy scales, have the enticing possibility that they can be observed in the next generation of LHC colliders. Our model, which may be a form of supersymmetric M-Theoretic T-Duality, is different, tabletop and low energy; if successful it will put an end to the need for supercolliders [90].

> In a variant of the original proposal, in which the second brane does not end space but resides in an infinite extra dimension (essentially combining RS1 and RS2), one would have missing energy signatures identical to those one would obtain with six large ADD-type extra dimensions ... A five-dimensional AdS space is equivalent to a four dimensional scale-invariant field theory, in the sense that all properties of the four-dimensional theory can be computed from the five-dimensional gravitational theory, and in principle one can learn about the gravitational theory from the conformal field theory (this is known as a holographic correspondence) … These include the existence of a four-dimensional domain in a higher dimensional space … It is possible that one or several of these ideas will be relevant to the question of how string theory evolves from a higher dimensional theory to one that reproduces observed four-dimensional physics [7].

4.5. Insight into the Measurement Problem

In order to surmount quantum uncertainty and empirically access the hidden 3rd regime of reality (Classical → Quantum → Unified) new physics is required.

Here we introduce a new ontological type of homeomorphic transformation (a holomorphic-antiholomorphic duality) that Toffoli calls a 'topological switching' [75] by what Stern calls 'topological charge' [91,92] that we propose as an empirical basis for the Micromagnetics of spacetime/matter information exchange without usual phenomenological exchange quanta. Mediation occurs instead as an 'ontological becoming' or 'being' by operation of an energyless coherently controlled resonant hierarchy of the topology of LSXD brane interactions [4,87,88] which is not a local

Hamiltonian phenomenon but perhaps a new form of ontological U_F Lagrangian topology. Topological switching can be represented metaphorically as the perceptual switching of the central vertices of a Necker Cube (Ambiguous cube) when stared at.

For example, imagine a usual 4D qubit or quantum particle in a box. In our noetic UFM interpretation the LSXD Calabi-Yau mirror symmetric regime contains a hierarchy of conformal scale-invariant 'copies' of the original 4D quantum state not independent Everett-Wheeler parallels [94,95]. Then in way of simplistic introduction in terms of our new operationally completed interpretation of quantum theory the 'mirror image of the mirror image is causally free' of the underlying uncertain 4D quantum state and is accessible by manipulating the resonance hierarchy of our empirical protocol! Many physicists have been reluctant to embrace HD or LSXD physics. We suspect success of our protocol would ease this philosophical conundrum.

In this volume a putative protocol is delineated not for another sophisticated improvement of the varied stepwise degrees of reducing the uncertainty relation by the several extant IFM protocols [93]; but for completely surmounting the uncertainty relation directly, in a straight forward manner, for any and every single action of the experiment with probability, $p \equiv 1$. In an unexpected way our model has similarities to IFM but by using extended theory fully completes the task of uncertainty violation. One could say the new noetic UFM protocol turns the IFM methodology upside down and inside out. The LSXD regime of the noetic UFM protocol accesses the complete 'hall of mirrors' simultaneously (ontologically) because the whole battery of IFM interferometers and multiple cycling routines is inherent in the conformal scale-invariant mirror symmetry of the LSXD regime, such that only one 'measurement' is required to achieve probability, $p \equiv 1$ when resonance is properly coupled and timed with the inherent continuous-state mirror symmetric synchronization backbone beat frequency.

The methodology of this new empirical protocol is fully ontological (rather than the usual phenomenology of field interactions) because action in the LSXD regime is in causal violation of Copenhagen phenomenology not in an Everett 'many-worlds' sense but in a manner that extends to completion the de Broglie-Bohm-Vigier causal interpretation of quantum theory [50]. In summary the ontological basis is realized utilizing the additional degrees of freedom of a unique 12D iteration of M-Theory along with the key supposition of conformal scale-invariance pertaining to the physicality of the dual mirror symmetric state of LSXD quantum information as geometric topology [4,5,44].

In Fig. 4.4a the suggestion is that the 3-cube (bottom left) represents the region of a Cavity-QED or 3D quantum 'particle in a box' that through conformal scale-invariance remains physically real when the metaphor is carried to 12D where the 'mirror copy' becomes like a 'mirror image of a mirror image' and in that sense, is causally free of the E_3 quantum state thereby open to ontological information transfer in violation of Copenhagen uncertainty. A 5D hypercube would unfold into a cross of 4D hypercubes and so on to 12D.

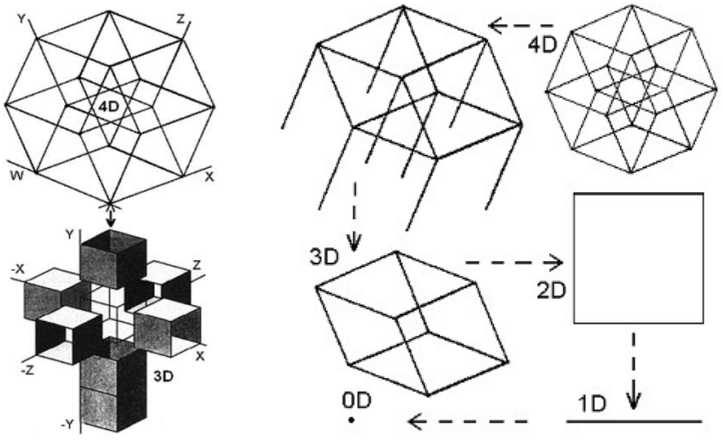

Fig. 4.4. a) Left, a 4D hypercube unfolds into a 3D cross of 8 cubes. b) Right. Dimensional reduction cycle from 4D to 1D.

Beyond 4D mirror symmetry adds a complexity in that the unfolding (Fig. 4.4b) has a knot or Dirac twist (not shown) that is part of the gating mechanism insulating quantum mechanics from the 3rd regime of UFM [5]. In Copenhagen the 'handcuffs' are on but during the LSXD cycle the handcuffs are periodically off and thus accessible resonantly.

4.6. New Physics from Anthropic Cosmology

Issues of the nature of the fundamental cosmological background continue to be debated with disparate views jockeying for philosophical supremacy; a scenario remaining tenable because experimental avenues for testing physics beyond the standard model have remained elusive until now. For the scientific perspective to evolve beyond the usual Copenhagen Interpretation of quantum theory requires a new cosmological paradigm. Full delineation of the new cosmology is beyond the scope of this volume, but introduced in [4,5,44,71,72]. In summary we axiomatically review pertinent concepts. The new noetic UFM cosmology is required to explain, utilize and design experimental access to the U_F regime where parameters required for UQC and for biophysical-bridging reside.

- The Planck scale can no longer be considered the most fundamental level of reality. Three regimes of reality must be addressed: Classical⇔Quantum⇔Unified Field; all of which cycle continuously [4].

- No 'observer' quantum state reduction exists in the usual sense of wave function collapse [71]; in the de Broglie-Bohm and extended Cramer interpretations of quantum theory [49-52] a continuous evolution operates instead [4,5,71]. Collapse of the wavefunction reduces a quantum state to a classical state, which does not generally happen in the nonlocal flux of qualia as the locus of awareness; especially since now more pertinently qualia are not quantum phenomena per se but unified field phenomena. Quale interface with the quantum regime as part of the sensory data transduction apparatus.

- The Planck scale is not an impenetrable barrier [5,44] even though considered so as an empirical fact demonstrated by the quantum uncertainty principle. This is a main problem with utilizing a Darwinian Naturalistic Big Bang cosmology originating from a putative singularity in time as the basis for cognitive theory. In an anthropic multiverse cosmology utilizing extended quantum theory and M-Theory the answer is simply: 'do something else!' which opens physical investigation into a new U_F realm of large scale additional dimensions (LSXD) [5,7,44,89]. The anthropic multiverse is closed and finite in time, i.e. the 14.7 billion light year Hubble radius, H_R, but open and infinite in atemporal eternity [4]. 'Worlds without number, like grains of sand at the seashore' [96] the multiverse has room for an infinite number of nested Hubble spheres each with their own fine-tuned laws of physics [4].

Fourteen empirical protocols are proposed [97,98] (9 reviewed here) for UQC, demonstrating, gaining access to and leading to a variety of experimental platforms for first hand investigation of awareness (qualia) breaking down the 1st person 3rd person barrier called for by Nagel [99].

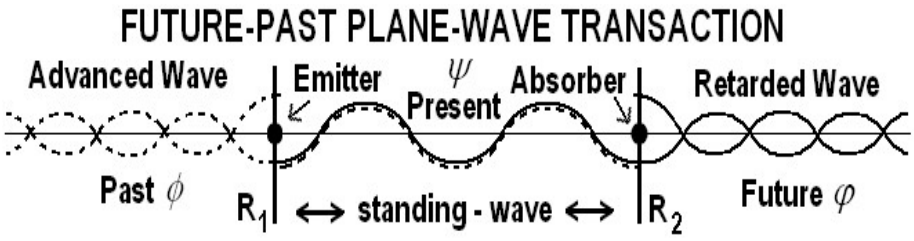

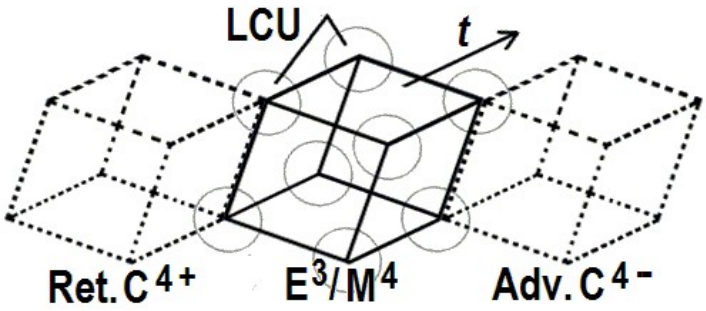

Figure 4.5. a) Conceptualized structure of a Cramer transaction (present state or event) where the present (simplistically) is a standing-wave of future-past potential elements. A point is not a rigid singularity (although still discrete) as in the classical sense, but has a complex structure like a mini-wormhole where R_1 & R_2 (like the frets holding the wire of a stringed instrument) represent opposite ends of its diameter. b) How observed (virtual) 3D reality arises from the infinite potentia of HD space (like a macroscopic transaction). The 'standing-wave-like' (retarded-advanced future-past) mirror symmetric elements C^{4+} / C^{4-} (where C^4 signifies 4D potentia of complex space distinguished from the realized 3D of visible space) of continuous-state spacetime show a central observed Euclidian, E_3, Minkowski, M_4 space resultant. Least Cosmological Units (LCU) governing evolution of the 'points' of 3D reality are represented by circles. The Advanced-Retarded future-past 3-cubes in HD space guide the evolution of the central cube (our virtual reality) that emerges from elements of HD space.

String theory only has one parameter, string tension, T_S fraught with the dilemma of a Googolplex (10^{googol}) or infinite number of vacuum possibilities. Utilizing the Eddington, Dirac, and Wheeler large number hypothesis [5] we derived an alternative derivation of T_S leading to one unique string vacuum and what we call the 'continuous-state hypothesis' an alternative to the expansion/inflation parameters of Big Bang cosmology [4,5]. Simplistically the perceived inflation energy of Big Bang cosmology postulated as a Doppler expansion from a primordial *ex nihilo* temporal singularity, instead according to the UFM noetic continuous-state hypothesis, is localized in an 'eternal present' as if in permanent 'gravitational free-fall' [4,5]. Since we are relativistically embedded in and made out of matter this condition means that all objects (in our 3D virtual reality) exist (in HD) as if they were in gravitational 'free-fall'. This is better explained by two other interpretations of quantum theory generally ignored by the physics community because they are myopically considered to add nothing. That of the de Broglie-Bohm Causal Interpretation [49-51] and the Cramer Transactional Interpretation [52]; where spacetime and the matter within it (all matter is made of de Broglie waves) are created-annihilated and recreated cyclically over and over as part of the perceived arrow of time and creation of our 3D reality as a resultant from HD infinite potentia as a 'standing-wave' (Fig. 4.5) [4,5].

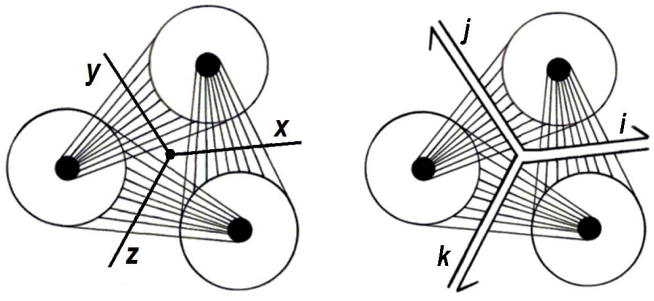

Fig. 4.6. Conceptualization of the cosmological Least-Unit (LCU) tessellating space which like quark confinement cannot exist alone. a) Current view of a so-called point particle or metric *x,y,z* vertex. The three large circles are an LCU array slice. It is a form of close-packed spheres forming a 3-torus; missing from the illustration are an upper and bottom layer covering the *x,y,z* vertex and completing one fundamental element of an LCU complex. The field lines emanating from one circle to another represent the de Broglie-Bohm concept of a quantum 'pilot wave or potential' governing evolution. b) Similar to a) but drawn with a central 'Witten string vertex' [100] and relativistic quantum field potentials (lines) guiding its evolution in spacetime. The Witten vertex is not a closed singularity and because of its open structure provides a key element to the continuous-state process and rotation of the Riemann sphere cyclically from zero to infinity which represents rotational elements of the HD exciplex brane topology.

The problem has to do with the nature of a point or 3D vertex in physical theory [4,100]. What extended versions of de Broglie-Bohm and Cramer bring to the table is a basis for defining a fundamental 'point' that instead of being rigidly fixed classically (Fig. 4.6a) is continuously transmutable (Fig. 4.6b) as in string theory. This represents in essence the elevation of the so-called wave-particle duality for quanta to a Principle of continuous-state cosmology. What this does is cancel the troubling infinites in the standard model of particle physics in a natural way rather than by use of a mathematical gimmick called renormalization. We also build the continuous-state hypothesis around an object in string theory called the Witten Vertex [100] (Fig. 4.6b after noted M-Theorist David Witten). This means that when certain parameters (compactification, dimensional reduction etc.) associated with the Riemann sphere reach a zero-point; the Riemann sphere relativistically rotates back to infinity and so on continuously (Reminiscent of how water waves operate). The HD branes of so-called Calabi-Yau mirror symmetry are forms of Riemann 3-spheres or Kahler manifolds [15,46,47]. Instead of the insurmountable Plank foam, the gate keeper in this cosmology is an array of least cosmological units (LCU) [4,5,71,101] of which part (like the tip of an iceberg) resides in our virtual 4-space and the other part resides in the HD (12D) regime of a UFM version of M-Theory. These LCU exciplex gates govern the continuous-state process in the coherent ordering of matter embedded in a localized spacetime manifold (Chap. 4).

4.6.1. *Spacetime Exciplex - U_F Noeon Mediator*

The spacetime exiplex or 'excited complex' of least cosmological units (LCU) is key to mediation of the U_F principles related to the observer. In the usual 4D interpretation of quantum theory limited by the uncertainty principle, virtual quanta in the zero point field wink in and out of existence limited to the Planck time, 10^{-43} s. For the noetic UFM spacetime exiplex the situation is radically different. The duality of its HD structure (i.e. living in both local 4-space and nonlocal 8-space) allows it to remain in an excited state in 4-space never fully coupling with the Planck-scale ground state. This holophote interaction is a noeon flux (exchange unit of the U_F) into every point (and thus atom) in spacetime (also animating living systems) by interaction with neural dendrons etc. for example as the flow of qualia as a form of superradiance into the brain.

Kowalski discovered that photon emission occurs only after electrons complete full Bohr orbits [102,103]. We apply this as a general principle for emission during rotation of the complex Calabi-Yau Riemann sphere which acts like a pinwheel-like scoop bringing in the next topologically switched hysteresis loop of semi-quantum interaction energy.

The exciplex concept as defined in engineering parlance is an 'excited complex' or form of excimer - short for excited dimer in chemistry nomenclature used to describe an excited, transient, combined state, of two different atomic species (like XeCl) that dissociate back into the constituent atoms rather than reversion to some ground state after photon emission. An excimer is a short-lived dimeric or heterodimeric molecule formed from two species, at least one of which is in an electronic excited state. Excimers are often diatomic and are formed between two atoms or molecules that would not bond if both were in the ground state. The lifetime of an excimer is very short, on the order of nanoseconds. Binding a larger number of excited atoms form Rydberg clusters extending the lifetime which can exceed many seconds.

An Exciplex is also defined as an electronically excited complex, 'non-bonding' in the ground state. For example, a complex formed by the interaction of an excited molecular entity with a ground state counterpart of a different structure. When it hits ground a photon or quasiparticle soliton is emitted. In Noetic UFM Cosmology we have adapted the exciplex concept as a tool to describe the LCU gating mechanism between the quantum regime and the regime of the U_F. The exciplex LCU gate is key to understanding interaction of the physical mind of the observer and the basis for developing empirical tests. The general equations for a putative spacetime exciplex are:

$$G^* + G^* \Leftrightarrow Z^*; \quad Z^* + m_\gamma \Leftrightarrow X^*$$
$$X^* - m_\gamma \xrightarrow{emission} Z^* \ \ or \ G^* \qquad (4.7)$$
$$X^* + m_\gamma \rightarrow Z^* \ \ or \ \ G^*$$

where as seen in Fig. 4.7a, G is the ZPF ground state, Z intermediate cavity excited states and X the spacetime C-QED (Cavity-Quantum Electrodynamics) exciplex coupling. The numerous configurations plus the large variety of photon frequencies absorbed allow for a full absorption-emission equilibrium spectrum. We believe the spacetime exciplex model also has sufficient parameters to allow for the spontaneous emission of protons by a process similar to the photoelectric effect but from HD spacetime C-QED brane spallation rather than from a charged metallic surface. Not having a sufficient spacetime vacuum proton creation mechanism led to the downfall of Steady-State cosmology.

The new U_F basis centers on defining what is called a Least Cosmological Unit (LCU) [4,5,101] tessellating the spacetime backcloth. An LCU (Figs. 4.6,4.7) conceptually parallels the unit cell that builds up crystal structure. The LCU entails the next evolutionary step for the basis of a point particle and has two main functions; it is the raster from which matter arises, and is a central mechanism that mediates the syntropic gating for physics of the observer parameters of the U_F. Syntropy is the negentropy process of expelling entropy by the teleological action of quantum biosystems.

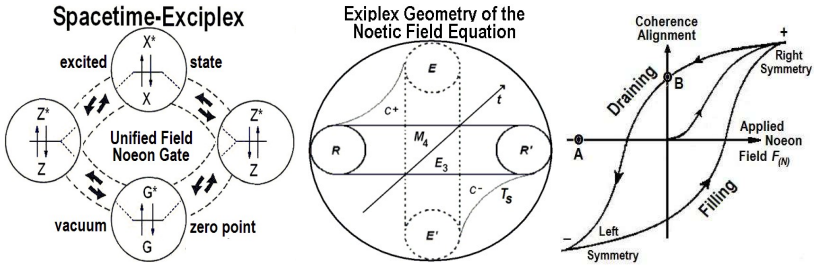

Fig. 4.7a) The geometry of the 'spacetime exciplex' (excited complex), a configuration of spacetime LCUs that act like a holophote laser pumping mechanism of U_F noeon energy and also how coherence of the U_F interacts with 3D compactified states. Locally the exciplex acts like an oscillating 'cootie catcher' [104]. b) Geometric representation of the Noetic Unified Field Equation, $F_{(N)} = \aleph / \rho$ for an array of cosmological LCUs. Solid lines represent extension, dotted lines field. Where $F_{(N)}$ is the anthropic or coherent force of the U_F driving self-organization, total energy, $\aleph$ equals the c) hysteresis loop energy of the hypervolume, ρ is the scale-invariant rotational radius of the action and the domain wall (curves) string tension, T_0.

The LCU change from the current concept of a fixed Planck scale point (Fig. 4.6a) to what is called a Witten string vertex [100] (Fig. 4.6b) is a form of Riemann sphere (model of the extended complex-plane with points at zero and infinity for stereographic projection to the Euclidean plane) cyclically opening into the LSXD regime of the U_F. Behind the current view of $\hbar$ (Planck's constant) as a barrier of stochastic foam is a coherent topology with the symmetry of a spin raster comprised of LCUs [4].

4.6.2. *Quantum Phenomenology Versus Noetic UFM Field Ontology*

There is a major conceptual change from Quantum Mechanics to Unified Field Mechanics (UFM). The 'energy' of the U_F is not quantized and thus is radically different from other known fields. Here is what troubled Nobelist Richard Feynman: *"...maybe nature is trying to tell us something new here, maybe we should not try to quantize gravity... Is it possible that gravity is not quantized and all the rest of the world is*?" [105]. It turns out that not only is gravity not quantized but neither is the UFM coherent noeon energy of the U_F which is a step deeper than gravity.

Here is one way to explain it. In a usual field like electromagnetism, easiest for us to understand

because we have the most experience with it, field lines connect to adjacent point charges. The quanta of the fields force is exchanged along those field lines (in this case photons). We perceive this as occurring in 4-space (4D). It is phenomenological. This is the phenomenon of fields. For topological charge as in the U_F with properties related to consciousness; the situation is vastly different. The fields are still coupled and there is tension between them but no phenomenological energy (i.e. field quanta) is exchanged. This is the situation in the ontological case. The adjacent branes 'become' each other as they overlap by a process called 'topological switching'. This is not possible for the 4-space field because they are quantized resultants of the HD topological field components. The HD 'units' (noeons) are free to 'mix' ontologically (ambiguous Necker cube vertices) as they are not resolved into points.

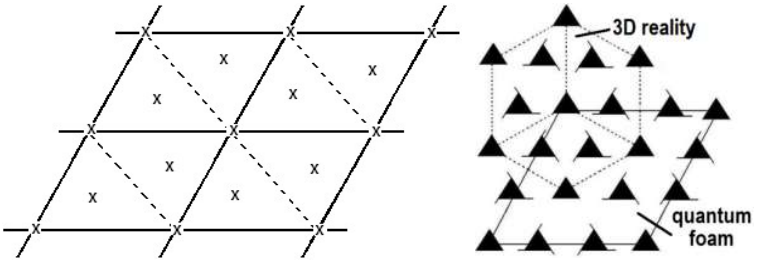

Fig. 4.4. a) 2D view of the LCU tiling of the spacetime backcloth (Fig. 4.6). b) Projective geometry topologically giving rise to HD (here the Fig. 4.8a 2D view extended to 3D). The triangles with tails represent trefoil knots and the naked triangles the resultant cyclic point or fermionic vertex quantum state in 3-space (Spheres in Fig. 4.7a,b).

The metric still has points, or it might be better to say coordinates; but in HD super space they are unrestricted and free to interact by topological switching which is not the case for an 'event' in 4-space. Whereas this singular quality (basis of our perceived reality) does not exist in the HD regime (U_F) of infinite potentia! So if the U_F is not quantized how can there be a force which is mediated by the exchange of energy? Firstly, the U_F does not provide a 5th force as one might initially assume; instead the ontological 'presence' of the U_F provides a 'force of coherence' which is based on 'topological charge'. It helps to consider this in terms of perception. If one looks along parallel railroad tracks they recede into a point in the distance, a property of time and space. For the unitary evolution of the mind of the observer [71] this would break the requirement of coherence. For the U_F which is outside of local time and space, a cyclical restoring force is applied to our *res extensa* putting it in a *res cogitans* mode. The exciplex mechanism [4] guides rotation of the Witten vertex Riemann spheres to maintain a consistent level of periodic coherence (parallelism). It is a relativistic U_F process. The railroad tracks do not recede into a point, but it is not observed because the Riemann sphere flips (our perception) by subtractive interference beforehand.

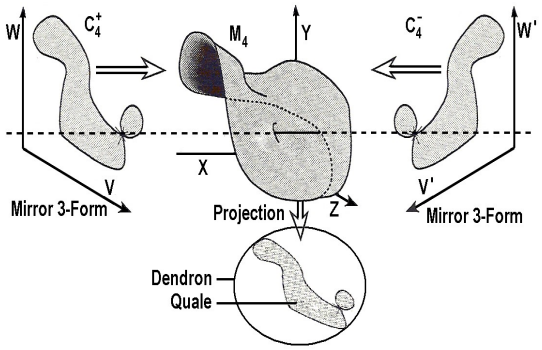

Fig. 4.9. Complex HD Calabi-Yau mirror symmetric 3-forms, C_4 become embedded in Minkowski space, M_4 and the U_F energy of this resultant is projected into localized matter as a continuous stream of evolving (evanescing) Bohmian explicate order. This represents the lower portion only that embeds in local spacetime; there is an additional duality above this projection embedded in the infinite potentia of the U_F from which it arises.

The U_F provides an inherent force of coherence just by its cyclical presence (perhaps a form of superradiance). This means that it is ontological in its propagation of information or 'interaction'. The railroad tracks remain parallel and do not recede to a point as (perceived) in the 3D phenomenological realm where forces are mediated by a quantal energy exchange. Another way of looking at this is that the 3D observer can only look at one page of a book at a time while the HD observer (omniscient) can see all pages continuously. The LCU space-time exciplex is a mechanism allowing both worlds to interact locally-nonlocally.

Most are familiar with the ambiguous 3D Necker cube (center of Fig. 4.4a bottom is like a Necker cube) that when stared at central vertices topologically reverse. This is called topological switching [75]. There is another paper child's toy called a 'cootie catcher' [104] that fits over the fingers and can switch positions. What the cootie catcher has over the Necker cube is that it has an easier to visualize a defined center or vertex switching point. So in the LCU Exciplex spacetime background we have this topological switching which represents the frame that houses the gate which is the lighthouse holophote with the rotating light on top.

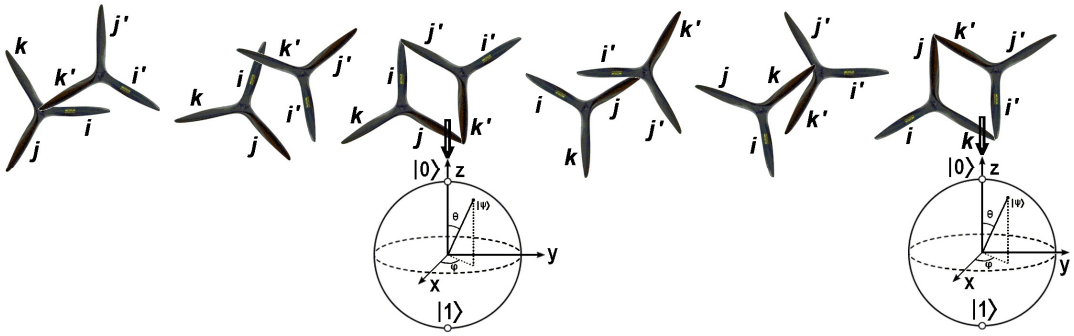

Fig. 4.10. Locus of nonlocal HD mirror symmetric Calabi-Yau 3-tori (here technically depicted as quaternionic trefoil knots) spinning relativistically and evolving in time. Nodes in the cycle are sometimes chaotic and sometimes periodically couple into resultant (faces of a cube) quantum states in 3-space depicted in the diagram as Riemann Bloch spheres, possibly indicative of the emergence of observed 3D reality. An animated version of Fig.4.9.

Now inside the structure there is also a 'baton passing'. The baton is like the lens that the light shines through but only at the moment of transfer (or coupling). In the HD U_F regime the 'light' is always on omni-directionally but only 'shines' into 3-space when the gate is open during the moment of baton passing. In addition to baton passing there is also a form of 'leap-frogging'. The leap-frogging represents wave-particle duality (remember we elevated it to a principle of cosmology). The leaping moment represents the wave, and the crouched person being leapt over is the particulate moment. The particle moment acts like a domain wall and no noeon light passes when its orientation is aligned towards the 3-D world resultant. This is also an important aspect of the gating mechanism. This is of course a relativistic process such that the 'beat frequency' giving rise to the arrow of time as a continuous LCU creation-annihilation cycle.

The trefoil knot, drawn as Planck-scale quaternion vertices in Fig. 4.10, is holomorphic to the circle. Since energy is conserved we may ignore the complexity of the HD symmetries and use the area of the circle for the noeon hysteresis loop (Fig. 4.7c), in this case a 2D resultant as a 2-sphere quantum state as the coupling area of one LCU complex coupled to a HD noeon brane array. This idea is further conceptualized in Fig. 4.8 illustrating how a 3D object emerges from close-packed spacetime LCUs.

4.7. The Basement of Reality - Through the Glass Ceiling

The anyon braid is topologically protected from decoherence but seemingly doubly inaccessible by the uncertainty principle. Few yet understand why UQC cannot be done from within the confines of the 4D standard model. The full power of quantum entanglement only comes to bear with access to the

holographic properties of non-locality. Not as utilized now by parametric down conversion of a pair of EPR photons (points) embedded in spacetime. Many now realize space-time is emergent – not fundamental. So we want to gain access to a more fundamental arena, which is the HD regime of UFM. We need to Gödelize beyond quantum mechanics in the same way we Gödelized beyond classical mechanics; which we know everything about because of this transition. Gödelizng QM will give us full access to all that is quantum readily facilitating UQC. By Gödelizng, we mean going beyond the limits of the domain under study. Generalizing philosophically what Gödel said, '*a thing cannot be understood in terms of itself*'.

Let's try to understand how to Gödelize beyond the Standard Model. Firstly, the world we observe is an asymptotically flat Euclidean 3-space of infinite size dimensionality. Current thinking suggests this reality has a 'basement'; a fixed Zero-Point Field (ZPF) stochastic barrier or 'quantum foam' with *zitterbewegung* virtual particles winking in and out of existence for the Planck time, t_P. The Planck time, $t_P \equiv \sqrt{\hbar G/c^5} \approx 5.39106 \times 10^{-44}$s represents the duration required for light to travel a distance of one Planck length ($l_P = \sqrt{\hbar G/c^3} \approx 1.61619 \times 10^{-33}$cm), where, $\hbar$ is the reduced Planck constant, G the gravitational constant, c the speed of light in vacuum and s the second. Quantum field theory covers aspects of both special relativity and quantum theory, $\hbar$ sets the scale at which the uncertainty principle applies. In quantum theory $\hbar$ appears in the commutation relation between momentum, p and position, q of a particle: $pq - qp = -i\hbar$, and similar commutation relations involving other complementary pairs of measurable quantities. Because our ability to measure two quantities simultaneously with complete precision is limited by their *inability to commute*, $\hbar$ quantifies uncertainty for simultaneous measurement of all quantum properties!

If LSXD are shown to exist, the Planck length would have no fundamental physical significance. In string theory, the Planck length is claimed to be the mathematical order of magnitude of the oscillating strings that form elementary particles. The string scale l_s is related to the Planck scale by $\ell_P = g_s^{1/4} l_s$, where g_s is the string coupling constant, which in actuality is not constant, but depends on the value of a volume factor when the size of XD is allowed to vary. Any physical calculation predicting length using only the constants c, G and $\hbar$ must include the Planck length, possibly multiplied by a usually considered unimportant numerical factor like 2π. But these arguments are far from being settled; it may be, and this is our conjecture, that a numerical factor like 2π might be very important and take a value that is very large or very small [26]. If $\hbar$ has physical significance (beyond its current use as a mathematical tool) it would apply to compactified black hole material.

How does this correlate the concept of a photon as a traveling **wave** along a 2D surface projecting at right angles to the **direction** of propagation with a photon with a particulate radius limiting the slit diameter it is able to pass through to ~ 10^{-9} cm? These are unsettled issues in both the basis of quantum field theory itself and measurement theory. What we are getting at is that the uncertainty principle is hiding an inherent backcloth of cyclic bumps and holes in the Dirac polarized backcloth [4].

n	*V*(*n*,1)	
0	0	0
1	2	2
2	π	$\approx$ 3.1416
3	$4/3\pi$	4.1888
4	$1/2\pi^2$	4.9348
5	$8/15\pi^2$	5.2638
6	Degenerate ?	∞

TABLE 4.1. Standard Hypervolume values for increasing *n*-dimensionality and radius, *r* of a unit sphere or *n*-ball equal to 1.

We have postulated a Manifold of Uncertainty (MOU) with a finite dimensional radius somewhat aligned with what string theory calls T-Duality [3-5]. For preliminarily predictions we could calculate hyperspherical volume or surface area of 2D-5D MOU (Fig. 4.11). The general *n*-volume equation is

$$V(n,r) = \pi^{\frac{n}{2}} r^n / \Gamma\left(\tfrac{n}{2}+1\right) \qquad (4.8)$$

where $V_{n,r}$ is volume per number of dimensions, *n* of radius *r* and Γ a factorial constant. These *n*-volume equations relate to volumetric properties of the MOU for calculating an HD C-QED volume hierarchy for predicting new Tight-Bound State (TBS) spectral lines in hydrogen [31,35]. If LSXD exist, degeneracy would occur at the limit of *r* discovered in the same manner the outermost energy level of an atom is detected when an outer electron acquires sufficient energy to escape to infinity.

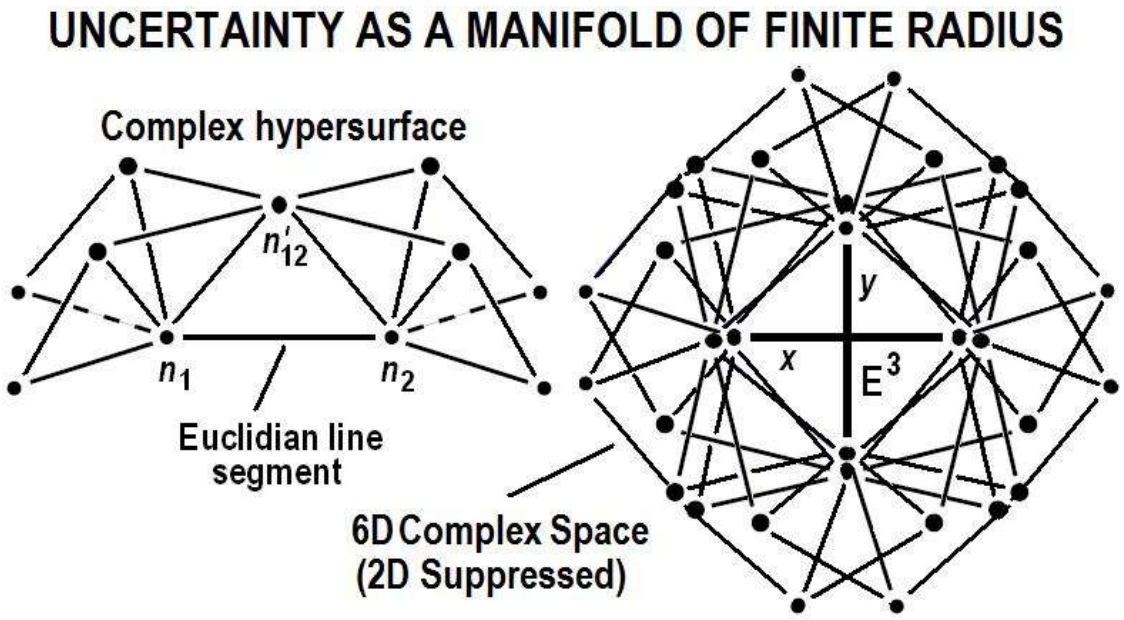

Fig. 4.11. Proposed 5/6D Manifold of Uncertainty (MOU) 'guarding the door to LSXD. Dimensional suppressed planar views of quaternion vertices.

As shown in Fig. 4.11 we postulate existence of a 'semi-quantum limit' MOU 5D with the 6thD being degenerate (like the outermost atomic electron radius where the outer electron can escape to infinity when acquiring sufficient energy). We assume a 6D MOU based on an M-Theoretic Calabi-Yau dual 3-torus [3]. This is a 12D model with 6 spatial, 3 temporal and 3 super-quantum potential-like control parameters of the unified field. But because we don't fully understand how to close-pack the LCU array tessellating spacetime we do not have much rigor yet [87,88].

4.8. Empirical Tests of UFM Cosmology Summarized

Viable experimentation will lead to new UFM research platforms for studying fundamental syntropic properties of quantum systems. We have proposed fourteen tests of UFM; in this chapter we summarize the main experimental protocol to test the for the UFM noeon, Tight-Bound States (TBS) in hydrogen and the teleological 'life-principle' hypotheses. Note: Not all of the experiments relate directly to mediation of the U_F noeon, but all of the experiments manipulate the new physical regime of the U_F or importantly mediate the 'gating mechanism' by which access is gained to the 3rd regime of reality, thus facilitating mind-body research in addition to M-Theory, UQC and nuclear physics.

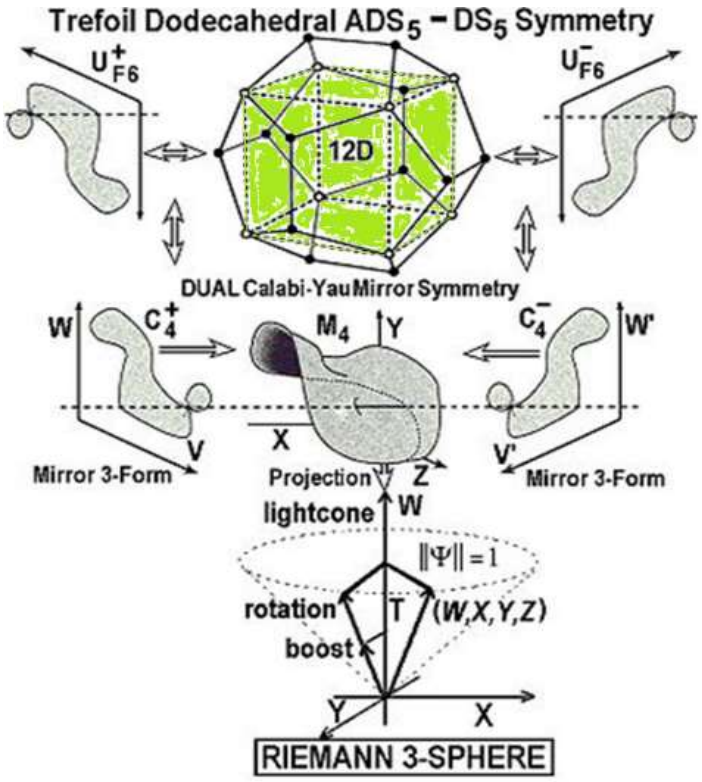

Fig. 4.12. Completion of Figs. 4.9 & 4.10 illustrating full extension to an HD ontological-phase topological field in continuous-state dual Calabi-Yau mirror symmetric UFM cosmology with Dodecahedral involute properties, as well as the continuous-state exciplex 'hysteresis loop' of noeon injection (not shown) as far as currently understood. The Bloch 2-sphere representation is also replaced with an extended Riemann 4-sphere resultant with sufficient parameters to surmount the uncertainty principle representing a unique M-Theoretic model of 'Continuous-State' U_F dynamics as it relates to UFM and its putative exchange quanta of the U_F - the noeon.

The 3-cube embedded in the dodecahedron (top of Fig. 812) represents what we term the 'mirror image of the mirror image' enfolding a scale-invariant 'causally free' copy of the Euclidean 3-space quantum 'particle in a box', accessible under a precise protocol surmounting uncertainty.

4.8.1 *Summary of Experimental Protocols*

If experimentation proves viable a new class of UQC biophysical research platform for studying fundamental properties of the spacetime vacuum as it relates to long-range coherence in living systems. We summarize eight derivatives of the main experimental protocol to test the LSXD continuous-state Long-Range Coherence hypotheses:

1. Basic Experiment - Fundamental test that the concatenation of new OPTFT U_F principles is theoretically sound. A laser oscillated rf-pulsed vacuum resonance hierarchy is set up to interfere with the periodic (continuous-state) structure of the inherent 'beat frequency' of a covariant Dirac polarized spacetime vacuum exciplex to detect the new coherence principle associated with a cyclical holophote entry of the U_F into 4-space. This experiment 'pokes a hole in spacetime' in order to bring the energy of the U_F into a detector. The remaining protocols are variations of the parameters of this experiment.
2. Bulk Quantum Computing - Utilizing protocol (1) Bulk Scalable UQC can be achieved by superseding the quantum uncertainty principle. (see [31,35,87,88,97,98] for details) Programming and data I/O are performed without decoherence by utilizing the inherent mirror symmetry properties

that act like a 'synchronization backbone' [4,] whereby 'LSXD copies' of the local 3-space quantum state are causally free (measureable without decoherence) at specific resonance nodes in the continuous-state conformal Calabi-Yau symmetry cycle hierarchy.

3. Protein Conformation - (similar to discussion in [13]). Utilizing more macroscopic aspects of protocols (1 & 2) dual Hadamard quantum logic gates are set as a Cavity-QED spacetime cellular automata [4,27] experiment to facilitate conformational propagation in the prion protein from normal cellular form, PrP^{C} to the pathological, PrP^{Sc} form by noeon bombardment with the 'force of coherence' of the U_F.
4. Manipulating a special case of the Lorentz Transformation [72] - Aspects of a spacetime exciplex model [4] in terms of restrictions imposed by Cramer's Transactional Interpretation [52] on mirror symmetry can be used for the putative detection of virtual tachyon-tardyon interactions in *zitterbewegun* [37].
5. Extended Quantum Theory - Test of causal properties of de Broglie-Bohm-Vigier quantum theory by utility of the U_F holophote effect (protocol 1 parameters) as a 'super quantum potential' to summate by constructive interference the density of de Broglie matter waves [4].
6. Coherent Control of Quantum Phase - Additional test of the de Broglie-Bohm interpretation for existence of a nonlocal 'pilot wave - quantum potential' for manipulating the phase 'space quantization' in the double slit experiment by controlling which slit quanta passes through. Application to quantum measurement and transistor lithography refinement.
7. Manipulating Spacetime LCU Structure - (similar to protocol 6) Test of conformal scale-invariant properties of the putative Dirac conformal polarized vacuum, a possible 'continuous-state' property related to an arrow of time [4,21,34] (Also similar to basic experiment, but more advanced).
8. Testing for and Manipulating Tight Bound States (TBS) - (similar to protocol 4) Vigier [31,35] has proposed TBS below the 1st Bohr orbit in the Hydrogen atom. Utilizing tenets of the original hadronic form of string theory [4] such as a variable string tension, T_S where the Planck constant, $\hbar$ is replaced with a version of the original Stoney, $\lambda\!\!\!^{-}$ [4], where $\hbar$ is an asymptote never reached, instead oscillating from virtual Planck to the Larmor radius of the hydrogen atom, i.e. the so-called Planck scale is a restriction imposed by the limitations of the Copenhagen Interpretation and is not a fundamental physical barrier. LSXD exist putatively behind the barrier of uncertainty and the oscillation of the Planck constant is part of the exciplex gating mechanism [4]. Utilizing ontological-phase topological field theory (OPTFT) at the moment of spin-spin coupling or spin-orbit coupling an rf-pulse is kicked at various nodes harmonically set to coincide with putative phases in the cycle between local and LSXD cavity TBS properties. [4,31,35]
9. Test for the noetic Unique String Vacuum - Until now the structure of matter has been explored by building ever bigger supercolliders like the CERN LHC. If the LSXD access model in terms of a Dirac covariant polarized energy dependent vacuum proves correct utilizing the inherent conformal scale-invariant mirror symmetry properties of de Broglie matter waves will allow examining various cross sections in the structure of matter in symmetry interactions during cyclic continuous-state future-past annihilation-creation modes of matter in the LCU tessellated spacetime metric without the need for supercolliders.

There are a number of very specific postulated cosmological properties required in order to perform these experiments [4,5,44].

4.8.2. *Review of Key Experimental Details*

To empirically gain access to the U_F, regime one must pass through the so-called Planck scale stochastic barrier. In order to do this one must violate the heretofore sacrosanct quantum uncertainty principle. Since by definition the standard methods of quantum theory produce the uncertainty principle; the simple solution is to do something else! Because of the great success of gauge theory physicists have ignored the existence of a covariant Dirac polarized vacuum because they believe its existence would violate gauge principles. The methods of gauge theory however are only an approximation suggesting

that there is additional new physics. Next we outline the general method for accessing the HD superspace of the U_F. Technical details can be found in references [4,87,88].

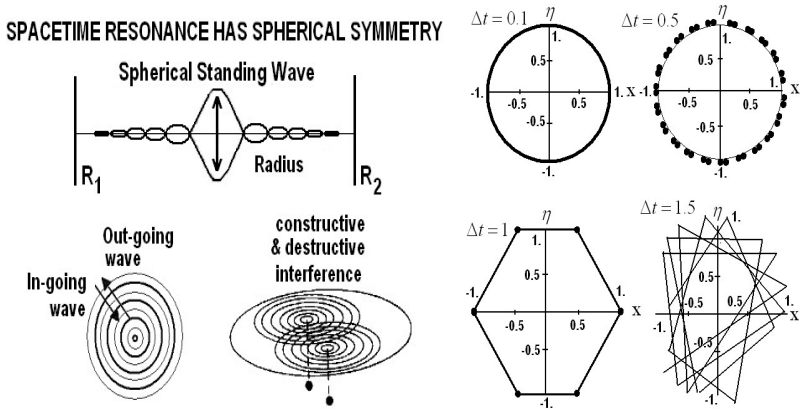

Fig. 4.13. The Dirac polarized vacuum has hyperspherical symmetry. a) Top left, metaphor for TI standing-wave present showing future-past elements, R_1, R_2, eleven of twelve dimensions suppressed for simplicity. b) Bottom left, top view of a) 2D spherical standing-wave; c) Bottom left, right portion, manipulating the relative quantum/brane phase of oscillations creates nodes of destructive and constructive interference for incursive oscillation. d) Right, Four numerical simulations of the phase space trajectory of the Dubois *superposed incursive oscillator.*

The Dubois superposed incursive oscillator based on coordinates and velocities takes the form:

$$x_n = 1/2[x_n(1) + x_n(2)], \quad v_n = 1/2[v_n(1) + v_n(2)] \qquad (4.9)$$

And is shown in Fig. 4.13 (right) for values of $\Delta\tau = \omega t$ equal to 0.1, 0.5, 1.0 and 1.5. Initial conditions are $\chi_0 = 1, \eta_0 = 0 \,\&\, \tau_0 = 0$ with total simulation time $\tau = \omega t = 8\pi$. Figure 4.13b adapted from [106-110].

Postulates introduced in this chapter are utilized; in general, the de Broglie-Bohm, ontological and Cramer, TI interpretations of quantum theory, the Dirac polarized vacuum, the Sagnac affect [4,49-55,111], the unique string vacuum derived from UFM cosmology and the special class of Calabi-Yau mirror symmetry conditions.

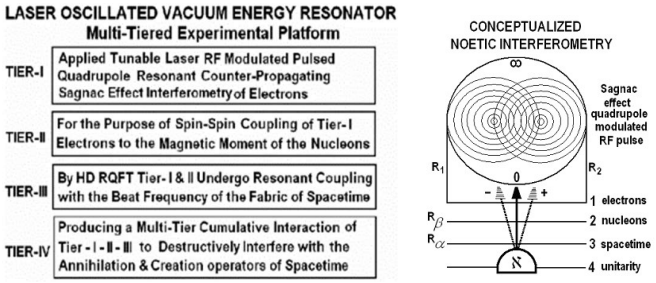

Fig. 4.14. a) Design elements of the Noetic Interferometer postulated to constructively-destructively interfere with the topology of the spacetime manifold to manipulate the unified field. The first three tiers set the stage for the critically important 4th tier which by way of an incursive oscillator 'punches a hole' in the fabric of spacetime creating a holophote or lighthouse effect of the U_F into the experimental apparatus momentarily missing its usual coupling node into an atom or biophysical system. b) Conceptualized Witten vertex Riemann sphere cavity-QED multi-level Sagnac effect interferometer designed to 'penetrate' space-time to emit the 'noeon wave, $\aleph$ ' of the unified field. Experimental access to vacuum structure or for surmounting the uncertainty principle can be done by two similar methods. One is to utilize an atomic resonance hierarchy and the other a spacetime resonance hierarchy. The spheroid is a 2D representation of a HD complex Riemann sphere complex able to spin-flip from zero to infinity continuously.

It is important to recall one of our main proposals concerning the wave structure of matter and that emergent spacetime is created, annihilated and recreated continuously. If one throws a stone in a pool of water concentric ripples occur. If one drops two stones into the water, regions of constructive and destructive interference occur. This is essentially how our resonant hierarchy operates as shown in Fig. 4.14b. The basic idea of the radio frequency or rf-modulated resonance hierarchy is as follows: in the first tier (Fig. 4.14a) a radio frequency is chosen to oscillate the electrons in the atom or molecule used in such a way that the nucleons will resonate. This is related to the principles of nuclear magnetic resonance (NMR). This couples electrons to the magnetic moment of the nucleons in tier 2. By the principles of relativistic quantum field theory (RQFT) tiers one and two undergo resonant coupling to the beat frequency of the fabric of space-time. The multitier cumulative interaction of tiers 1, 2 and 3 by application of the incursive oscillator can be set to destructively or constructively interfere with the annihilation or creation operators of space-time.

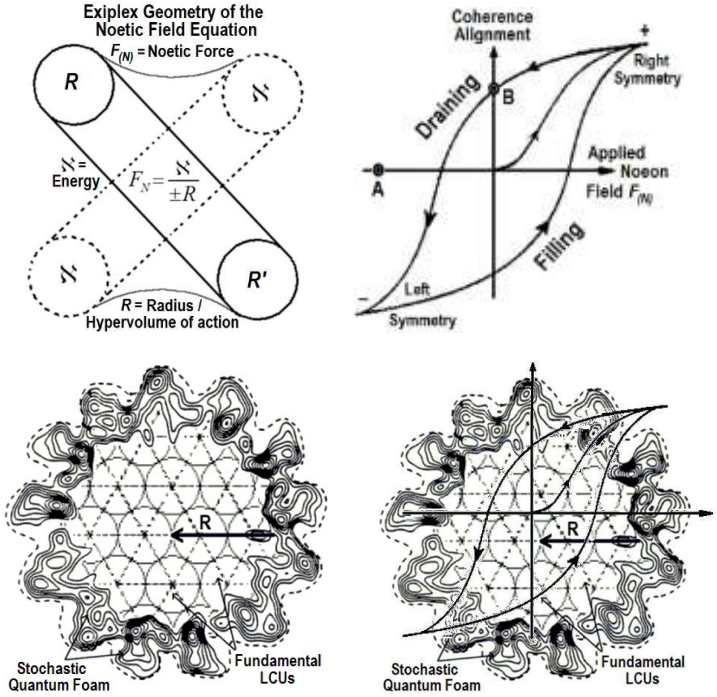

Fig. 4.15. a) Geometric topology of Noetic Field Equation $F_{(N)} = \aleph / \rho$ acting as a holophote (rotating lighthouse beacon) gating mechanism for entry of the nonlocal HD *UF* into local M_4-E_3 3(4)-space. a) Wave-particle-duality is elevated to a principle of cosmology such that the solid bar, R_1-R_2 at one moment transforms to the dotted bar, $\aleph$ at the next in a continuous relativistic wave-particle cycle with *t* the arrow of time. Fluctuating string tension, T_S (curves) helps drive the oscillation. b) *UF* Hysteresis Loop. Point A is a Zero-point where the driving field reverses and increases. Point B is where the driving field drops but still retains considerable charge as a *UF* force of coherence related to the life-principle and quale. c) Noeon spacetime coupling to LCU tessellating space. d) Overlap of hysteresis loop with noeon coherent force spacetime interaction.

A final essential component of the vacuum interferometer is called an incursive oscillator [106-110] which acts as a feedback loop on the arrow of time [21,34]. Parameters of the Dubois incursive oscillator are also required for aligning the interferometer hierarchy with the beat frequency of spacetime by $x(t+\Delta t)$ $v(t+\Delta t)$. Critically the size of Δt correlates with the bandwidth of the 'hole' to be punched in spacetime which also correlates with the wavelength, λ of the rf-resonance pulse.

Hysteresis is an important part of understanding how to quantify the topological charge with a unit of energy measure because it relates not to residual magnetization as in common usage but to the residual *UF* noeon charge. When the driving force drops to zero, the material retains considerable

charge (coherence) for a period. The driving (noen) field must be continuously reversed and increased (holophote action) driving the charge to zero again. A Hysteresis Loop is a history dependence of a material (atom) at saturation (driven to). When the field is removed some retention occurs for a period of time. As noeon input alternately increases and decreases, hysteresis is the loop that the output forms (Fig. 4.15). A simple form of hysteresis is the lag-time between input (filling) and output (draining). An example of hysteresis is sinusoidal or harmonic input $X(t)$ and output $Y(t)$ separated by a phase lag, ϕ : $X(t) = X_0 \sin \omega t;;\ Y(t) = Y_0(\omega t - \phi)$ this is the principle of hysteresis [11] - switching cycles that retain considerable charge (coherence in the case of the *UF* LCU noeon cycle.

In the current understanding of quantum cosmology where the Planck scale is the 'basement of reality' [4] there is a stochastic Zero Point Field (ZPF) where virtual quantum particles wink in and out of existence with a half-life of the Planck time. This is considered an impenetrable barrier imposed by the Uncertainty Principle. UFM has sufficient degrees of freedom to surmount uncertainty and allow a cyclic or harmonic emergence of the noeon into localized matter. This holophote mechanism can be metaphorically described as an Exciplex (Fig. 4.7a). In an exciplex (short for excited complex) heteronuclear molecules or molecules having more than two species are ***exciplex*** molecules that are often diatomic and composed of two atoms or molecules that would not bond if both were in the ground state - An Exciplex is a complex existing in an excited state that dissociates in the ground state.

4.9. Unified Field Mechanical (UFM) Précis - Required Parameters

Most physicists believe a *UF* theory (coined by Einstein) should be a quantum theory uniting the four fundamental interactions; but there is no *a priori* reason this should be the case and many physicists in recent decades transferred the search to an 11D M-Theoretic (4D + 2D to 6D) brane world instead of the original 1D string) regime. The 11th dimension in M-Theory unites the five forms of string theory; and the 12th dimension of noetic UFM cosmology (OPTFT) introduces the coherent action of the *UF*. Classical Mechanics describes an event between two coordinate systems by what is called the Galilean transformation for uniform motion at velocities less than the speed of light in 3D Euclidean space.

Quantum mechanical events with relativistic velocities are described by the Lorentz-Poincairé group of transformations in 4D Einstein-Minkowski spacetime. To cross the manifold of uncertainty, noetic cosmology utilizes an extension of M-Theory requiring a new 12D set of transformations called the Noetic or UFM Transform [4] (provides actual bridge between the 2nd and 3rd regimes of reality) because it includes properties of inherent UFM principles in a 'sea' of infinite potentia simplistically like the entangled alive-dead quantum state of Schrödinger's cat before realized local events occur and from which 4D reality of the observer cyclically emerges as nilpotent resultants (Figs. 4.9, 4.10). Norm zero nilpotency - technically meaning 'sums to zero' [111].

The key ingredients the HD regime of UFM provides for surmounting uncertainty and solving the observer or mind-body problem are:

1) Sufficient additional degrees of freedom to surmount the Uncertainty Principle,
2) an exciplex gating mechanism to allow *UF* entry into 4-space [4],
3) Ontological UFM 'Force of Coherence' mediated by noeon topology and
4) Ability to define new physical unit of measure called the noeon to quantify mental energy [97,98].
5) Matter is not only a 3(4)D Euclidean/Minkowski substance; but an nD (12) nonlocal topological space, with a local manifold (shadow) homeomorphic to Euclidean space near each 3D point.

The force of coherence is described by the UFM Field Equation, $F_{(N)} = \aleph / \rho$ defining how to manipulate the topological charge of the Exciplex gate to perform UFM experiments. Since noeon flux is like a holophote, hysteresis loops can quantify the energy and duration of the coherence period applicable to a C-QED volume or surface area. This energy transfers information instantaneously as observed by the EPR experiment; presenting duality between our temporal 3-space and the atemporal unity of the UFM regime.

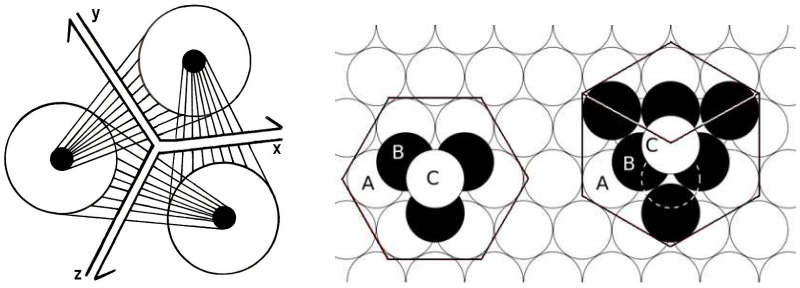

Fig. 4.16. a) Solitary triune LCU complex 'component' with a Whitten string vertex in 3-space represented by central *x,x,z* parallel lines; The 3 circles are super quantum potential field components coherently controlling the evolution of a local fermionic vertex with field lines of the *UF*. b) Possible ways to close-pack LCU arrays in spacetime tessellations.

4.10. Formalizing the Noeon, New Physical Unit Quantifying UFM Energy

Defining 'noeon' energy as a unit of physical measure helps formulate a comprehensive empirically testable UFM science. The Einstein, another physical unit of energy measure, named in honor of Albert Einstein for his explanation of the photoelectric effect in terms of light quanta (photons) bears conceptual similarity; thus our starting point.

The Einstein measures the power of em-radiation in photosynthesis where one Einstein represents one mole (Avogadro's number) of photons (6.02 x 10^{23}). In general physics the energy of *n*-photons is $E = n\hbar\nu = n\hbar(c/\lambda)$ where $\hbar$ is Planck's constant and ν frequency. The second part of the equation is energy in terms of wavelength, λ (in nanometers, *nm*) and speed of light, *c*. Adaptation of this photon energy equation to measure Einsteins is similar, $E = N_0\hbar\nu = N_0\hbar(c/\lambda)$ where energy of N_0 photons is instead in Einsteins, *E*. In photometrics the measure used is one microeinstein per second per m^2, where one microeinstein, *u*E is one-millionth of an Einstein (6.02 x 10^{17}) photons imping leaf area.

We create a similar unit of measure to quantify noeon energy of the U_F. The same unit can be applied to mental energy quantifying the mind of the observer (*quale* in terms of the Eccles' Psychon) as one mole (Avogadro's number) of 'noeons'. Forces of the four known phenomenological fields (electromagnetic, strong, weak and gravitational) have exchange quanta mediating field interactions by energy exchange. For em the exchange quanta is the photon. This quantal mediation has been experimentally verified for all fields except gravity because the graviton has not been discovered; and according to UFM is not expected to be, as the regime of unification is not quantum but instead correlates with ontological parameters of 3rd regime UFM [4,105].

Hypervolume charge in HD Calabi-Yau brane topology is complex and difficult to calculate at this stage of theoretical development. Since energy is conserved let's ignore this complexity and simply use area of the circle, or in this case resultant continuous rotations of two circles as a 2-sphere quantum state or perhaps better as a 3-torus as the noeon coupling area to one LCU complex. In considering noeon energy measure it seems easier to calculate nonlocal brane area of the spacetime exciplex (gating mechanism for passage of *UF* energy, Fig. 4.7a) rather than the volume or surface area of atoms which is unknown in this respect. Recall the surface area of small intestinal villi is about 4500 m^2 ~area of a football field. We will not calculate here but leave for later publication since we still struggle with conceptual problems relating to the geometric-topology of noeon interaction coherence. The de Broglie-Bohm interpretation entails nonlocal pilot-waves or quantum-potentials guiding evolution of wavefunctions ontologically. This concept was not very successful in 4D, but when carried to Large-Scale Additional Dimensions (LSXD) [44] it works elegantly and the pilot-wave-quantum potential becomes a 'Super Quantum Potential' synonymous with coherent *UF* aspects in an arena seemingly corresponding to Bohm's super-implicate order.

More noeon-LCU theory: A torus is generated by rotating a circle about an extended line in its plane where the circles become a continuous ring. According to the torus equation,

$\left[\left(\sqrt{x^2}+y^2\right)-R\right]^2+z^2=r^2$, where r is the radius of the rotating circle and R the distance between the center of the circle and axis of rotation. Torus volume is $2\pi^2Rr^2$ and surface area is $4\pi^2Rr$. In this Cartesian formula the z axis is the axis of rotation. We apply this to the holophote action of noeon exciplex flux with a hysteresis loop. In atomic theory electron charged particle spherical domains fill toroidal volumes of atomic orbits by their wave motion. If a photon of specific quanta is emitted while an electron is resident in an upper (U_F domain) more excited Bohr orbit, the orbit radius drops back down to the next lower energy level decreasing volume of the torus in the emission process (noeon-psychon exciplex hysteresis loop maintaining a periodic syntropic force of coherence).

Summarizing pertinent aspects of noeon-LCU cosmology:

- Nature of point particles or singularities in physics has long been debated. In Noetic Cosmology it becomes a continuous Witten vertex [100] (Central *x,y,z* parallel lines, Fig. 4.16a).
- Energyless interaction of the U_F occurs by 'topological switching'. Metaphorically like what happens by staring at an ambiguous Necker cube as the vertices ontologically oscillate back and forth. Like the exciplex gate in noetic cosmology [4].
- Like the Einstein, the noeon defines a measure of one mole of noeons, purported to be the topological exchange complex of the U_F providing the force of coherence that forms local material.

Using the noetic field equation, $F_{(N)}=\aleph/\rho$ (Fig. 4.15a) we could calculate the energy of the noeon field from its spacetime hysteresis loop (Fig. 4.15b,c). This is a practical and conceptual challenge currently hard to meet. Imagine a helicopter like those used to put out forest fires carrying a bucket of water retrieved from a nearby lake (*UF*). The volume of that bucket is known. So it is infinitely easier to work with the volume of the helicopter water bucket than to try to measure the surface area of trees and other objects on the ground. Until the experiment is performed; we could approximate the volume of the helicopter bucket with the energy of one LCU complex from parameters of Tbl. 4.1. As shown in Fig. 4.11 we are postulating that the Manifold of Uncertainty (MOU) has from 2D to 5D with either the 3rd or 6thD being degenerate (like atomic radius where an outer electron flies off to infinity). We don't know yet if the MOU is 3D or 6D because we don't fully understand how to close-pack the LCU array tessellating spacetime (Fig. 4.16). This model is compatible with M-Theoretic Calabi-Yau dual 3-tori [3,46,47]; but our theory cannot fully predict this until we know how many space-antispace doublings are required in LCU packing [112]. We discovered that a complex quaternion Clifford algebra can perform this task but our team hasn't finished developing the equations at time of writing.

When first considering the noeon as a new unit of measure a correlation with an Avogadro's number of noeons entering the picture wasn't considered. Can we correlate helicopter buckets of *UF* brane topology with the volume or surface area of an array of LCUs modulating energy of coherence entering local spacetime? Yes, but we defer the calculation until we have more maths or perform the experiment [31]. The exciplex LCU gate transforms continuously through HD M-Theoretic brane topology with cyclic compactification modes [4] until reaching a 4D 'standing-wave' [52,111] Minkowski spacetime of the standard model. Observed virtual reality, a gated domain-wall for entry of *UF* noeon energy pervading all spacetime and matter is mediated by a new set of transformations beyond the Galilean-Lorentz-Poincairé. Named the UFM Transform in deference to the anthropic multiverse it is cast in [4].

For preliminarily predictions we could calculate hyperspherical volume or surface area of 4D-5D MOU (Fig. 4.11). The general n-volume equation is $V(n,r)=\pi^{\frac{n}{2}}r^n/\Gamma\left(\frac{n}{2}+1\right)$ where $V_{n,r}$ is volume per number of dimensions, n of radius r and Γ a factorial constant. These n-volume equations relate to volumetric properties of the MOU for calculating noeon brane volume of topological charge.

UF dynamics entails a 'force of coherence' not a 5th fundamental force. This 'coherence' is the resultant unitary unified action of the *UF* which is primary - originator of all other forces 'pumping' noeons, which are then immediately returned to the infinite sea of *UF* potentia. This cyclical process

creates and annihilates matter. More work must be done on noeon dynamics. This is what the experimental protocols are designed for - rigorous investigation of '*some crazy theory*', as Nobel Laureate D. Gross called it at the 2015 Singapore, NIAS 60 Years of Yang-Mills conference.

4.11. Quarkonium Flag Manifold Topology

In sections above, we made a current best effort to describe in principle how an 'Exciplex Topology' acts as a gating mechanism for real *UF* noeons to pass from the 3rd regime of UFM to 4-space; a paradigm shift from current thinking of ZPF virtual particles of the 2nd regime of Quantum Mechanics. We know this gating mechanism pulses or oscillates cyclically like a lighthouse holophote beacon.

In this section we shed additional light on how the structure of the gating manifold hierarchy might operate:

1) 1st regime: A classical local Euclidean 3-space x, y, z fermion vertex with space-antispace *zitterbewegung*.
2) 2nd regime: In terms of an extended Cramer standing-wave transaction, is a mid-level future-past complex quantum space of which 3-space is the 'resultant shadow'.
3) 3rd regime: UFM topology governing brane dynamics which is at the core of the gating mechanism.

In 1945 Wheeler and Feynman proposed an Absorber Theory as the mechanism for energy transfer by calculating em-radiation emitted from an accelerated electron. The electron generated outward and inward waves. Cramer's Transactional Interpretation of quantum theory is based on the Wheeler-Feynman Absorber Theory. M. Wolff further proposed a parallel model where spherical standing-waves created a 'particle effect' at their Wave-Center**,** suggesting a solution to the 70-year-old paradox of the Wave-Particle Duality of Matter [4]**.**

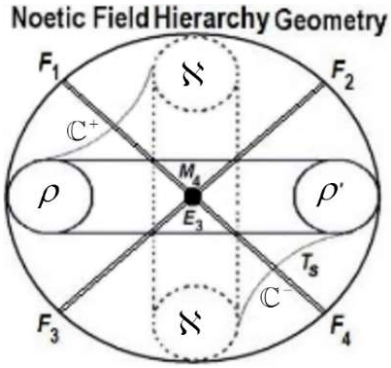

Fig. 4.17. Hierarchy of the three regimes of reality. a) Central black dot; a point in Euclidean space. b) Double lines, F_1, F_2, F_3 F_4 (eq. 4.12) as future-past components of a Cramer transaction. c) Four LCU circles representing geometric topology of the UF and UF equation $F_{(N)} = \aleph / \rho$ for coherent control.

For a Cramer transaction emission locus at $x,t = 0, 0$; we are concerned with the boundary conditions in the region outside the event horizon. The scalar equation in spherical coordinates for wave motion in spacetime which has spherical symmetry

$$\nabla^2 \Phi - \frac{1}{c^2} \partial^2 \frac{\Phi}{\partial t^2} = 0 \qquad (4.10)$$

where, Φ is the wave amplitude. The equation has two solutions

$$\Phi_{out} = \frac{1}{r}\Phi_{\max}\exp\left(i\omega t - ikr\right)$$
$$\Phi_{in} = \frac{1}{r}\Phi_{\max}\exp\left(i\omega t + ikr\right) \tag{4.11}$$

which for the programming of spacetime can be applied to the propagation of Cramer's advanced retarded waves from an emission locus at x,t = 0,0 by Eqs. (4.11 & 4.12) which form the advanced-retarded components of a transaction (Fig.4.5) [52].

$$F_{1-Ret} = F_0 e^{-ikx} e^{-2\pi ift},\ F_{2-Ret} = F_0 e^{ikx} e^{-2\pi ift}$$
$$F_{3-Adv} = F_0 e^{-ikx} e^{2\pi ift},\ F_{4-Adv} = F_0 e^{ikx} e^{2\pi ift} \tag{4.12}$$

Another approach to formalizing noeon flux is in terms of the 6D flag manifold describing the geometry of quark confinement. A possible relationship to the noeon-LCU complex can make correspondence to work by Shipman correlating the flag manifold to a hexagonal structure of spacetime [113-115]. The structure of quarks in hadrons bears an uncanny geometric relation to the noetic UFM LCU.

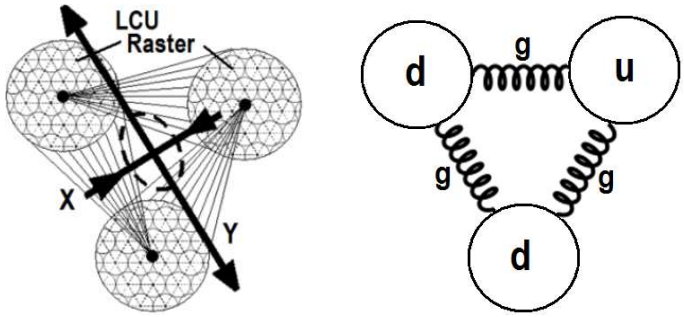

Fig. 4.14. Comparison of a) LCU array (with Euclidean *x, y* vertex) and b) Three quarks d, u, d with gluon, *g* force couplings.

4.12 Singularities, Unitary Operators and Domains of Action

Quantum systems decohere because they are open systems that couple to the environment. As we now begin to supersede Quantum Mechanics, leaving the challenges of decoherence and the Uncertainty Principle behind, by entering a 3rd regime of reality – that of Unified Field Mechanics (UFM); we have finally come full circle to Einstein's challenge of refuting indeterminism, that '*God does not play dice with the universe'*! Einstein felt that natural laws could not be like the throw of dice, incorporating an inherent structural randomness with access only probabilistically. But this is exactly what Quantum Mechanics tells us empirically – that at the fundamental level Nature is inherently stochastic or random, codified in Heisenberg's famous Uncertainty Principle. Physicists have now begun to suspect that spacetime is not fundamental but emergent. Spacetime is the domain of Quantum Mechanics; so now the challenge is that Quantum Mechanics along with its rigorous empirical tests of stochasticity can no longer be considered fundamental and will be superseded in a manner similar to Classical Mechanics. Here is where at the newly discovered 'semi-quantum limit' we begin to make correspondence to a regime of natural science where Einstein's wager finally becomes valid. Measurement with certainty is key to the Unified Field Mechanical or Noetic model of Universal Quantum Computing (UQC) being able to address quantum states without facilitating decoherence as it completely removes all aspects of that issue in QC operations.

If the Church-Turing Hypothesis (simplistically, any function that can be computed by a physical system can be computed by a Turing Machine) is correct, and that all quantum operators must be unitary (reversible), then UFM adds the ability to surmount uncertainty as a Gödelization beyond QM by the additional degrees of freedom.

4.12.1 *Semi-Classical Limit*

The Semi-classical limit refers to theoretical models or domains where one part of a physical system is described quantum mechanically and another corresponding part is treated classically [116]. This scenario is related to Bohr's Correspondence Principle, used generally to represent the idea that new theories should reproduce the results of established theories (as limiting cases) in domains where the earlier theories work. The Semi-classical limit is the arena in which quantum mechanics reduces to classical mechanics**.** For example, Einstein's special relativity satisfies the correspondence principle because it reduces to classical mechanics in the limit where velocities are small compared to the speed of light. Another example is the Wentzel-Kramers-Brillouin (WKB) Approximation [117].

4.12.2 *Semi-Quantum Limit*

The Semi-quantum limit refers to the domain where one part of a physical system is described by UFM and another corresponding part quantum mechanically [90]. This scenario is related to Bohr's Correspondence Principle, stating that new theories should reproduce the results of established theories in the limit where the earlier theory operates. The Semi-quantum limit is the arena in which UFM reduces to quantum mechanics; it is the one concerned with the duality of the interface with the finite dimensional radius of the manifold of uncertainty (MOU)**.**

4.13 Measurement

A quantum system can be in a ground state $|0\rangle$ or excited state $|1\rangle$; but the superposition principle states that the system is in a linear superposition or combination of the two, $\alpha_0|0\rangle+\alpha_1|1\rangle$, simple if α represented probabilities, nonnegative real numbers adding to 1. However, the superposition principle allows them to be complex numbers if the square of their norms add to 1, $|\alpha_0|^2+|\alpha_1|^2=1.$ The coefficient α_0 represents the amplitude of the state $|0\rangle$, so it can thus refer to the probability, be negative or imaginary.

A linear superposition is the 'private world of the quantum state', $\alpha_0|0\rangle+\alpha_1|1\rangle$ with measurement outcome 0 having probability $|\alpha_0|^2$ and outcome 1 with probability $|\alpha_1|^2$, normalized to $|\alpha_0|^2+|\alpha_1|^2=1.$ This act of measurement causes the system to change state. This holds for *k*-level systems, such as $|0\rangle,|1\rangle,|2\rangle,...,|k-1\rangle.$ Under these circumstances the superposition principle states, $\alpha_0|0\rangle+\alpha_1|1\rangle+...\alpha_{k-1}|k-1\rangle,$ with $\sum_{j=0}^{k-1}|\alpha_j|^2=1.$ A measurement then has an outcome between 0 and $k-1$, with *j*'s probability $|\alpha_j|^2$ disturbing the system to $|j\rangle$ or the *j*th excited state.

To encode *n* qubits for two electrons for example, we have four possible states, 00, 01 10, 11 (2 qubits) which in linear combination becomes

$$|\alpha\rangle=\alpha_{00}|00\rangle+\alpha_{01}|01\rangle+\alpha_{10}|10\rangle+\alpha_{11}|11\rangle, \qquad (4.13)$$

Normalized to $\sum_{x\in\{0,1\}^2}|\alpha_x|^2=1$ where the probability of outcome is $x\in\{0,1\}^2$ is $|\alpha_x|^2$.

Now here's the rub; let's consider a general case of n = 500 qubits in a linear superposition of all 2^{500} possible classical states, much larger than the number of particles estimated in the classical universe (10^{80}):

$$\sum_{x\in\{0,1\}^n}\alpha_x|x\rangle. \tag{4.14}$$

This exponentially huge superposition is 'the private world' of the electrons involved and measurement only allows us to find the n bits (500) of information, $|\alpha_x|^2$. If our UFM model proves successful in surmounting uncertainty, then measurement does not change the system leaving all 2^{500} possible superposed states intact. This also leads to violation of the no-cloning theorem.

Input to quantum algorithms is by n classical bits - an n-bit string, x. After QC operations are performed, the n qubits have been transformed to the superposition, $\sum_y \alpha_y|y\rangle$ with output probability $|\alpha_y|^2$. This works by placing molecules in a magnetic field aligning spins of the nuclei and then flipping the spins with radio waves. Because each nucleus sits in a slightly different position in the molecule, each is addressed with slightly different frequencies, by a process known as nuclear magnetic resonance. The spins can also be made to interact with each other so that the molecule acts like a tiny logic gate when zapped by a carefully prepared sequence of radio pulses. In this way the molecule processes data. And because the spins of each nucleus can exist in a superposition of spin up and spin down states, the molecule acts like a tiny quantum computer [118-120].

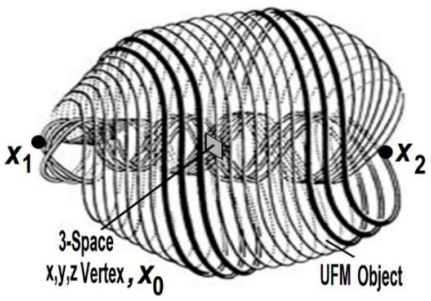

Fig. 4.19. Matter can no longer be considered as 3-space point particles; but needs to be studied with the inclusion of an HD topological brane manifold that it is embedded in and cyclically emerges from as a hyperspherical standing-wave.

A big question is, does an ontological measurement change the basis for quantum algorithms? Would such a scenario (other than putatively removing the need for error correction cycles) provide another category of speedup? We have considered that UFM based UQC is primarily a boon to measurement and possibly in that case classes of quantum algorithms might remain the same. Let's not call it 'parallel QC", but rather could we discover a class of 'holographic UQC' with asymptotically infinite speedup? As we devise in Chap. 13, it is not to be called infinite; but with EPR-like dual-Amplituhedron connectivity it is termed a new class of 'instantaneous' ontological algorithms!

The Larmor or cyclotron radius is the radius of the circular motion of a charged particle in the presence of a uniform magnetic field. Given in SI units by

$$r_L=\frac{mv_\perp}{|q|B} \tag{4.15}$$

where m is the mass of the particle, $v_{\perp}$ the component of velocity perpendicular to the direction of the magnetic field, q the charge of the particle, and B the strength of the magnetic field. Proton, Electron, Photon? Gödelizng Fine Structure will reveal additional Unified Field Mechanical atomic structure beyond the current 4D model of the 3D Fermionic 0D singularity.

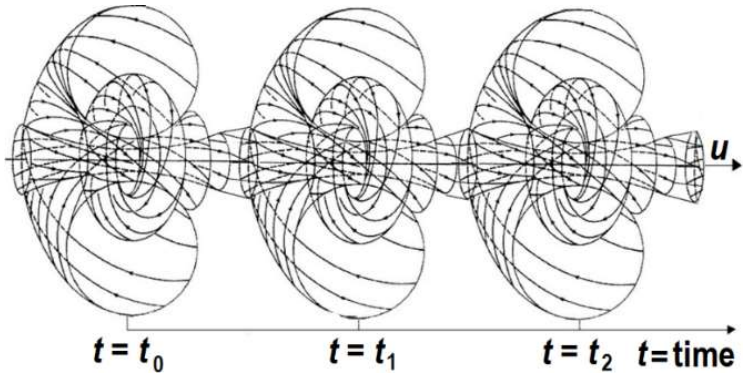

Fig 4.20. Symbolic diagram for LCU radius beat frequency of spacetime. Could be achieved by π rotations of the Riemann sphere LCU complex.

Coherent energy exchange can be achieved by dynamically coupling the mechanical oscillations of the two beams. This is realized by periodically modulating the spring constant of one beam at the frequency difference between the two beams. This periodic modulation, namely pumping, can be induced by applying gate voltage via the piezoelectric effect in this sample. This pumping enables strong vibrational coupling, leading to the cyclic (Rabi) oscillations between the two vibrational states (the beam-L state and the beam-R state) on the Bloch sphere. The Rabi cycle period, i.e., the coupling strength, is fully adjustable by changing the pump amplitude via the gate voltage. As a result, the vibration energy can be quickly transferred from one beam to the other enabling the vibration of the original beam to be switched off on a time-scale orders of magnitude shorter than its ring-down time. This quick energy transfer to the adjacent oscillator opens up the prospect of high-speed repetitive operations for sensors and logics using Nano-mechanical systems [121,122].

4.14 The No-Cloning Theorem (NCT)

The no-cloning theorem explicitly states that it is impossible to create an identical copy of an arbitrary unknown quantum state. We profess the NCT is only valid for the Copenhagen Interpretation, not for UFM. In theoretical physics no-go theorems state that some situation is physically untenable. Specifically, the term describes results in quantum mechanics like Bell's theorem and the Kochen-Specker theorem that constrain the permissible types of hidden variable theories attempting to explain the apparent randomness of quantum mechanics as a deterministic model featuring hidden states [123,124].

This no-go theorem of quantum mechanics was articulated by Wooters and Zurek [125] and Dieks [126], and has profound implications in quantum computing and related fields. The state of one system can be entangled with the state of another system. For instance, one can use the controlled NOT gate and the Walsh–Hadamard gate to entangle two qubits. This is not cloning. No well-defined state can be attributed to a subsystem of an entangled state. Cloning is a process whose result is a separable state with identical factors. The no-cloning theorem was prompted by a proposal of Herbert [127] for a superluminal communication device using quantum entanglement.

The no-cloning theorem is normally stated and proven for pure states; the no-broadcast theorem generalizes this result to mixed states [128-130].

§ The Quantum No-Cloning Theorem: *An unknown quantum state cannot be duplicated*.

4.14.1 *Proof of the Quantum No-Cloning Theorem (NCT)*

Let $|\phi\rangle$ be the state of quantum system A that we want copied. In order to clone state $|\phi\rangle$ we must take another quantum system *B* that has the same state space (general Hilbert abstract vector space) and its initial empty state $|e\rangle B$ which must be independent of state $|\phi\rangle A$ which must also be completely unknown. The composite *A, B* quantum system is designated by the tensor product $|\phi\rangle A \otimes |e\rangle B$. According to the tenets of quantum theory there are only two permissible quantum operations by which the composite system may be manipulated:

• An irreversible observation on the system could be made, collapsing the system into some observable eigenstate thereby corrupting the qubits information. This is not satisfactory.

• The Hamiltonian of the system can be controlled. Thus if the time-evolution operator, *U* up to some fixed time interval, yields a unitary operator *U* for a time-independent Hamiltonian, $U(t) = e^{-iHt/\hbar}$, with $-H/\hbar$, the 'translations in time' generator, then *U* acts as a copier so long as $U|\phi\rangle A|e\rangle B = |\phi\rangle A|e\rangle B$ for all possible states $|\phi\rangle$ in the state space.

For the latter case we can select an arbitrary pair of states $|\phi\rangle A$ and $|\psi\rangle A$ drawn out of the Hilbert space. Since *U* is unitary, the inner product $\langle e|B\langle\phi|A\langle\psi|A|e\rangle B = \langle e|B\langle\phi|AU^{\dagger}U\langle\psi|A|e\rangle B = \langle\phi|B\langle\phi|A|\psi\rangle A|\psi\rangle B,$ is preserved; and because all quantum mechanical states are assumed to be normalized, $\langle\phi a|\psi a\rangle\langle\phi b|\psi b\rangle = \langle\phi|\psi\rangle^2 = 1 = \langle\phi|\psi\rangle$.

Since this implies that either $\langle\phi|\psi\rangle = 1$ or $\langle\phi|\psi\rangle = 0$, two possibilities occur, either $\phi = \psi$ or that ϕ is orthogonal to ψ. Quantum theory however states that this cannot be true for two arbitrary states. Thus it is not possible for a single universal *U* to have the ability to clone a general quantum state which simply enough proves the Non-Cloning Theorem (NCT). However, one should be aware that that it is possible to find specific pairs that satisfy the algebraic requirement above. The following orthogonal states provide such an example $|\phi\rangle = 1/\sqrt{2}(|0\rangle + |1\rangle)$, $|\psi\rangle = 1/\sqrt{2}(|0\rangle - |1\rangle)$ and for this special case one can verify that $\langle\phi|\psi\rangle = 0 = \langle\phi|\psi\rangle^2$. And as one might surmise the relation doesn't hold for more general quantum states [125].

And again, supposing the unknown quantum state, $|\psi\rangle = \alpha|0\rangle + \beta|1\rangle$, is it possible to take state $|\psi\rangle$ and produce copies of this state $|\psi\rangle \otimes |\psi\rangle$, essentially cloning it?

Proof: Show that for the evolution $|\psi\rangle \otimes |0\rangle \rightarrow |\psi\rangle \otimes |\psi\rangle$ for all possible states $|\psi\rangle$, there is no unitary cloning map operator, *U* allowing a $|0\rangle$ and $|1\rangle$ cloning operation: $U|0\rangle \otimes |0\rangle = |0\rangle \otimes |0\rangle$ and $U|1\rangle \otimes |0\rangle = |1\rangle \otimes |1\rangle$. If this operation holds, by the linearity of quantum theory, $U\frac{1}{\sqrt{2}}(|0\rangle + |1\rangle) \otimes |0\rangle = \frac{1}{\sqrt{2}}(|0\rangle \otimes |0\rangle + |1\rangle \otimes |1\rangle)$; but this is not equal to the $\frac{1}{\sqrt{2}}(|0\rangle + |1\rangle) \otimes \frac{1}{\sqrt{2}}(|0\rangle + |1\rangle)$ required for a cloning unitary. The contradiction demonstrates that no such unitary exists for states that are elements of an unknown orthonormal basis [125,145].

4.14.2 *Quantum No-Deleting Theorem*

Similar in many ways to the no-cloning theorem, the quantum no-deleting theorem states that no quantum operation can erase an unknown quantum state. In order to manipulate, copy or delete quantum information a measurement must be performed by access to the state. While anyonic braiding TQC provides protected quantum states; they are currently too protected and inaccessible.

Ontological-phase topological field (OPTFT) theory will change this scenario. OPTFT has the ability to override the quantum no-cloning and non-erasure theorems; also allowing access to the topologically protected quantum Hall anyon braid states. See Chap. 12.

4.15 The Tight-Bound State Protocol

Because Euclidean space is a 'shadow' of HD reality, gated by the Uncertainty Principle, and the current belief that the stochastic quantum foam is the 'basement of reality'; it has not been evident that behind this veil (provided by a manifold of uncertainty of finite radius) there is a harmonic oscillation of the unified field, that opens and closes this gating mechanism with a 'continuous-state' periodicity. This is the key element of this scenario: in this regard there is a 'beat frequency' to the cyclic creation and annihilation of spacetime from the nilpotent potentia it is reduced (shadow) from. The symmetry occurs because of its inherent Cramer-like standing-wave structure with de Broglie-Bohm control parameters driving its evolution. The perceived extreme radical nature of these premises, they will be difficult to accept initially; but in our favor we have an experimental paradigm waiting in the wings to be performed.

We assume that all matter emerges from spacetime. In order to perform our experiment, we need to 'destructively-constructively' interfere with this process of continuous emergence. In the model being developed this requires finding a cyclical beat-frequency to the creation and annihilation process of space-time and matter. We believe this is best done by utilizing HD completed forms of the de Broglie-Bohm-Vigier causal and Cramer transactional interpretations of quantum theory. Once we know the size of the close-packed LCU and apply this to our 'zero to infinity' rotation of the Riemann sphere (Kahler manifold) we will know the radius/time of this putative inherent beat-frequency. This is where the Sagnac Effect Dubois incursive oscillator is applied to the structure where the Δt hyperincursion [106-110] would correspond to a specific phase in the beat-frequency of spacetime and size of the hole utilized (punched by destructive interference) to send our signal through in order to detect several new TBS spectral lines in hydrogen [31].

We set the resonance hierarchy up in this case with hydrogen (simplest case with least amount of artifact from other electrons) where we jiggle the electron tuned to resonate with the nucleus tuned with the annihilation - creation vectors in the beat frequency of spacetime which putatively opens a hole into the HD 'manifold of uncertainty' cavities by a process which we have stated numerous times is a direct violation of the quantum uncertainty principle. Which as you recall occurs when a field is arbitrarily set up along the z-axis to separate the states in the Stern-Gerlach apparatus, the historical beautiful empirical proof of the uncertainty principle.

So simplistically we're going to do something else which you should by now have a glimmer of and the additional degrees of freedom required to perform this something else. This is why we have to have access to the physics inherent in this new cosmology. In the current model with the Planck basement there is no understanding of how to pass through; there is no XD cavities behind the Planck basement. It is finding the LCU beat frequency in the Dirac polarized vacuum that will give us success.

In summary we have the 3-level tiered Sagnac Effect resonance hierarchy of electrons nucleons and spacetime. The counter-propagating properties of the Sagnac Effect that violates special relativity in the small-scale will most likely be relevant to this resonance process.

For the standing-wave oscillator, the gap between R_1 & R_2 in the beat frequency of spacetime we take our 'little laser blaster' starting at the R_1 bandwidth, when we reach the right point we will get a reflected blip, which will be our first new spectral line in hydrogen. So in a sense if you've been

following along; you see in general how straightforward and really simple this experiment is. This is a paradigm shift and beneath this infinite as yet to the reader, concatenation of mumbo-jumbo lies the framework for performing the TBS experiment. Unfortunately, one can see that any part of these elements that I've been gerrymandering could each take several hours to describe properly. The continuous-state, deriving the alternative formula for string tension - any of these is in hour lecture in itself. The importance of the LCU could require thousand-page treatises. I've been trying to give an overview of the framework for UFM that we're in the process of discovering.

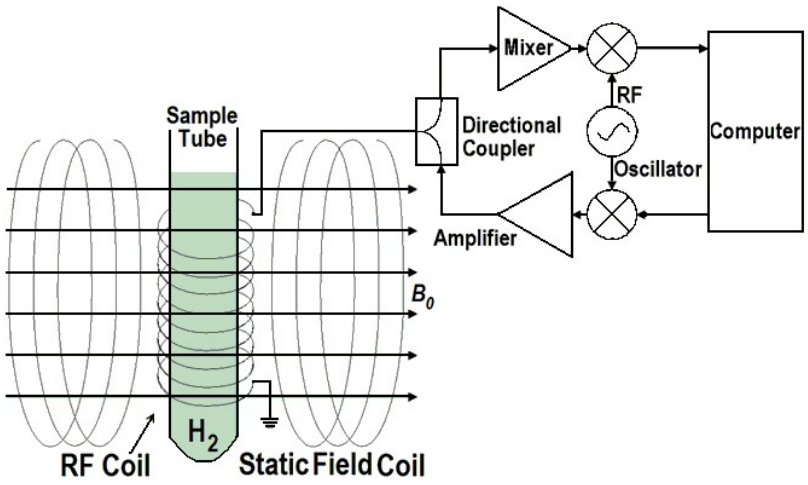

Fig. 4.21. NMR apparatus designed to manipulate TBS in Hydrogen. The Fig. only shows possible details for rf-modulating TBS QED resonance, not the spectrographic recording and analysis components. Conceptual model of a proposed TBS experiment where hydrogen is put in the sample tube to which resonances are applied in a manner opening the manifold of uncertainty for access to HD cavities correlated with new spectral lines in hydrogen.

Some experimental evidence has been found to support this view showing the possibility that this is the same property that the interaction of these extended structures in space involve real physical vacuum couplings by resonance with the subquantum Dirac ether. Because of photon mass the CSI model, any causal description implies that for photons carrying energy and momentum one must add to the restoring force of the harmonic oscillator an additional radiation (decelerating) resistance derived from the em (force) field of the emitted photon by the action-equal-reaction law. Kowalski has shown that emission and absorption between atomic states take place within a time interval equal to one period of the emitted or absorbed photon wave. The corresponding transition time correlates with the time required to travel one full orbit around the nucleus [102,103]. Individual photons with m_γ are extended spacetime structures containing two opposite point-like charges rotating at a velocity near *c,* at the opposite sides of a rotating diameter with a mass, $m = 10^{-65}\ g$ and with an internal oscillation $E = mc^2 = h\nu$. Thus a new causal description implies the addition of a new component to the Coulomb force acting randomly and may be related to quantum fluctuations. We believe this new relationship also has some significance for our model of vacuum C-QED blackbody absorption/ emission equilibrium [130].

4.16. Indicia of the UFM Tight Bound State CQED Model

A) SEARCH FOR LARGE-SCALE ADDITIONAL DIMENSIONS

CERN has begun a new program to find evidence of another host of particles that can only exist if there are more dimensions than found in the Standard Model of particle physics; experiments proposed, but not yet successfully performed.

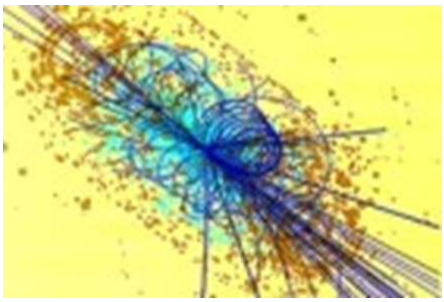

Fig. 22. CERN high energy collision cross section particle spray of the type that uncovered the Higgs mechanism.

CERN is trying to build larger and larger more powerful colliders like the LHC in the hopes of creating cross sections closer and closer to the Planck scale. Our UFM model is radically different; it is table-top and low energy. Why is that? If the matter right in front of our nose only appears solid and impenetrable because of a constructively interfered phase amplitude – of which we are made out of and imbedded in so that we have the same occlusion, then the uncertainty principle provides a simple gating mechanism to preclude us. Remember when 'they' first tried to fire a machine gun through the propeller of WWI airplanes – 'They' shot the propellers off until they timed the shots properly. Recall our mention of the inherent beat frequency hidden within the manifold of uncertainty.

B) THE CONTINUOUS-STATE HYPOTHESIS

Derivation of continuous-state multiverse postulates led to a unique string vacuum with as I've mentioned contains a variable string tension and a virtual tachyon [6,7]. I will do my best to define this continuous-state process which is still very difficult for me to do. The Planck scale is currently called the basement of reality starting from an essentially infinite size Hubble radius cosmology that reduces to a rigid microscopic Planck scale. In the holographic multiverse model, built partly by the way on an extension of Elizabeth's complex 8-space, where she added a 4D complex space, $\mathbb{C}^4$ to standard 4D Minkowski space, M^4 which didn't quite work for me because her 4D complex space still reduced to a fixed rigid Planck barrier.

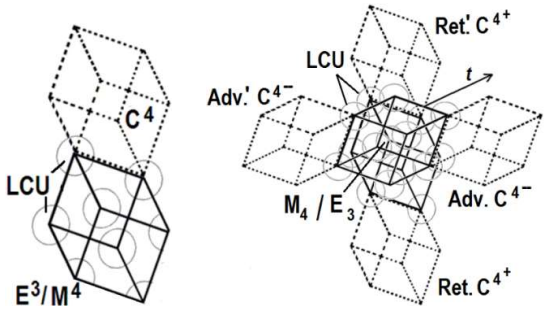

Fig. 4.23. a) Conceptual view of the Rauscher HD Complex C^4 space added to Minkowski space. b)12D UFM Multiverse cosmology with the addition of a 2nd dual mirror symmetric complex 4-space resulting in $\tilde{M}_4 \pm C^4$. The $\pm C^4$ spacetime packages must become involute (like a trefoil or L-R dual Mobius Klein bottle (Fig. 4.26) before the continuous-state process flow can occur. Or better yet for Calabi-Yau manifolds, folded into a torus.

What was needed to develop the continuous-state model was to have a fundamental basis of reality that acted as if it was in a self-contained inherent freefall. So we added another set of complex dimensions to allow reality to cycle continuously at the fundamental level. However, Rauscher's complex 8-space also included superluminal Lorenz transformations that boosted a spatial dimension, *s* into a temporal dimension, *t* enhancing my process for conceptualizing the continuous-state scenario

[10]. We then applied a second set of superluminal Lawrence transformations boosting a temporal dimension, t to dimension of energy, e. The energy dimension becomes compatible with a super-quantum potential eventually becoming synonymous with the ontological force of coherence of the unified field. This addition along with the second complex 4-space, $\pm\mathbb{C}^4$ dimensions completed geometrically at least the necessary components for continuous-state cyclicality providing a key framework for one of the most key elements of the model within which we propose new TBS spectral lines in hydrogen [31].

Concerning the importance of the original hadronic form of variable string tension; the main reason we were able to discover a unique string vacuum was by finding an alternative derivation of string tension; for which the traditional formula is, $T_s = e/l = (2\pi\alpha')^{-1}$. The multiverse UFM formula in unexpanded form became,

$$F_{(N)} = \frac{\aleph}{\rho} \tag{4.16}$$

where instead of energy, e over the length of the string, l topological charge or UF brane energy, $\aleph$ was put over the brane topological radius, ρ of the relativistically rotating Riemann sphere LCU hyperstructure. $F_{(N)}$ is the noetic force of coherence of the unified field [31].

4.17 Building the UFM TBS Experimental Protocol

The best indicia for our model experimentally is suggested by work done by Chantler [132,133]. The data from his experiments over the last 10 years or so on hydrogen showed only a minute artifact proposed to violate QED; but more recently in 2012 for work on Titanium the QED violation effect was much larger. The beauty of this is that they stripped all the electrons off the Titanium atom except one creating a large hydrogen-like atom [133]. One wants to maintain the simplicity of the hydrogen atom to perform the experiment.

Vigier's seminal papers in 1999/2003 [134,135] are similar theoretically in some ways to Chantler's model. Vigier describes the first exploration made by Corben in an unpublished paper. Corben noticed that motion of a point charge in the field of magnetic dipole at rest, is highly relativistic and that the orbits are of nuclear dimensions. Further investigation has been undertaken by Schild [136], but the most systematic treatment of this problem is given by Barut (see for example [137]) A 2-body system where magnetic interactions play the most significant role is in positronium. Both electron and positron have large magnetic moments which contribute to the second potential well in an effective potential, at distances much smaller than the Bohr radius. Barut and his coworkers predicted that this second potential well can support resonances. A 2-body model, suitable for non-perturbative treatment of magnetic interactions is presented by Barut [137] and Vigier [l34,135].

Our approach doesn't fully correlate with Vigier's because at that time he had no consideration of additional dimensionality which is a dominant element in our multiverse model. For the first 10 years of Chantler's work the artifact said to violate QED was so small that it was essentially ignored by the physics community. But in the 2012 experiment [133] the QED violation was great enough $(>\sigma 5)$ that media suggested Nobel Prize; but the majority of the physics community said the artifact is insufficient.

Now the reason we think the continuous-state model will work is for example if you take the Bohr model of the hydrogen atom, spectroscopic measurements are taken as a 3D volume measurement from the space between the nucleus and the electrons orbit. For hydrogen the first Bohr orbit has a radius of a .5 Angstrom, and the second or orbit a radius of ~2 Å. This is the 100-year history of spectroscopic measurements from within the fixed regime of the 4D standard model. A spectroscopic cavity is going to have different properties in a 12D holographic multiverse regime.

Firstly, we postulate the volumes of XD both within the finite radius MOU and beyond into the

regime of LSXD. We continue to mention in terms of the complex quaternion Clifford algebra required to describe the continuous state process; that the cyclicality has an inherent commutativity anti-commutativity that the algebra can handle with a 3D or 4D Euclidean/Minkowski space resultant with 8D or 9D complex cycling dimensions built on top of it. Initially for a single space anti-space doubling, the MOU represents a 4th 5th and 6th hyperspherical XD.

Recall our use of the Rauscher superluminal Lorentz transformation that boosts a spatial dimension into a temporal dimension, wherein multiverse UFM cosmology has added a second boost of dimensionality from temporal to that of energy as the exchange mechanism for topological charge in unified field theory. Behind or within the veil of uncertainty these XDs open and close volumetrically from zero i.e. the usual 3D Euclidean QED cavity to the added volumetric structure of the 4th 5th and 6th XD yielding: $r_1V_{3D}, r_2V_{4D}, r_3V_{5D}, r_4V_{6D}$ enabling us to calculate the wavelength of three additional spectral lines in hydrogen based on the volume of these respective hyperspherical cavities.

We haven't given enough thought to consider whether it's a viable addition to interpretation, but Von Neumann postulated a 'speed for collapse' of the wave function, suggesting that if we also used a hydrogen-like Titanium atom there might be an additional helpful time delay factor. In any case the success of this experiment would provide the first indicia that something exists beyond the regime of Gauge theoretic SM QED.

Opening the 4D resonance hierarchy cavity will be relatively easy, but to open the 5th and 6D cavities probably requires the addition of some kind of precision Bessel function to the resonance hierarchy because additional artifacts like found in the refinements of the Born-Sommerfeld model; it will be a little tricky to master the protocol to measure these additional spectral lines. I do not mean this in calculating the wavelength, but the tiniest property we do not sufficiently understand will probably keep the uncertainty principle sufficiently active to keep the 5D cavity closed!

This TBS model only works within the continuous-state holographic multiverse scenario simply because without that utility physics would not go beyond 5D Kaluza-Klein and remain 'curled up at the Planck scale' model of XD. It is only the inherent continuous-state process of open-closed cyclicality that allows access (violating the uncertainty principle) to the additional infinite LSXD. This restriction is not a negative aspect of this proposed multiverse cosmology, but we feel rather that it is suggestive of the correct path to take as it is the actuality of physical reality.

The key element in this cosmology is the Least Cosmological Unit (LCU), not fully invented by us; but an extension of the idea found within a chapter called, "*The size of the least unit*" in a collection edited by Kafatos [101]. But Stevens of course utilizing only the 4D of the standard model attempted to describe a Planck scale least unit. But hopefully you have realized by now that our LCU oscillates from asymptotic virtual Planck, $(\hbar + T_S)$ to the Larmor radius of the hydrogen atom relative to the nature of its close-packing tiling the spacetime foam.

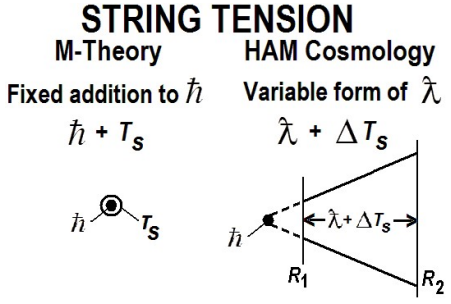

Fig. 4.24. Fixed string tension in M-Theory (left) and variable (right) as in the original hadronic form of string theory and HAM cosmology that also reverts to the original Stoney, $\hat{\lambda}$ rather that Planck's constant, $\hbar$.

The left-hand part of Fig. 4.24 shows the current thinking of string tension but, on the right we see a multiverse version with a variable string tension that oscillates from virtual plank to the Larmor radius

of hydrogen. Notice that the symbol for the Planck constant is different, we use the original Stony [4] that preceded Planck because it is electromagnetic and correlates better with the Dirac polarized vacuum which we want available for our resonance hierarchy component of the experimental protocol. Virtual plank is the asymptotic zero point on the Riemann sphere that flips back to infinity in the continuous-state cycle.

Since the Planck scale is no longer considered the basement of reality the 12D continuous-state process changes the size of the LCU in the process of Riemann sphere rotation from zero back to infinity continuously. Choice of the upper limit as the Larmor radius is somewhat arbitrary. We cannot define this rigorously yet without experiment; but assume it is in this ballpark. So just to make a note we have this oscillating Planck unit, $\Delta\hbar$ at the microscopic level in conjunction with an oscillating $\Delta\Lambda$ lambda or cosmological constant at the macroscopic level.

As an aside this gives us the ability to describe dark matter/energy as an artifact of the rest of the multiverse outside our ~ 14.7 bly radius Hubble sphere. The multiverse has 'room for an infinite number of nested Hubble spheres each with their own fine-tuned laws of physics'. That scenario provides our model of dark energy. These nested Hubble spheres are closed and finite in time and causally separate in the XD where gravity would take effect, so it's not like there is an infinite mass acting on us but something subtler. As generally known the postulate of dark energy and dark matter comes from the knowledge that galactic rotation occurs like a phonograph record not a vortex.

Think of these nested Hubble spheres as a stalk of grapes; they are invisible to current empirical means because the nature of the stalk holding the grapes, however, UFM allows design of a 'Q-telescope' to visualize them [4]. Also see the Drake equation therein.

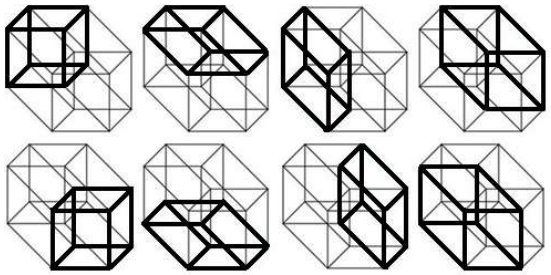

Fig. 4.25. View of 8 3D cubes comprising a 4D hypercube. See continuous-state involution metaphor in Fig. 4.5.

A main condition of the continuous-state hypothesis comes from an HD extension of Cramer's Transactional Interpretation of future-past elements resulting in a present moment [52]. Cramer considers this as a standing-wave of the future-past. In XD we build on superluminal Lorentz transformations, coupled to advanced-retarded future-past complex pairs.

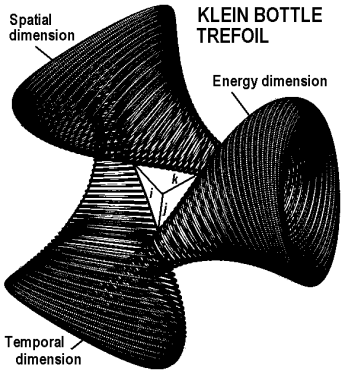

Fig. 4.26. A Klein bottle trefoil. A 6D Calabi-Yau 3-torus could also be used. A primitive metaphor to show rotation of continuous-state components. Does not really work in 4D. But I wanted to try to illustrate the cycling of dimensional parameters if the eight cubes of the hypercube put into motion not just exploded as in the figure.

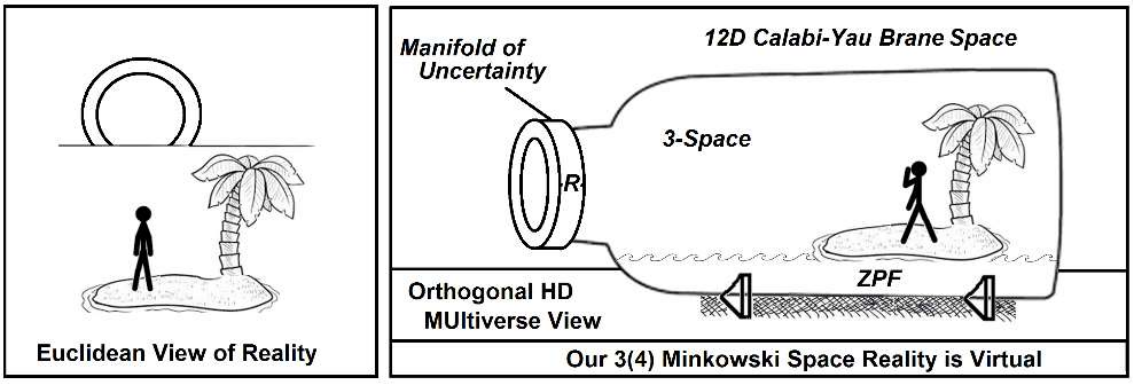

Fig. 4.27. Beyond The 4D Standard Model Lies Infinite Size Dimensionality (LSXD) 'Hidden' by Uncertainty.

What I have poorly tried to illustrate in Figs. 4.25 to 4.27 is some of the underlying topology of continuous-state topology. Figure 4.25 shows the dramatic increase in the number of cubes comprising HD space as we travel rectilinearly up the XD ladder. Figure 4.26 shows a key condition of involution allowing the continuous-state process to cycle continuously when set in motion by the nature of HD reality. Figure 4.27 is also an attempt to speak to the rotational properties of cyclicality. Out 12D model must cycle through nodes of commutativity and anti-commutativity where one mode is degenerate and the other closed to observation. There are not sufficient degrees of freedom to cyclically break closure otherwise. Rowlands supports an inherent necessity of 3D for reality [138], so we have a doubling of the 1st 3D into another triplet of HD space. This might suggest indicia for the necessity of the 12D where UFM wants to lead us.

Imagine a 3-blade ceiling fan symbolic of a quaternion fermion vertex. If one puts one of these fans in front of a mirror (real space) rotating clockwise the mirror image (anti-space) rotates counterclockwise with the blades coming occasionally into phase as in Fig. (4.10). Now we give a key insight into the TBS experiment that Fig. 4.10 doesn't have. If there is a light on near the fan in real space, i.e. the rf-pulse of our TBS experiment. Periodically when the blades come into phase (Fig. 4.10 again) meaning when a blade from real space comes into phase with a blade in the mirror antispace the light is reflected off each blade (the mirror image of the mirror image) and a pulsating, reflected flash of light occurs in the direction back towards the source/detector! This is representative of how we intend to find the new TBS spectral lines in hydrogen; that we would expect to see a flashing back, like a rotating lighthouse beacon when the resonance hierarchy is aligned properly!

Rowlands suggests these additional space anti-space dimensions are redundant (no new information) [138] That's actually what we want from an infinite potentia that is nilpotent and redundant. Surmounting the quantum mechanical uncertainty principle occurs by this same process that gives us a beat frequency inherent in the spacetime backcloth.

In order to demonstrate existence of new spectral lines the experiment itself requires surmounting the quantum uncertainty principle. I hope when we apply the complex quaternion Clifford algebra it will tell us whether one or two additional doublings of Peter's original space anti-space model are required and then let us know if there's two or three or more consecutive doubling needed to find four or five additional spectral lines which of course tells us the complete size of the manifold of uncertainty.

From the common simple example of a Bessel function, with α an arbitrary complex number:

$$x^2 \frac{d^2 y}{dx^2} + x \frac{dy}{dx} + \left(x^2 - \alpha^2 \right) y = 0 \qquad (4.17)$$

we solve the Helmholtz equation in spherical coordinates by variable separation such that the radial equation takes the form

$$x^2\frac{d^2y}{dx^2}+2x\frac{dy}{dx}+\left[x^2-n(n+1)\right]y=0\,. \tag{4.18}$$

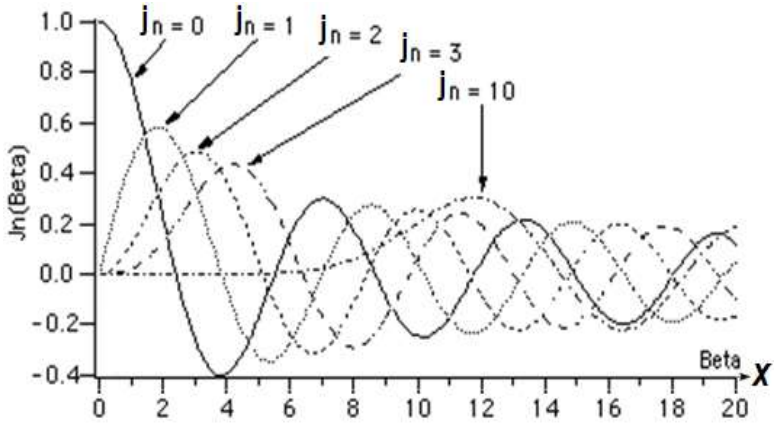

Fig. 4.28. Example of a Bessel Function that may be necessary to couple synchronization with the Dubois incursive oscillator in order access additional TBS beyond the first. Even though we think we know how, surmounting uncertainty will probably not be trivial.

The spherical Bessel functions, j_n, y_n are the two linearly independent solutions relate to the ordinary Bessel functions, J_n, Y_n as:

$$\begin{aligned} j_n(x) &= \sqrt{\frac{\pi}{2x}}J_{n+\frac{1}{2}}(x), \\ y_n(x) &= \sqrt{\frac{\pi}{2x}}Y_{n+\frac{1}{2}}(x) = (-1)^{n+1}\sqrt{\frac{\pi}{2x}}J_{-n-\frac{1}{2}}(x). \end{aligned} \tag{4.19}$$

When written as Rayleigh's formulas

$$\begin{aligned} j_n(x) &= (-x)^n\left(\frac{1}{x}\frac{d}{dx}\right)^n\frac{\sin(x)}{x}, \\ y_n(x) &= (-x)^n\left(\frac{1}{x}\frac{d}{dx}\right)^n\frac{\cos(x)}{x}, \end{aligned} \tag{4.20}$$

the first spherical Bessel functions are

$$\begin{aligned} j_0(x) &= \frac{\sin(x)}{x} \\ j_1(x) &= \frac{\sin(x)}{x^2}-\frac{\cos(x)}{x} \\ j_2(x) &= \left(\frac{3}{x^2}-1\right)\frac{\sin(x)}{x}-\frac{3\cos(x)}{x^2} \end{aligned} \tag{4.21}$$

[139]

and

$$y_0(x) = -j_{-1}(x) = -\frac{\cos(x)}{x}$$
$$y_1(x) = -j_{-2}(x) = -\frac{\cos(x)}{x^2} - \frac{\sin(x)}{x} \qquad [139]. (4.22)$$
$$y_2(x) = -j_{-3}(x) = \left(-\frac{3}{x^2} + 1\right)\frac{\cos(x)}{x} - \frac{3\sin(x)}{x^2}$$

We show the 1st three Bessel function solutions of the 1st and 2nd kind to illustrate our process to locate the first TBS spectral line in hydrogen which will be relatively easy to find in comparison to finding the 2nd and 3rd. The additional lines will be more challenging as there will be some unexpected complexity in the Bessel harmonic oscillator that must be overcome. The restrictions related to this refinement hasn't revealed itself to us as yet, that will require some additional adjustment to the spin-spin coupling parameters of the algebra describing the HD hyperspherical volume. Parallel transport of the gravitational curvature deficit angle kick in, in mirror symmetric brane topological form, with noeon topological charge corrections (not a quantized gravity).

The choice of linear combinations of Bessel solutions (4.5) depends on their asymptotic behavior at ∞,

$$J_n(x) \simeq \sqrt{\frac{\pi}{2x}}\cos(x - \tfrac{\pi}{2}n - \tfrac{\pi}{4});\;\; Y_n(x) \simeq \sqrt{\frac{\pi}{2x}}\sin(x - \tfrac{\pi}{2}n - \tfrac{\pi}{4}) \qquad (4.23)$$

thus

$$H_n^{\pm}(x) \simeq \sqrt{\frac{\pi}{2x}}\exp\left[\pm i\left(x - \tfrac{\pi}{2}n - \tfrac{\pi}{4}\right)\right] \quad [140]. \qquad (4.24)$$

With the harmonic oscillator Bessel function solutions, the next step in the experimental design is to apply the Dubois incursive oscillator parameters as the final step in designing the Sagnac effect rf-pulses. The incursive algorithms are numerically stable and the numerical simulation of the pendulum will show the conservation of the energy. Let us consider the example of the harmonic oscillator, with m the oscillating mass and *k* the spring constant, represented by the ordinary differential equations:

$$\mathrm{dx(t)/dt = v(t)} \qquad (4.25a)$$

$$dv(t)/dt = -\omega^2 x(t)\;\; \mathrm{dv(t)/dt} \qquad (4.26b)$$

where $x(t)$ is the position and v(t) the velocity as functions of the time *t*, and where the pulsation ω is related to *k* and *m* by $\omega^2 = k/m$ [141].

The solution is given by

$$x(t) = x(0)\cos(\omega t) + \left[v(0)/\omega\right]\sin(\omega t) \qquad (4.27a)$$

$$v(t) = -\omega x(0)\sin(\omega t) + v(0)\cos(\omega t) \qquad (4.27b)$$

with the initial conditions $x(0)$ and $v(0)$. In the phase space, given by $(x(t), v(t))$, the solutions are given

by closed curves (orbital stability). The period of oscillations is given by $T = 2\pi / \omega$. The energy $e(t)$ of the harmonic oscillator is constant and is given by

$$e(t) = k\, x^2(t) / 2 + m\, v^2(t) /2 = k\, x^2(0) / 2 + m\, v^2(0) /2 = e(0) = e_0 \qquad (4.28)$$

The simulation of differential equations is impossible. This is only the discrete transformation which is computable with recursive function.

In differential equations there is only the current time. In discrete systems, there are the current time t and the interval of time $\Delta t = h.$ The discrete time is defined as: $t_k = t_0 + kh$ with k = 0,1,2,… where t_0 is the initial value of the time and k is the counter of the number of interval of time h [141].

The discrete variables are defined as $x_k = x(t_k)$ and $y_k = y(t_k)$. The discrete equations used in the harmonic oscillator case for computing the position and the velocity at consecutive moments have the general form

$$x_{k+1} = Ax_k + Bv_k \qquad (4.29a)$$

$$v_{k+1} = Cv_k - D\omega^2 x_k \qquad (4.29b)$$

where *A, B, C* and *D* are coefficients with values specific to the numerical integration methods applied. In eliminating v_k of Eq. (4.29a) in Eq. (4.29b), a second order discrete equation in x_k is given by

$$x_{k+2} - (A + C)x_{k+1} + (AC + BD\omega^2)x_k = 0 \qquad (4.30)$$

The stability analysis for this discrete system can be performed by using the Z-transform

$$z^2 - (A + C)z + (AC + BD\omega^2) = 0 \qquad (4.31)$$

which presents two poles:

$$z_{1,2} = ((A + C) \pm i\sqrt{-(A + C)^2 + 4(AC + BD\omega^2)}) / 2 \qquad (4.32)$$

that are complex when

$$(A + C)^2 < 4(AC + BD\omega^2)\ [141]. \qquad (4.33a)$$

The position of the poles relative to the unit circle defines the system stability: a system is stable if the poles lie inside the unit circle, is unstable if the poles lie outside the unit circle and shows an orbital stability if the poles lie on the unit circle. It follows that the condition for stability is:

$$((A + C)^2 - (A + C)^2 + 4(AC + BD\omega^2)) / 4 \le 1 \qquad (4.33b)$$

or $AC + BD\omega^2 \le 1$ and the orbital stability must satisfy the strict equality

$$AC + BD\omega^2 = 1 \qquad (4.33c)$$

so, for the harmonic oscillator, the conditions for obtaining an orbital stability are given by relations (8a) and (8c), rewritten as

$$(A+C)^2 < 4 \text{ and } AC + BD\omega^2 = 1 \qquad (4.34a,b)$$

in using the equality from the relation (8c), in the relation (8a) [141].

Let us first consider the well-known Euler and Runge-Kutta integration methods, e.g. Scheid [142]; and after that, the incursive methods will be analysed.

In terms of incursive discrete algorithms, Dubois defined a generalized forward-backward discrete derivative

$$D(w) = w\, Df + (1 - w)\, Db \qquad (4.35)$$

where w is a weight taking the values between 0 and 1, and where the discrete forward and backward derivatives on a function f are defined by

$$D_f(f) = \Delta^+ f / \Delta t = \left[f_{k+1} - f_k \right] / h \qquad (4.36a)$$

and

$$D_b(f) = \Delta^- f / \Delta t = \left[f_k - f_{k-1} \right] / h \qquad (4.37b)$$

The generalized incursive discrete harmonic oscillator is given as:

$$(1\text{-}w)\, x_{k+1} + (2w\text{-}1)\, x_k - w\, x_{k-1} = h v_k \qquad (4.38a)$$

$$w\, v_{k+1} + (1\text{-}2w) v_k + (w\text{-}1) v_{k-1} = -h\, \omega^2 x_k \qquad (4.38b)$$

When w = 0, $D(0) = D_b$, this gives the first incursive equations:

$$x_{k+1} - x_k = h\, v_k \qquad (4.39a)$$

$$v_k - v_{k-1} = -h\, \omega^2\, x_k \qquad (4.39b)$$

When w = 1, $D(1) = D_f$, this gives the second incursive equations:

$$x_k - x_{k-1} = h\, v_k \qquad (4.40a)$$

$$v_{k+1} - v_k = -h\, \omega^2\, x_k . \qquad (4.40b)$$

When w = 1/2, $D(1/2) = [D_f + D_b]/2$, this gives the averaged (hyperincursive) equations:

$$x_{k+1} - x_{k-1} = 2\, h\, v_k \qquad (4.41a)$$

$$v_{k+1} - v_{k-1} = -2\, h\, \omega^2\, x_k \qquad (4.41b)$$

These Eqs. (4.41a,b) integrate the two incursive equations.

This deals with a deduction of this forward-backwards discrete derivative, with the deduction of this time-symmetric discretization of the harmonic oscillator [141].

Next Dubois discusses ssimulation of the incursive and hyperincursive algorithms of the classical harmonic oscillator. First, for the simulation of the classical harmonic oscillator, the dimensionless variables X, V and H, will be used [8], for the variables, *x, v* and $h: X(k) = \sqrt{[k/2]}x_k$, $V(k) = \sqrt{[m/2]}v_k$, $\tau = \omega t$ with $\omega = \sqrt{[k/m]}$, and $\Delta\tau = \omega\Delta t = \omega h = H$. So, the two incursive dimensionless harmonic oscillators are given by

$$X_1(k+1) = X_1(k) + H\,V_1(k) \qquad (4.42a)$$

$$V_1(k+1) = V_1(k) - H\,X_1(k+1) \qquad (4.42b)$$

$$V_2(k+1) = V_2(k) - H\,X_2(k) \qquad (4.43a)$$

$$X_2(k+1) = X_2(k) + H\,V_2(k+1) \qquad (4.43b)$$

and the hyperincursive dimensionless harmonic oscillator is given by

$$X(k+1) = X(k-1) + 2H\,V(k) \qquad (4.44a)$$

$$V(k+1) = V(k-1) - 2H\,X(k) \text{ [141]}. \qquad (4.44b)$$

Table 4.2 shows the numerical simulations of algorithms (4.42-4.44).

TABLE 4.2. Simulation of Eq. (4.42, 4.43) of the two incursive harmonic oscillators with a cycle of N = 6 iterates and interval of time H = 1.0. The averaged energy <E(k)> = ($E_1(k) + E_2(k)$)/2 of the two oscillating energies is constant.

			INCURSION 1			INCURSION 2			Energy
N	**H**	**k**	**$X_1(k)$**	**$V_1(k)$**	**$E_1(k)$**	**$X_2(k)$**	**$V_2(k)$**	**$E_2(k)$**	**<E(k)>**
6	**1**	**0**	**4.66**	**0.00**	**75**	**10.00**	**5.00**	**125**	**100**
		1	**4.66**	**-8.66**	**150**	**5.00**	**-5.00**	**50**	**100**
		2	**0.00**	**-8.66**	**75**	**-5.00**	**-10.00**	**125**	**100**
		3	**-8.66**	**0.00**	**75**	**-10.00**	**-5.00**	**125**	**100**
		4	**-8.66**	**8.66**	**150**	**-5.00**	**5.00**	**50**	**100**
		5	**0.00**	**8.66**	**75**	**5.00**	**10.00**	**125**	**100**
		6	**8.66**	**0.00**	**75**	**10.00**	**5.00**	**125**	**100**

So, this confirms that the incursive and hyperincursive algorithms are totally numerically stable with the conservation of energy [141].

When the parameters for the experiment are coordinated and the rf-pulse sent into the MOU HD QED TBS hydrogen cavity, a positive result will retrieve a spectroscopic signal like the one represented in Fig. 4.29. A negative result would send back 0 amplitude [31].

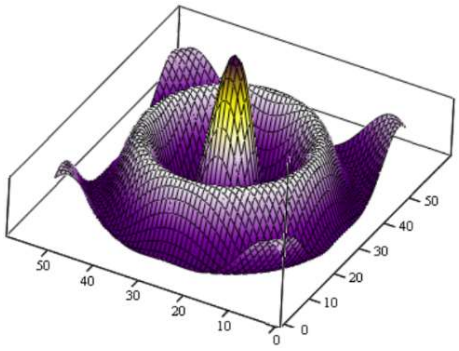

Fig. 4.29. First 4D TBS spectral line in hydrogen emerging from the 4D spherical potential well for $\alpha = \pm 1$. Fig. adapted from [143].

4.18. Issues of Experimental Design

In the simplistic model of doing the TBS experiment we put hydrogen in a sample tube (Fig. 4.21) and apply a series of resonant pulses in conjunction with the beat-frequency of space-time to open the HD QED-UFM cavity, send the signal in and allow the new TBS spectral line signal to be emitted back to the detector.

Remember we postulated that the HD continuous-state cycle must incorporate cycles of commutativity and anti-commutativity. This can be shown metaphorically in terms of logarithmic spirals applied to what is called perfect rolling motion (Figs. 4.30, 4.31).

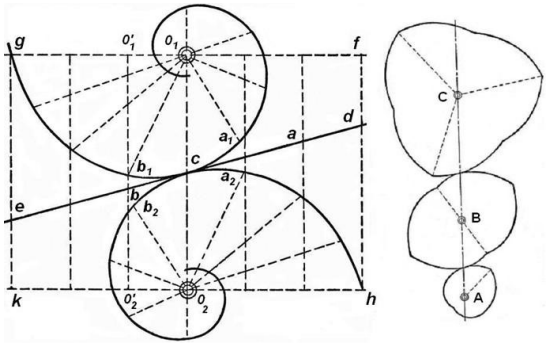

Fig. 4.30. Logarithmic spirals and 'Perfect Rolling Motion. Segments of the logarithmic spiral are put together into the three spheroids on the right, A,B,C. Like the 320° - 720° spinor rotation of the Dirac electron; the speroids will only return to the same configuration after a number of 360° rotations.

We've been arguing with colleagues for the last couple of years about aspects of quaternion algebra. I'm thankful especially to Peter Rowlands for helping me learn some of the properties of quaternions. As well-known, Hamilton wanted to extend the complex number system algebraically by adding an additional *j* term to the *i* series; but the algebra didn't work. It was only when Hamilton added the 3rd *k* term that quaternion algebra became complete by closing the algebra and in the process, sacrificing commutativity. Is it any wonder that Rowlands resisted when I told him I wanted to open the algebra again so that it could cycle between modes of commutativity and anti-commutativity. Rowlands was very gracious and allowed me to visit him for a week in Liverpool. We did find something interesting (see [143]) that is not yet a complete study, and not quite the cycle we've been looking for which with all profundity is going to be possible with a rather simple complex quaternion Clifford algebra [145].

How can we find this cycle in HD Calabi-Yau mirror symmetry? The logarithmic spirals in Fig. 4.30a are not free to rotate (Euclidean shadow). If we take pieces of the curve as in Fig. 4.30b and paste

them together as shown; the three cycloids can cycle continuously. Perfect rolling motion in this case means a mechanical process where there is no slippage if this is applied to the mechanics of gears. As hopefully clear well before now to the reader, this represents a 'closed' non commuting algebra.

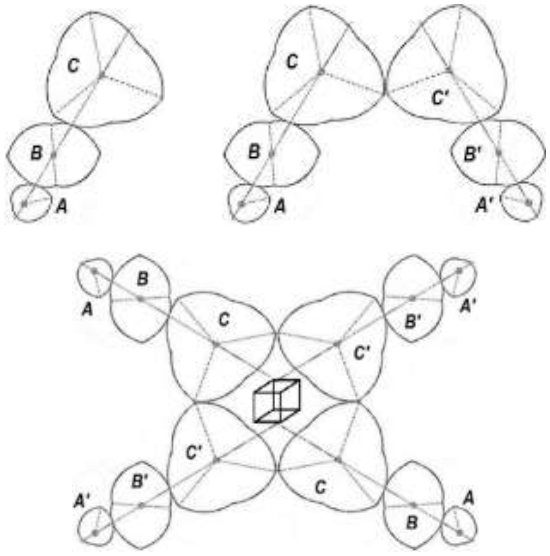

Fig. 4.31. a) Perfect rolling motion of logarithmic spiral components. b) Applied to left-right symmetry transformations of Calabi-Yau brane topology such that while the A,B,C tower is meant to represent the usual closed quaternionic space-antispace algebra; the A,B,C and A'B'C' towers together when doubled again as in c) will be able to cyclically commute and anti-commute (requires an additional mirror symmetric doubling with trefoil-like involution and parameters of parallel transport to finally cyclically break closure of the algebra. c) Hierarchical structure of HD space reducing to a 3-space resultant. The redundant A,B,C quaternionic copies shown for 2 cubic vertices, should be made to correlate with each of the 8 vertices of the Euclidean 3-space cube in order to fully represent complex 8-space, $\pm\mathbb{C}^4$; done beautifully with the Fano snowflake in Chap. 12.

If you're not a mechanical engineer, you may not have guessed already that after a certain number of cycles the set of three cycloids returns to the precise original position. Now in terms of the next figure (4.31) let's apply this to a second doubling or duality to Rowlands' space anti-space quaternion model which of course is going to have to include Calabi-Yau mirror symmetry. What we propose metaphorically here is that with the utility of the complex quaternion Clifford algebra we can mathematically describe how to break the closure inherent in one of the mirror symmetric partners and describe cycles relative to both mirror symmetric partners that additionally pass through cycles of commutativity and anti-commutativity with each other. We cannot surmount the uncertainty principle utilizing a closed algebra - the mathematical description of course.

This is similar to the property revealed in Fig. 4.10 with the rotating of the wind generator propellers cycling from Chaos to Order; and also similar to passing by a fruit orchard, rows of chairs in an auditorium or the tombstones in a graveyard where one's line of sight is alternatingly blocked and alternatingly open to infinity in similitude also to wave particle duality again in terms of the rotations inherent to the cyclicality of the LCU backcloth tessellating space antispace - talking about nodes in the hyperspherical structure inherent in the HD components 'behind' our 3-space virtual reality. We assume that all matter cyclically emerges from spacetime. In order to perform our experiment, we need to 'destructively-constructively' interfere with this process. In the model being developed this requires finding a cyclical beat-frequency to the creation and annihilation process of spacetime and matter.

In summary we have the 3-level tiered Sagnac Effect resonance hierarchy of electrons nucleons and spacetime. The counter-propagating properties of the Sagnac Effect that violates special relativity in the small-scale will most likely be relevant to this process. For the standing-wave oscillator, the gap between R_1 & R_2 (Fig. 12) in the beat frequency of spacetime we take our 'little laser blaster' starting

at the R_1 bandwidth, when we reach the right point we will get a reflected blip, which will be our first new spectral line in hydrogen.

Some experimental evidence has been found to support this view showing the possibility that this is the same property that the interaction of these extended structures in space involve real physical vacuum couplings by resonance with the subquantum Dirac ether. Because of photon mass the CSI model, any causal description implies that for photons carrying energy and momentum one must add to the restoring force of the harmonic oscillator an additional radiation (decelerating) resistance derived from the em (force) field of the emitted photon by the action-equal-reaction law.

The corresponding transition time corresponds to the time required to travel one full orbit around the nucleus. Individual photons are extended spacetime structures containing two opposite point-like charges rotating at a velocity near *c,* at the opposite sides of a rotating diameter with a mass, m $=10^{-65}$ g and with an internal oscillation $E = m^2 = h\nu$. Thus a new causal description implies the addition of a new component to the Coulomb force acting randomly and may be related to quantum fluctuations. We believe this new relationship has some significance for our model of vacuum C-QED blackbody absorption/emission equilibrium.

The purpose of this simple experiment is to empirically demonstrate the existence of LSXD utilizing a new model of TBS in the hydrogen atom until now hidden behind the veil of the uncertainty principle. If for the sake of illustration, we arbitrarily assume the *s* orbital of a hydrogen atom has a volume of 10 and the *p* orbital a volume of 20, to discover TBS we will investigate the possibility of heretofore unknown volume possibilities arising from cyclical fluctuations in large XD Calabi-Yau mirror symmetry dynamics. This is in addition to the Vigier TBS model. As in the perspective of rows of seats in an auditorium, rows of trees in an orchard or rows of headstones in a cemetery, from certain positions the line of sight is open to infinity or block. This is the assumption we make about the continuous-state cyclicality of HD space. Then if the theory has a basis in physical reality and we are able to measure it propose that at certain nodes in the cycle we would discover cavity volumes of say 12, 14, and 16. We propose the possibility of three XD cavity modes like 'phase locked loops' depending the cycle position - maximal, intermediate and minimal.

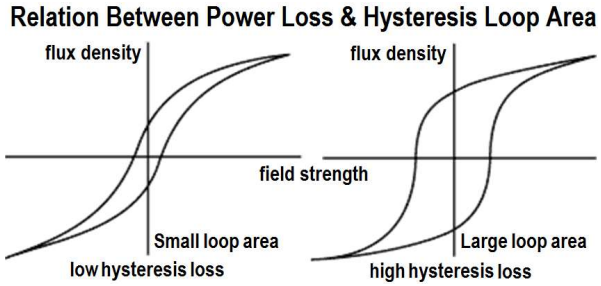

Fig. 4.32. We model our spacetime MOU QED cavity as a hysteresis loop of UFM charge. The cavity opens and closes; timing is crucial.

The lag of a magnetic material called Magnetic Hysteresis**,** relates to the magnetization properties of a material by which it first becomes magnetized and then de-magnetized. The magnetic flux generated by an electromagnetic coil is the amount of magnetic field force produced within a given area, called Flux Density. Using symbol B, the unit of flux density is the Tesla, T. Also, the Magnetic Strength, H of an electromagnet depends on the number of turns of the coil around the core, and the current flowing through the core. The relative permeability, μ_r is defined as the ratio of the absolute permeability μ and the permeability of free space μ_o (vacuum) which is a constant. The relationship of flux density, B and the magnetic field strength, H can be defined by the fact that the relative permeability, μ_r is not a constant but a function of the magnetic field intensity, so that the magnetic flux density is $B = \mu H$. Then the magnetic flux density in the material will be increased by a larger factor

as a result of its relative permeability for the material compared to the magnetic flux density in vacuum, $\mu_0 H$ and for an air-cored coil this relationship is given as: $B = \Phi / A$ with $B / H = \mu_0$.

The magnetic flux does not completely disappear since the core material retains some of its magnetism even when the current has stopped flowing in the coil. The ability of a coil to retain some magnetism within the core after the magnetization process has stopped is called retentivity or remanence, while the amount of flux density still remaining in the core is **called** Residual Magnetism, B_R.

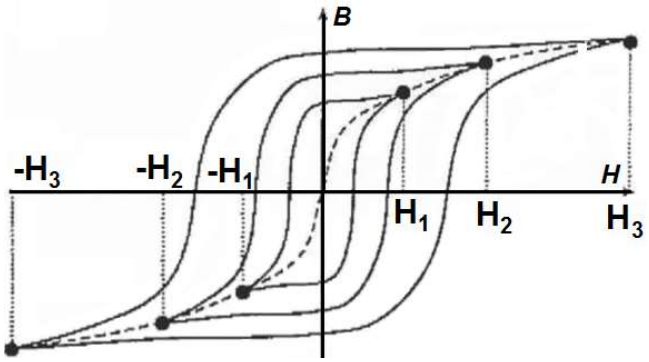

Fig. 4.33. The charge characteristics of nested Hysteresis loops can be used as a method for modeling the cyclic cavity dynamics of fermionic space-antispace parameters. Our postulate is that the Dirac polarized vacuum can demonstrate hysteresis properties.

References

[1] Dirac P.A.M. (1930/1958) The Principles of Quantum Mechanics, p. 12. Oxford: Oxford Clarendon Press.
[2] Allanach, B.C. (2014) Multiple solutions in supersymmetry and the Higgs, Phil. Trans. Roy. Soc. Lond. A373, 0035; arXiv:1401.8185 [hep-ph].
[3] Becker, K., Becker, M. & Schwarz, J.H. (2007) String Theory and M-Theory: A Modern Introduction, Cambridge: Cambridge, Univ. Press.
[4] Amoroso, R.L. & Rauscher, E.A. (2009) The Holographic Anthropic Multiverse Formalizing the Complex Geometry of Reality, London: World Scientific.
[5] Amoroso, R.L., Kauffman, L.H. & Rowlands, P. (eds.) (2016) Unified Field Mechanics: Natural Science Beyond the Veil of Spacetime, Hackensack: World Scientific.
[6] Arkani-Hamed, N., Dimopoulos, S., & Dvali, G. (1998) The hierarchy problem and new dimensions at a millimeter, Physics Letters B, 429(3), 263-272.
[7] Randall, L., & Sundrum, R. (1999) Large mass hierarchy from a small extra dimension, Physical Review Letters, 83(17), 3370.
[8] Cohen, A.G. & Kaplan, D.B. (1999) Solving the hierarchy problem with noncompact extra dimensions, Physics Letters B, 470(1), 52-58.
[9] Amoroso, R.L. (2009) (ed.) The Complementarity of Mind and Body: Realizing the Dream of Descartes, Einstein and Eccles, New York: Nova Science Publishers.
[10] Rauscher, E.A., & Amoroso, R.L. (2011) Orbiting the Moons of Pluto: Complex Solutions to the Einstein, Maxwell, Schrödinger, and Dirac Equations (Vol. 45) London: World Scientific.
[11] Amoroso, R.L. (2010) Simple resonance hierarchy for surmounting quantum uncertainty, in R.L. Amoroso et al. (eds.) AIP Conf. Proceedings, Vol. 1316, p. 185.
[12] Amoroso, R.L. (2009) Consciousness: The philosophical foundations of noetic field theory, in R.L. Amoroso (ed.) The Complementarity of Mind and Body: Realizing the Dream of Descartes, Einstein and Eccles, New York: Nova Science Publishers.
[13] Chu, M-Y.J. & Amoroso, R.L. (2008) Empirical mediation of the primary mechanism initiating protein conformation in prion propagation, in D. Dubois (ed.) Partial Proceedings of CASYS07, IJCAS, Vol. 22, Univ. Liege Belgium.
[14] Amoroso, R.L. (2005) Application of double-cusp catastrophe theory to the physical evolution of qualia: Implications for paradigm shift in medicine & psychology, in G.E. Lasker & D.M. Dubois (eds) Anticipative & Predictive Models in Systems Science, Vol. 1, pp. 19-26, Windsor: The Intl Inst Adv Studies in Systems Research & Cybernetics.
[15] Amoroso, R.L., & Amoroso, P.J. (2004) The fundamental limit and origin of complexity in biological systems: A new model for the origin of life, in D. Dubois (ed.) AIP Conference Proceedings (Vol. 718, p. 144).

[16] Amoroso R.L. (2003) Awareness: physical cosmology of the fundamental least unit, Noetic J, 4:1, 1-15
[17] Amoroso, R.L. (2003) The Fundamental Limit and Origin of Biological Systems, Noetic J, 4:1; 24-32.
[18] Amoroso, R.L. (2003) The physical basis of qualia: Overcoming the 1st person 3rd person barrier, Noetic J, 4:3, pp. 212-230.
[19] Amoroso, R.L. & Martin, B.E. (2002) Consciousness: 'A thousand points of light', The emergence of self-organization from the noumenon of the conscious universe, The Noetic Journal, 3:4, 289-311.
[20] Amoroso, R.L. (2002) The physical basis of consciousness: A fundamental formalism, Part 1 Noesis, XXVI, Bucharest: Romanian Acad.
[21] Amoroso, R.L. (2000) The parameters of temporal correspondence in a continuous-state conscious universe, in R. Buccheri & M. Saniga (eds.) Studies in the Structure of Time: From Physics to Psycho(patho)logy, Dordrecht Kluwer Academic.
[22] Amoroso, R.L, (2000) Consciousness, a radical definition: Substance dualism solves the hard problem, in R.L. Amoroso, R. Antunes, C. Coelho, M. Farias, A. Leite, & P. Soares (eds.) Science & the Primacy of Consciousness, Orinda: Noetic Press.
[23] Amoroso, R.L (1999) An introduction to noetic field theory: The quantization of mind, Noetic J. 2:1, pp. 28-37.
[24] Amoroso, R.L. (1997) Consciousness a radical definition: The hard problem made easy, Noetic Journal 1:1, pp. 19-27.
[25] Amoroso, R. L. (1997) A brief introduction to noetic field theory: The quantization of mind, in L. Rakic, G. Kostopoulos, D. Rakovic, & D. Koruga (eds.) Brain and Consciousness, Belgrade: ECPD.
[26] Amoroso, R.L. & Martin, B. (1995) Modeling the Heisenberg matrix: Quantum coherence & thought at the holoscape matrix and deeper complementarity, in J. King & K.H. Pribram (eds.) Scale in Conscious Experience, Mahwah: Lawrence Earlbaum.
[27] Osoroma, D.S. (2013) A programmable cellular automata polarized Dirac vacuum, 71-80, in R.L. Amoroso et al., The Physics of Reality: Space, Time, Matter, Cosmos, 504-509, New York: World Scientific.
[28] Amoroso, R.L. Rowlands, P & Kauffman, L.H. (2013) Exploring novel cyclic extensions of Hamilton's dual-quaternion algebra, 81-91, in R.L. Amoroso et al., The Physics of Reality: Space, Time, Matter, Cosmos, 504-509, New York: World Scientific.
[29] Amoroso, R.L (2013) Geometrodynamics: a complementarity of newton's and Einstein's gravity 152-163, in R.L. Amoroso et al., The Physics of Reality: Space, Time, Matter, Cosmos, 504-509, New York: World Scientific.
[30] Amoroso, R.L & Dunning-Davies, J. (2013) A scintilla of unified field mechanics revealed by a conceptual integration of new fundamental elements associated with wavepacket dispersion, 239-248, in R.L. Amoroso et al., The Physics of Reality: Space, Time, Matter, Cosmos, 504-509, New York: World Scientific.
[31] Amoroso, R.L & Vigier, J-P (2013) Evidencing 'tight bound states' in the hydrogen atom: empirical manipulation of large-scale XD in violation of QED, 254-272, in R.L. Amoroso et al., The Physics of Reality: Space, Time, Matter, Cosmos, 504-509, New York: World Scientific.
[32] Amoroso, R.L Kauffman, L.H. & Giandinoto, S. (2013) Universal quantum computing; 3rd gen prototyping utilizing relativistic 'trivector' r-qubit modeling surmounting uncertainty, 316-325, in R.L. Amoroso et al., The Physics of Reality: Space, Time, Matter, Cosmos, 504-509, New York: World Scientific.
[33] Dunning-Davies, J. & Amoroso, R.L (2013) Some thoughts on redshift and modern cosmology, 358-363, in R.L. Amoroso et al., The Physics of Reality: Space, Time, Matter, Cosmos, 504-509, New York: World Scientific.
[34] Amoroso, R.L (2013) Time? in R.L. Amoroso et al., The Physics of Reality: Space, Time, Matter, Cosmos, 504-509, New York: World Scientific.
[35] Amoroso, R.L (2013) "Shut The Front Door!": Obviating the challenge of large-scale extra dimensions and psychophysical bridging, 510-522, in R.L. Amoroso, L.H. Kauffman & P. Rowlnds (eds.) The Physics of Reality: Space, Time, Matter, Cosmos, 504-509, New York: World Scientific.
[36] Amoroso, R.L. (2012). Through the looking glass: Discovering the cosmology of mind with implications for medicine, psychology and spirituality, in I. Fredriksson (ed.) Aspects of Consciousness: Essays on Physics, Death and the Mind, 147, McFarland.
[37] Amoroso, R.L., & Rauscher, E.A. (2010) Empirical Protocol for Measuring Virtual Tachyon/Tardon Interactions in a Dirac Vacuum, in R.L. Amoroso et al. (eds.) AIP Conference Proceedings (Vol. 1316, p. 199).
[38] Kafatos, M. Roy, S. & Amoroso, R.L. (2000) Scaling in cosmology & the arrow of time, in R. Buccheri, V. Di Gesu & M. Saniga, (eds.) Studies on Time, Dordrecht: Kluwer Academic.
[39] Amoroso, R.L. (2004) The fundamental limit and origin of complexity in biological systems: A new model for the origin of life, in D.M. Dubois (ed.) Computing Anticipatory Systems, AIP Conf. Proceedings Vol. 718, pp. 144-159, Melville: American Inst. of Physics.
[40] Amoroso, R.L. (2002) Developing the cosmology of a continuous-state universe, in R.L. Amoroso, G. Hunter, M. Kafatos & J-P Vigier (eds.) Gravitation & Cosmology: From the Hubble Radius to the Planck Scale, Dordrecht: Kluwer Academic.
[41] Amoroso, R.L. (2005) Paradigm for a continuous-state holographic conscious multiverse, in R.L. Amoroso & B. Lehnert (eds.) Extending the Standard Model: Searching for Unity in Physics, Oakland: Noetic Press.
[42] Amoroso, R.L. (2009) Defining a context for the cosmology of awareness, in R.L. Amoroso (ed.) The Complementarity of Mind and Body: Realizing the Dream of Descartes, Einstein and Eccles,

[43] Amoroso, R.L. (2009) The physical origin of the principle of self-organization driving living systems, in R.L. Amoroso (ed.) The Complementarity of Mind and Body: Realizing the Dream of Descartes, Einstein and Eccles, New York: Nova Science Publishers.
[44] Amoroso, R.L., Kauffman, L.H. & Rowlands, P. (2013) The Physics of Reality: Space, Time, Matter, Cosmos, London: World Scientific Publishers.
[45] Amoroso, R.L. (1996) The production of Fröhlich and Bose-Einstein coherent states in in vitro paracrystaline oligomers using phase control laser interferometry, Bioelectrochem. & Bioenergetics, 41:1, pp. 39-42; http://vixra.org/pdf/1305.0106v1.pdf.
[46] Kaku, M. (1999) Introduction to Superstrings and M-Theory. Springer Verlag.
[47] Polchinski, J. (1998) String Theory (Vols. 1&2) Cambridge university press.
[48] Hübsch, T. (1992) Calabi-Yau Manifolds: A Bestiary for Physicists, Singapore: World Scientific.
[49] Bohm, D. (1963) Quantum Theory, pg. 353, Englewood Cliffs: Prentice-Hall.
[50] Bohm, D. & Vigier, J-P (1954) Model of the causal interpretation of quantum theory in terms of a fluid with irregular fluctuations, Phys. Rev. 96:1; 208-217.
[51] Holland, P.R. (1995) The Quantum Theory of Motion: An Account of the de Broglie-Bohm Causal Interpretation of Quantum Mechanics, Cambridge: Cambridge Univ. Press.
[52] Cramer, J.G. (1986). The transactional interpretation of quantum mechanics, Reviews of Modern Physics, 58(3), 647.
[53] Dirac, P.A.M. (1952) Is there an ether? Nature, 169: 172.
[54] Pettroni, N.C. & Vigier, J-P (1983) Dirac's aether in relativistic quantum mechanics, Foundations Phys., 13:2, 253-285.
[55] Vigier, J-P (1980) De Broglie Waves on Dirac Aether: A Testable Experimental Assumption, *Lettere. al Nuovo Cimento*, *29*; *467*-475.
[56] Feynman, R.P. (1986) Quantum mechanical computers, Found. Phys. 6: 507-531.
[57] Elitzur, A.C. & Vaidman, L. (1993) Quantum mechanical interaction-free measurements. Found. Phys. 23; 987-997.
[58] Kwiat, P., Weinfurter, H., Herzog, T., Zeilinger, A. & Kasevich, M. (1995) Interaction-free quantum measurements. Phys. Rev. Lett. 74, 4763-4766; Kwiat, P.G., Weinfurter, H., Herzog, T., Zeilinger, A. & Kasevich, M. (1995) Experimental realization of 'interaction-free' measurements, in D.M. Greenberger & A. Zelinger (eds.) Fundamental Problems in Quantum Theory, A Conference held in Honor of Professor John A. Wheeler, Annals of the New York Academy of Science, Vol. 755, p. 383, New York: New York Academy of Science.
[59] du Marchie Van Voorthuysen, E.H. (1996) Realization of an interaction-free measurement of the presence of an object in a light beam, Am. J. Phys. 64:12; 1504-1507; or arXiv:quant-ph/9803060 v2 26.
[60] Simon, S.H. & Platzman, P.M. (1999) Fundamental limit on "interaction free" measurements, arXiv:quant-ph/9905050v1.
[61] Vaidman, L. (1996) Interaction-free measurements, arXiv:quant-ph/9610033v1.
[62] Paraoanu, G.S. (2006) Interaction-free measurements with superconducting qubits, Physical Rev. Letters 97, (2006) 180406.
[63] Vaidman, L. (2001) The meaning of the interaction-free measurements arXiv:quant-ph/0103081v1.
[64] Vaidman, L. (2001) The paradoxes of the interaction-free measurements, arXiv:quant-ph/0102049v1.
[65] Vaidman, L. (2000) Are interaction-free measurements interaction free? arXiv:quant-ph/0006077v1.
[66] Helmer, F., Mariantoni, M., Solano, E. & Marquardt, F. (2008) Quantum Zeno effect in the quantum non-demolition detection of itinerant photons, arXiv:0712.1908v2.
[67] Facchi, P. Lidar, D.A. & Pascazio, S. (2004) Unification of dynamical decoupling and the quantum Zeno effect, Phys Rev A 69, 032314; or arxiv:quant-ph/0303132.
[68] Sudarshan, E.C.G. & Misra, B. (1977) The Zeno's paradox in quantum theory, J Mathematical Physics 18:4; 756–763.
[69] Facchi, P. & Pascazio, S. (2002) Quantum Zeno subspaces, arXiv:quant-ph/0201115v2.
[70] Kwiat, P.G. White, A.G., Mitchell, J.R., Nairz, O., Weihs, G. Weinfurter, H. & Zeilinger, A. (1999) High-efficiency quantum interrogation measurements via the quantum Zeno effect, Phys. Rev. Lett. 83, 4725-4728; or arXiv:quant-ph/9909083v1.
[71] Amoroso, R.L. (2010) (ed.) Complementarity of mind and body: Realizing the dream of Descartes. Einstein and Eccles, New York: Nova Science.
[72] Amoroso, R.L., & DiBiase, F. (2013) Crossing the psycho-physical bridge: Elucidating the objective character of experience, J Consc. Explor & Res.
[73] Allen, L. & Eberly, J.H. (1987) Optical Resonance and Two-Level Atoms, New York: Dover.
[74] Feynman, R.P. (1965) The Feynman Lectures on Physics: Vol. 3. Reading: Addison- Wesley.
[75] Kotigua, R.P. & Toffoli, T. (1998) Potential for computing in micromagnetics via topological conservation laws, Physica D, 120:1-2, pp. 139-161.
[76] Georgiev, L.S. (2006) Topologically protected gates for quantum computation with non-Abelian anyons in the Pfaffian quantum Hall state, Physical Review B, 74(23), 235112.
[77] Jiang, L., Brennen, G.K., Gorshkov, A.V., Hammerer, K., Hafezi, M., Demler, E., & Zoller, P. (2008) Anyonic interferometry and protected memories in atomic spin lattices, Nature Physics, 4(6), 482-488.
[78] Saeedi, K., Simmons, S., Salvail, J.Z., Dluhy, P., Riemann, H., Abrosimov, N.V., Becker, P., Pohl, H-V, Morton, J.J.L. & Thewalt, M.L.W. (2013) Room-temperature quantum bit storage exceeding 39 minutes using ionized donors in silicon-28, Science, Vol. 342, No. 6160, pp. 830-833.
[79] Benenti, G. & Strini, G. (2007) A bird's eye view of quantum computers, arXiv:quant-ph/0703105v1.
[80] Benenti, G., Casati, G., & Strini, G. (2004-2007), Principles of quantum computation and information, Vol. I: Basic

concepts; Vol. II: Basic tools and special topics, Singapore: World Scientific.
[81] Nielsen, M.A., & Chuang, I.L. (2000) Quantum Computation and Quantum Information, Cambridge: Cambridge University Press; Lloyd, S. (1996), Universal quantum simulators, Science 273, 1073.
[82] Lidar, D.A. & Wang, H. (1999) Calculating the thermal rate constant with exponential speedup on a quantum computer, Phys. Rev. E 59, 2429.
[83] Moore, G.E. (1965) Cramming more components onto integrated circuits, Electronics, 38, N. 8, April 19.
[84] Aspect, A. (1976) Proposed experiment to test the nonseparability of quantum mechanics, Phys. Rev. D 14, 1944.
[84] Ghirardi, G.C., Rimini, A., & Weber, T. (1986) Unified dynamics for microscopic and macroscopic systems, Phys. Rev. D 34, 470.
[86] Kieu, T.D. (2003) Computing the noncomputable, Contemporary Physics 44, 51.
[87] Amoroso, R.L., & Vigier, J-P (2013) Evidencing 'tight bound states' in the hydrogen atom: Empirical manipulation of large-scale XD in violation of QED, in R.L. Amoroso et al. (eds.) The Physics of Reality: Space, Time, Matter, Cosmos, pp. 254-272, Singapore: World Scientific.
[88] Amoroso, R.L. (2010) Simple resonance hierarchy for surmounting quantum uncertainty, in R.L. Amoroso, P. Rowlands & S. Jeffers (eds.) AIP Conference Proceedings-American Institute of Physics, Vol. 1316, No. 1, p. 185.
[89] Randall, L. (2005) Warped Passages, Unraveling the Mysteries of the Universe's Hidden Dimensions, New York: Harper-Collins.
[90] Amoroso, R.L. (2015) Yang-Mills Kaluza-Klein equivalence: An empirical path extending the standard model of particle physics, Address given at the International Conference on 60 Years of Yang-Mills Gauge Field Theories, 25-28 May 2015, IAS, Singapore; http://vixra.org/abs/1511.0257; video: https://onedrive.live.com/?authkey=%21APfM4hcl_Mcv8dk&cid=F94F1346F17EA060&id=F94F1346F17EA060%21158&parId=F94F1346F17EA060%21117&o=OneUp.
[91] Stern, A. (1992) Matrix logic and the Mind, a probe into a unified theory of mind and matter, Amsterdam: Northern-Holland.
[92] Stern, A. (2000) Quantum Theoretic Machines, New York: Elsevier Science.
[93] Gerlach, W & Stern, O. (1922) *Das magnetische moment des silberatoms, Zeitschrift Physik* 9, 353-355.
[94] Cramer, J.G. (2006) A transactional analysis of interaction-free measurements, Foundations of Physics Letters 19: 1; 63-73; or arXiv:quant-ph/0508102v23, 2008.
[95] Everett, H. (1957) Relative state formulation of quantum mechanics, Reviews of Modern Physics, Vol 29, pp 454-462.
[96] Holy Bible, King James Version.
[97] Amoroso, R.L. (2013) Empirical protocols for mediating long-range coherence in biological systems, J Consciousness Exploration & Research, Vol. 4, No. 9, pp. 955-976.
[98] Amoroso, R. L. (2015) Toward a pragmatic science of mind, Quantum Biosystems, 6(1), 99-114.
[99] Nagel, T. (1974) What's it like to be a bat? Philosophical Rev., 83, pp. 435-450.
[100] Witten, E. (1993) Quantum background independence In string theory, arXiv:hep-th/9306122v1.
[101] Stevens, H.H. (1989) Size of a least unit, in M. Kafatos (ed.) Bell's Theorem, Quantum Theory and Conceptions of the Universe, Dordrecht: Kluwer Academic.
[102] Kowalski, M. (1999) Photon Emission from Atomic Hydrogen, Physics Essays, Vol.12, 312-331.
[103] M. Kowalski (2000) The process of photon emission from atomic hydrogen, in Amoroso, R.L. et al. (eds.) From the Hubble Radius to the Planck Scale, Dordrecht: Kluwer Academic, pp. 207-220.
[104] Go to: www.Images.Google.com and type in "cootie Catcher" in the search box.
[105] Feynman, R.P. (1971) Lectures on Gravitation, Pasadena: California Inst. Technology.
[106] Dubois, D.M. (2001) Theory of incursive synchronization and application to the anticipation of delayed linear and nonlinear systems, in D.M. Dubois (ed.) Computing Anticipatory Systems: CASYS 2001, 5th Intl Conf., Am Inst of Physics: AIP Conf. Proceedings 627, pp. 182-195.
[107] Antippa, A.F. & Dubois, D.M. (2008) The synchronous hyperincursive discrete harmonic oscillator, in D. Dubois (ed.) proceedings of CASYS07, preprint.
[108] Dubois, D.M. (2008) The quantum potential and pulsating wave packet in the harmonic oscillator, in D. Dubois (ed.) proceedings of CASYS07, preprint.
[109] Antippa, A.F. & Dubois, D.M. (2004) Anticipation, orbital stability and energy conservation in discrete harmonic oscillators, in D.M. Dubois (ed.) Computing Anticipatory Systems, AIP Conf. Proceedings Vol. 718, pp.3-44, Melville: American Inst. of Physics.
[110] Dubois, D. (2016) Hyperincursive algorithms of classical harmonic oscillator applied to quantum harmonic oscillator separable into incursive oscillators, in R.L. amoroso, L.H. Kauffman, & p. Rowlands (eds.) Unified Field Mechanics: Natural Science Beyond the Veil of Spacetime, Hackensack: World Scientific.
[111] Cramer, J.G. (2005) The quantum handshake: A review of the transactional interpretation of quantum mechanics, Time-Symmetry in Quantum Mechanics Conference, Sydney 23 July 2005.
[112] Rowlands, P. (2007) Zero to Infinity: The Foundations of Physics. Singapore: World Scientific.
[113] Shipman, B. A. (2002) On the fixed-point sets of torus actions on flag manifolds. Journal of Algebra and Its Applications, 1(03), 255-265.
[114] Shipman, B. A. (1997). On the geometry of certain isospectral sets in the full Kostant–Toda lattice. pacific journal of mathematics, 181(1), 159-185.

[115] Shipman, B. A. (2000) The geometry of the full Kostant–Toda lattice of sl (4, C). Journal of Geometry and Physics, 33(3), 295-325.
[116] Child, M.S. (1991) Semiclassical Mechanics with Molecular Applications Oxford: Clarendon Press.
[117] Spigler, R. & Vianello, M (1998) A Survey on the Liouville-Green (WKB) approximation for linear difference equations of the second order, in S. Elaydi, I. Győri, & G.E. Ladas (eds.) Advances in Difference Equations: Proceedings of the 2nd Intl. Conf. on Difference Equations: Veszprém, Hungary, August 7–11, 1995, p. 567, CRC Press.
[118] Dasgupta, S., Papadimitriou, C.H. & Vazirani, U.V (2008) Algorithms, McGraw-Hill, New York.
[119] Rosenbaum, D. & Perkowski, M. (2010) Superposed quantum state initialization using disjoint prime implicants (SQUID), http://www.davidjrosenbaum.net/SQUID.pdf.
[120] Schulman, L.J. & Vazirani, M. (1999) Molecular scale heat engines and scalable quantum computation, STOC, ACM.
[121] Petta, J.R., Johnson, A.C., Taylor, J.M., Laird, E.A., Yacoby, A., Lukin, M.D., Marcus, C.M., Hanson, M.P. & Gossard, A.C. (2005) Coherent manipulation of coupled electron spins in semiconductor quantum dots, Science, 309, 2180-2184.
[122] Okamoto, H., Gourgout, A., Chang, C-Y, Onomitsu, K., Mahboob, I., Chang, Y. & Yamaguchi, H. (2013) Coherent phonon manipulation in coupled mechanical resonators, Nature Physics, 9, 480-484.
[123] *Bub, J. (1999) Interpreting the quantum world, revised ed., Cambridge: Cambridge University Press.*
[124] Holevo, A. (2011) Probabilistic and Statistical Aspects of Quantum Theory (2nd English ed.) Pisa: Edizioni della Normale.
[125] Zurek, W.H. & Wootters, W.K. (1982) A single quantum cannot be cloned, Nature Vol. 299 , 802.
[126] Dieks, D. (1982) Communication by EPR devices, Phys. Letters A 92 (6): 271-272.
[127] Herbert, N. (1982) FLASH- A superluminal communicator based upon a new kind of quantum measurement, Foundations of Physics, Vol. 12. No. 12.
[128] Lamas-Linares, A., Simon, C., Howell, J.C. & Bouwmeester, D. (2005) Experimental quantum cloning of single photons, arXiv:quant-ph/0205149.
[129] Barnum, H., Caves, C.M., Fuchs, C.A., Jozsa, R. & Schumacher, B. (1996) Noncommuting mixed states cannot be broadcast, arXiv:quant-ph/9511010v1.
[130] Chiribella, G., Yang, Y. & Yao, A.C-C (2013) Reliable quantum replication at the Heisenberg limit, arXiv:quant-ph/1304.2910v1.
[131] Amoroso, R.L., & Vigier, J-P (2002) The origin of cosmological redshift and CMBR as absorption/emission equilibrium in cavity-QED blackbody dynamics of the Dirac vacuum, in R.L. Amoroso, Hunter, G., Kafatos, M. & Vigier, J-P (eds.) Gravitation & Cosmology: From the Hubble Radius to the Planck Scale.
[132] Chantler, C.T. (2004) Discrepancies in quantum electro-dynamics, Radiation Physics and Chemistry, 71(3), 611-617.
[133] Chantler, C.T. et al. (2012) Testing three-body quantum electrodynamics with trapped Ti^{20} ions: evidence for a *Z*-dependent divergence between experiment and calculation, PRL 109, 153001.
[134] Dragic´, A. Maric´, Z. Vigier, J-P (2000) New quantum mechanical tight bound states and 'cold fusion' experiments, Physics Letters A: 265;163-167.
[135] Vigier, J-P (1993) New Hydrogen (Deuterium) Bohr Orbits, Proceedings ICCF4, Hawaii, Vol 4, p. 7.
[136] Bhabha, H.J., & Corben, H.C. (1941) General classical theory of spinning particles in a Maxwell field, Proceedings of the Royal Society of London Series A: Mathematical, Physical & Engineering Sciences, 178:974, 273-314.
[137] Barut, A.O. (1980) Surv. High Energy Phys. 1, 113.
[138] Rowlands, P. (2015) How many dimensions are there? in R.L. Amoroso et al. (eds.) Unified Field Mechanics: Natural Science Beyond the Veil of Spacetime, Proceedings of the IX Symposium Honoring Noted French Mathematical Physicist Jean-Pierre Vigier (p. 46) Singapore: World Scientific.
[139] Rowlands, P. (2013) Space and antispace, in R.L. Amoroso, P. Rowlands & L.H. Kauffman (eds.) Physics of Reality: Space, Time, Matter, Cosmos, London: World Sci.
[140] Abramowitz, M. & Stegun, I.A. (eds.) (1983) Handbook of Mathematical Functions with Formulas, Graphs, and Mathematical Tables. Applied Mathematics Series 55, National Bureau of Standards; New York: Dover.
[141] Gurarie, D. (2013) Bessel zoo and harmonic oscillator, http://www.cwru.edu/artsci/math/gurarie/classes/445/lecture/bessel.pdf.
[142] Dubois, D.M. (2016) Hyperincursive algorithms of classical harmonic oscillator applied to quantum harmonic oscillator separable into incursive oscillators, in R.L. Amoroso, L.H. Kauffman & P.Rowlands (eds.) Unified Field Mechanics: Natural Science Beyond the Veil of Spacetime, London: World Scientific.
[143] Scheid F. (1986) Theory and Problems of Numerical Analysis. McGraw-Hill.
[144] Riffee, D.M. (2013) Lecture notes, http://www.physics.usu.edu/riffe/3750/lecture_notes.htm.
[145] Bacon, D. (2006) CSE 599d - Quantum computing, the no-cloning theorem, classical teleportation and quantum teleportation, superdense coding, http://courses.cs.washington.edu/courses/cse599d/06wi/lecturenotes4.pdf

PART 5
New Classes of Quantum Algorithms

Quantum algorithm research and development remains in its infancy, because although a fair number of quantum gates and qubit technology platforms exist, it is safe to say that until an actual Universal Quantum Computer (UQC) implementation capable of bulk operation occurs, a complete conception of what sufficient quantum algorithms are seems unlikely; especially if much of the novel new parameters proposed in this monograph are required. Meaning for example, that the first bulk quantum computing system might in actuality be scalable, but there may be a dearth of quantum algorithms to implement sufficient quadratic speedup for practical utility beyond classical computing. We propose a new class of unified field mechanical (UFM) based holographic quantum algorithms with asymptotic speedup beyond the purely classical holographic reduction algorithmic process currently under development even to the point of a new class of instantaneous algorithms. There is recent talk of an end to locality and unitarity as a new basis for QC, along with the new field relativistic information processing (RIP); these scenarios may cause dramatic changes in QC research.

5.1 Introduction - From al-Khwarizmi to Unified Field-Gorhythms

The concept of 'Algorithm' reaches back to the creation of Arabic numerals in the 9th Century by Abu Jafar Muhammad ibn Musa al-Khwarizmi (Latin *Algoritmi*) and the methods of calculation utilizing them. He developed solutions to six varieties of linear and quadratic equations. His famous treatise on the subject, *Hisab al-jabr w'al-muqabala*, translated into Latin as *Liber algebrae et almucabala*, gave us the word 'algebra' [1,2]. The House of Wisdom at Baghdad during his lifetime was the Golden Age of Arabic science and mathematics.

In simplest terms, a classical algorithm is a finite sequence of instructions, step-by-step process or set of rules followed in calculations or other computed logical operations which always terminates. A quantum algorithm runs on a realistic model of quantum information processing, usually applied to algorithms that are inherently quantum using some essential feature of quantum computation such as quantum superposition or entanglement. The development of algorithms for simulating quantum mechanical systems was Feynman's original motivation for proposing a quantum computer [1]. Quantum algorithms require modules that are uniformly scalable and reversible (unitary) that can be efficiently implemented; the most commonly used model has been the quantum circuit model [3,4].

Generally, an algorithm is the procedure or set of instructions used to perform an information processing task. According to the strong Turing-Church thesis: Any algorithmic process can be simulated efficiently using a probabilistic Turing machine. Here, the word efficiently classifies algorithms into two main complexity classes - P and NP, where P is a polynomial type algorithm and NP the non-deterministic polynomial type algorithm. An algorithm is of the P-class if it has an 'efficient solution', meaning it runs in a polynomial time the size of the problem to be solved. An NP-class algorithm does not have an efficient solution or requires super-polynomial (usually exponential) time. For example, prime factorization of an integer is NP-type algorithm because no efficient solution is known for solving the problem. Deutsch first showed by a simple example the existence of an efficient QC solution for a classically classified NP problem [5]. In 1994, Shor demonstrated that prime factorization has an efficient solution in QC. But only a few NP-class problems can be solved efficiently with a QC [6]. Numerous NP-class problems exist for which no efficient algorithm is known even in QC. Although it is clear that P is a subset of NP, but whether P6 = NP or P = NP is still an unsolved puzzle to the QC research community [4].

In general, input to a quantum algorithm consists of n classical bits, and the output also consists of n classical bits. If the input is an n-bit string x, then the QC takes input as n qubits in state $|x\rangle$. Then a series of quantum operations are performed, at the end of which the state of the n qubits is transformed

to some superposition $\sum_y \alpha_y |y\rangle$. Afterwards, a measurement is made, which has as output the *n*-bit string *y* with probability $|\alpha_y|^2$ [4].

5.2 The Church-Turing Hypothesis

The Church-Turing thesis states that any function that can be computed by a physical system can be computed by a Turing Machine. Many mathematical functions cannot be computed on a Turing Machine such as the halting function $h:\mathbb{N}\to\{0,1\}$ that decides whether the i^{th} Turing Machine halts or the function that decides whether a multivariate polynomial has integer solutions. Therefore, the physical Church-Turing thesis is a strong statement of belief about the limits of both physics and computation. Some functions can be computed faster on a quantum computer than on a classical one, but, as noticed by Deutsch [5,7], this does not challenge the physical Church-Turing thesis itself: a QC could even be simulated by pen and paper, through matrix multiplications. Therefore, what they compute can be computed classically.

Several researchers have pointed out that Quantum theory does not forbid, in principle, that some evolutions would break the physical Church-Turing thesis [8-10]. Technically, the only limitation upon quantum evolution is that it be by unitary operators. Then, as Nielsen argues, it suffices to consider the unitary operator, $U=\sum |i,h(i)\oplus b\rangle\langle i,b|$, with *i* over integers and *b* over $\{0,1\}$, to have a counterexample [9].

The paradox between Deutsch's and Nielsen's arguments is only an apparent one as both are valid; the former applies specifically to Quantum Turing Machines and the latter to full-blown quantum theory. This is not satisfactory; if Quantum Turing Machines are to capture Quantum theory's computational power, it falls short, and needs amending. Unless in contrast, quantum theory itself needs to be amended, and its computational power brought down to the level of the Quantum Turing Machine [11,12]. Most likely quantum theory will be amended.

It was known very early on that quantum algorithms cannot compute functions that are not computable by classical computers, however they might be able to efficiently compute functions that are not efficiently computable on a classical computer [5]. This scenario may evolve also.

5.3 Algorithms Based on the Quantum Fourier Transform

The first QC algorithms were called the 'black-box or 'oracle' framework, where part of the input is a black-box implementing a function *f*(*x*). The only way to extract information about *f* was to evaluate it on the *x* inputs. These early algorithms used a special case of the quantum Fourier transform, the Hadamard gate. This allowed a problem to be solved with fewer black-box evaluations of *f* than a classical algorithm would need [12]. Deutsch [7] formulated the problem of deciding whether a function, $f:\{0,1\}\to\{0,1\}$ was constant. If one has access to a black-box implementing *f* reversibly by mapping $x,0\mapsto x,f(x);$ one further assumes that the black box does implement a unitary transformation U_f mapping $|x\rangle|0\rangle\mapsto|x\rangle|f(x)\rangle$. Deutsch's problem is to output "constant" if *f*(0) = *f*(1) and to output "balanced" if $f(0)\neq f(1)$, given a black-box for evaluating *f*. Thus, to determine $f(0)\oplus f(1)$ ($\oplus$ denotes addition modulo 2). Outcome '0' means *f* is constant and outcome '1' means *f* is not constant [12].

Classical algorithms would have to evaluate *f* twice to solve the problem. A quantum algorithm can only apply U_f once to produce

$$\frac{1}{\sqrt{2}}|0\rangle|f(0)\rangle+\frac{1}{\sqrt{2}}|1\rangle|f(1)\rangle. \tag{5.1}$$

With an end to the no-cloning theorem by UFM parameter based QC, another basis change will probably occur for QC development.

Under these conditions, if $f(0)=f(1)$, applying the Hadamard gate to the first register yields $|0\rangle$ with probability 1, and if $f(0)\neq f(1)$, then applying the Hadamard gate to the first register and ignoring the second register leaves the first register in the state $|1\rangle$ with probability 1/2; thus a result of $|1\rangle$ can only occur if $f(0)\neq f(1)$ [12].

Of special interest, given

$$\frac{1}{\sqrt{2}}|0\rangle|\psi_0\rangle+\frac{1}{\sqrt{2}}|1\rangle|\psi_1\rangle \tag{5.2}$$

a 'Hadamard test' can be performed if a Hadamard gate is applied to the first qubit. A measurement will give '0' with probability $\frac{1}{2}+\mathrm{Re}\left(\langle\psi_0|\psi_1\rangle\right)$ [12].

5.4 Exponential Speedup by Quantum Information Processing

The salient utility of UQC is the offering of algorithms that will provide a fully exponential speed-up over classical algorithms, making them the most sought after research avenue for unleashing the power of QCs. Let's follow the work of Aaronson for finding a general theorem for developing exponential speedups from quantum algorithms; in recent efforts he makes two advances toward such a theorem in the black-box model where most quantum algorithms operate [13].

- First, Aaronson shows for any problem invariant under permuting inputs and outputs that has sufficiently many outputs (like collision and element distinctness problems), the quantum query complexity is at least the 7th-root of classical randomized query complexity. Earlier he found a 9th-root [14], resolving a conjecture of Watrous [15].

- Second, inspired by work of O'Donnell [16] and Dinur [17], he conjectured that every bounded low-degree polynomial has a 'highly influential' variable. (A multivariate polynomial p is *bounded* if $0 \leq p(x) \leq 1$ for all x in the Boolean cube.) Assuming this conjecture, he then showed that every T-query quantum algorithm can be simulated on most inputs by a $TO(1)$-query classical algorithm. Essentially one cannot hope to prove P ≠ BQP relative to a random oracle.

> Perhaps the central lesson gleaned from fifteen years of quantum algorithms research is this: Quantum computers can offer superpolynomial speedups over classical computers, but only for certain "structured" problems. The key question, of course, is what we mean by "structured." In the context of most existing quantum algorithms, "structured" basically means that we are trying to determine some global property of an extremely long sequence of numbers, assuming that the sequence satisfies some global regularity [13].

Aaronson offers period finding as a canonical example, the core of Shor's factoring algorithms and computing discrete logarithms [18] where black-box access to exponentially-long sequences of integers $X=(x_1,\ldots,x_N)$ is given; that is, to compute x_i for a given i. We find the *period* of X, that is, the smallest $k>0$ such that $x_i=x_{i-k}$ for all $i>k$ with the promise that X is indeed periodic, with period $k \ll N$ (and that the x_i values are approximately distinct within each period). The requirement of periodicity is crucial: it lets us use the Quantum Fourier Transform to extract the information we want from a superposition of the form

$$\frac{1}{\sqrt{N}}\sum_{i=1}^{N}|i\rangle|x_i\rangle. \tag{5.3}$$

For other known quantum algorithms, X needs to be a cyclic shift of quadratic residues [19], or constant on the cosets of a hidden subgroup.

By contrast, the canonical example of an 'unstructured' problem is the Grover search problem. Black-box access is given to an N-bit string $(x_1,...,x_N)\in\{0,1\}^N$, and we are asked whether there exists an i such that $x_i = 1$. Grover formulated a quantum algorithm to solve this problem using $O(\sqrt{N})$ queries [20], as compared to the $\Omega(N)$ needed classically. However, Bennett et al. showed this quadratic speedup is optimal [21]. For other "unstructured" problems see [22-26].

This 'need for structure' limits prospects for super-polynomial quantum speedups to areas of mathematics likely to produce similar periodic sequences or sequences of quadratic residues. This is the fundamental reason why the greatest successes of quantum algorithm research have been cryptographic, specifically in number-theoretic cryptography. This helps to explain why there are no fast quantum algorithm to solve NP-complete problems, or to break arbitrary one-way functions [13,27].

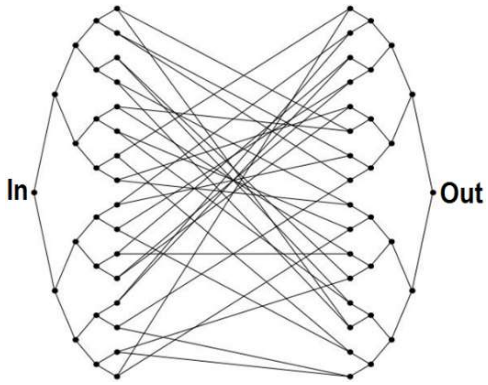

Fig. 5.1. Quantum walk algorithm graph. Figure adapted from [27].

Quantum walk algorithms can achieve provable exponential speedups over any classical algorithm (in query complexity), but according to Childs et al. only for extremely fine-tuned' graphs [27].

In the 20 years since the appearance of Shor's factoring algorithm only a few additional quantum algorithms like Grover's search and quantum walks have appeared. Aaronson claims that while there are a number of exponential and polynomial speedup algorithms, "*there just aren't that many compelling candidates left for exponential quantum speedups*" [28].

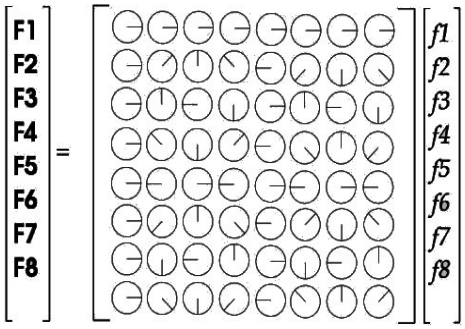

Fig. 5.2. Shor-like Fourier transform algorithms.

Factoring algorithms can break almost all public-key cryptosystems used today, but theoretical public-key systems exist that are unaffected, causing one to ask, '*Can Shor's algorithm be generalized to nonabelian groups?'* [28].

Grover-like algorithms provide Quadratic speedup for any problem involving searching an unordered list, provided the list elements can be queried in superposition. This implies subquadratic speedups for many other basic problems [21]. For black-box searching, the square root speedup of Grover's algorithm is the best possible approach [29-31].

It was shown, if a fast, classical exact simulation of boson sampling is possible, then the polynomial hierarchy collapses to the third level. Experimental demonstrations with 3-4 photons were achieved [29-31].

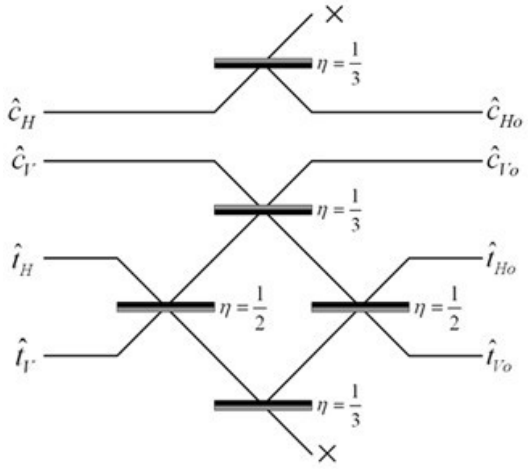

Fig. 5.3. Boson sampling algorithm. Identical single photons sent through network of interferometers, then measured at output modes. Figure adapted from [28].

5.5 Classical Holographic Reduction Algorithms

Yes, holographic algorithms (HA) already exist, a concept originated by Valiant in 2004 [32]. HA utilize a process called 'holographic reduction' mapping solution fragments 'many-to-many' so that the summation of solution fragments remains unchanged. Valiant coined the term HA because "*their effect can be viewed as that of producing interference patterns among the solution fragments*" [32]. The power of HA comes from the mutual cancellation of many contributions to a sum, analogous to the interference patterns in a hologram [33]. So far HA have discovered solutions to previously unsolved polynomial problems. Although HA have some similarities to quantum computation, they are currently completely classical in nature [34].

Holographic algorithms occur in the context of what is called Holant problems, which generalize counting Constraint Satisfaction Problems (#CSP). A #CSP example is the hypergraph G = (V,E) also called a constraint graph. Each hyperedge is a variable and each vertex, v is assigned a constraint, f_v. A vertex is connected to a hyperedge if the constraint on the vertex involves the variable on the hyperedge. The counting problem is to compute

$$\sum_{\sigma: E \to \{0,1\}} \prod_{v \in V} f_v \left(\sigma \middle| E_{(v)} \right), \tag{5.4}$$

which is a sum over all variable assignments, the product of every constraint, where the inputs to the constrain f_v are the variables on the incident hyperedges of v.

A Holant problem is similar to a #CSP except the input must be a graph, not a hypergraph. For a #CSP instance, one replaces each hyperedge, *e* of size, *s* with a vertex, *v* of degree, *s* with edges incident to the vertices contained in *e*. The constraint on *v* is the equality function of *s* identifying all the variables on the edges incident to *v*. For Holant problems, Eq. 5.4 is called the Holant after a related exponential sum introduced by Valiant [35]. To further clarify, Holant is a framework of counting characterized by local constraints. It is closely related to other well-studied frameworks such as #CSP and Graph Homomorphism. An e dichotomy for such frameworks can immediately settle the complexity of all combinatorial problems expressible in that framework. Both #CSP and Graph Homomorphism can be viewed as sub-families of Holant with the additional assumption that the equality constraints are always available [35].

Considering holographic reduction, for a bipartite graph G = (U,V,E} the constraint assigned to each vertex $u \in U$ is f_u, likewise for vertex $v \in V$ is f_v. This counting problem is $\text{Holant}(G, f_u, f_v)$. Thus for a complex 2 x 2 invertible matrix T, there is a holographic reduction between $\text{Holant}(G, f_u, f_v)$ and $\text{Holant}(G, f_u, T^{\otimes(\deg u)}, (T^{-1})^{\otimes(\deg v)} f_v)$. Thus, $\text{Holant}(G, f_u, f_v)$ and $\text{Holant}(G, f_u, T^{\otimes(\deg u)}, (T^{-1})^{\otimes(\deg v)} f_v)$ have precisely the same Holant value for all constraint graphs, essentially defining the same counting problem, which can also be proved using holographic reduction. Valiant's original application of holographic algorithms used holographic reduction which has since been used in polynomial time algorithms and proofs of #P-hardness [36].

5.6 Ontological-Phase UFM Holographic Algorithms

> To try to stop all attempts to pass beyond the present viewpoint of quantum physics could be very dangerous for the progress of science and would furthermore be contrary to the lessons we may learn from the history of science. This teaches us, in effect, that the actual state of our knowledge is always provisional and that there must be, beyond what is actually known, immense new regions to discover – de Broglie [37].

A fundamental theory is needed which would tell us from first principles when quantum speedups are possible. There is a related longstanding open problem: Is there any Boolean function with a quantum quantum/classical gap better than quadratic? A Boolian function, *f* is simply

$$f : \{0,1\}^n \to \{0,1\} \tag{5.5}$$

with n input bits and a single output bit [4]. We will answer yes below.

There are new results from Ben-David: If $F : S_N \to \{0,1\}$ is any Boolean function of permutations, then D(F) = O(Q(F)^{12}). If F is any function with a symmetric *promise*, and at most M possible results of each query, then R(F) = O(Q(F)$^{12(M-1)}$) [38]. We need a 'structured' promise if we want an exponential quantum speedup. Exponential quantum speedups depend on structure. For example, abelian group structure, glued-trees structure, or relational structure…

The term Semiclassical in common usage means: intermediate between a classical Newtonian description and one based on quantum mechanics or relativity. Semiclassical physics, refers to a theory in which one part of a system is described quantum-mechanically whereas the other is treated classically. For example, external fields will be constant, or when changing will be classically described. In general, it incorporates a development in powers of Planck's constant, resulting in the classical physics of power 0, and the first nontrivial approximation to the power of (−1). In this case, there is a clear link between the quantum mechanical system and the associated semi-classical and classical approximations.

Now for UFM, we create a new term, semi-quantum where one part will be quantum and the other part UFM. This is a small regime of finite radius called the Manifold of Uncertainty (MOU). This is the 1st step in the realization that the central pillars of quantum field theory, spacetime, locality and unitarity

are to be superseded. In assuming the universe is a huge information processor, in terms of unitarity and locality (phenomenal) each distinct point is like a central processing unit (CPU), but in the move to nonlocality and holographic (ontological) ballistic processing, there is no CPU; there is a simultaneity of information at each tessellated node. Clearly, I am trying to say this scenario is not classical or quantum, but a unified field mechanical ontology. It is hard to fathom what kind of algorithm, from a new class of holographic ontological algorithms able to operate without decohering the wavefunction, this leads to.

Creative thinking has already begun to skirt this empyrean realm:

> *All we experience is nothing but a holographic projection of processes taking place on some distant surface that surrounds us.* - Brian Greene

> *Discovery of the amplituhedron could cause an even more profound shift … That is, giving up space and time as fundamental constituents of nature and figuring out how the … universe arose out of pure geometry … In a sense, we would see that change arises from the structure of the object, but it's not from the object changing. The object is basically timeless.* - Nima Arkani-Hamed

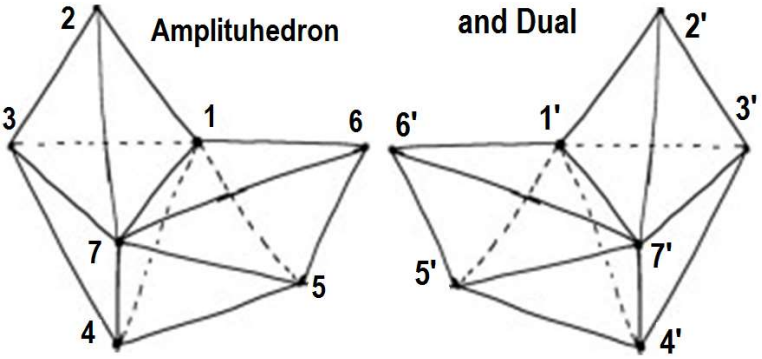

Fig. 5.4. 7-point Amplituhedron in P^3 with Amplitude for $\left[1^-2^+3^+4^+5^+6^+7^-8^-\right]$ and its dual. The Hubble sphere, H_R may be one huge geometric Amplituhedron.

Figure 5.4 is a sketch of the basic amplituhedron element, $A_{n,k,L;m}$ which lives in $G(k,k+m;L)$, the space of *k*-planes *Y* in *k* + *m* dimensions, together with *L* 2-planes L1, … ,LL in the m-dimensional compliment of Y [41], representing an 8-gluon particle interaction using Feynman diagrams. The amplituhedron is a newly discovered mathematical object resembling a multifaceted jewel in HD. Encoded in its volume are the most basic features of reality that can be calculated - the probabilities of outcomes of particle interactions. This, or a similar geometric object, could help remove two deeply rooted physical principles: locality and unitarity from quantum field theories' basic assumptions [39-41].

> The amplitude form is positive when evaluated inside the amplituhedron. The statement is sensibly formulated thanks to the natural 'bosonization' of the superamplitude associated with the amplituhedron geometry. However, this positivity is not manifest in any of the current approaches to scattering amplitudes, and in particular not in the cellulations of the amplituhedron related to on-shell diagrams and the positive Grassmannian. The surprising positivity of the form suggests the existence of a 'dual amplituhedron' formulation where this feature would be made obvious [41].

Locality is the idea that particles can interact only from adjoining positions in space and time, and unitarity states that the probabilities of all possible outcomes of a quantum mechanical interaction must add up to one. The amplituhedron is not built out of spacetime and probabilities; these properties merely arise as consequences of the jewel's geometry. The usual picture of space and time, with particles moving around in them, is a construct. "*Locality and unitarity emerge hand-in-hand from the positive geometry of the amplituhedron*" [39-41]. What is beyond the end to locality and unitarity as we know it?

In a confoundingly humorous parody Scott Aaronson has this to say about the amplituhedron:

> My colleagues and I have been investigating a mathematical structure that contains the amplituhedron, yet is even richer and more remarkable. I call this structure the 'unitarihedron'…The unitarihedron encompasses, within a single abstract 'jewel,' all the computations that can ever be feasibly performed by means of unitary transformations, the central operation in quantum mechanics (hence the name). Mathematically, the unitarihedron is an infinite discrete space: more precisely, it's an infinite collection of infinite sets, which collection can be organized (as can every set that it contains!) in a recursive, fractal structure. Remarkably, each and every specific problem that quantum computers can solve - such as factoring large integers, discrete logarithms, and more - occurs as just a single element, or 'facet' if you will, of this vast infinite jewel. By studying these facets, my colleagues and I have slowly pieced together a tentative picture of the elusive unitarihedron itself [42]. – Scott Aaronson.

Aaronson's parody is of course justified, especially at this stage of development. The QC paradigm until now has been local and semiclassical. Aaronson himself said, '*UQC will require a new discovery in physics*'. Our *hypothesis non fingo* is that this putative discovery in physics is in fact a Gödelization beyond quantum mechanics (unitarity and locality) into the 3rd regime of reality dubbed UFM. We have seen that holographic computing algorithms are classical; we are not just looking for a quantum holography (already exists in NMR spectroscopy), we are proposing a special new class of UFM algorithms. In the course of preparing this volume our opinion on this matter has evolved. We thought that the existing body of QC research would suffice; and what we had to add to the mix was ontological measurement without collapse and violation of the no-cloning theorem. We hope it is obvious that opinion has changed. If one has the stamina to read this whole volume, one sees we expend a lot of effort skirting around issues without doing much of the math. This is our excuse; NASA flew around the moon a couple times before actually landing on it.

Since the framework of quantum mechanics seems to rest on unitarity, most physicists will tend to look for possible ways to get around such a drastic modification. In quantum physics, unitarity is a restriction on the allowed evolution of quantum systems that ensures the sum of probabilities of all possible outcomes of any event is always 1.

Giving up space and time as fundamental constituents of nature and figuring out how the cosmological evolution of the universe arose out of pure geometry is a fascinating opportunity. In a sense, we would see that change arises from the structure of the object. But it's not from the object changing. The object is basically timeless. The revelation that particle interactions, the most basic events in nature, may be consequences of geometry significantly advances a decades-long effort to reformulate quantum field theory, describing elementary particles and their interactions. Interactions that were previously calculated with mathematical formulas thousands of terms long can now be described by computing the volume of the corresponding jewel-like 'amplituhedron,' which yields an equivalent one-term expression [39-41].

In the quantum world probabilities were expressed as complex numbers, with both a quantity and a phase, and these so-called amplitudes were squared to produce probability. This was the mathematical procedure necessary to capture the wavelike aspects of particle behavior. Probability amplitudes were normally associated with the likelihood of a particle's arriving at a certain place at a certain time [43]. Feynman said he would associate the probability amplitude *'with an entire motion of a particle'-with a path*. He stated the central principle of quantum mechanics: '*The probability of an event which can happen in several different ways is the absolute square of the sum of complex contributions, one from each alternative way*'. These complex numbers, amplitudes, were written in terms of classical action; Feynman showed how to calculate the action for each path as a certain integral [44-55].

5.7 The Superimplicate Order and Instantaneous UQC Algorithms

Who might have guessed there might be a class of QC algorithms better than polynomial and exponential speed QIP. Let's take a peek at the basis for possible instantaneous algorithms. It is generally known that information passes instantaneously in systems of EPR correlated photons. We

know how to parametric down-convert entangled EPR pairs; what if we can learn parametric up-conversion utilizing the tenets of UFM?

Following Bohm, we assume a field, $\phi(x,t)$ will take the form of a wavepacket, $\alpha_c F_c(x,t) + \alpha_s F_s(x,t)$ with α_c, α_s real and positive proportionality factors; then functions, $\Gamma(x,t)$ orthogonal to $F_c(x,t)$ and $F_s(x,t)$ will have no effect on the factor in front of Ψ_0, meaning their variation will be the same as in the ground state. Thus chaotic variation of the field will be modified by statistical tendencies to change around an average form of the wavepacket,

$$\Psi = \sum_k{}' f_k q_k \Psi_0 . \tag{5.6}$$

In (5.6) the sum is over all k and no restriction made that $f_{-k} = f_k^*$ because the wave function is complex even though $f_{(x)}$ is real. Considering $q_{-k} = q_k^*$ we write

$$\Psi = \sum_k{}' \left[f_k q_k + f_{-k} q_k^* \right] \Psi_0 \tag{5.7}$$

where $\sum_k{}'$ indicates summation over a suitable half of the total set of k values. With the assumption in (5.7) that the space average of the field, $f_0 = 0$ we write

$$\Psi = \sum_k{}' f_k q_k \exp\left[-ikt\right] \Psi_0 . \tag{5.8}$$

Then write $g = \sum_k{}' f_k q_k \exp\left[-ikt\right]$, giving $R = \sqrt{\Psi^* \Psi} = \sqrt{g g^*}\,\Psi_0$ [37].

According to Bohm, inside this wave packet the super-quantum potential introduces nonlocal connections between fields at different points separated by a finite distance (unlike ground state). Now we write the quantum potential as

$$Q = -\sum_k{}' \frac{\partial^2 R}{\partial q_k^* \partial q_k} / R. \tag{5.9}$$

Now we evaluate the quantum potential change from the ground state,

$$\Delta Q = -\frac{1}{4} \sum_k{}' \frac{f_k f_k^*}{g^* g} + \frac{1}{2} \sum_k{}' \frac{k f_k q_k \exp\left[-ikt\right]}{g} + c.c. \tag{5.10}$$

For a wave packet with only a small range of wave vectors, the factor, k on the right reduces to the fixed number, k_0, while the remaining factors reduce to unity. This term varies with time, but we are only interested in the wave packets for which the spread of k makes negligible contributions. But when the q_k are expressed in terms of $\phi(x)$ as in

$$q_k = 1/\sqrt{V}\int \exp\left[-ik\cdot x\right]\phi(x)dV \tag{5.11}$$

the quantum potential reduces to

$$\Delta Q = \frac{1}{4}\sum_k{}' \frac{f_k f_k^*}{\sqrt{\int F(x,t)\phi(x)dV}\sqrt{\int F^*(x',t)\phi(x')dV'}}. \tag{5.12}$$

It should be obvious the term implies nonlocal interaction between $\phi(x)$ at one point and $\phi(x')$ at other points where the integrand is substantial. Writing $Q = \Delta Q + Q_0,$ with Q_0 the quantum potential of the ground state as given in

$$\Psi_0 = \exp\left[-\iint \phi(x)\phi(x')f(x'-x)dVdV'\right] \tag{5.13}$$

as taken from (5.11) with the t coordinate suppressed and where $f(x'-x) = 1/V\sum_k{}' k\exp\left[ik\cdot\le(x'-x)\right]$, we can write the field equation

$$\frac{\partial^2\phi}{\partial t^2} = \nabla^2\phi - \frac{\delta Q}{\delta\phi} \tag{5.14}$$

as

$$\frac{\partial^2\phi}{\partial t^2} = \nabla^2\phi - \frac{\delta\Delta Q}{\delta\phi} - \frac{\delta Q_0}{\delta\phi}. \tag{5.15}$$

Using (5.13) and expressing Q in terms of $\phi(x)$ by Fourier analysis Bohm obtains, [37]

$$\frac{\partial^2\phi}{\partial t^2} = \frac{1}{8}\left(\sum_k{}' f_k f_k^*\right)\times \frac{f_k f_k^*}{\left(\int F(x,t)\phi(x)dV\right)^{3/2}\left(\int F^*(x',t)\phi(x')dV'\right)^{1/2}} + c.c. \tag{5.16}$$

Remember from the ground state, the field is static because the effect of the quantum potential cancels out the Laplacian, $\nabla^2\phi$ in the field equation. ∇^2 is the Laplacian or divergence of the gradient of a function, $\Delta f(p)$ on a point, p in Euclidean space. Now with (5.16) in the excited state there is an additional term causing the wavepacket to move, and as happens with the quantum potential, the field equation is nonlocal and nonlinear [37].

The point we have been building up to in this section, is that the nonlocality represents an instantaneous connection of the field at different points in space. However, as Bohm reminds us, this is significant only over the extent of the wavepacket. In the usual interpretation, the spread of the wavepacket applies to a region within which, according to the uncertainty principle, nothing whatsoever can be said regarding what is happening. Therefore, the de Broglie-Bohm-Vigier causal interpretation [56] attributes nonlocality only to situations in which the usual interpretation cannot attribute well-defined properties [37].

It is of key importance to note that a wavefunction of the form $\Psi = q_k \exp\left[-ikt\right]\Psi_0$ does not correspond to the usual picture of an oscillation. This is shown by (5.16) because the term $\nabla^2\phi$ is absent. This result follows because stationary wavefunctions usually correspond to static situations contradicting intuitive expectations of a dynamic state of motion [37].

But Bohm was only thinking from a 4D Standard Model perspective, in terms of an amplituhedronic-type (volume) for a Wheeler-DeWitt wavefunction of the universe, $H\Psi = 0$ instantaneous EPR-holographic algorithms should prove possible with sufficient UFM insight.

When considered in terms of our UFM brane topological additions to the structure of matter and Bohm's superimplicate order, full utility of nonlocal information as hinted by EPR correlations hints at the possibility of instantaneous algorithms.

5.8 Some Ontological-Phase Geometric Topology

The simplest example of ontological-phase eversion is in the transformation of the ambiguous vertices of the Necker cube. The form of a cube by itself is not oriented; any set diagonal pairs could apply to eversion. With 6 faces and 4 vertex positions each, this gives 24 possible directed orientations; the important point is that the phase eversion must be directed by the topological charge of the unified field.

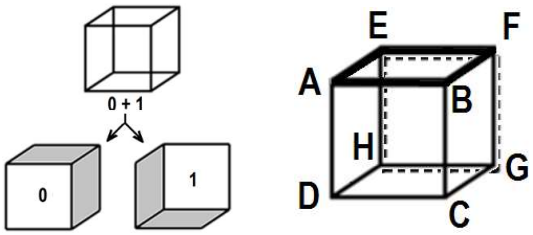

Fig. 5.5 a) The two ontological states of the ambiguous or Necker cube, 0 and 1. b) Vertices and ambiguous vertices labeled. Solid lines (B) front, dashed lines (H) rear.

With the 8 vertices labeled and 25 orientations, steps to create an algebra to describe rotations or dual-morphic projections can be taken. In Fig. 5.5a there is no distinction between as to whether 0 or 1 represents the front or rear face. This is called the Topology of Ambiguity.

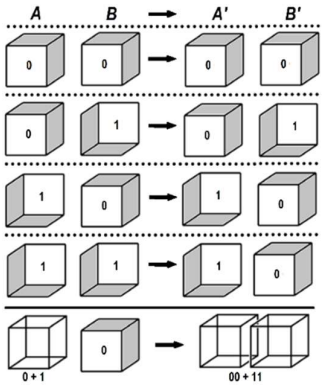

Fig. 5.6 Ambiguous truth table, showing how holographic r-qubits might be built up.

Ambiguous geometric/topology is the most rudimentary indicia of ontological information processing. For instantaneity to occur each point (no longer a point but structure beyond in nonlocality) must be a

ballistic processor. In simplest form evolution is governed by a Bohmian super-quantum potential or force of coherence of the unified field, $F_{(N)} = \aleph / \rho$, where $\aleph$ is UFM topological charge, and ρ the radius of action.

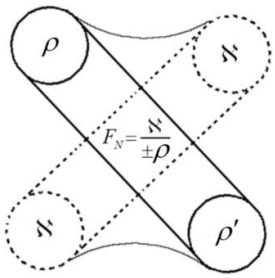

Fig. 5.7. Topological geometry of an isolated LCU described by the UFM equation. The center might be one oscillating L-R static-dynamic 'Casimirror' half producing the knotted shadow fermion vertex in an *x,y* plane in 3-space.

The quaternions, *H*, are a 4D algebra with basis 1,*i,j,k*. To describe the product, we could give a multiplication table, but it is easier to remember that:

- 1 is the multiplicative identity, *i,j*,
- and *k* are square roots of -1,
- we have *ij* = *k, ji* = -*k*, and all identities obtained from these by cyclic permutations of (*i,j,k*) [57].

The last rule is summarized in Fig. 5.8. below:

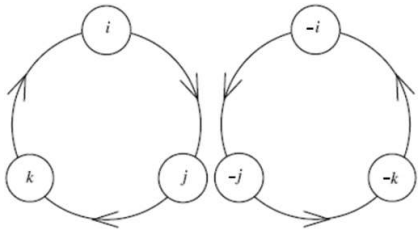

Fig. 5.8. Clockwise counterclockwise cyclicality of the quaternion algebra.

When we multiply two elements going clockwise around the circle we get the next one: for example, *ij* = *k*. But when we multiply two going around counterclockwise, we get *minus* the next one: for example, *ji* = -*k*.
We can use the same sort of picture to remember how to multiply octonions:

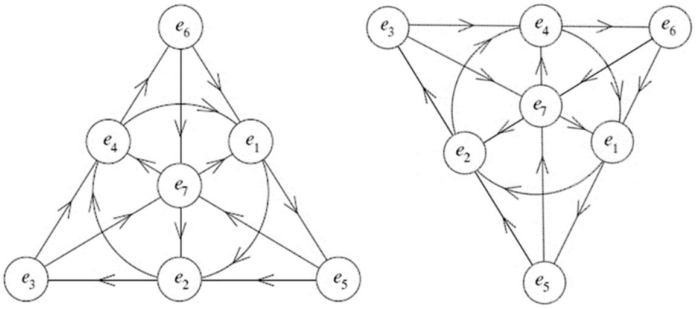

Fig. 5.9. The Fano plane, a) Graph showing the cyclic relationship of the Octonions. b) Index doubling by rotating the Fano plane 1/3 of a turn.

The Fano plane (Fig. 5.9), a graphic with 7 lines and 7 points, completely describes the algebraic structure of the octonions, and the central circle describes the quaternions. The 'lines' are the sides and altitudes of the triangle, and the central circle contains all the midpoints of the sides. Each pair of distinct points lies on a unique line. Each line contains three points, and each of these triples has a cyclic ordering shown by the arrows. Index-doubling corresponds to rotating the plane 1/3 of a turn (right). If $e_i, e_j,$ and e_k are cyclically ordered in this way then $e_i e_j, = e_k$, $e_j e_i, = -e_k$. Together with these rules:

- 1 is the multiplicative identity,
- $e_1,\ldots,e_7$ are all square roots of -1 [57].

Can we go deeper? The Fano plane is the projective plane over the 2-element field $\mathbb{Z}_2$. In other words, it consists of lines through the origin in the vector space $\mathbb{Z}_2^3$. Since every such line contains a single nonzero element, we can also think of the Fano plane as consisting of the seven nonzero elements of $\mathbb{Z}_2^3$. If we think of the origin in $\mathbb{Z}_2^3$ as corresponding to $1 \in O$, we get the following picture of the octonions:

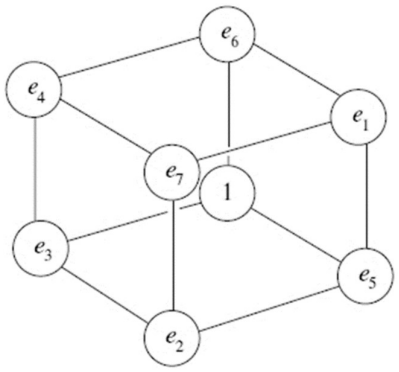

Fig. 5.10. Octonions subalgebras.

Planes through the origin of this 3D vector space give subalgebras of O isomorphic to the quaternions, lines through the origin give subalgebras isomorphic to the complex numbers, and the origin itself gives a subalgebra isomorphic to the real numbers. This is a description of the octonions as a 'twisted group algebra'. Given any group G, the group algebra $\mathbb{R}[G]$ consists of all finite formal linear combinations of elements of G with real coefficients. This is an associative algebra with the product coming from that of G. We can use any function $\alpha : G^2 \to \{\pm 1\}$ to 'twist' this product, defining a new product $* : \mathbb{R}[G] \times \mathbb{R}[G] \to \mathbb{R}[G]$ by $g * h = \alpha(g,h)\, gh,$ where $g, h \in G \subset \mathbb{R}[G].$ One can figure out an equation involving α that guarantees this new product will be associative. In this case we call α a '2-cocycle'. If α satisfies a certain extra equation, the product $*$ will also be commutative, and we call α a 'stable 2-cocycle' [57].

For example, the group algebra $\mathbb{R}[Z_2]$ is isomorphic to a product of 2 copies of $\mathbb{R}$, but we can twist it by a stable 2-cocyle to obtain the complex numbers. The group algebra $\mathbb{R}\left[Z_2^2\right]$ is isomorphic to a product of 4 copies of $\mathbb{R}$, but we can twist it by a 2-cocycle to obtain the quaternions. Similarly, the group algebra $\mathbb{R}\left[Z_2^3\right]$ is a product of 8 copies of $\mathbb{R}$, and what we have really done in this section is describe a function α that allows us to twist this group algebra to obtain the octonions. Since the octonions are nonassociative, this function is not a 2-cocycle. However, its coboundary is a 'stable 3-

cocycle', which allows one to define a new associator and braiding for the category of $\mathbb{R}\left[Z_2^2\right]$-graded vector spaces, making it into a symmetric monoidal category [58]. In this symmetric monoidal category, the octonions are a commutative monoid object. In less technical terms: this category provides a context in which the octonions are both commutative and associative [57].

Figure 5.11 is an adaptation of the Fano plane with many more degrees of freedom. Notice that the so-called Fano snowflakes involute into a 3-cube. The Fano snowflake graph also makes use of the 8th Necker ambiguous point. The central quaternionic cycle may also progress clockwise or counter-clockwise. Thus with rotations, mirror reflections, dimensional reduction and expansion of the Necker double covering point and other topological moves, there are sufficient degrees of freedom for ballistically programming a nonlocal class of instantaneous UFM QIP algorithms. We would like to name the full set of moves - Ontological-phase eversion cycles.

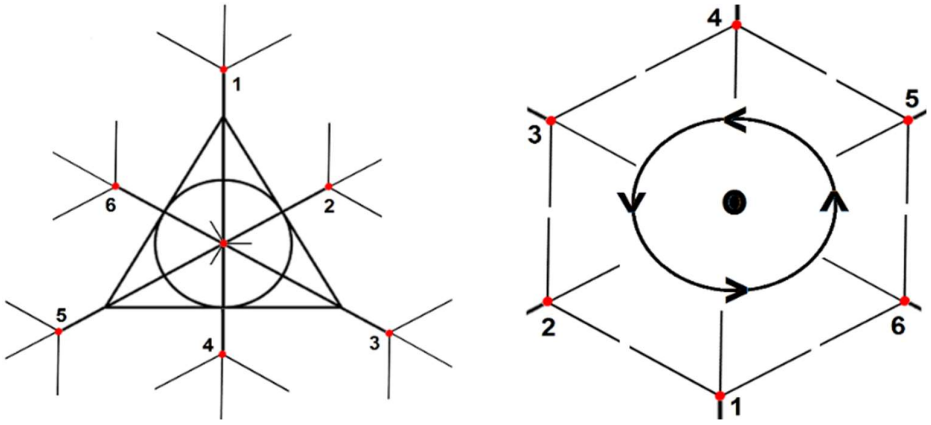

Fig. 5.11. a) Six snowflakes on the rim of fano plane. b) Notice that that the 6 snowflakes involute to form a 3-cube which also contains the dual projection $\left(+\omega,-\omega\right)$ double covering point of the ambiguous Necker cube.

5.9 Summation

I recall a critic of Aaronson's Unitarihedron parody blog of the Amplituhedron calling Aaronson's Unitarihedron a diaperhedron! There is always risk when a 'bear'goes over the mountain '*to see what he could see'* as the old nursery song goes. I still remember vividly Tom Toffoli chastising Vlasov a young Russian postdoc at the time at Physcomp96 regarding his paper putting forth a relativistic qubit; now 20 years later, finally, there is more and more talk of r-qubits and a new field of relativistic information processing is well under way. In any case there is no need for us to 'shut up' because we have 'put up' viable protocols, much simpler and more revealing than those being processed by the CERN LHC.

Now here's the rub; let's consider a general case of n = 500 electron qubits in a linear superposition of all 2^{500} possible classical states, much larger than the number of particles estimated in the classical universe (10^{80}):

$$\sum_{x\in\{0,1\}^n} \alpha_x \left|x\right\rangle. \tag{5.17}$$

This exponentially huge superposition is 'the private world' of the electrons involved and measurement only allows us to find the n bits (500) of information, $\left|\alpha_x\right|^2$. If our UFM model proves successful in

surmounting uncertainty, then measurement does not change the system leaving all 2^{500} possible superposed states intact. This also leads to violation of the no-cloning theorem.

I remember a quote by Feynman or Kip Thorne, (I forget which) 'to be the 1st person on Earth to discover a new principle'. That's the great fun of doing physics; enjoy a tiny moment before the hordes mass. I have to admit, 'ontological-phase eversion cycles for instantaneous algorithms', puts a spread of jam on my toast. I remember what noted Stanford neuroscientist (holographic brain) said to me once while we were watching a sunset by the ocean in Long Beach, CA USA arguing about how many images there were of the sun on the water surface, "*aren't we all in this together*?". Technological evolution continues to move asymptotically faster, 150 years for acceptance of Copernicus' revolutions, 15 years to perform Einstein's simple photoelectric effect experiment (after he was called an idiot and moron to his face). Any chance of getting one of the experiments proposed herein performed in 1.5 years? That would be about 2018… UQC could be that close if 'angel investors' appear in the midst.

References

[1] Chabert, J.L. (1999) A History of Algorithms: From the Pebble to the Microchip, Berlin: Springer-Verlag.
[2] Berlinski, D. (2001) The Advent of the Algorithm: The 300-Year Journey from an Idea to the Computer, Fort Washington: Harvest Books.
[3] Alsuwaiyel, M.H. (2010) Algorithms: Design Techniques and Analysis, Singapore: World Scientific.
[4] Nielsen, M.A. & Chuang, I.L. (2004) Quantum Computation and Quantum Information, Cambridge: Camb. Univ. Press.
[5] Deutsch, D. (1985) Quantum theory, the Church-Turing principle and the universal quantum computer, Proceedings of the Royal Society of London A, V. 400, pp. 97-117.
[6] Shor, P.W. (1994) Algorithms for quantum computation: Discrete logarithms and factoring, Foundations of Computer Science, 1994 Proceedings., 35th Annual Symposium, pp. 124-134, IEEE.
[7] Deutsch, D. (1989) Quantum computational networks, Proceedings of the Royal Society of London A: Mathematical, Physical and Engineering Sciences (Vol. 425,
No. 1868, pp. 73-90).
[8] Gu, M., Weedbrook, C., Perales, A. & Nielsen, M.A. (2009) More really is different, Physica D: Nonlinear Phenomena, 238 (9-10): 835-839.
[9] Kieu. T.D. (2003) Computing the non-computable, Contemp. Physics, 44(1):51-71.
[10] Nielsen, M.A. (1997) Computable functions, quantum measurements, and quantum dynamics, Phys. Rev. Lett., 79 (15): 2915-2918.
[11] Arrighi, P. & Dowek, G. (2011) The physical Church-Turing thesis and the principles of quantum theory, arXiv:1102.1612v1 [quant-ph].
[12] Smith, J. & Mosca, M. (2010) Algorithms for quantum computers, arXiv:1001.0767v2 [quant-ph].
[13] Aaronson, S. & Ambainis, A. (2014) The need for structure in quantum speedups, Theory of Computing, V. 10 (6), pp. 133-166; http://theoryofcomputing.org/articles/
v010a006/v010a006.pdf.
[14] Aaronson, S. & Ambainis, A. (2011) The need for structure in quantum speedups, Proc. 2nd Innovations in Computer Science Conference (ICS'11) pp. 338-352, Tsinghua, [arXiv:0911.0996] 138, 140.
[15] Watrous, J. (2002) Limits on the power of quantum statistical zero-knowledge, Proceedings of the 43rd Annual IEEE Symposium on Foundations of Computer Science, pp. 459-468.
[16] O'donnell, R., Saks, M.E., Schramm, O. & Servedio, R.A. (2005) Every decision tree has an influential variable, Proc. 46th FOCS, pp. 31-39. IEEE Comp. Soc. Press.
[17] Dinur, I., Friedgut, E., Kindler, G. & O'donnell, R. (2007) On the Fourier tails of bounded functions over the discrete cube, Israel J. Math., 160 (1):389-412; Preliminary version in STOC'06.
[18] Shor, P.W. (1999) Polynomial-time algorithms for prime factorization and discrete logarithms on a quantum computer, SIAM review, 41(2), 303-332.
[19] Van Dam, W., Hallgren, S. & Lawrence, I.P. (2006) Quantum algorithms for some hidden shift problems, SIAM J. Comput., 36 (3): 763-778.
[20] Grover, L.K. (1996) A fast quantum mechanical algorithm for database search, in Proc. 28th STOC, pp. 212-219, ACM Press.
[21] Bennett, C.H., Bernstein, E., Brassard, G. & Vazirani, U.V. (1997) Strengths and weakensses of quantum computing, SIAM J. Comput., 26 (5): 1510-1523.
[22] Beals, R., Buhrman, H., Cleve, R., Mosca, M. & De Wolf, R. (2001) Quantum lower bounds by polynomials, J. ACM, 48 (4): 778-797.
[23] Ambainis, A. & De Wolf, R. (2001) Average-case quantum query complexity, Journal of Physics A: Mathematical and General, 34 (35): 6741.

[24] Szegedy, M. (2004) Quantum speed-up of Markov chain based algorithms, in FOCS '04: Proceedings of the 45th Annual IEEE Symposium on Foundations of Computer Science, pp. 32-41, IEEE Computer Society, Washington, DC.
[25] Bhaskar, M.K., Hadfield, S., Papageorgiou, A. & Petras, I. (2015) Quantum algorithms and circuits for scientific computing, arXiv:1511.08253v1 [quant-ph].
[26] Cockshott, W.P. & Mackenzie, L.M. (2012) Computation and its Limits, https ://books.google.com/books?ISBN=0199640327.
[27] Childs, A.M., Cleve, R., Deotto, E., Farhi, E., Gutmann, S. & Spielman, D.A. (2002) Exponential algorithmic speedup by quantum walk, MIT-CTP #3309; arXiv:quant-ph/0209131v2.
[28] Aaronson, S. (2015) When exactly do quantum computers provide a speedup?, www.scottaaronson.com/talks/speedup-austin.ppt.
[29] Bremner, M.J., Jozsa, R., & Shepherd, D.J. (2011). Classical simulation of commuting quantum computations implies collapse of the polynomial hierarchy, in Proceedings of the Royal Society of London A: Mathematical, Physical and Engineering Sciences (Vol. 467, No. 2126, pp. 459-472) The Royal Society.
[30] Ambainis, A. (2004) Quantum search algorithms, ACM SIGACT News, 35(2),
22-35.
[31] Ambainis, A. (2007). Quantum walk algorithm for element distinctness, SIAM Journal on Computing, 37(1), 210-239.
[32] Valiant, L. (2004) Holographic algorithms (Extended Abstract) FOCS 2004, Rome, Italy: IEEE Computer Society. pp. 306-315.
[33] Hayes, B. (2008) Accidental algorithms, American Scientist.
[34] Cai, J-Y (2008) Holographic algorithms: guest column. SIGACT News, New York: ACM 39 (2): 51-81.
[35] Huang, S., & Lu, P. (2012) A dichotomy for real weighted Holant problems, in Computational Complexity (CCC), 2012 IEEE 27th Annual Conference on, pp. 96-106, IEEE.
[36] Cai, J-Y, Pinyan, L. & Mingji, X. (2008) Holographic algorithms by Fibonacci gates and holographic reductions for hardness, FOCS, IEEE Computer Society, pp. 644-653.
[37] de Broglie, L. (2004) Forward to, D. Bohm, Causality and Chance in Modern Physics, New York: Routledge.
[38] Shalev-Shwartz, S., & Ben-David, S. (2014) Understanding Machine Learning: From Theory to Algorithms, Cambridge: Cambridge University Press.
[39] Arkani-Hamed, N., & Trnka, J. (2013) The amplituhedron, arXiv:1312.2007.
[40] Bai, Y., He, S., & Lam, T. (2015) The amplituhedron and the one-loop Grassmannian measure, arXiv:1510.03553.
[41] Arkani-Hamed, N., Hodgesb, A. & Trnka, J. (2013) Positive amplitudes in the amplituhedron, arXiv:1412.8478v1 [hep-th].
[42] Aaronson, S. (2013) The unitarihedron: The jewel at the heart of quantum computing, http://www.scottaaronson.com/blog/?p=1537.
[43] De Angelis, S.F. (2013) http://www.enterrasolutions.com/2013/09/are-space-and-time-real.html.
[44] D'Ariano, G.M., Van Dam, W. & Mosca, M. (2007) General optimized schemes for phase estimation, Physical Review Letters 98(9), 090,501.
[45] Papageorgiou, A. & Traub. J.F. (2014) Quantum algorithms for continuous problems and their applications, Vol. 154, Advances in Chemical Physics, pages 151-178, Hoboken: Wiley.
[46] Harrow, A.W, Hassidim, A. & Lloyd, S. (2009) Quantum algorithm for linear systems of equations, Phys. Rev. Lett., 103:150502.
[47] Portugal, R. & Figueiredo, C.M.H. (2006) Reversible Karatsubas algorithm, Journal of Universal Computer Science, 12(5):499-511.
[48] Cao, Y., Papageorgiou, A., Petras, I., Traub, J.F. & Kais, S. (2013) Quantum algorithm and circuit design solving the Poisson equation, New Journal of Physics, 15: 013021.
[49] Draper, T.G. (2000) Addition on a quantum computer, arXiv, quant-ph/0008033.
[50] Wegner, P. (1997) Why interaction is more powerful than algorithms, Communications of the ACM, Vol. 40.
[51] Wegner, P. (1998) Interactive foundations of computing, Theoretical Computer Science, Vol. 192, Issue 2, pp. 315-351.
[52] Wegner, P. & Goldin, D. (2003) Computation Beyond Turing Machines, Communications of the ACM, Vol. 46, Iss. 4.
[53] Hopcroft, J.E. & Ullman, J.D. (1969) Formal Languages and Their Relation to Automata, Reading: Addison-Wesley.
[54] Rice, J.K. & Rice J.N. (1969) Computer Science: Problems, Algorithms, Languages, Information and Computers, New York: Holt, Rinehart and Winston.
[55] Goldin, D.Q., Smolka, S.A., Attie, P.C. & Sonderegger, E.L. (2004) Turing
machines, transition systems, and interaction, Information and Computation, Vol. 194, Iss. 2, pp. 101-128.
[56] Bohm, D. & Vigier, J. P. (1954) Model of the causal interpretation of quantum theory in terms of a fluid with irregular fluctuations, Physical Review, 96 (1), 208.
[57] Baez, J. (2013) The Fano plane, http://math.ucr.edu/home/baez/octonions/node4.html.
[58] Albuquerque, H. & Majid, S. (2012) Quasialgebra structure of the octonions, arXiv:math/9802116.